Roll and Yaw Stability Evaluation of Class 8 Trucks with Single and Dual Trailers in Low- and High-speed Driving Conditions

Yunbo Hou

Dissertation submitted to the faculty of the Virginia Polytechnic Institute and State University in partial fulfillment of the requirements for the degree of

Doctor of Philosophy
In
Mechanical Engineering

Mehdi Ahmadian, Chair
Steve Southward
Pablo A. Tarazaga
Saied Taheri
Linbing Wang

08/28/2017
Blacksburg, Virginia

Keywords: Vehicle dynamics, Roundabout, Modeling and simulation, Testing, RSC, ESC

Roll and Yaw Stability Evaluation of Class 8 Trucks with Single and Dual Trailers in Low- and High-speed Driving Conditions

Yunbo Hou

ABSTRACT

A comprehensive evaluation of roll and yaw stability of tractor/semitrailers with single and dual trailers in city and highway conditions is conducted. Commercial vehicles fundamentally behave differently in city driving conditions than at high speeds during highway driving conditions. In order to closely examine each, this study offers two distinct evaluations of commercial vehicles: 1) low-speed driving in tight turns, representative of city driving; and 2) high-speed lane change and evasive maneuvers, typical of highway driving. Specifically, for city driving, the geometric parameters of the roadway in places where tight turns occur—such as in roundabouts—are closely examined in a simulation study in order to evaluate the elements that could cause large vehicle body lean (or high rollover index), besides the truck elements that have most often been studied. Two roundabout geometries, 140-ft single-lane and a 180-ft double-lane, are examined for various truck load conditions and configurations. The vehicle configurations that are considered are a straight 4x2 truck, a tractor with a 53-ft semi-trailer (commonly known as WB-67), and two trucks in double-trailer configurations. Five potential factors are identified and thoroughly studied: circulatory roadway cross-section, roundabout tilt, truck configurations, truck apron geometry, and truck load condition. The results of the study indicate that when the rear axles of the trailer encounter the truck apron in the roundabout, the climbing and disembarking action can cause wheel unloading on the opposite side, therefore significantly increasing the risk of rollover. Interestingly, in contrast to most high-speed rollovers that happen with fully-loaded trailers, at low speeds, the highest risks are associated with lightly loaded or unloaded trucks. For high-speed driving conditions, typical of highway driving, a semi-truck with a double 28-ft trailer configuration is considered, mainly due to its increasing use on U.S. roads. The effect of active safety systems for commercial vehicles, namely Roll Stability Control (RSC) for trailers and Electronic Stability Control (ESC) for the tractor, is closely examined in a test study. Various trailer loading possibilities are evaluated for different combinations of ESC/RSC on the tractor and trailer, respectively. The results of the study indicate that 1) RSC systems reduce the risk of high-speed rollovers in both front and rear trailers, 2) the combination of ESC (on tractor) and RSC (on trailer) reduce the risk of rollover and jackknifing, and 3) RSC systems perform less effectively when the rear trailer is empty.

Roll and Yaw Stability Evaluation of Class 8 Trucks with Single and Dual Trailers in Low- and High-speed Driving Conditions

Yunbo Hou

GENERAL AUDIENCE ABSTRACT

Traffic accidents involved with heavy trucks are more likely to result in fatality, excessive property damage, and traffic congestion. Unfortunately, heavy trucks commonly have lower stability than passenger cars due to heavy axle load and high center of gravity, which means they are easier to roll over or lose control. Therefore, it is necessary for us to understand the dynamics of heavy trucks in order to improve their stability and reduce the likelihood of severe accidents.

Because heavy trucks are commonly operated for freight transport, they are subjected to two different driving conditions. When a truck is used within an urban area, it will be driven at low speeds and will need to negotiate tight turns, such as those normally seen at city traffic intersections and roundabouts. In this condition, the tight turns and roadway geometry (i.e. curb, truck apron, etc.) can considerably increase the likelihood of truck rollovers. On the contrary, non-collision accidents like rollovers that happen to heavy trucks during highway driving, where there are no tight turns or significant roadway input, are commonly due to the unstable dynamics of trucks rather than external excitation. This is because heavy trucks are more prone to exhibiting unstable dynamics at high speeds, especially when performing quick and aggressive maneuvers, such as those applied when changing lanes or avoiding an obstacle on the road.

In this dissertation, the dynamic stability of heavy trucks in both driving conditions are evaluated. For low-speed conditions, a simulation study is conducted to learn how roadway geometry and truck elements affect the likelihood of rollovers during city driving. For high-speed conditions, a test study is performed to investigate how active safety systems reduce the likelihood of heavy truck rollovers and other non-collision accidents during highway driving. This dissertation provides valuable information for researchers or engineers who are interested in urban traffic design, heavy truck dynamics, and active safety systems for commercial vehicles.

ACKNOWLEDGMENT

I would like to thank my advisor, Prof. Mehdi Ahmadian, for his endless support and encouragement throughout my doctoral studies at Virginia Tech. It is his great wealth of knowledge, unbelievable patience, and wonderful kindness that have guided me through this amazing journey. I could never express enough gratitude for all those times when he went above and beyond the call of duty to help me with both my research and future career. He is truly the best advisor that I could ever ask for.

I would also like to thank my committee members–Prof. Steve Southward, Prof. Pablo A. Tarazaga, Prof. Saied Taheri, and Prof. Linbing Wang–for serving on my PhD committee and providing valuable advice on my research. The classes I took from them also helped me gain great knowledge in mechanical engineering, and let me learn the true spirit of being a research engineer.

I have been so pleased to have the opportunity of joining the CVeSS family. I would like to thank Sara Vallejo for always taking good care of us in the office. I am also very grateful to Dr. Andrew W. Peterson, Dr. Masood Taheri Andani, Dr. Yang Chen, and Andrew E. Kim for their great contributions to the testing project. Those long but fun days we had in South Carolina will always be in my memories. I would also like to thank Zebo Zhu, Dejah Singh, and Ashish Jain for the great friendship we developed during the past years. Some people say the life of a graduate student could be boring, but you guys definitely made sure mine was not one of those. There are also other good CVeSS friends that helped me through the years, including Dr. Sajjad Meymand, Dr. Milad Hosseinipour, Dr. Mehdi Taheri, and Dr. Abdullah Mohammed Hassan.

Pursuing a PhD degree is not easy, but I am so blessed to have my fiancée, Dr. Yifan Dong, to take this journey together with me. It feels like yesterday when we were sitting by the North Lake at Beijing Institute of Technology, picturing what our life would be like in the future. But we could have never imagined that seven years later we would be able to participate in the fall 2017 Graduate Commencement Ceremony at Virginia Tech side by side. If I could get a chance to start my life over, I would follow the exact same path so that I would not miss her and all those ups and downs we have been through together.

More importantly, I would like to express my greatest gratitude to my parents–Min Hou and Huiying Meng–for their unconditional love and endless encouragements. Not all parents are willing to let their only child move to the other side of the world, as they did so unselfishly. They gave me the best gift in life. They allowed me to follow my dreams! My love for them is endless!

Yunbo Hou
August 2017
Blacksburg, VA

Table of Contents

List of Figures

List of Tables

Chapter 1 – Introduction

1.1 Motivation

Heavy commercial trucks have been used as one of the major cargo transport methods for decades all over the world. In 2014, 4.34% of all registered vehicles in the United States were large trucks (with a gross weight rating greater than 10,000 lb), but they traveled 9.34% of all the vehicle miles [1]. Unlike passenger car crashes, truck-related crashes always have greater exposure due to the high fatality and injury rates, as well as excess property damage and traffic congestion. In the United States, 3,744 fatal and 52,360 injury crashes involving large trucks occurred in 2014, where 2,436 (65.1%) of the fatal crashes and 26,132 (50%) of the injury crashes were related to Class 8 articulated trucks (with a gross weight rating greater than 33,000 lb) [1]. The dynamics of articulated vehicles has been studied actively for over sixty years, and great progress was achieved during the 1970s to 1990s. Various types of commercial stability control systems have been designed based on the knowledge of truck dynamics, and some of them have been successfully applied to articulated heavy vehicles (AHV), such as the Anti-lock Braking System (ABS), the Electronic Stability Control (ESC) system, and the Roll Stability Control (RSC) system. However, the relatively low roll and yaw stability of AHVs are still presenting issues to traffic safety today, due to the inherent complicated dynamic properties. Therefore, there is still strong necessity and interest to research deeper into heavy truck dynamics in order to further improve truck stability.

Commercial vehicles fundamentally behave differently in city driving conditions than at high speeds during highway driving conditions. For city driving, the geometric parameters of roadway in places where tight turns occur, such as in roundabouts, usually bring challenges to the roll stability of commercial vehicles. Roundabouts are relatively newer traffic intersection designs and are commonly used in urban settings, compared to the conventional four-way signalized intersection. Roundabouts can bring many benefits to traffic operation and safety, and therefore have become more and more popular in the United States since the 1960s. However, roundabouts also cause some challenges to heavy

trucks that could trigger truck rollover [2], and there are relatively few studies that have been conducted to investigate this issue. Hence, a simulation-based case study is performed to evaluate the effect of critical roadway geometric parameters and truck properties on truck rollover likelihood in roundabouts, representative of city-driving conditions.

Unlike low-speed truck roll stability issues in roundabouts where road excitation acts as one of the main causes of rollover, the dynamic property of the truck itself can also lead to unstable situations in high-speed, highway-driving conditions. For example, rearward amplification is an inherent phenomenon that happens to articulated vehicles, especially for trucks with multiple trailers during high-speed dynamic maneuvers. When this phenomenon occurs, the trailing units tend to experience greater lateral accelerations than the tractor, which significantly increases the likelihood of rollover and jackknifing events. As trucks with double trailers are more and more favored within freight carriers for operational efficiency, it is necessary to further investigate the dynamic stability of trucks in such configurations. In addition, since the National Highway Traffic Safety Administration (NHTSA) submitted a new Federal Motor Vehicle Safety Standard (FMVSS) that requires truck tractors and certain large buses with a GVWR greater than 11,793 kg (26,000 lb) to be equipped with tractor-based ESC systems [3], it raises the interest of examining how tractor-based ESC and trailer-based RSC systems perform on trucks with double-trailer configurations. Therefore, a comprehensive test study is conducted to closely examine the effect of active safety systems for commercial vehicles, namely RSC for trailers and ESC for tractors, on the dynamic stability of typical 28-ft A-train doubles.

1.2 Objectives

The primary objectives of this study are to:

1. Evaluate the elements that would increase the likelihood of commercial truck rollover during both low-speed, city-driving and high-speed, highway-driving conditions;

2. Determine the elements that can increase the risk of rollover during city and highway driving;
3. Examine the effect of both roadway geometry and truck conditions in city driving rollovers; and
4. Evaluate the effect of active safety systems on tractors and trailers in reducing the likelihood of rollovers in high speeds.

1.3 Approach

This study uses a combination of dynamic simulation and testing to achieve the above objectives. Where possible, dynamic testing of the tractor-trailer combinations are performed. When such tests are not possible, we will resort to simulations. Most of the simulation studies are conducted using specific models in such accepted tools as TruckSim. The TruckSim model is augmented with component models that are developed in Simulink for better representing the dynamics that are important to our analysis.

The key steps taken during the study include the following:

- Extensive literature research is conducted to learn critical factors for low-speed truck stability during city driving. To this end, the geometry and design of roundabouts are identified as critical factors.
- Experts are consulted to learn more about the specific geometries of roundabouts and also how typically an experienced truck driver negotiates a roundabout. The findings are used for setting up an extensive case plan that includes *both* the truck variations and the critical roadway parameters.
- Simulation-based case studies are conducted to evaluate the effect of the identified factors on truck rollover in various conditions.
- A similar path is taken for evaluating the high-speed roll stability of trucks under typical steering maneuvers that can occur on highways. The high-speed study, however, is conducted on a dedicated test track with a professional driver in order to more accurately capture the complex dynamics that occur during steering maneuvers that include collision avoidance, exit ramp driving, lane change maneuvers, etc.

- A series of simulation-based case studies are conducted to estimate the specifications required in the design of the tests and the needed safety equipment, such as anti-roll outriggers and anti-jackknifing systems.
- Customized load frames are designed and fabricated for better representing a realistic load location and center of gravity (CG) during the tests.
- A comprehensive and innovative instrumentation suite is installed onboard the test tractor and trailers, including integrating load cells into outriggers for contact force measurement, and a 16-channel LiDAR system for measuring tractor-trailer and trailer-trailer articulation angles.
- A simple but effective method is devised and used to synchronize analog and video data. The synchronized video data is used to validate analog data (i.e., outrigger contact) and to exhibit truck transient response that cannot be reflected in analog data (i.e., wheel lift).
- Standard test maneuvers suggested by past test reports and industry experts are evaluated using simulation. The maneuvers that best suit the testing objective of the study are adopted for the tests.
- A steering robot is employed to perform maneuvers that require exact steering profile, with high repeatability.
- Preliminary laboratory and track tests are conducted in advance of the track tests to ensure proper functioning of the safety structures and accurate performance of the data acquisition system.
- A new Sine-with-Dwell (SWD) maneuver is developed and applied specifically for the test truck, which leads to better rear-trailer dynamic excitation than the standard SWD maneuvers.
- An additional criterion is added to the existing method of evaluating SWD test results for quantifying the understeer experienced by the test truck.

1.4 Contributions

This study presents the most comprehensive and scientific-based evaluation of tractor semitrailers in both low- and high-speed conditions of which we are aware. The study provides:

- A comprehensive evaluation of the effect of roundabout geometry on heavy truck roll stability in roundabouts, assisting civil engineers in designing safer roundabouts.
- Highlighting for the first time the elements that can be designed into or avoided in roundabouts in order to reduce the likelihood of apron-induced tripping, in particular in lightly-loaded and unloaded conditions.
- A comprehensive roadmap for instrumenting tractors and trailers for analog, digital, and video data collection, while synchronizing them together.
- Test conditions and maneuvers that best assist in determining the roll stability and jackknifing propensity of trucks with double trailers in steering maneuvers that can arise during highway driving.
- Evaluations of the dynamic benefits of RSC systems on double trailers with different trailer loading configurations.
- A thorough analysis of the effect of mixed ESC/RSC usage on trucks with double trailers.

1.5 Outline

- Chapter 1 provides the objectives, approach, potential contributions from the research, and the outline of the dissertation.
- Chapter 2 introduces the background and technical review for the dissertation.
- Chapter 3 details the truck and roundabout models developed in TruckSim, as well as the simulation case study plan for heavy truck low-speed stability evaluation in roundabouts.
- Chapter 4 presents the low-speed simulation results and analysis for the evaluation of heavy truck roll stability in roundabouts.
- Chapter 5 provides an overview of truck dynamics in high-speed driving conditions.
- Chapter 6 presents the simulation-based dynamic stability analyses of 28-ft A-train doubles.
- Chapter 7 provides an overview of the testing and evaluation of dynamic stability of 28-ft A-train doubles with electronic stability control, as well as the test preparation work and preliminary tests.

- Chapter 8 presents and discusses the test results for 28-ft A-train doubles with trailer-based RSC systems.
- Chapter 9 presents and discusses the results of tests to evaluate the effect of configuration changes on the dynamic stability of a 28-ft A-train double.
- Chapter 10 provides conclusions and recommended future work.

Chapter 2 − Background and Technical Review

This chapter provides the technical background necessary for understanding the yaw and roll stability issue of an articulated heavy vehicle (AHV). An overview of vehicle units, couplings, and configurations of AHVs is presented. Next, the typical directional safety and stability issues experienced by AHVs are reviewed, along with a brief introduction of common stability enhancement systems for heavy trucks. Last, a relatively new traffic intersection design–the modern roundabout–is introduced, and the challenge it brings to heavy trucks is reviewed.

2.1 AHV Units, Couplings, and Configurations

AHVs, as indicated by the name, are an assemblage of two or more ridged (i.e. non-articulating) vehicle units [4]. An AHV is composed of a lead unit, and one or multiple trailing unit(s). The lead unit is at the front of the configuration, processes one or more steering axles, and normally provides power to move the entire vehicle combination. A lead unit that does not carry any cargo but only tows trailing units is typically called a tractor. Otherwise, it can be considered as an individual truck.

The common AHV units and couplings are shown in Figure 2-1. Trailing units, which are commonly known as trailers, can be categorized into two main classes: full trailers and semitrailers. A full trailer possesses both front and rear running gears, and a pintle hitch coupling is normally used to tow a full trailer and provide steering input. On the contrary, a semitrailer only possesses rear running gear, which requires the towing unit to provide vertical support when traveling. Such support can be provided by a tractor or by a converter dolly that "converts" the semitrailer into a full trailer. A semitrailer uses a kingpin to connect to a fifth-wheel coupling installed on the towing unit, which transfers towing force and steering input to the semitrailer. In addition, there is another type of trailer, the center-axle trailer, which is used less widely than those introduced above. A center-axle trailer has its running gear located slightly behind the center of gravity (CG). Hence, the running gear supports most of the vertical load of the center-axle trailer. A pintle hitch coupling is commonly used to connect the center-axle trailer to the towing unit.

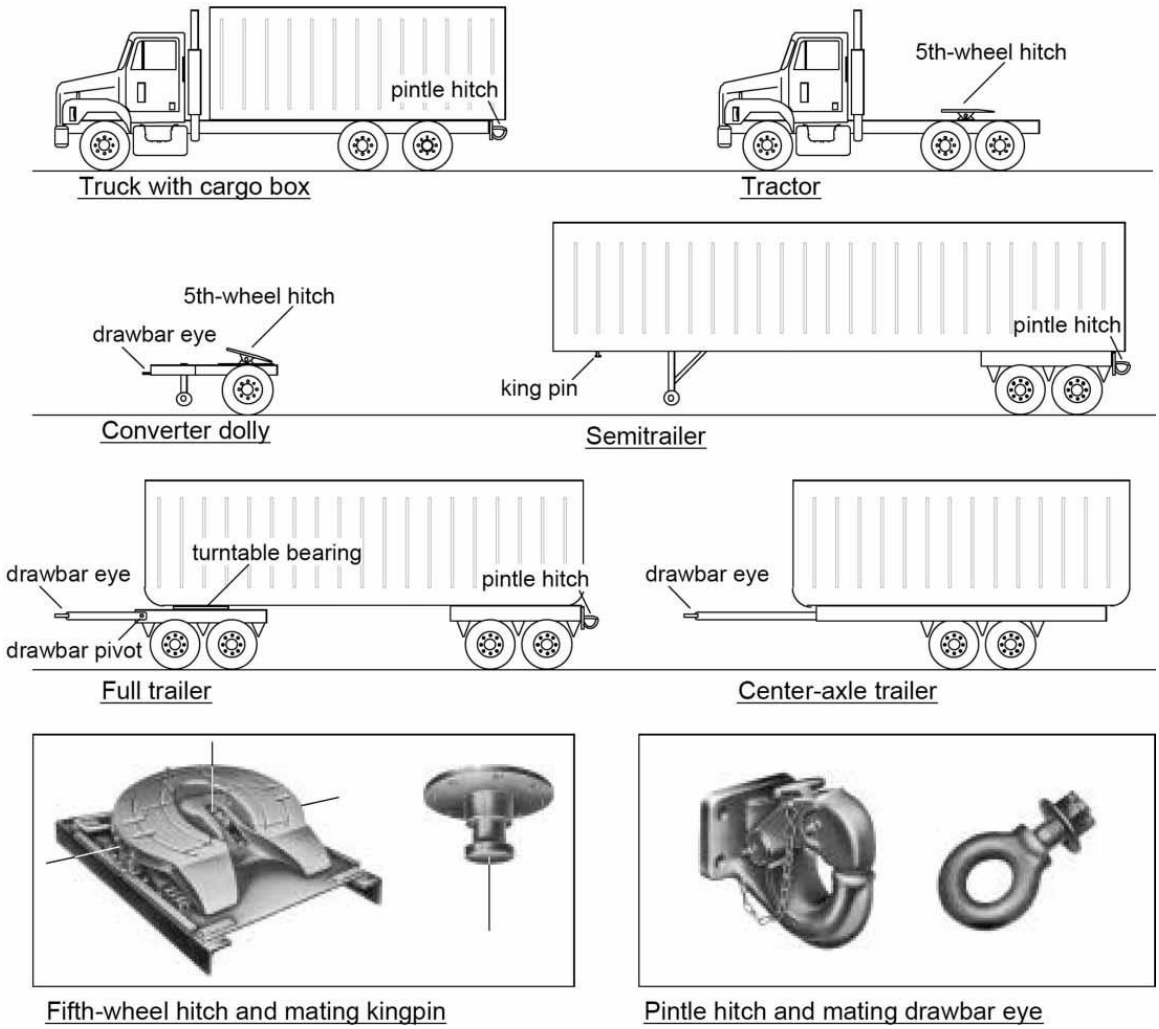

Figure 2-1. Common AHV vehicle units and couplings [4].

As introduced above, a pintle hitch coupling and a fifth-wheel coupling are the two devices widely applied to couple towing and trailing units. A pintle hitch coupling is more commonly used to connect a full trailer or converter dolly tow bar to a towing unit, which approximates a spherical joint by providing three rotational degrees of freedom within the normal operating range [5]. A fifth-wheel coupling is most commonly applied to connect a semitrailer to a towing vehicle unit, which allows free yaw rotational motion, and limited roll and pitch rotational motion. Both pintle hitch coupling and fifth-wheel coupling provide translational constraints in all three directions.

Different vehicle units and couplings can lead to various vehicle combinations and configurations. In general, the two most widely used AHV configurations are the tractor/semitrailer and truck/full trailer combinations, where the tractor/semitrailer

configuration is the most popular type in the United States and is commonly referred to as a “semi-truck.”

An AHV that has more than one trailing unit is usually called a vehicle train or a road train. A tractor with two trailers is known as a double, whereas a tractor with three trailers is called a triple. The doubles can have three configurations, A-, B-, and C-train, based on the coupling mechanics between the trailers. Figure 2-2 shows that an A-train double possesses a front semitrailer, a converter dolly (A-dolly), and a rear semitrailer. The front trailer is coupled with the tractor via a fifth-wheel coupling; the converter dolly is connected to the front trailer with a pintle hitch coupling; and another fifth-wheel coupling is used to couple the converter dolly to the rear trailer. Hence, the A-train configuration has three degrees of freedom (DOF) for articulation motion. A B-train double consists of a tractor, a front semitrailer with a fifth-wheel coupling attached to its rear end, and a rear semitrailer, as shown in Figure 2-3. The major difference between an A-train and B-train double is that a B-train uses a fifth-wheel installed on the rear end of the front trailer to connect the rear trailer, rather than employing a converter dolly, as shown in Figure 2-3. Therefore, B-train doubles have two DOF for articulation motion. A C-train is very similar to an A-train, except that the converter dolly in this configuration, which is called a C-dolly here, has a double draw-bar arrangement attached to two pintle hitch couplings installed on the front semitrailer. Hence, a C-train also has two DOF in articulation motion.

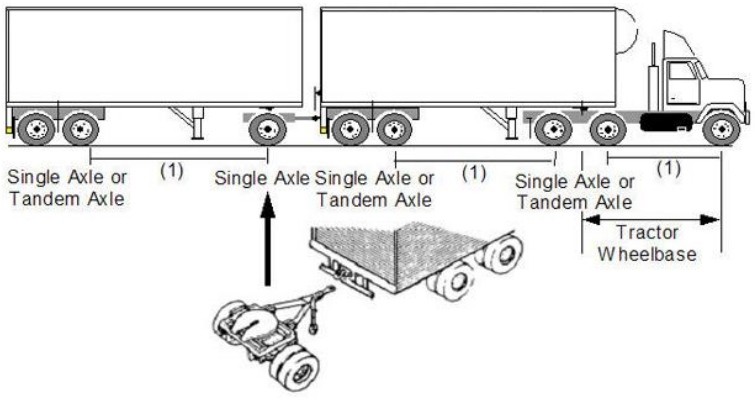

Figure 2-2. A-train double configuration [6].

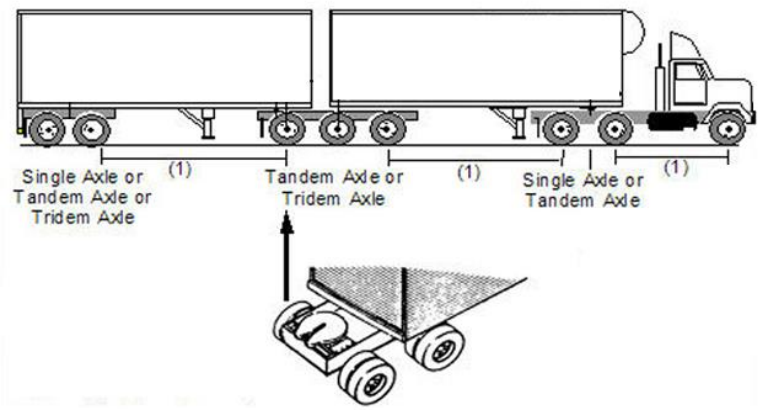

Figure 2-3. B-train double configuration [6].

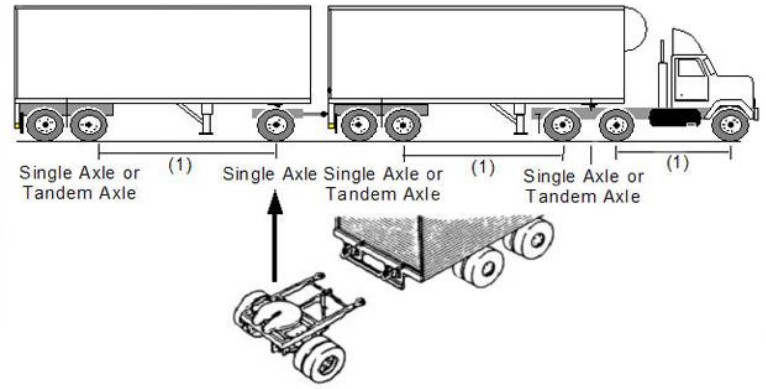

Figure 2-4. C-train double configuration [6].

Doubles have become more and more popular in the United States, mainly due to the logistical advantage, which could increase productivity by fifty percent for very little additional expense [7]. Among all three double-trailer configurations introduced above, A-train doubles are more widely used in the United States. Because both the semitrailers in an A-train double are identical, they can be used as either front or rear trailers. Unlike A-trains, the front semitrailer in a B-train double has different frames than the rear semitrailer. Hence, if a rear trailer is dropped at a shipping center, the cargo that needs to be picked up has to be loaded into another rear trailer, which might cause logistical inefficiency. However, A-train doubles are known for experiencing a great directional stability issue, referred to as rearward amplification, where the lateral acceleration experienced by the trailers are larger than that at the tractor during dynamic maneuvers. The rearward amplification only happens to articulated vehicles, and becomes stronger as the combined vehicle's DOF for articulation motion increases. Therefore, a B-train double has better directional stability than an A-train double regarding the rearward amplification,

since it has less DOF in articulation motion than an A-train. As for C-train doubles, they have the same number of vehicle units as the A-train, but the DOF for articulation motion is less than A-trains. This is because the two draw-bar arrangement provides constraints for relative yaw and roll motion between the C-dolly and the front semitrailer. In addition, the front and rear semitrailers of a C-train are interchangeable, and hence it does not lead to logistical problems as a B-train does. C-dollies usually have self-steering axles for reducing the tire wear at tight turns, which may increase maintenance cost. Innovative converter dollies have been designed to improve the AHV dynamics, including modifying the arrangement of the drawbar hitch, revising the mechanism of linkage between the drawbar and dolly body, adding a forced-steering axle to A-dollies, and adjusting the steering mechanism of C-dollies, etc. [8]. Simulation and test studies have been conducted to evaluate the dynamic performance of these innovative dollies [9, 10].

2.2 Typical AHV Directional Safety and Stability Issues

A study conducted by NHTSA [11] shows that in the United States, 41,059 people were killed and 2,491,000 people were injured in motor vehicle crashes in the year 2007, which resulted in a fatality rate of 1.65%. However, in the crashes in which large trucks were involved, 4,808 people were killed and 101,000 people were injured, leading to a fatality rate of 4.76%. Obviously, large-truck-related accidents result in a higher fatality rate, which makes it important to study and understand heavy truck dynamics in order to improve stability and therefore reduce traffic accidents.

The dynamics of AHVs are more complicated than those for a single-unit vehicle, such as a passenger car. One of the major differences between them is the directional dynamics. Unlike single-unit vehicles that can be regarded as a single rigid body, articulated vehicles behave as multiple rigid bodies coupled by joints (couplings), and therefore the dynamics are more complicated and additional stability issues appear. This section will introduce the common directional safety and stability issues experienced by AHVs.

2.2.1 Driver Being Isolated from Sensing the Motion of Trailing Vehicle Units

Before discussing the vehicle kinematics and dynamics, the first issue is that an AHV driver can be isolated and may not be able to directly sense the vehicle motion, especially for

trailing vehicle units, and therefore be unable to react accordingly. This is because the couplings between the towing and trailing vehicle units allow certain relative motions. Commonly, a fifth-wheel coupling allows free relative yaw motion and limited pitch motions (7 ~ -11 degrees), whereas a pintle hitch coupling only provides limited roll constraint (10 ~ 25 degrees). For example, if an A-train double negotiates a curve at an excessive speed, the driver may not be able to sense the roll angle of the rear semitrailer even though the trailer is about to roll over, due to the pintle hitch that connects the front trailer and the converter dolly. In addition, there is another situation where the driver is not able to sense the trailer motion, as shown in Figure 2-5, where the trailer has already rolled over but the tractor is still held upright. This is because the structure strength of trailing units of AHVs in the vertical direction is usually more considered in design while the torsional strength is not. Therefore, when a trailing unit that has a long wheelbase and high torsional flexibility rolls and twists, the driver may not be able to feel the motion and react responsively.

Figure 2-5. The driver cannot sense the trailer roll motion due to the trailer's high torsional flexibility. (Screenshot, https://www.youtube.com/watch?v=zEsVsVGH6o4, assessed Aug. 2017)

2.2.2 Off-Tracking in a Steady-State Turn

Off-tracking is a characteristic issue for articulated vehicles, and is defined as the lateral distance between the path followed by the tractor front axle's center point and those of the trailer axles when an AHV turns. The off-tracking that happens to AHVs is different at

low and high speeds. Low-speed off-tracking occurs when an articulated vehicle tracks a steady-state circular path at low speeds, where each axle of the vehicle train follows a path that lies inside of that inscribed by the preceding axle [12], as shown in Figure 2-6 [13]. Equation 2-1 is a simplified equation for low-speed off-tracking in a steady-state turn for an *n*-unit articulated vehicle [4].

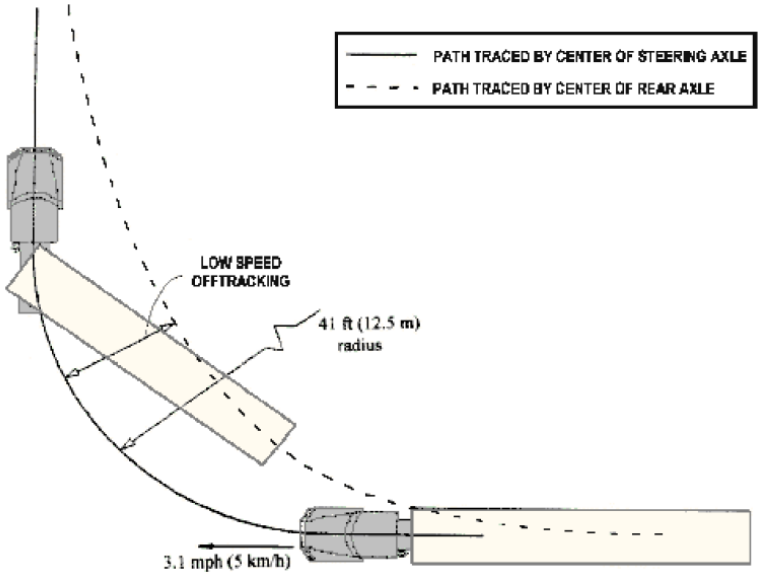

Figure 2-6. Low speed off-tracking of articulated vehicles [13].

$$R_1 - R_{n+1} = R_1 - \left(R_1^2 - \sum_{1}^{n} (WB_i^2 - AH_i^2) \right)^{0.5} \qquad (2-1)$$

This equation is derived based on the geometry analysis of a simple yaw-plane model, where R_1 is the turning radius of the tractor's front axle, R_{n+1} is the turning radius of the rear axle on the *n*th trailer (the last unit), WB_i is the effective wheelbase from the front hitch to the rear axle of the *i*th unit, and AH_i is the distance from the rear hitch to the rear axle of the *i*th trailer. The low-speed off-tracking requires extra space, especially when the truck negotiates a tight curve, which results in the risk of hitting the inside road shoulder or curb, as well as the adjacent traffic participators.

High-speed off-tracking is a speed-dependent phenomenon that results from the tendency of the rear of the trailing units to move outward due to the lateral acceleration of the vehicle as it follows a curve at higher speeds [13]. As the AHV speed increases, the off-tracking

to the inside of the curve decreases and becomes zero at a certain speed, which indicates that the trailer axle follows the same path as that of the tractor front axle. If higher speeds are applied, the trailer will track outside the trajectory of the tractor, as shown in Figure 2-7.

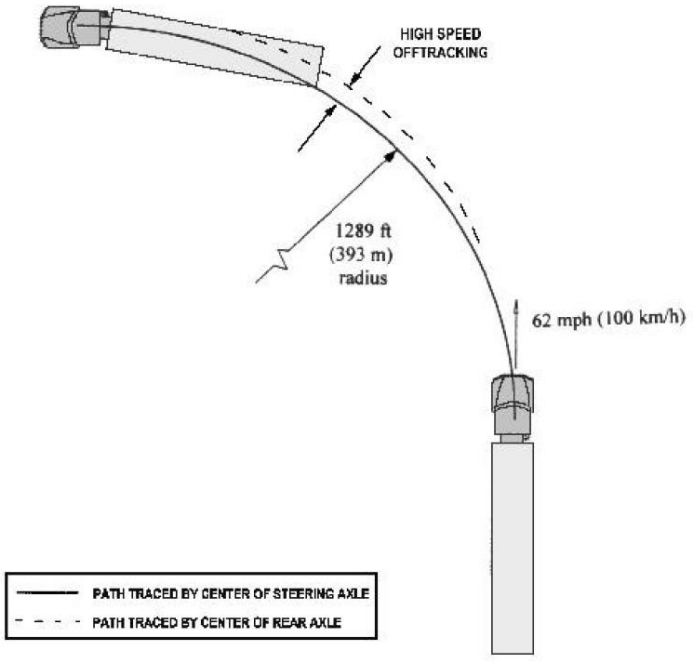

Figure 2-7. High-speed off-tracking of articulated vehicles [13].

2.2.3 Rollover

Rollover of heavy articulated trucks presents serious hazards to safety for all motorists, and an out-of-control heavy truck has the potential to cause injury or death to its operator as well as to other motorists, and can inflict significant damage to property because of its size [14]. Table 2-1 summarizes crashes involving large trucks that happened in the United States in 2014 [1]. It shows that heavy truck rollover accidents resulted in higher fatality and injury rates than the average accidents.

Rollover events can be categorized into two classes: tripped rollovers and untripped rollovers. Tripped events commonly occur when a vehicle slides sideways and digs its tires into soft a road surface or strikes an object such as a curb or guardrail. Driver-induced un-tripped rollover can occur during typical driving situations, such as excessive speed during cornering, obstacle avoidance, and severe lane change maneuver, where rollover occurs as a direct result of the lateral wheel forces during the maneuver [15].

Table 2-1. Crashes involving large trucks that happened in the United States in 2014 [1].

	Fatal Crashes		Injury Crashes		Property Damage Only Crashes		Total
	Number	Percent	Number	Percent	Number	Percent	
General	3,424	0.83%	82,000	19.93%	326,000	79.24%	411,424
Rollover	156	1.70%	5,000	54.61%	4,000	43.69%	9,156

Most rollovers that happen to passenger cars are tripped events. In contrast, un-tripped rollovers more occur to heavy trucks that have lower roll stability, due to the heavy load and high center of gravity (CG). Figure 2-8 shows the static rollover threshold of different types of vehicles [16].

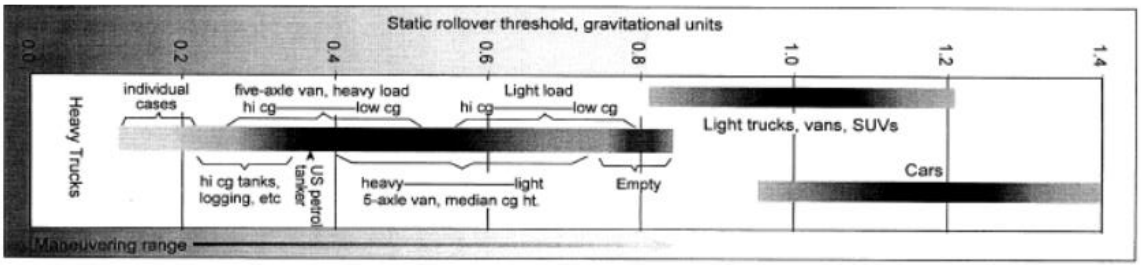

Figure 2-8. The static rollover threshold of different types of vehicles [16].

Figure 2-9 illustrates a simplified free-body diagram of a heavy vehicle in steady turn, and the corresponding roll equation is provided in Equation 2-2 [16].

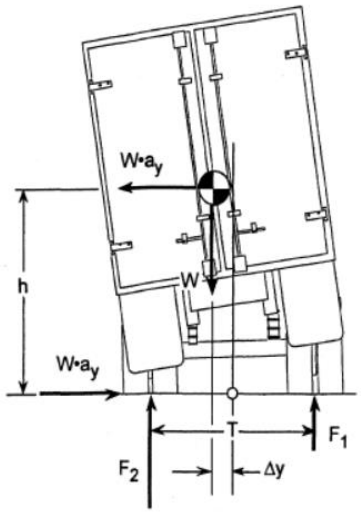

Figure 2-9. A simplified free body diagram of a heavy vehicle in steady turn [16].

$$W \cdot h \cdot a_y = (F_2 - F_1) \cdot \frac{T}{2} - W \cdot \Delta y \qquad (2-2)$$

Where

a_y = lateral acceleration

F_i = vertical tire force, i = 1,2

h = height of the CG

T = vehicle track width

W = vehicle weight

Δy = the lateral distance that the CG travels due to a_y

Equation 2-2 can also be expressed with respect to roll angle as shown in Equation 2-3, where φ = vehicle roll angle, and $\varphi = \Delta y/h$.

$$W \cdot h \cdot a_y = (F_2 - F_1) \cdot \frac{T}{2} - W \cdot h \cdot \varphi \qquad (2-3)$$

The graphic presentation of Equation 2-3 is shown in Figure 2-10.

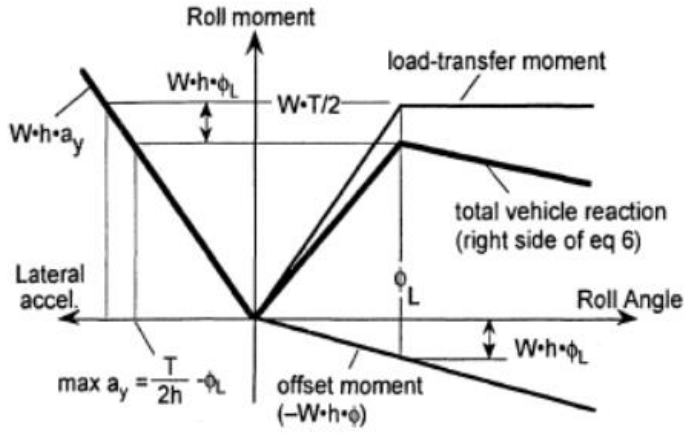

Figure 2-10. Graphic presentation of Equation 2-3 for a vehicle with compliant tires and suspension [16].

2.2.4 Jackknifing

Jackknifing is a type of accident that exclusively happens to articulated vehicles. Jackknifing occurs when the articulation angle between the towing and trailing unit becomes so excessive that a kinematic constraint is formed, or even collision between two

units occurs. Figure 2-11 illustrates an example of a jackknifed semi-truck. Jackknifing events are commonly triggered by aggressive dynamic maneuvers, such as obstacle avoiding, or braking on a road surface with a low friction coefficient where tire traction is significantly reduced. In 2012, 5,163 jackknifing crashes happened in the United States, including 163 fatal, 1,000 injury, and 4,000 property-damage-only crashes [17].

Figure 2-11. A jackknifed semi-truck (Wallaceburg Courier Press, accessed August 2016).

2.2.5 Rearward Amplification

Rearward amplification is not a type of accident, but it is a phenomenon experienced by articulated vehicles that may induce both rollover and jackknifing accidents. Rearward amplification can be described as, in general, the lateral acceleration experienced by the trailing units is larger than that of the leading unit during a dynamic maneuver at high speeds. Rearward amplification can be expressed and measured as the ratio of the lateral acceleration at the tractor and that on the trailer(s), as shown in Equation 2-4.

$$RA_i = \frac{a_{y1}}{a_{yi}} \qquad (2-4)$$

RA_i is the rearward amplification ratio between the tractor and the i-th unit, and a_{yi} is the lateral acceleration applied to the i-th unit. Figure 2-12 illustrates the rearward amplification that happens to a semi-truck during a lane change maneuver. The second trailer experiences a larger peak lateral acceleration than the tractor, and there is also a phase delay between the front and rear vehicle units due to the long wheelbase.

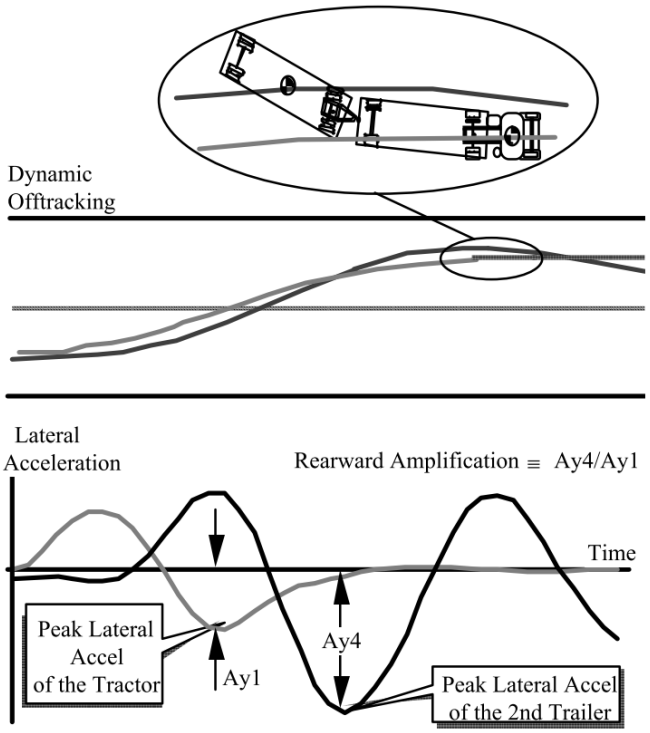

Figure 2-12. Rearward amplification happening to a truck with double trailers [7].

2.3 Heavy Truck Dynamic Stability Issues at Low and High Speeds

Similar to passenger cars, the forward traveling speed plays a significant role in determining the dynamic behavior of heavy trucks. Therefore, heavy trucks are subjected to different dynamic stability issues at low and high speeds.

When traveling at low speeds during city-driving conditions, the geometric parameters of the roadway in places where tight turns occur are major factors that contribute to truck rollover accidents. For example, heavy commercial vehicles commonly carry heavy cargo loads with great CG heights, resulting in a considerably lower rollover threshold compared with passenger cars. Thus, heavy commercial trucks would experience larger body roll and thus greater load transfer when traveling on roadways with cross-slopes, leading to a stronger likelihood of rollovers. Unfortunately, heavy commercial vehicles also need to negotiate tight curves in city-driving conditions, and in some places−such as in roundabouts−heavy commercial vehicles are not only subjected to tight turns, but are also traveling on roadways that have cross-slopes towards the outside of the turn. This outward cross-slope works together with centrifugal forces to further increase truck body roll and thus lead to even stronger rollover risk. As urbanization has developed rapidly in the past

several decades, the truck dynamic stability in low-speed, city-driving conditions should be thoroughly investigated, especially when traveling through new traffic designs, such as modern roundabouts.

Different from low-speed rollover accidents that are mainly caused by roadway input and tight turns, rollover or jackknifing accidents that happen to heavy commercial vehicles traveling in high-speed, highway-driving conditions are mostly due to evasive steering wheel input, such as lane-change or evasive maneuvers. Such aggressive steering input could result in large lateral accelerations to tractors and trailers, posing great risks of rollover and jackknifing accidents. In addition, having more trailing units or traveling at higher speeds both increase the phenomenon of rearward amplification, which further contributes to large lateral forces applied to the rearmost trailing unit. For example, a tractor with double trailers is subjected to a stronger rearward amplification effect than a tractor with a single semitrailer at the same speed. Moreover, an A-train double also experiences more rearward amplification than a B-train double due to its additional DOF in yaw motion. Therefore, the dynamic stability issues for heavy commercial vehicles at high speeds are related to steering input, traveling speed, and truck configurations. As most heavy truck dynamics studies are focused on semi-trucks, and trucks with multiple trailers are becoming more favored by freight carriers for better operational efficiency, it is important to conduct further in-depth research on the dynamic stability of trucks with multi-trailers.

2.4 Stability Enhancement Systems for Heavy Trucks

The stability issue for heavy trucks has been apparent since heavy trucks started to become widely operated for cargo transport. In order to enhance heavy truck stability, many electronic and mechanical systems have been designed and tested. This section introduces common stability enhancement systems for heavy trucks.

2.4.1 Anti-lock Braking System (ABS)

The Anti-lock Braking System (ABS) is a safety system that prevents the vehicle wheels from locking up during braking in order to obtain more braking force from the contact

patch. ABS is widely employed by both passenger cars and commercial vehicles, and has become mandatory for all new passenger cars in Europe since 2004.

For a vehicle tire, the longitudinal friction force that it could generate from the ground is governed by the slip ratio, which is defined by

$$slip\ ratio = \frac{r\omega - v}{v} \qquad (2-5)$$

Where

r = rolling radius of the tire

ω = tire rotational speed (rad/s)

v = vehicle forward velocity

The relation between the braking force and slip ratio is shown in Figure 2-13. Most commercial ABS packages monitor angular accelerations and slip ratios of each wheel and compare them against certain thresholds to activate ABS operation [18]. In detail, an ABS controls the vehicle brake system to maintain the slip ratio of each individual tire within a range to gain optimal friction force. For example, if a driver applies full brakes to the vehicle and locks up a wheel (100% slip ratio), the ABS would release the brake pressure on this wheel to reduce the slip until the ratio drops down to the desired range.

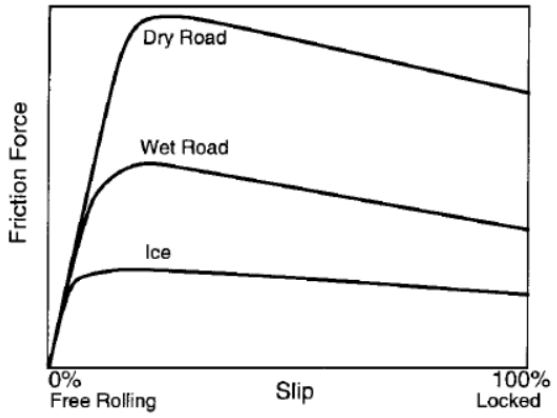

Figure 2-13. Relation between slip ratio and friction force [19].

2.4.2 Electronic Stability Control (ESC) System

The terminology of the Electronic Stability Control (ESC) system can be generally used to describe any electronic stability enhancement system on a vehicle. However, here it specifically refers to the system that automatically provides roll and yaw control based on measuring the lateral acceleration, yaw rate, steering angle, wheel speed, vehicle mass, etc. The vehicle mass can be estimated using engine torque and transmission data that is available to the ESC Electronic Control Unit (ECU) via the SAE J1939 CAN bus [18]. However, in some cases, the mass of those heavy trucks equipped with pneumatic suspension systems can also be estimated by measuring airbag pressures. An ESC system uses lateral acceleration and yaw rate as the main factors to determine control action by comparing them with threshold values. The threshold values are determined from a look-up table, which is commonly calculated based on the measured data and predefined vehicle information. In addition, considering that the ESC system may not be able to engage at the exact moment when the threshold lateral acceleration is reached, due to the dynamic delay caused by the vehicle inertia and time consumed for transferring and processing data, an ESC ECU also estimates a second value of lateral acceleration referred to as "Preview Lateral Acceleration" [20], which is given by

$$a_{y\_preview} = \frac{\delta v_x^2}{R_\delta v_x^2 + L} \qquad (2-6)$$

Where

δ = steering angle (rad)

R_δ = vehicle roll coefficient ($rad \cdot s^2/m$)

V_x = vehicle longitudinal speed (m/s)

L = vehicle wheelbase

The preview lateral acceleration enables an ESC system to engage at least 200-300 milliseconds before the threshold acceleration is actually achieved, and therefore enhances the performance of ESC systems.

A commercial ESC system takes over the engine and brake control when engaging. Commonly, it first reduces throttle to slow down the vehicle in order to attenuate lateral acceleration, and then it selectively brakes the wheels to generate a counter-yaw moment. This moment, on the one hand, could directly reduce the chance of yaw instability; on the other hand, it could also "straighten" an articulated vehicle and therefore prevent it from jackknifing.

2.4.3 Roll Stability Control (RSC) System

The Roll Stability Control (RSC) system is a less sophisticated version of the ESC system, which is commonly used on the trailers of articulated vehicles. An RSC system senses the lateral acceleration and yaw rate, and compares them with the threshold value calculated from a look-up table. When excessive values are sensed, an RSC system will selectively brake one or both trailer axles to reduce vehicle speed and thus decrease the likelihood of rollover.

2.4.4 Balanced Pneumatic Suspension System

Unlike the electronic stability control systems introduced in the previous sections, a balanced pneumatic suspension system is a mechanical system that enhances the roll stability of heavy commercial vehicles. A pneumatic suspension system usually consists of:

- Air supply tank: The reservoir that stores compressed air.
- Check valve: A unidirectional valve that only allows air flow from the air supply tank to the airbags.
- Leveling valve: A valve that controls when to supply or dump the air in airbags by sensing the suspension travel.
- Airbag: A cylinder made from textile-reinforced rubber that uses compressed air to provide spring forces.
- Hose and fitting: Components that are used to connect the air tank, check valve, leveling valve, and airbag.

The leveling valve is the control unit in a pneumatic suspension system. It is normally installed on the truck frame with its control arm connected to the targeted truck axle via a solid rod. Therefore, a leveling valve can sense the suspension travel and decide to charge or dump airbags when the suspension is compressed or expanded, respectively, in order to maintain the truck at a specific ride height. Figure 2-14 shows a leveling valve installed on a semi-truck.

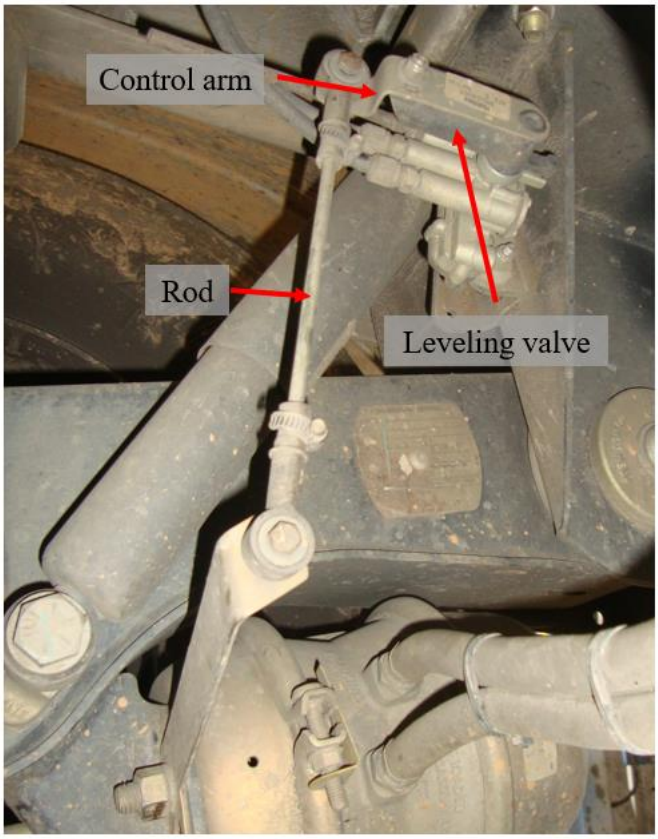

Figure 2-14. A leveling valve installed on a semi-truck.

Figure 2-15(a) illustrates a common Original Equipment (OE) suspension plumbing arrangement [21]. The OE system possesses one leveling valve on the tractor and another one on the trailer, and these leveling valves are usually installed closer to the driver's side. In contrast, the balanced system, as shown in Figure 2-15(b), has two leveling valves on the tractor as well as on the trailer. Therefore, the plumbing arrangement of the balanced system obtains better symmetry and enables the system to adjust ride height more responsively and precisely. The effect of the balanced system on improving heavy truck roll stability was studied using simulation [22, 23].

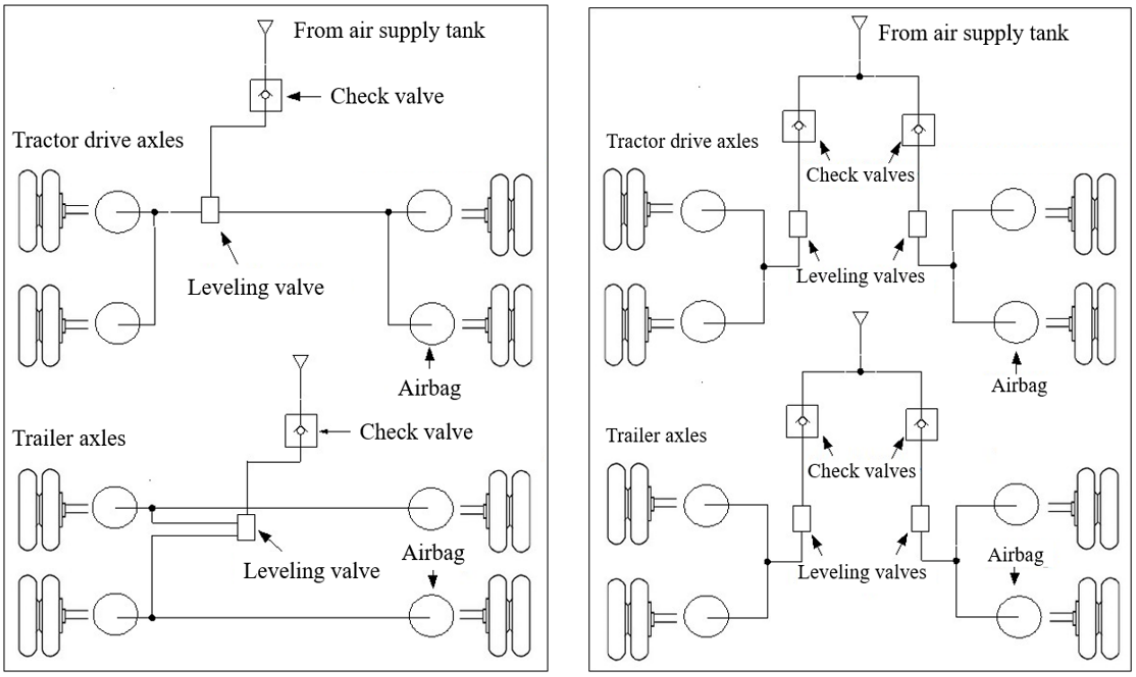

(a) OE system plumbing arrangement (b) Balanced system plumbing arrangement

Figure 2-15. Plumbing arrangements of OE and balanced pneumatic suspension systems [22]: (a) OE system; (b) Balanced system.

2.5 Heavy Truck Directional and Stability Studies Review

This section introduces the studies that have been conducted on heavy truck directional dynamics and stability.

2.5.1 Heavy Truck Modeling and Stability Analysis

The modeling of heavy truck dynamics mainly started in the 1960s, when analog computers became practically available for calculating linear ordinary differential equations. Jindra [24] developed a simplified linear tractor-semitrailer model in yaw plane for directional stability analysis. This bicycle model has three DOF including side-slip and yaw of the tractor, as well as articulation angle of the semitrailer with respect to the tractor. Later, a mathematical model for a tractor with double trailers was also developed by Jindra [25]. This model consisted of five DOF, and the effects of forward speed, fifth-wheel location, semitrailer length, and other parameters on truck directional stability were investigated.

Hazemoto [26] developed three double-trailer models that were similar to that of [25]. Frequency-domain analysis was conducted to study different parameters on lateral stability, including various trailer lengths, trailer load combinations, second trailer weight,

etc. Mallikarjunarao and Fancher [27] developed five linear truck models with different configurations in yaw plane. The directional stability of these trucks was analyzed based on the eigenvalues of corresponding characteristic matrices, where various parameters were applied, such as different load conditions, wheelbases, cornering stiffnesses, etc. Sanyal and Karmakar [28] developed a four-DOF mathematical model for a truck with a dolly and a trailer. The equations of motion (EOM) were derived using Bond Graph, and the Routh-Hurwitz criterion was applied to determine the stability of the vehicle system. Alexander et al. [29] performed experiments with ramp steering maneuvers to validate a mathematical semi-truck model. The cornering stiffness of the front and rear axles of the truck were adjusted based on the test results to enhance model accuracy. Verma and Gillespie [30] studied the roll dynamics of commercial vehicles based on a five-DOF nonlinear analytical roll-plane model without small angle assumptions. The results indicated that rollover could occur at lateral acceleration levels less than the static acceleration limit due to resonance of the roll motions.

Winkler [31] improved existing mathematical vehicle models by considering more factors that affected slip angles on tires, such as vehicle velocity and path curvature, compared to previous models where only lateral acceleration was taken into consideration to determine slip angles. This study concluded that the actual wheelbase of a two-axle vehicle is longer than that derived from geometric measurement. Esmailzadeh and Tabarrok [32] developed a mathematical model for a specific type of Canadian truck−"Super B Train"−and performed parametric studies on how vehicle weight and cornering stiffness affected the yaw stability. Wideberg [33] developed a new mathematical model for a heavy articulated truck, where a Finite Element Analysis (FEA) model for the truck frame was integrated into a classic three-DOF bicycle model. It concluded that the elasticity of the frame has an important impact on the direction response. Elhemly and Fayed [34] developed a tractor-semitrailer model in MATLAB/Simulink, including vehicle subsystem models of the tractor, semitrailer, axle, suspension, tire, and brake. Tabatabaei et al. [35] examined the effects of cornering stiffness variation on directional stability of an AHV through analysis and simulations. A classic linear semi-truck model was applied with varying cornering stiffness on different axles. It was concluded that the directional stability of the articulated vehicle is not significantly affected by the cornering stiffness of the front tractor axle, and

reducing the cornering stiffness of the rear tractor or trailer axles might lead to unstable situations. Morrison [36, 37] developed a 16-DOF mathematical model of a semi-truck, which was implemented in Simulink and validated again test data.

Ervin et al. [38] found that fully-loaded double tankers employed in Michigan had a gain between the lateral accelerations of the tractor and the last trailer that exceeded 2.0 in an obstacle-avoidance maneuver at 50 mph. This phenomenon was later tested and analyzed in [39] and [40]. Fancher [41] further investigated this phenomenon−"Rearward Amplification"−in frequency domain to determine the contributions of full trailers, trucks, and semi-trucks on the rearward amplification between the lateral accelerations of the towing and trailing vehicle units. The parameters studied included forward velocity distances from pintle hitches to CG locations, and cornering coefficients. Ei-Gindy et al. [42] designed a vehicle handling controller for a six-axle truck with a full trailer. Rearward amplification ratio was employed as the control criterion, and the controller was implemented by applying active anti-yaw moment to each unit's CG. Jin et al. [43] and Zhang et al. [44] investigated and improved the conventional rollover index for better rollover prediction.

2.5.2 Heavy Truck Directional Stability Enhancement Studies

Considering the relative low directional stability of heavy trucks and the great severity of heavy-truck-related accidents, a number of studies have been conducted to either predict rollover events and warn the driver before it actually happens, or design a stability control system to directly enhance the truck stability.

Chen and Peng [45] developed an algorithm to assess rollover likelihood for an articulated vehicle. This Time-To-Rollover (TTR) metric was implemented on a simplified yaw-roll plane model and further enhanced by a trained Neural Network (NN) for better accuracy. Chen and Tomizuka [46] used Lagrange's Equations to develop a complex semi-truck model that could capture both yaw and roll dynamics. Two lateral stability control algorithms for a semi-truck were designed, and their performance was evaluated on the complex vehicle model. The first one corrected the tractor steering wheel angle when necessary, while the second one enhanced stability by both controlling the tractor steering

wheel angle and selectively applying brakes to certain wheels. Hyun and Langari [47] developed a predictive model for rollover events using simple roll-plane models of the vehicle sprung and unsprung masses in conjunction with online vehicle parameter identification. This model estimated and predicted Load Transfer Ratio (LTR) on the trailer axle, which was used as the rollover likelihood index. A 12-DOF vehicle model was applied to verify the proposed predictive model and the associated parameter-identification algorithm.

Dahlberg and Stensson [48] came up with a concept of Dynamic Rollover Threshold (DRT) and compared it with Steady-State Rollover Threshold (SSRT). Parameter sensitivity analysis was conducted to calculate the influence of roll stiffness and roll center heights on SSRT and DRT. Jo et al. [49] developed a vehicle stability control system to enhance steerability, lateral stability, and roll stability. This system controlled the vehicle by applying brakes to individual wheels for maintaining the yaw rate to a target value. Hecker et al. [50] presented the Vehicle Dynamic Control (VDC) for commercial vehicles developed by BOSCH. This system monitored vehicle lateral motion and engaged when sensing unstable situations by controlling the engine and applying brakes to specific wheel(s). MacAdam et al. [51] developed an automatic brake control system that could suppress unwanted trailer oscillations, namely rearward amplification. This system was tested on both dry and wet surfaces with double and triple trailers. Rao et al. [18] developed RSC and ESC models in Simulink and coupled them with a 6x4 truck model in TruckSim. The jointed models were validated by performing dynamic maneuvers and straight-ahead braking tests, and the results were compared against field testing data.

Lin et al. [52] investigated three proposed roll-control strategies on a validated non-linear articulated vehicle model. The results showed that (1) a roll angle feedback controller could eliminate the steady-state roll angle, but not the steady-state load transfer; (2) a load transfer feedback controller could eliminate the steady-state load transfer by balancing the vehicle back; and (3) a lateral acceleration controller could roll the vehicle back towards the turn center but could not eliminate the steady state load transfer. Sampson and Cebon [53] investigated modeling requirements and design issues for developing active roll control systems for heavy commercial vehicles. A mathematical model for an articulated

commercial vehicle that could simulate both yaw and roll dynamics was applied, and the torsional flexibility of the vehicle frame was also considered. Sampson et al. [54] developed an active roll control system for a semi-truck. The performance of the control system was evaluated by simulations based on a mathematical model that could capture both yaw and roll dynamics, as well as the flexibility of vehicle frames. The control system was planned to be implemented on trucks by five active anti-roll bars to control roll motion at each axle. Sampson and Cebon [55] performed a controllability analysis to study the fundamental limitations in achievable roll stability of heavy vehicles with active roll control systems, based on a vehicle model similar to that of [54]. Simulations were then conducted to evaluate the performance of a semi-truck with a full-state feedback active roll control system. It was found that the roll stability of the vehicle could be increased by 30-40 percent for steady-state and transient maneuvers. This control system was later validated by Miege and Cebon [56].

2.5.3 Heavy Truck Directional Dynamics Testing Studies

Even though analytical models for vehicle dynamics have been improved over the years, they are still not capable of capturing all dynamic behavior due to the inherent complicated nonlinear characteristics of a vehicle system. Therefore, full-scale vehicle testing is necessary for either direct evaluation of vehicle dynamic behavior or analytical model validation.

NHTSA [57] conducted a thorough testing project on tractor semi-trailer objective roll stability performance. In Phase 1I of this project, stability control systems were installed on two Class 8 tractors and a 53-ft van box trailer, and performance maneuvers were conducted with and without the stability control. In Phase II, three tractors and six trailers were further tested with Ramp Steer Maneuvers (RSM) with different load conditions, as well as with and without stability control enabled. NHTSA [58] also conducted research on tractor semi-trailer yaw stability by testing. Six test maneuvers were evaluated, including Sine with Dwell (SWD), Half-Sine with Dwell (HSWD), Ramp with Dwell (RWD), RSM, 150-ft. Brake-in-Curve (BIC), and Slowly Increasing Steer (SIS). Three tractors with four stability conditions and four trailers were tested with different road conditions. This project mainly focused on developing performance tests that challenged

the capabilities of a tractor-based stability control system designed to mitigate loss-of-control situations related to tractor semitrailer yaw stability.

Pape et al. [74] investigated the safety and stability of a triple trailer combination behind a commercial tractor. Full-scale field tests were conducted first to generate data with simple maneuvers, and then two vehicle models were developed using TruckSim and Adams based on the test results. The simulation results indicated that the models could duplicate the experimentally-measured rearward amplification behavior of the truck. Wang and He [59] developed a new test maneuver for determining rearward amplification of multi-trailer articulated vehicles with active trailer steering. This new maneuver was evaluated in TruckSim and could be potentially applied in future field tests.

2.5.4 Heavy Vehicle Directional Dynamics Review Articles

Ervin et al. [12] provided an overview of the dynamic performance properties of long truck combinations. The performance of each examined truck combination was compared with that of a conventional five-axle tractor-semitrailer, and a conventional five-axle double trailer. The discussion included different designs of dollies that could be potentially applied to increase truck stability. Fancher et al. [60] reviewed the mechanical properties of the components used in heavy trucks, including geometric layout, mass distribution, tires, suspensions, steering systems, brakes, frames, and hitches. The influences of these component properties on maneuvering performance were discussed. Winkler and Ervin [16] provided a comprehensive review on heavy commercial vehicle rollover mechanics. The fundamentals of static roll stability were described in detail and enhanced with a discussion of dynamic considerations of the rollover process. Fancher and Winkler [4] reviewed the dynamics of heavy road vehicle systems that emphasized directional performance. The topics covered in this article included: the usage of articulated vehicles; units, hitches, and vehicle combinations; multiple axle suspensions and steering systems; important performance issues; models and simulation tools; and methods to improve directional performance.

2.6 Modern Roundabout

A modern roundabout is a form of circular intersection in which traffic travels counterclockwise (in the United States and other right-hand traffic countries) around a central island and in which entering traffic must yield to circulating traffic, as shown in Figure 2-16 [61]. Architect John McLaren designed the first American circular traffic intersection in San Jose, California in 1907; however, such traffic circles considerably differ from modern roundabouts. The modern roundabouts were developed by the Transport Research Laboratory in the United Kingdom in the 1960s, were introduced to the United States in the 1990s, and have become more and more popular since then. Two key characteristics of modern roundabouts (hereafter referred to as roundabouts) include (1) a requirement for entering traffic to yield to circulating traffic, and (2) geometric constraints that slow entering vehicles [62].

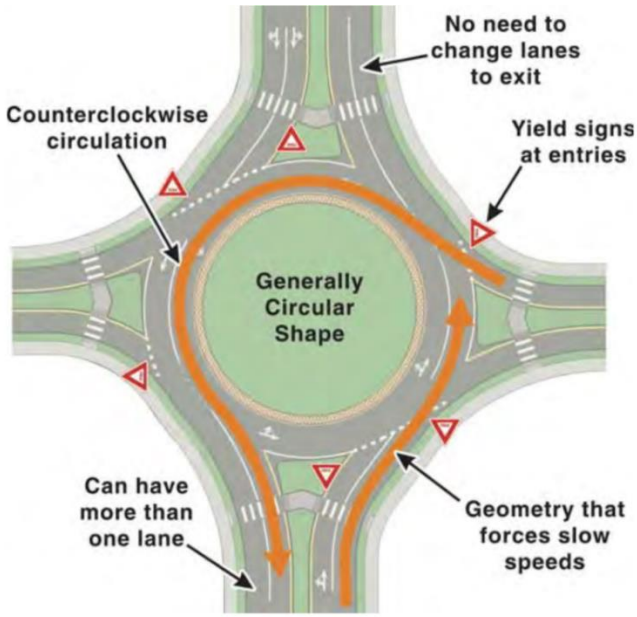

Figure 2-16. Key roundabout characteristics [61].

2.6.1 Basic Geometric Element of a Roundabout

Figure 2-17 illustrates the basic geometric elements of a typical single-lane roundabout. A roundabout commonly includes approaching roadway (entering roadway), entry curve, circulatory roadway, central island, and exit roadway. In addition, some roundabouts also have a truck apron to provide extra space to accommodate large trucks. As shown in Figure 2-17, when a vehicle approaches the roundabout from the bottom of the figure, first it will

be forced to slow down as it negotiates the entry curve, then it starts circulating the central island on circulatory roadways counterclockwise, and finally it exits the roundabout through an exit curve.

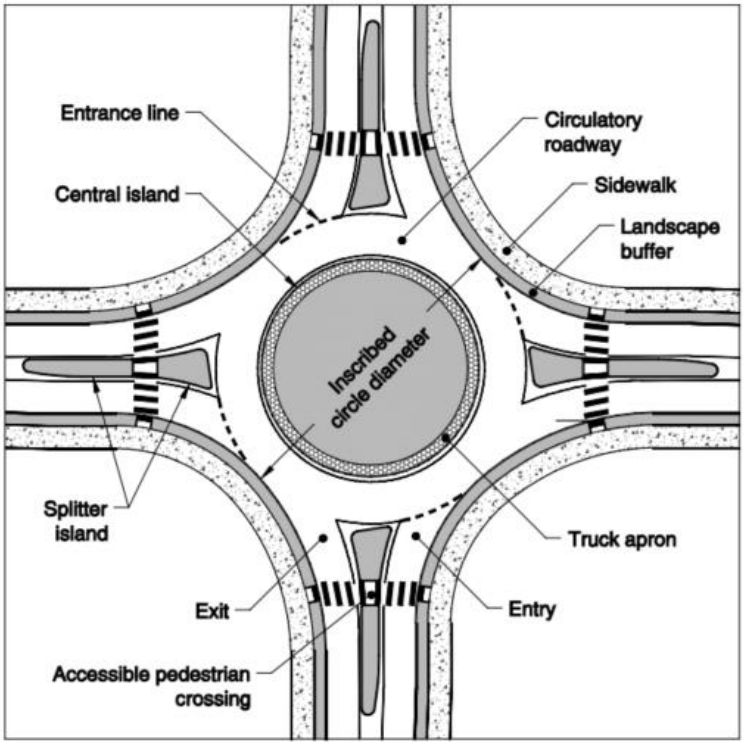

Figure 2-17. Basic geometric element of a roundabout [61].

2.6.2 Advantages and Disadvantages of Roundabouts for Traffic Control and Safety

Roundabouts can bring many benefits to both traffic flow control and safety. The advantages of roundabouts for traffic flow include (1) allowing vehicles to perform a U-turn within the traffic flow, (2) reducing traffic delay since vehicles do not need to make a complete stop before traveling through roundabouts if there is no conflict presented, especially at off-peak hours, and (3) allowing traffic to still move if there are queues on one or more approaching directions, which is more tolerable for drivers compared to signalized intersections where drivers have to stop in queue. The benefits of roundabouts for traffic safety include (1) the special entry design that forces approaching vehicles to reduce speed before entering roundabouts, thereby decreasing the likelihood of severe vehicle accidents, and (2) the unidirectional design where all vehicles travel in one direction, reducing conflict points of different vehicle traveling paths.

Even though the advantages introduced above make roundabouts more and more popular, they still have disadvantages. The major disadvantage of roundabouts for traffic flow control is that they are unable to balance the traffic at a location that connects high-volume major roads and low-volume local roads. To be more specific, roundabouts tend to treat all approaching traffic equally, and entering traffic is required to yield to circulating traffic. Therefore, roundabouts cannot assign priority to high-volume roads even though they have longer queues than low-volume roads. For the disadvantage regarding traffic safety, the major concern is that the vehicle maneuver in the roundabout can result in other traffic issues that are not commonly seen at regular intersections, especially for commercial vehicles with long wheelbases and heavy loads. For example, if a truck intends to perform a through-movement or a left turn at a roundabout, it has to negotiate successive reverse curves and follow a path that is similar to a double lane-change maneuver. Such a maneuver can result in large lateral accelerations that may cause truck rollovers.

2.6.3 Heavy Truck Issues at Roundabouts

As introduced in the previous section, the successive reverse curves that a truck needs to negotiate through a roundabout could lead to excessive lateral accelerations. In addition, the circulatory roadway in a roundabout usually has a cross-slope for drainage that may additionally increase the lateral load transfer to heavy trucks. Unfortunately, heavy articulated trucks, such as those commonly operated on U.S. roads, have a far lower roll stability than passenger cars, and thus they are more sensitive to lateral input induced by the roadway geometry.

A report prepared by the Federal Highway Administration (FHWA) [63] shows that of the 37 identified truck crashes at roundabouts in the United States, rollover crashes (over 30 crashes) were the most common crash type, followed by trucks getting stuck (3 crashes), fixed-object (1 crash), and sideswipe (1 crash). Therefore, rollover can be intensified as the major issue that a truck would experience when traveling through roundabouts.

There are relatively few studies that provide in-depth evaluations of the effect of the roadway geometry on heavy truck lateral dynamics in roundabouts. Waddell et al. [2] investigated emerging issues regarding the accommodation of trucks in North American

roundabouts from a civil engineering perspective. Cerezo and Gothie [64] studied the influence of roundabout geometric parameters on heavy goods vehicle accidents in roundabouts using simulation, including the cross-slope and ground friction coefficient.

Chapter 3 – Heavy Truck Low-speed Stability Evaluation: Model Setup and Case Study Plan

This chapter introduces the TruckSim simulation studies for the vehicles considered for the study on city roadways that could cause an increased risk of rollovers. Specifically, two typical roundabouts are considered: a single-lane and double-lane roundabout. The truck models include a straight truck, a WB-67 semi-truck, an A-train with two 28-ft trailers, and another A-train with two 40-ft trailers. These truck configurations represent those widely operated on U.S. roads. The roundabout models were also created in TruckSim. The geometric parameters of the roundabout models are selected to represent roundabouts common to U.S. cities. Eighty-three individual cases are studied in total, representing various roundabout geometries, travel paths, truck loading conditions, and types of vehicles.

3.1 Overview

As introduced in Chapter 2, the geometric parameters of the roadway in places where tight turns occur greatly increase the likelihood of rollover for heavy commercial vehicles in city-driving conditions. Modern roundabouts, which are commonly used in urban settings with increasing frequency, are unfortunately one of those places that bring challenges to heavy truck roll stability. A vehicle needs to negotiate successive tight reverse curves to travel through a roundabout, requiring maneuvers that can result in large lateral accelerations which may lead to vehicle rollovers. Moreover, some cross-sectional geometric designs of roundabouts, such as the roadway's cross-slope and truck apron, may additionally increase the likelihood of rollover. Therefore, a simulation-based study was conducted to closely examine the effect of geometric parameters of roundabouts, as well as truck load conditions and configurations on roll stability in roundabouts.

3.2 TruckSim Introduction

A commercially-available software, TruckSim, was applied to develop truck and roundabout models. TruckSim is a professionally-designed software for simulating and analyzing the dynamic behavior of medium to heavy trucks, buses, and articulated vehicles. The vehicle math models in TruckSim are built on decades of research in characterizing

vehicles and reproducing their behavior, and are well-recognized for providing reasonably accurate simulation results. In addition, TruckSim also includes a road design package that is able to create complex road models, such as roundabouts. Hence, TruckSim was employed in this study.

3.3 Truck Models

Four truck models were developed to represent those commonly operated on the roads.

3.3.1 Truck Configurations

The first truck model represents a single-unit truck as shown in Figure 3-1(a), which has two axles and a van box cargo area. As indicated by the name, the cargo area of a single-unit truck is fixed to the truck body.

The second truck model represents a WB-67 semi-truck, which is the most popular truck configuration in the United States, as shown in Figure 3-1(b). A WB-67 consists of one tri-axle 6×4 tractor, and a 53-ft semitrailer. The term "WB-67" indicates that the overall wheelbase is 67 feet, which is the distance from the center of the tractor steering axle to the center of the trailer's tandem axles. A fifth-wheel coupling is used to couple the tractor and trailer, which allows no relative roll motion, limited pitch motion (~±10°), and free yaw (articulation) motion. Therefore, unlike the single-unit truck, the WB-67 semi-truck performs as two jointed bodies in dynamics. In other words, when a semi-truck travels, the tractor and trailer may have different dynamic responses to the steering, speed, or road input.

Figure 3-1(c) illustrates the truck model for an A-train with two 28-ft trailers, which is also called "STAA Double" or "double pups." The tractor in this configuration is the same as that in the WB-67 semi-truck. The tractor is connected to the front semitrailer via a fifth-wheel coupling, whereas the front and rear semitrailer is coupled via a converter dolly. The converter dolly used in an A-train is called an "A dolly." The A dolly uses a pintle hitch coupling to connect with the front trailer, and a fifth-wheel coupling to couple the rear trailer. Therefore, the 28-ft double trailers perform as three jointed bodies in dynamics.

The last truck modeled is a tractor with two 40-ft trailers, called "Turnpike doubles," as shown in Figure 3-1(d). This truck configuration is similar to the 28-ft double trailers, except that both trailers are longer and have tandem axles. The converter dolly in this configuration also has tandem axles, and is coupled with the front and rear semitrailers with a pintle hitch and a fifth-wheel coupling, respectively. The tractor in this configuration is the same as that used in the WB-67 semi-truck and 28-ft double trailers.

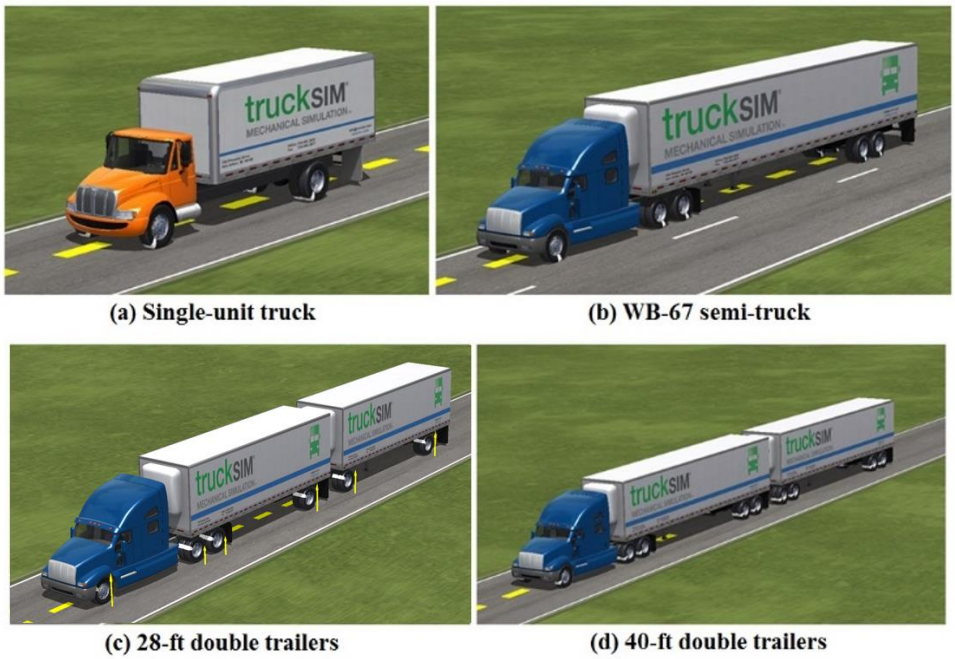

Figure 3-1. Truck models developed in TruckSim: (a) Single-unit truck; (b) WB-67 semi-truck; (3) 28-ft double trailers; and (4) 40-ft double trailers.

3.3.2 Truck Dimensional and Weight Parameters

The parameters for the four truck models introduced in the previous section are included in Table 3-1 to Table 3-7. The dimensions were selected mainly from the "typical design vehicles" from "Policy on Geometric Design of Highways and Streets (2004)", published by the American Association of State Highway and Transportation Officials (AASHTO) [65]. The weight parameters for each configuration were determined based on the trailer arrangement. The gross weight for the single-unit truck was selected based on the truck commonly operated on the roadways. The WB-67 semi-truck was loaded to meet the maximum gross weight limit enforced by the interstate system in the United States, which is 80,000 lb. For the 28-ft double trailers, the weight was determined based on the logistics company's information guide [66]. In practice, 28-ft double trailers are commonly

operated by freight carriers to transport low-density cargo, which means the load on such trucks is limited by volume rather than weight. Therefore, the gross weight for this configuration is lower than the 80,000-lb weight limit. The 40-ft double trailers are often operated with an overload permit, and therefore the weight for this configuration was set to be 140,000 lb, representing average overloaded truck weight limits in Minnesota and its neighboring States or Provinces [67], where such a truck configuration is widely used for cargo transport.

The loads fixed to the trailers were assumed to have a uniform density and rectangular shape. For simulating full-load conditions, the load was assumed to fill the entire trailer. In the half-full cases, the simulated load was assumed to fill the bottom half of the trailer. Shifting loads were not considered here.

Table 3-1. Dimensions of the single-unit truck.

Property	Value	
Wheelbase	240.0 in.	
Overall length	360.0 in.	
Overall height	150.0 in.	
Overall width	96.0 in.	
Track width	Front axle: 80.0 in.	Rear axle: 73.0 in.

Table 3-2. Dimensions of the WB-67 semi-truck

Property	Tractor		Trailer
Wheelbase	224.0 in.		522.0 in.
Length	294.5 in.		636.0 in.
Height	113.0 in.		150.4 in.
Overall width	96.0 in.		102.0 in.
Track width	Steering axle: 80.0 in.	Drive axles: 72.0 in.	77.5 in.

Table 3-3. Dimensions of the 28-ft double trailers.

Property	Tractor		Dolly	Trailers*
Wheelbase	224.0 in.		76.0 in.	276.0 in.
Length	294.5 in.		N/A	336.0 in.
Height	113.0 in.		50 in.	149.0 in.
Overall width	96.0 in.		N/A	98.0 in.
Track width	Steering axle: 80.0 in.	Drive axles: 72.0 in.	76.0 in.	73.0 in.

* For double-trailer configurations, the front and rear trailers are assumed to be the same.

Table 3-4. Dimensions of the 40-ft double trailers.

Property	Tractor		Dolly	Trailers
Wheelbase	224.0 in.		84.4 in.	430.0 in.
Length	294.5 in.		N/A	480.0 in.
Height	113.0 in.		50 in.	150.0 in.
Overall width	96.0 in.		N/A	100.0 in.
Track width	Steering axle: 80.0 in.	Drive axles: 72.0 in.	76.0 in.	77.5 in.

Table 3-5. Weight properties for four truck configurations.

Truck configuration		Individual gross weight	Total gross weight
Single-unit truck		28,000 lb	28,000 lb
Wb-67 semi-truck	Tractor	18,600 lb	80,000 lb
	Trailer	61,400 lb	
28-ft double trailers	Tractor	18,600 lb	58,865 lb
	Front trailer	22,000 lb	
	Dolly	2,513 lb	
	Rear trailer	22,000 lb	
40-ft double trailers	Tractor	18,600 lb	140,000 lb
	Front trailer	57,580 lb	
	Dolly	6,240 lb	
	Rear trailer	57,580 lb	

Table 3-6. Vehicle CG locations of four truck configurations.

Truck configuration		CG location		
		X*	Y	Z
Single-unit truck		-131.2 in.	0	66.0 in.
WB-67 semi-truck	Tractor	-100.3 in.	0	50.0 in.
	Trailer	-293.7 in.	0	96.9 in.
28-ft double trailers	Tractor	-100.3 in.	0	50.0 in.
	Front trailer	-141.6 in.	0	95.1 in.
	Rear trailer	-141.6 in.	0	95.1 in.
40-ft double trailers	Tractor	-100.3 in.	0	50.0 in.
	Front trailer	-226.4 in.	0	94.3 in.
	Rear trailer	-226.4 in.	0	94.3 in.

* The tractor coordinate system is located at the center of the steering axle, and the trailer coordinate system is located at the ground underneath the kingpin. Both X-axes point forward, the Y-axes point to the driver's side, and the Z-axes point upward.

Table 3-7. Weight properties of the WB-67 semi-truck model with different load conditions.

Component (s)	Weight
Tractor	18,600 lb
Trailer (Empty)	14,400 lb
Tractor + Trailer (Empty)	33,000 lb
Tractor + Trailer (Half full)	56,500 lb
Tractor + Trailer (Full)	80,000 lb

3.3.3 Baseline Truck Model

Since the WB-67 semi-truck is the most popular configuration operated in the United States [13], it is selected as the baseline truck model in the simulation study. The baseline truck model has a full load that makes the total truck weight reach 80,000 lb.

3.3.4 Truck Suspension and Tire Parameters

All four truck models were equipped with linear leaf springs and linear dampers. The parameters of springs and dampers are included in Table 3-8.

Table 3-8. Suspension parameters for four truck configurations.

Truck configuration			Leaf spring				Damping (lbf-s/in.)
			Spring rate (lbf/in.)	Friction (lbf)	Beta (compression) (in.)	Beta (extension) (in.)	
Single-unit truck		Steering axle	1,427.5	450.0	0.079	0.079	85.6
		Rear axle	3,997.1	1,124.0	0.079	0.079	171.3
WB-67 semi-truck	Tractor	Steering axle	1,427.5	450.0	0.079	0.079	85.6
		Drive axles	5,139.1	1,124.0	0.079	0.079	171.3
	Trailer	Tandem axles	5,139.1	1,124.0	0.079	0.079	171.3
28-ft double trailers	Tractor	Steering axle	1,427.5	450.0	0.079	0.079	85.6
		Drive axles	5,139.1	1,124.0	0.079	0.079	171.3
	Front trailer	Tandem axles	5,139.1	1,124.0	0.079	0.079	285.5
	Dolly	Single axle	5,139.1	1,124.0	0.079	0.079	285.5

	Rear trailer	Tandem axles	5,139.1	1,124.0	0.079	0.079	285.5
40-ft double trailers	Tractor	Steering axle	1,427.5	450.0	0.079	0.079	85.6
		Drive axles	5,139.1	1,124.0	0.079	0.079	171.3
	Front trailer	Tandem axles	5,139.1	1,124.0	0.079	0.079	285.5
	Dolly	Tandem axles	5,139.1	1,124.0	0.079	0.079	285.5
	Rear trailer	Tandem axles	5,139.1	1,124.0	0.079	0.079	285.5

A default tire model provided by TruckSim was applied to all vehicle models, which represents the property of a typical 305/74R22.5 truck tire. The tire spring rate was 5,595.9 lbf/in., and the longitudinal force and lateral force were calculated from look-up tables, which considered the tire slip ratio, slip angle, and vertical load. The look-up tables for longitudinal and lateral tire force are illustrated in Figure 3-2 and Figure 3-3, respectively.

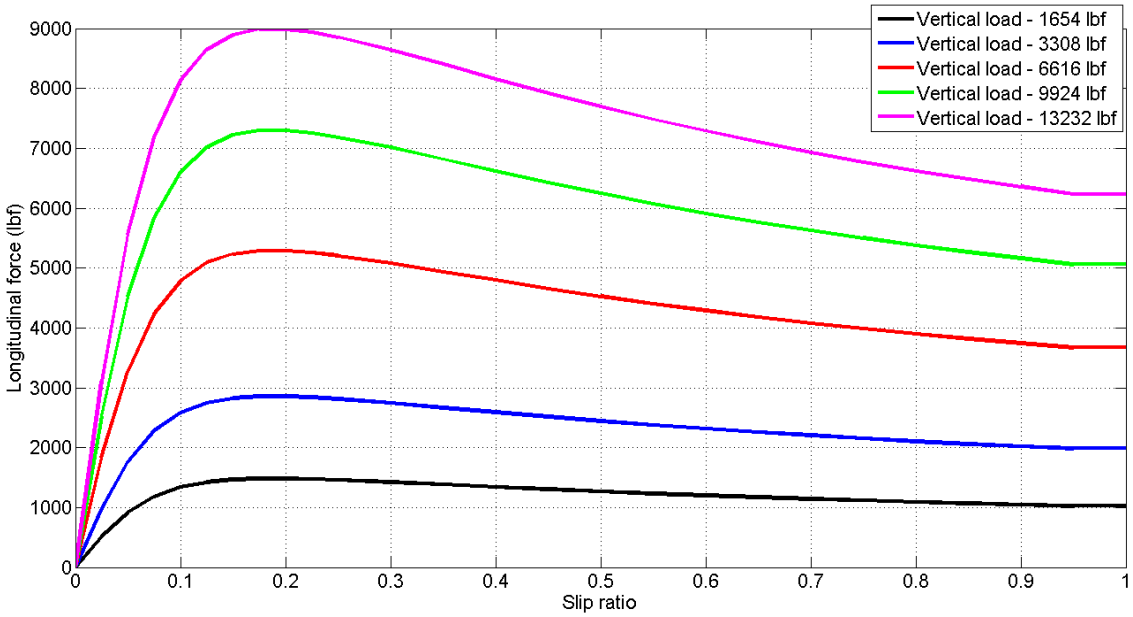

Figure 3-2. Longitudinal tire force with respect to different vertical loads.

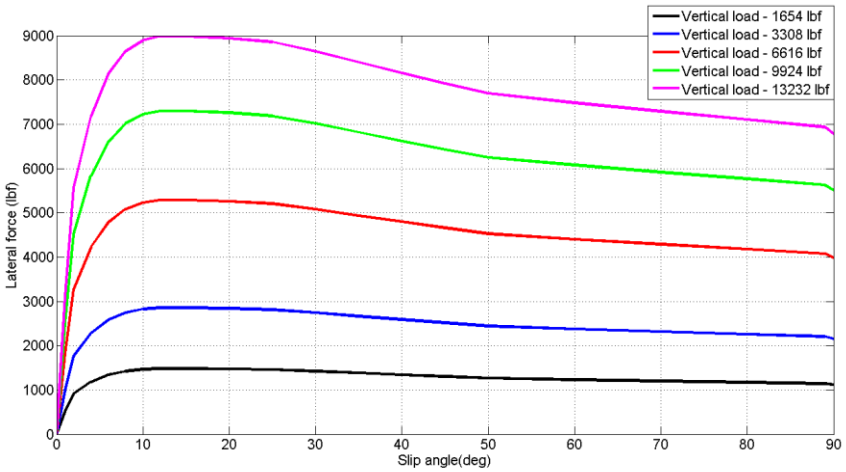

Figure 3-3. Lateral tire force with respect to different vertical loads.

3.4 Roundabout Models

As introduced in Chapter 2, a roundabout is a form of circular intersection in which traffic travels counterclockwise (in the United States and other right-hand traffic countries) around a central island and in which entering traffic must yield to circulating traffic [61]. Figure 3-4 illustrates a two-lane roundabout in Brattleboro, Vermont. A roundabout consists of several components, including approaching roadway, entry curve, circulatory roadway, central island, truck apron (optional), exit curve, and exit roadway. Figure 3-5 provides a street view of the same roundabout shown in Figure 3-4. Two types of roundabout models are developed in TruckSim: the single-lane and two-lane roundabouts. In order to create an accurate roundabout model, it is a good practice to first review the functionality and features of each roundabout segment.

Figure 3-4. A two-lane roundabout in Brattleboro, Vermont (Google Earth image, accessed August 2016).

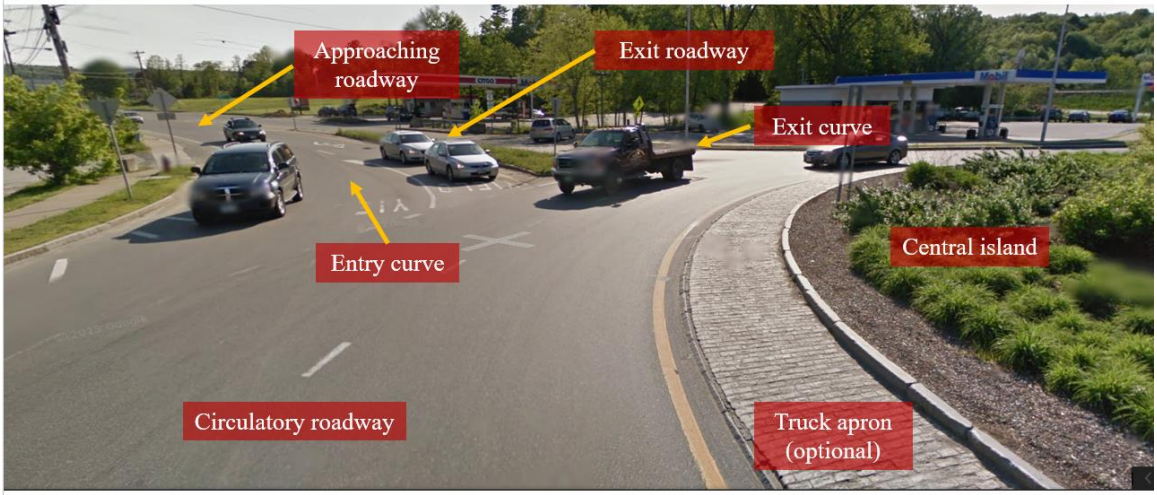

Figure 3-5. Street view of the two-lane roundabout in Brattleboro, Vermont (Google Earth image, accessed August 2016).

3.4.1 Roundabout Entry

Roundabout entry plays an important role in roundabout design, both for traffic safety and operation. An entry curve is designed to connect the approaching roadway and circulatory roadway. On the one hand, the entry curve can force the vehicle to slow down before entering the roundabout, thereby reducing the likelihood of several traffic accidents. On the other hand, it also helps guide the entering traffic to merge into the circulating traffic. The radius of an entry curve is normally determined according to the type of roundabout (single-lane or multilane), as well as the roundabout diameter. Approaching roadways are also considered as part of the roundabout entry here, which commonly has a 2% cross-slope to the passenger's side for drainage.

3.4.2 Roundabout Circle

The roundabout circle is the main segment of a roundabout that consists of a central island, circulatory roadway, and truck apron (for roundabouts that have a truck apron) as illustrated in Figure 2-16 and Figure 2-17. The central island is a non-traversable elevated area in the center of a roundabout. Vehicles circulate the central island along circulatory roadways, and a circulatory roadway may have one or multiple lanes. In addition, the cross-section of a circulatory roadway may possess a constant cross-slope or a road crown, as shown in Figure 3-6(a) and (b), respectively. The crowned roadway is a special design where the inner section has an inward cross-slope, and the outer section has an outward

cross-slope. As for a truck apron, the roundabout provides additional paved area to allow the off-tracking of large semi-trailer vehicles on the central island without compromising the deflection for smaller vehicles [61]. Figure 3-6 illustrates the typical section with a truck apron.

Designing a roundabout, like other intersection designs, is complicated work where many factors need to be considered, including traffic operation, safety, and context. The following key design elements for roundabouts were selected to develop the roundabout models for evaluating heavy truck dynamics in roundabouts:

- Number of lanes: Single lane or two lanes.
- Inscribed circle diameter (ICD): This is the diameter across the circle from outer edge to outer edge of the circulatory roadway pavement.
- Circulatory roadway width: This is the radial distance between the inner edge and the outer edge of the circulatory roadway.
- Circulatory roadway cross-section: The two circulatory cross-section scenarios considered consist of (1) a uniform 2% slope away from the inner edge to the outer edge (outward), and (2) a road crown where the inner two-thirds of the circulatory roadway is sloped to the inner edge (inward) at 2%, and the outer third is sloped to the outer edge at 2% (outward).
- Truck apron: The truck apron is designed to be 3 in. higher than the circulatory roadway, 13 ft wide, and to have a 2% cross-slope to the outside of the roundabout.
- Central island diameter: The central island diameter is calculated as the difference between the roundabout ICD and twice the circulatory roadway width.
- Roundabout tilt: Some intersections' topography requires that the roundabout be tilted on a constant plane. For a tilted roundabout, the entire roundabout is tilted at a constant slope. Three basic tilted slopes are considered, as shown in Figure 3-7: no tilt, positive tilt (roundabout is tilted outward), and negative tilt (roundabout is tilted inward). Four tilted slopes are considered: 4%, 2%, -4%, and -2%.

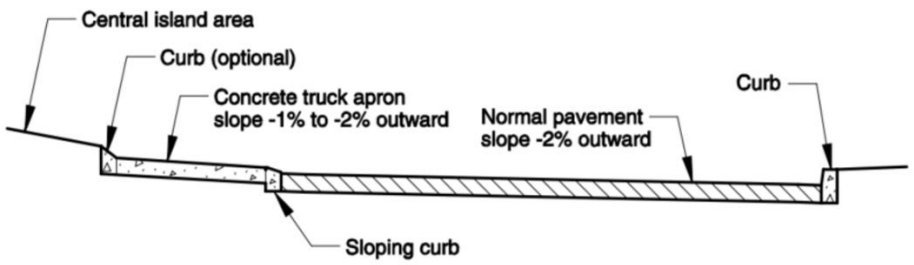

(a) Typical roundabout cross-section with a truck apron and a sloping circulatory roadway

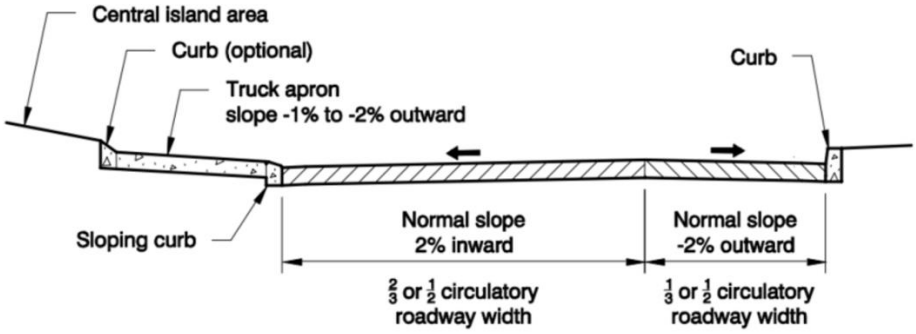

(b) Typical roundabout cross-section with a truck apron and a crowned circulatory roadway

Figure 3-6. Typical roundabout cross-section designs [61]: (a) typical roundabout cross-section with a truck apron and a sloping circulatory roadway; (b) typical roundabout cross-section with a truck apron and a crowned circulatory roadway.

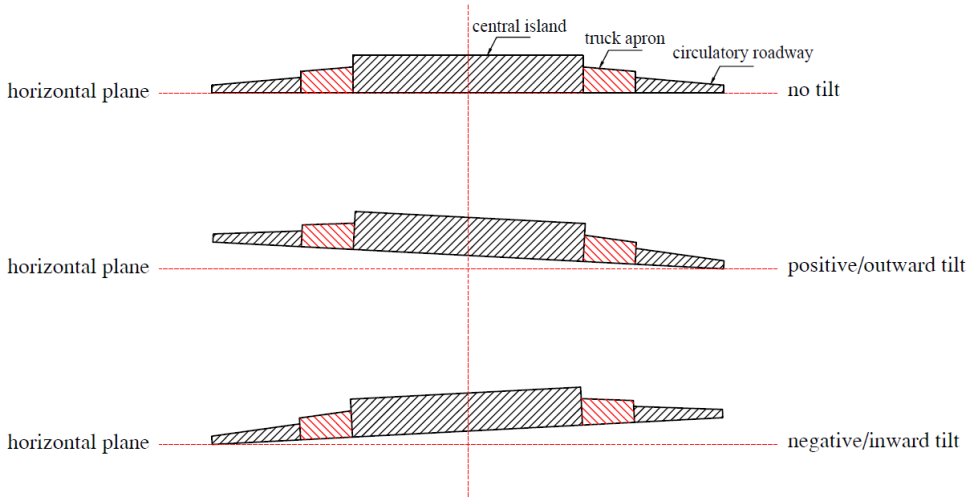

Figure 3-7. Roundabout tilt from the perspective of a driver on the approaching roadway [63].

3.4.3 Roundabout Exit

The layout of a roundabout exit section is similar to that for the entry. An exit curve connects the circulatory roadway and exit roadway. A roundabout exit curve is commonly greater than the entry curve in order to reduce the traffic delay and the likelihood of vehicle

crashes. The radius of an exit curve is determined based on the roundabout type (single-lane or multilane), as well as the roundabout size. The exit roadway, which is also considered as a part of the exit segment here, usually has a 2% cross-slope to the passenger's side for drainage.

3.4.4 Roundabout Geometric Parameters

The literature review shows that there is no strict or universal standard for roundabout design. Different agencies or designers tend to have various preferences when determining the geometric parameters for a roundabout. The roundabout parameters for the models here were selected based on consultation with a company that provides transportation engineering, planning, and research services. The geometric parameters of these models are listed in Table 3-9. It is noted that all roundabout models have a truck apron to accommodate the off-tracking of large articulated vehicles.

Table 3-9. Roundabout geometric parameters.

#	ICD (ft)	Type	Entry radii (ft)	Exit radii (ft)	Roadway width (ft)	Truck apron	Road crown	Tilt
1	140	Single	75	150	20	Applied	N/A	N/A
2	140	Single	75	150	20	Applied	N/A	Applied
3	180	Multi	100	400	30	Applied	N/A	N/A
4	180	Multi	100	400	30	Applied	Applied	N/A
5	180	Multi	100	400	30	Applied	N/A	Applied

3.4.5 Baseline Roundabouts

The baseline single-lane roundabout was selected (Table 3-9, #1) to represent the typical single-lane roundabout constructed in the United States. The horizontal geometry of the baseline single-lane roundabout is shown in Figure 3-8. The hatched area that encircles the central island represents the truck apron. Vehicles approach from the left-hand side to perform a right turn, through-movement, or left turn.

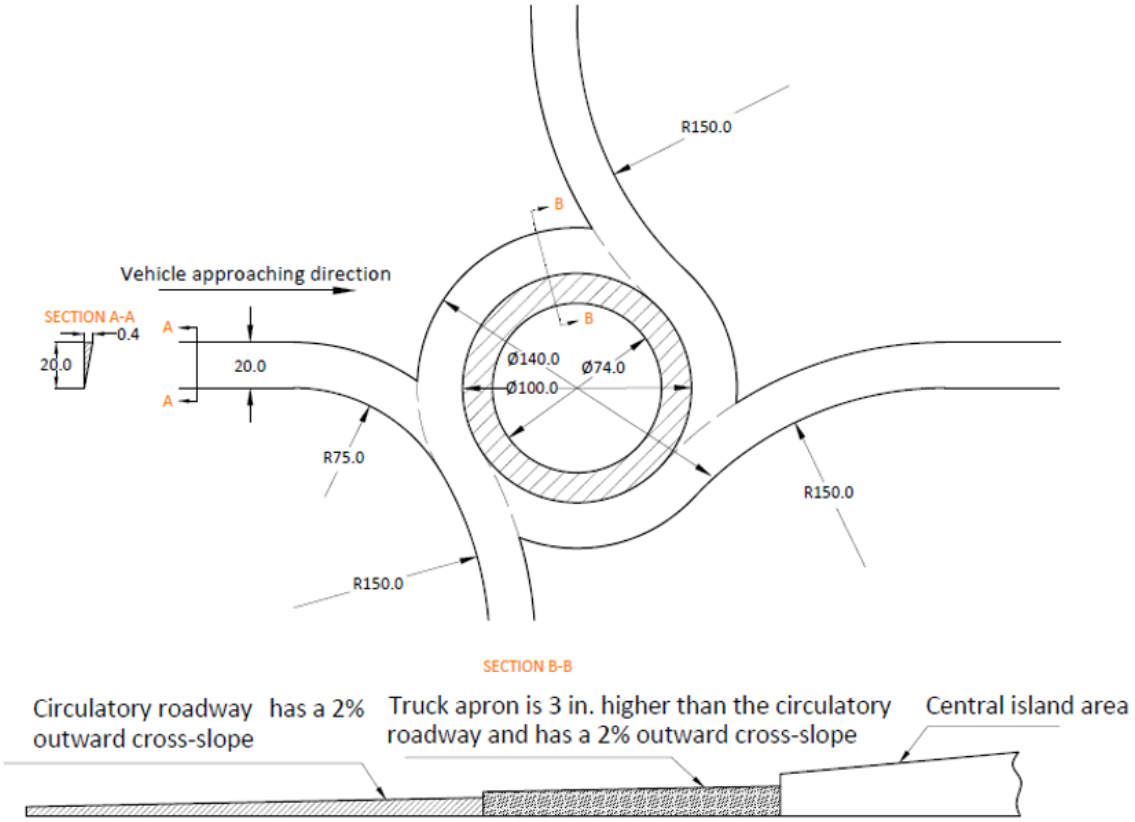

Figure 3-8. Horizontal geometry of 140-ft baseline single-lane roundabout model (Unit: ft).

The cross-sectional geometry of the baseline roundabout is shown in Figure 3-9. The numbers in the rectangles illustrate the vertical height. Detail ① shows the entry geometry, and detail ② shows the exit geometry (the exit geometry is the same for all three movements). The approaching roadway has a 2% outward cross-slope, and thus for a 20−ft−wide roadway, its left edge is 0.4 ft higher than the right edge. There are two transition areas that transfer the vertical roadway geometry from that of the approaching roadway to that of the circulatory roadway. Transition area 1 is where the left edge of the approaching roadway is lowered to match the outer edge of the circulatory roadway. This area is 20 ft long. Transition area 2 is where the lowered left edge of the roadway is raised to meet the circulatory roadway's inner edge. This area is 31.5 ft long. There are also two similar transition areas transferring the vertical roadway geometry from that of the circulatory roadway to that of the exit roadway, as shown in Figure 3-9. In all transition areas, the elevation increases or decreases linearly with respect to the length of the arcs or lines.

Section A-A in Figure 3-8 shows the cross-sectional geometry for the approaching roadway. Section B-B in Figure 3-9 shows the cross-sectional geometry of the circulatory roadway.

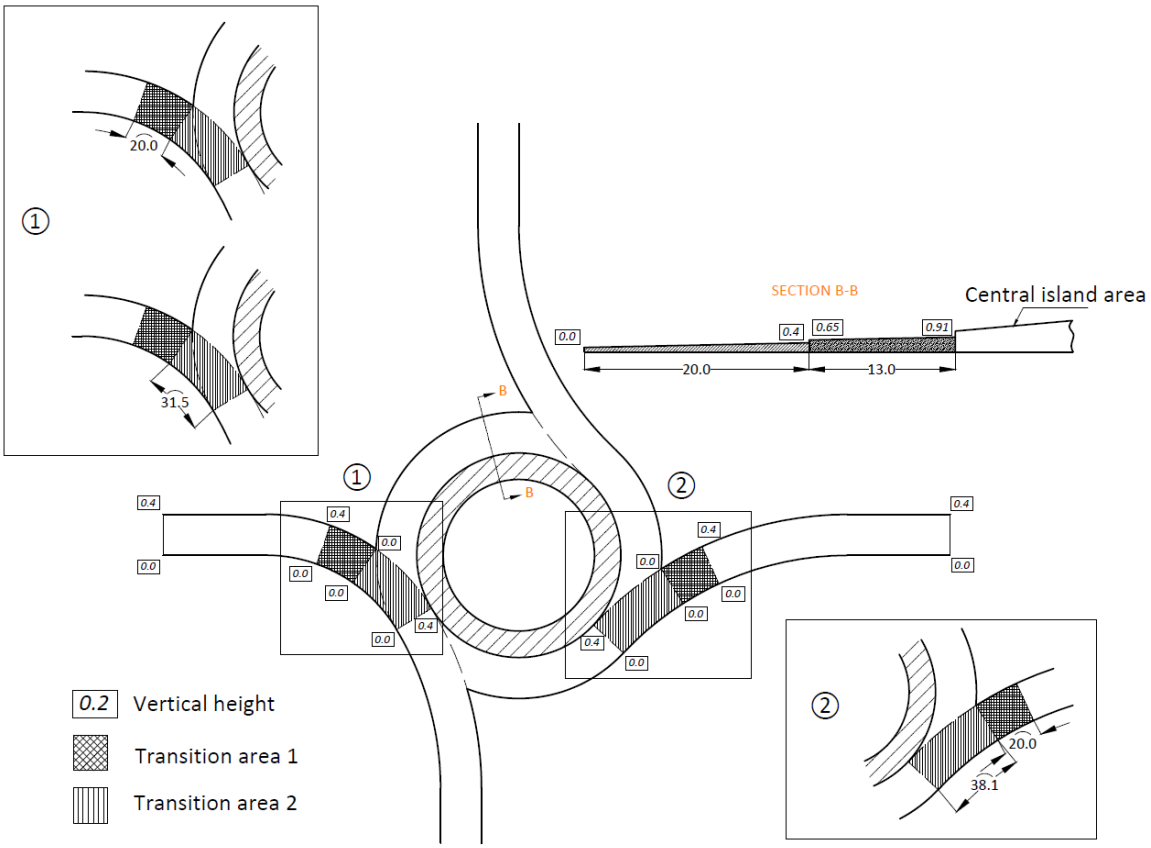

Figure 3-9. Cross-sectional geometry of 140-ft baseline single-lane roundabout model (Unit: ft).

The baseline two-lane roundabout was designed to have two lanes and a 180-ft ICD (Table 3-9, #3). The model of the two-lane baseline roundabout is similar to that of the single-lane baseline roundabout, except that the geometric parameters, such as entry radii, exit radii, and roadway width, are different.

Figure 3-10 illustrates the baseline two-lane roundabout's horizontal geometry and the cross-sectional geometry of the entry and circulatory roadways. Figure 3-11 illustrates the baseline two-lane roundabout's horizontal geometry, transition areas, and the cross-sectional geometry of the circulatory roadway. In Figure 3-11, detail ① shows the entry geometry, and detail ② shows the exit geometry. There are two transition areas where the vertical geometries of the approaching and exit roadways are matched to that of the circulatory roadway in a manner similar to that applied for the single-lane roundabout. For

the two-lane roundabout, transition areas 1 and 2 are 30− and 40−ft long, respectively. Again, the elevation increases or decreases linearly with respect to the length of the arcs or lines within transition areas.

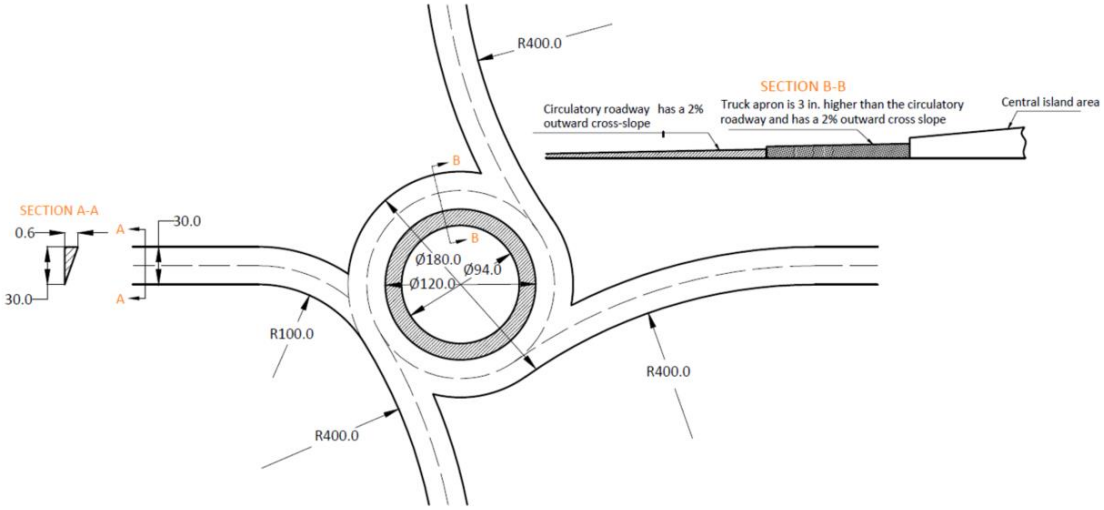

Figure 3-10. Horizontal geometry of 180-ft baseline two-lane roundabout model (Unit: ft).

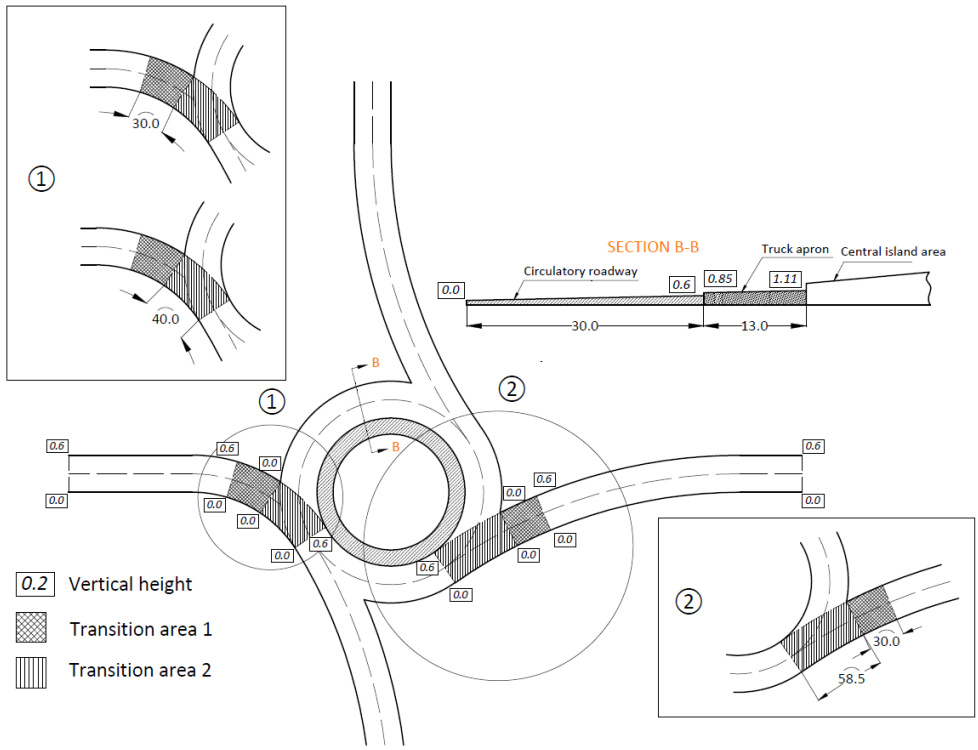

Figure 3-11. Cross-sectional geometry of 180-ft baseline two-lane roundabout model (Unit: ft).

3.5 Simulation Case Study Plan

This section introduces the simulation case study plan to study the heavy truck roll stability in roundabouts; 83 individual cases were designed in total. The truck travel path and the travel speed were also introduced.

3.5.1 Case Study Plan

The simulation case studies are designed to evaluate five features: circulatory roadway cross-section, roundabout tilt, truck configuration, truck apron, and load condition. For each simulation case, only one factor (truck characteristic or roundabout parameter, depending on the case) was modified from the baseline, while the other parameters were kept constant.

In total, 83 separate cases were created and simulated. The details for the cases are summarized in Table 3-10. The terms and abbreviations used in Table 3-10 are:

- ICD: inscribed circle diameter.
- Lanes: number of lanes (one or two).
- Truck apron: the first number indicates the truck apron curb height, and the second number indicates the slope. For example, "3 in. & 2%" means the truck apron curb is 3 in. higher than the circulatory roadway, and has a constant 2% outward cross-slope.
- Cross-slope: circulatory roadway constant cross-slope.
- Tilt: whether roundabout road is tilted.
- Truck config.: truck configurations–WB-67 semi-truck, single-unit truck, 28-ft double trailer, or 40-ft double trailers.
- Truck load: truck load conditions–empty, half full, or full.
- Maneuver: the movements that the truck performs to travel through the roundabout. In two-lane cases, 'through (left)' means the truck approaches in the left lane and then occupies both lanes to circulate, whereas 'through (right)' indicates the truck approaches in the right lane and occupies both lanes when circulating. In addition, 'through (apron)' or 'left turn (apron)' indicates that the truck approaches and stays in the left lane to travel through the roundabout, as the truck apron is present to

accommodate the off-tracking and therefore the truck does not need to occupy both lanes.

In Table 3-10, the modified element in each case is highlighted in green or gray.

Table 3-10. Roundabout dynamic modeling matrix.

Case	Test	ICD (ft)	Lanes	Truck apron	Cross-slope	Crown	Tilt	Truck config.	Truck load	Maneuver
1	1	180	2	3 in. & 2%	2%	N/A	N/A	WB-67	Full	Right turn
2		180	2	3 in. & 2%	2%	N/A	N/A	WB-67	Full	Through (right)
3		180	2	3 in. & 2%	2%	N/A	N/A	WB-67	Full	Through (left)
4		180	2	3 in. & 2%	2%	N/A	N/A	WB-67	Full	Through (apron)
5		180	2	3 in. & 2%	2%	N/A	N/A	WB-67	Full	Left turn
6		180	2	3 in. & 2%	2%	N/A	N/A	WB-67	Full	Left turn (apron)
7		180	2	3 in. & 2%	N/A	Applied	N/A	WB-67	Full	Right turn
8		180	2	3 in. & 2%	N/A	Applied	N/A	WB-67	Full	Through (right)
9		180	2	3 in. & 2%	N/A	Applied	N/A	WB-67	Full	Through (left)
10		180	2	3 in. & 2%	N/A	Applied	N/A	WB-67	Full	Through (apron)
11		180	2	3 in. & 2%	N/A	Applied	N/A	WB-67	Full	Left turn
12		180	2	3 in. & 2%	N/A	Applied	N/A	WB-67	Full	Left turn (apron)
13	2	140	1	3 in. & 2%	2%	N/A	4%	WB-67	Full	Right turn
14		140	1	3 in. & 2%	2%	N/A	4%	WB-67	Full	Through
15		140	1	3 in. & 2%	2%	N/A	4%	WB-67	Full	Left turn
16		140	1	3 in. & 2%	2%	N/A	2%	WB-67	Full	Right turn
17		140	1	3 in. & 2%	2%	N/A	2%	WB-67	Full	Through
18		140	1	3 in. & 2%	2%	N/A	2%	WB-67	Full	Left turn
19		140	1	3 in. & 2%	2%	N/A	-4%	WB-67	Full	Right turn
20		140	1	3 in. & 2%	2%	N/A	-4%	WB-67	Full	Through
21		140	1	3 in. & 2%	2%	N/A	-4%	WB-67	Full	Left turn
22		140	1	3 in. & 2%	2%	N/A	-2%	WB-67	Full	Right turn
23		140	1	3 in. & 2%	2%	N/A	-2%	WB-67	Full	Through
24		140	1	3 in. & 2%	2%	N/A	-2%	WB-67	Full	Left turn
25		180	2	3 in. & 2%	2%	N/A	4%	WB-67	Full	Right turn
26		180	2	3 in. & 2%	2%	N/A	4%	WB-67	Full	Through (left)

27		180	2	3 in. & 2%	2%	N/A	4%	WB-67	Full	Left turn
28		180	2	3 in. & 2%	2%	N/A	2%	WB-67	Full	Right turn
29		180	2	3 in. & 2%	2%	N/A	2%	WB-67	Full	Through (left)
30		180	2	3 in. & 2%	2%	N/A	2%	WB-67	Full	Left turn
31		180	2	3 in. & 2%	2%	N/A	-4%	WB-67	Full	Right turn
32		180	2	3 in. & 2%	2%	N/A	-4%	WB-67	Full	Through (left)
33		180	2	3 in. & 2%	2%	N/A	-4%	WB-67	Full	Left turn
34		180	2	3 in. & 2%	2%	N/A	-2%	WB-67	Full	Right turn
35		180	2	3 in. & 2%	2%	N/A	-2%	WB-67	Full	Through (left)
36		180	2	3 in. & 2%	2%	N/A	-2%	WB-67	Full	Left turn
37	3	140	1	3 in. & 2%	2%	N/A	N/A	Single-unit	Full	Right turn
38		140	1	3 in. & 2%	2%	N/A	N/A	Single-unit	Full	Through
39		140	1	3 in. & 2%	2%	N/A	N/A	Single-unit	Full	Left turn
40		140	1	3 in. & 2%	2%	N/A	N/A	28-ft double	Full	Right turn
41		140	1	3 in. & 2%	2%	N/A	N/A	28-ft double	Full	Through
42		140	1	3 in. & 2%	2%	N/A	N/A	28-ft double	Full	Left turn
43		140	1	3 in. & 2%	2%	N/A	N/A	40-ft double	Full	Right turn
44		140	1	3 in. & 2%	2%	N/A	N/A	40-ft double	Full	Through
45		140	1	3 in. & 2%	2%	N/A	N/A	40-ft double	Full	Left turn
46		180	2	3 in. & 2%	2%	N/A	N/A	Single-unit	Full	Right turn
47		180	2	3 in. & 2%	2%	N/A	N/A	Single-unit	Full	Through (right)
48		180	2	3 in. & 2%	2%	N/A	N/A	Single-unit	Full	Through (left)
49		180	2	3 in. & 2%	2%	N/A	N/A	Single-unit	Full	Left turn
50		180	2	3 in. & 2%	2%	N/A	N/A	28-ft double	Full	Right turn
51		180	2	3 in. & 2%	2%	N/A	N/A	28-ft double	Full	Through (right)
52		180	2	3 in. & 2%	2%	N/A	N/A	28-ft double	Full	Through (left)
53		180	2	3 in. & 2%	2%	N/A	N/A	28-ft double	Full	Through (Apron)
54		180	2	3 in. & 2%	2%	N/A	N/A	28-ft double	Full	Left turn
55		180	2	3 in. & 2%	2%	N/A	N/A	28-ft double	Full	Left turn (Apron)
56		180	2	3 in. & 2%	2%	N/A	N/A	40-ft double	Full	Right turn

57		180	2	3 in. & 2%	2%	N/A	N/A	40-ft double	Full	Through (right)
58		180	2	3 in. & 2%	2%	N/A	N/A	40-ft double	Full	Through (left)
59		180	2	3 in. & 2%	2%	N/A	N/A	40-ft double	Full	Left turn
60	4	180	2	3 in. & 6%	2%	N/A	N/A	WB-67	Full	Left turn (apron)
61		180	2	3 in. & 4%	2%	N/A	N/A	WB-67	Full	Left turn (apron)
62		180	2	3 in. & 0%	2%	N/A	N/A	WB-67	Full	Left turn (apron)
63		180	2	2 in. & 2%	2%	N/A	N/A	WB-67	Full	Left turn (apron)
64		180	2	1 in. & 2%	2%	N/A	N/A	WB-67	Full	Left turn (apron)
65		180	2	0 in. & 2%	2%	N/A	N/A	WB-67	Full	Left turn (apron)
66	5	140	1	3 in. & 2%	2%	N/A	N/A	WB-67	Empty	Right turn
67		140	1	3 in. & 2%	2%	N/A	N/A	WB-67	Empty	Through
68		140	1	3 in. & 2%	2%	N/A	N/A	WB-67	Empty	Left turn
69		140	1	3 in. & 2%	2%	N/A	N/A	WB-67	Half	Right turn
70		140	1	3 in. & 2%	2%	N/A	N/A	WB-67	Half	Through
71		140	1	3 in. & 2%	2%	N/A	N/A	WB-67	Half	Left turn
72		180	2	3 in. & 2%	2%	N/A	N/A	WB-67	Empty	Right turn
73		180	2	3 in. & 2%	2%	N/A	N/A	WB-67	Empty	Through (right)
74		180	2	3 in. & 2%	2%	N/A	N/A	WB-67	Empty	Through (left)
75		180	2	3 in. & 2%	2%	N/A	N/A	WB-67	Empty	Through (apron)
76		180	2	3 in. & 2%	2%	N/A	N/A	WB-67	Empty	Left turn
77		180	2	3 in. & 2%	2%	N/A	N/A	WB-67	Empty	Left turn (apron)
78		180	2	3 in. & 2%	2%	N/A	N/A	WB-67	Half	Right turn
79		180	2	3 in. & 2%	2%	N/A	N/A	WB-67	Half	Through (right)
80		180	2	3 in. & 2%	2%	N/A	N/A	WB-67	Half	Through (left)
81		180	2	3 in. & 2%	2%	N/A	N/A	WB-67	Half	Through (apron)
82		180	2	3 in. & 2%	2%	N/A	N/A	WB-67	Half	Left turn
83		180	2	3 in. & 2%	2%	N/A	N/A	WB-67	Half	Left turn (apron)

3.5.2 Truck Travel Path

Three movement scenarios were modeled for single-lane roundabouts, as shown in Figure 3-12. The first was a right turn, where trucks shifted to the left side of the roadway when approaching the roundabout, kept left to accommodate off-tracking, and drove back to the middle of the road to exit the roundabout. Next was a through movement, where trucks first made a slight right turn, then a left turn, and finally a second right turn. For each turn, drivers would keep the vehicle to the outside edge of the lane to accommodate the long wheelbase. Therefore, the vehicle shifted to the left of the roadway to make the first right turn, then drove to the right edge when circulating the central island, and finally swung back to the left edge to complete the second right turn. Last was a left-turn movement, where the path was similar to through movements, but the distance traveled in the circulatory roadway was longer.

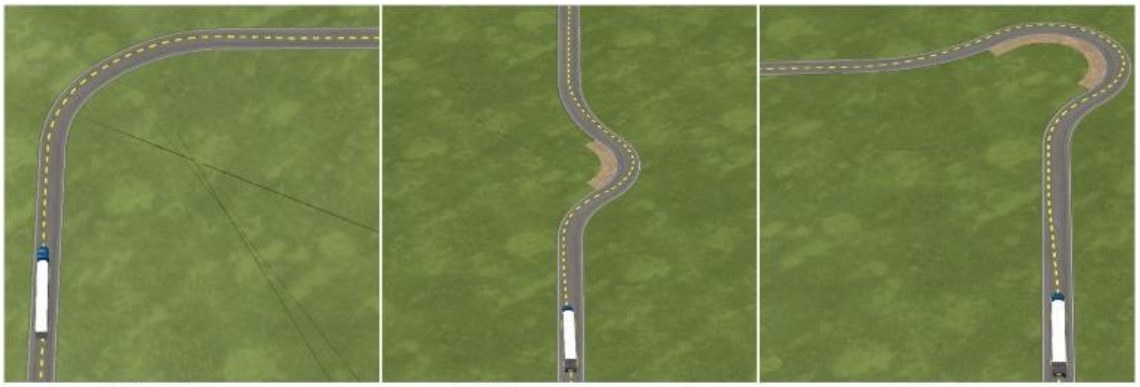

Figure 3-12. Travel path for the single-lane roundabout: (a) right turn; (b) through-movement; and (c) left turn [21].

A greater number of movement scenarios were modeled for two-lane roundabouts:

- Right turn: vehicles entered roundabouts from the right lane and then straddled both lanes to complete the right turn (Figure 3-13).
- Through-movement: there were three paths for a vehicle to perform a through-movement at two-lane roundabouts (Figure 3-14):
    - The first one assumed that the truck approached from the middle of the right lane, then straddled both lanes to perform the movement (Figure 3-14(a)).
    - Alternatively, the truck entered from the middle of the left lane, and then occupied both lanes to pass through the roundabout (Figure 3-14(b)).

- The third movement, which is commonly performed by trucks in roundabouts with a truck apron, was to keep the vehicles in the left lane and drive through the roundabout without occupying both lanes (Figure 3-14(c)).

- Left turn: two paths were designed for this movement (Figure 3-15):
  - The truck entered from the middle of the left lane, and then straddled both lanes to complete a left turn (Figure 3-15(a)).
  - The truck entered from the left lane, and stayed in the lane through its entire path around the circulatory roadway, without occupying both lanes but using a truck apron (Figure 3-15(b)).

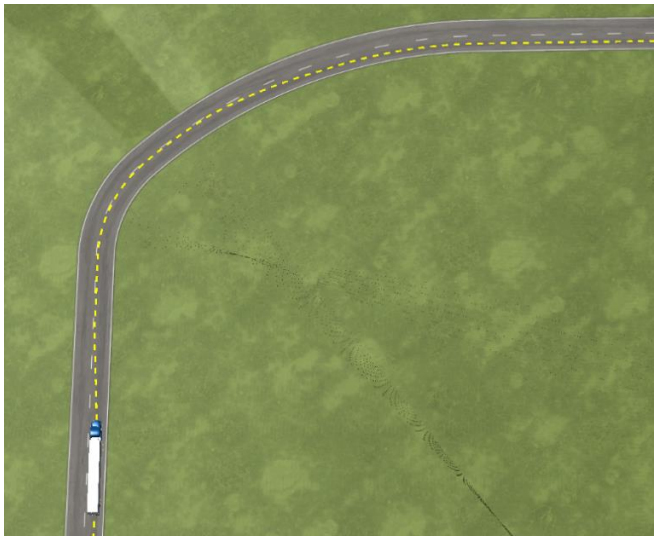

Figure 3-13. Travel path for a right turn in a two-lane roundabout [21].

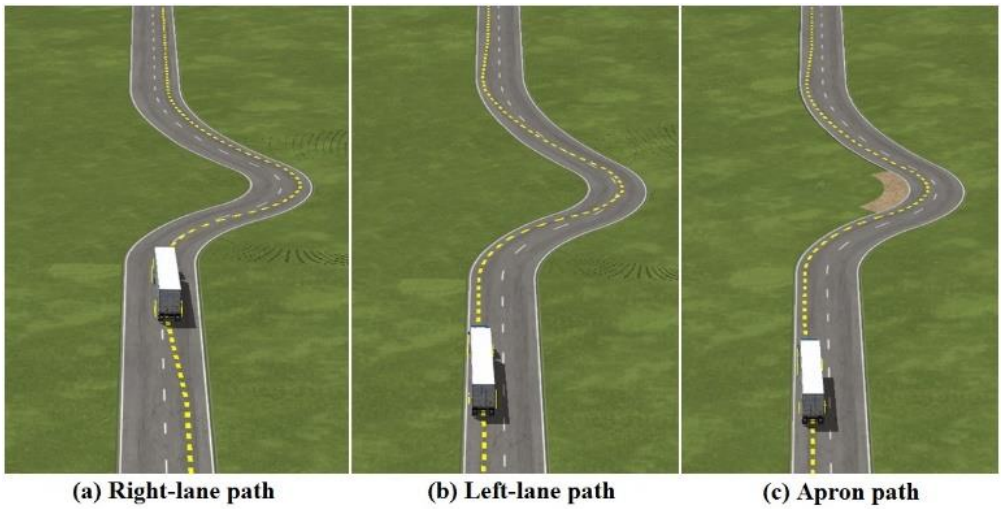

Figure 3-14. Travel path for through-movements in a two-lane roundabout: (a) right-lane path; (b) left-lane path; and (c) apron path [21].

Figure 3-15. Travel path for left turns in a two-lane roundabout: (a) left-lane path; and (b) apron path [21].

3.5.3 Truck Travel Speed

Given the long wheelbase, heavy load, and high CG, articulated-truck drivers usually drive slowly when negotiating roundabouts. This speed may vary from site to site, but is normally 10 mph for smaller roundabouts, and 15 mph for larger roundabouts.

In practice, semi-truck drivers commonly feel uncomfortable when they experience a lateral acceleration of more than 0.2g. Therefore, for this study, a lateral acceleration of 0.2g served as the limit for determining a proper circulating speed. When curvature is fixed, lateral acceleration is mainly determined by traveling speed, so the proper truck speed in this study was determined based on the roundabout diameters.

In this study, the truck entered the roundabout at 20 mph, slowed down to 15 mph within 2s, and accelerated back to 20 mph when exiting the roundabout. The speed diagram is illustrated in Figure 3-16 with respect to different movements.

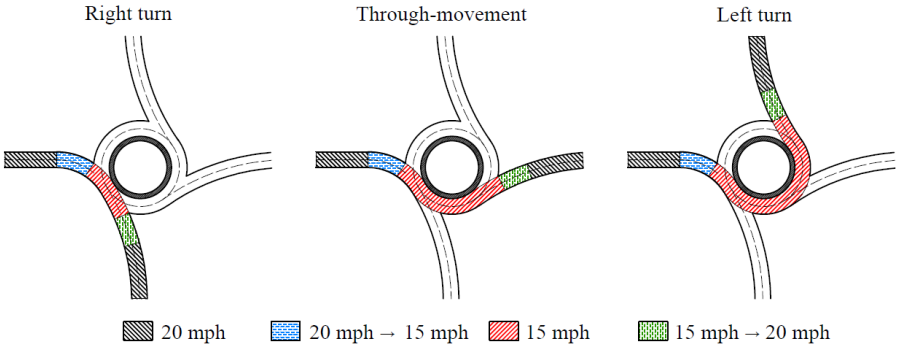

Figure 3-16. Speed diagram for different movements [21].

Chapter 4 – Low-speed Simulation Results and Analysis

The results of the case plans included in Table 3-10 are detailed in this chapter. Rollover index (RI) was selected as the metric for evaluating the likelihood of truck rollover. The RI for the rear-most trailing unit is determined to be used for representing the stability of an articulated truck, based on the result of a preliminary simulation study. The simulation results are presented and analyzed, indicating that roundabout geometry, truck configuration, and load condition significantly affect truck roll stability in roundabouts. A summary of the case studies is provided at the end of the chapter.

4.1 Rollover Index

Rollover index (RI) is used as the metric to indicate the likelihood of rollover:

$$RI = \frac{F_{z_{left}} - F_{z_{right}}}{F_{z_{left}} + F_{z_{right}}} \qquad (4-1)$$

Where

F_{z_left} = Total wheel-loads on the left

F_{z_right} = Total wheel-loads on the right

For example, the RI for a semi-trailer is calculated as:

$$RI_{semitrailer} = \frac{\left(F_{z4_{left}} + F_{z5_{left}}\right) - \left(F_{z4_{right}} + F_{z5_{right}}\right)}{\left(F_{z4_{left}} + F_{z5_{left}}\right) + \left(F_{z4_{right}} + F_{z5_{right}}\right)} \qquad (4-2)$$

Where

$F_{z4_{left}}$ = Total wheel-loads on the left of semi-trailer's front axle

$F_{z4_{right}}$ = Total wheel-loads on the right of semi-trailer's front axle

$F_{z5_{left}}$ = Total wheel-loads on the left of semi-trailer's rear axle

$F_{z5_{right}}$ = Total wheel-loads on the right of semi-trailer's rear axle

The maximum rollover index is defined as:

$$RI_{max} = ma\,x\left(\frac{\left|F_{z_{left}} - F_{z_{right}}\right|}{F_{z_{left}} + F_{z_{right}}}\right) \qquad (4-3)$$

Rollover index varies between -1 and 1. If there is no load transfer, the vertical loads on both the left and right sides are equivalent, and thus RI=0. If all loads are transferred to one side, the terms of Equation 4-1 become equal, resulting in RI =1 or -1. Therefore, an RI equal to 0 describes a perfectly weight-balanced vehicle. Based on our experience, in general, the risk of rollover increases significantly when RI exceeds 0.8 for any prolonged period, such as 200ms.

4.2 Preliminary Simulation Study to Compare the Roll Stability between Tractor and Trailer of Each Truck Configuration

Fifth-wheel couplings are commonly employed by articulated trucks to connect semitrailers to tractors, or to couple two trailing units. Therefore, the dynamics of these vehicle units are coupled with each other, and they are expected to have different roll stability. Previous research shows that trucks have a higher risk of rollover when circulating the central island in a left-turn movement [2]. Hence, trucks with the four configurations introduced in Chapter 5 were assigned to perform left-turn movements in the two-lane roundabout to examine the roll stability of each vehicle unit. For the left-turn maneuvers applied here, the trucks would occupy both lanes instead of using a truck apron, since this is the path that truck drivers would typically follow in roundabouts.

Figure 4-1 shows that trucks experienced body roll to the driver side when turning right at the entry, implied by positive RIs (from t=5s to t=11s). Trucks rolled to the passenger side and showed RIs when traveling on the circulatory roadway (from t=11s to t=23s). Finally, trucks exited the roundabout through a right turn at the exit curve and experienced body roll to the drive side again, indicated by positive RIs (from t=23s to t=33s). RIs exhibited greater values at the entry curve than those at the exit curve because the entry curve has a smaller radius which results in larger lateral accelerations, and thus more lateral load transfer where the same traveling speed is applied at the entry and exit curve. Based on Figure 4-1, the tractors in all the configurations experienced stable roll dynamics because they only exhibited RIs below 0.4, indicating a low likelihood of rollovers. On the

contrary, the trailers exhibited less roll stability than the tractors, especially for the WB-67 semi-truck and the 40-ft double trailers, which both experienced a peak RI of 0.7. Even though the 28-ft double trailers has a longer combined wheelbase than the WB-67 semi-truck, the trailers in this configuration showed smaller RIs due to the additional couplings that made them more flexible and better able to negotiate roundabouts. For the 40-ft double trailers, however, the long combined wheelbase required the use of the truck apron, although the truck had already occupied both lanes to take full advantage of the roadway width. Thus, the 40-ft double trailers experienced more aggressive roll dynamics due to traveling on a truck apron. Figure 4-1(d) shows that the rear trailer encountered and disembarked the truck apron at t=17s and t=24s, respectively, both resulting in transient dynamics indicated by RI spikes.

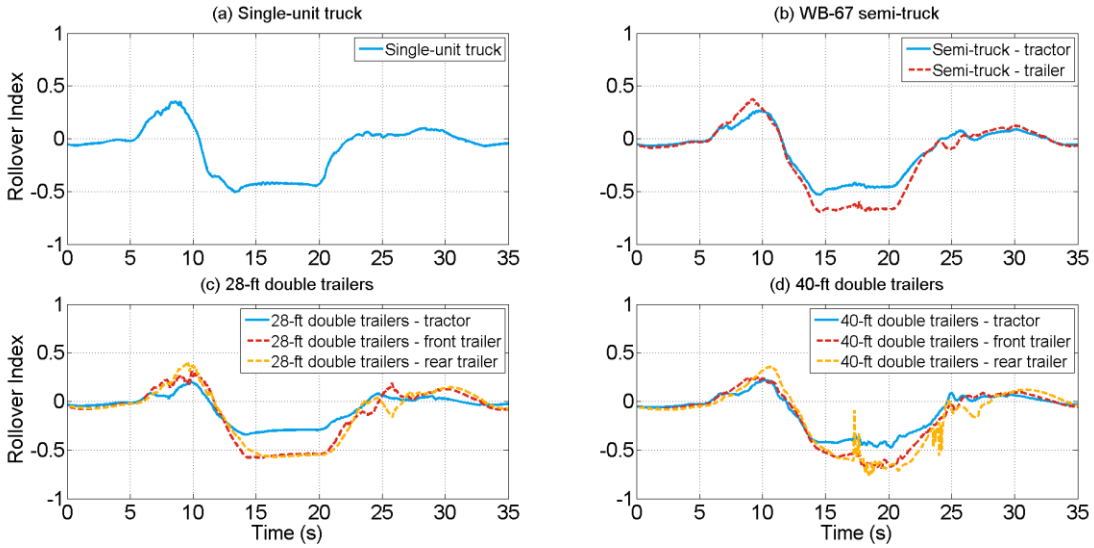

Figure 4-1. Rollover index of different truck configurations when performing left turns in the 54.9-m (180-ft) multilane roundabout: (a) single-unit truck; (b) WB-67 semi-truck; (c) 28-ft double trailers; (d) 40-ft double trailers.

Considering the fact that the trailer, or the rear trailer in double-trailer configurations, exhibited less roll stability than the other vehicle units because it experienced greater peak RIs, the rearmost trailing unit of each truck configuration is used to represent the roll stability of the entire truck combination.

4.3 Effect of Circulatory Roadway Cross-section on Truck Roll Stability in Roundabouts

In this test, two circulatory roadway cross-section designs were applied to the 180-ft two-lane roundabout model. The first one is the baseline model, where the circulatory roadway had a 2% outward cross-slope. The other model had crowned circulatory roadways, where the inner two-thirds of the roadway had a 2% inward cross-slope, and the outer one-third had a 2% outward cross-slope. Since single-lane roundabouts commonly do not have a crowned circulatory roadway due to the relatively smaller total roadway width, they were not considered for this study. The baseline WB-67 semi-truck model with a full load was applied in the simulation, and 12 cases were created and simulated, as listed in Table 4-1.

Table 4-1. Cases for evaluating the effect of different circulatory roadway cross-sections on truck roll stability.

Case #	Roundabout	Cross-slope	Road crown	Truck	Movement
1	180-ft two lane	2%	N/A	WB-67	Right turn
2	180-ft two lane	2%	N/A	WB-67	Through (right)
3	180-ft two lane	2%	N/A	WB-67	Through (left)
4	180-ft two lane	2%	N/A	WB-67	Through (apron)
5	180-ft two lane	2%	N/A	WB-67	Left turn
6	180-ft two lane	2%	N/A	WB-67	Left turn (apron)
7	180-ft two lane	N/A	Applied	WB-67	Right turn
8	180-ft two lane	N/A	Applied	WB-67	Through (right)
9	180-ft two lane	N/A	Applied	WB-67	Through (left)
10	180-ft two lane	N/A	Applied	WB-67	Through (apron)
11	180-ft two lane	N/A	Applied	WB-67	Left turn
12	180-ft two lane	N/A	Applied	WB-67	Left turn (apron)

4.3.1 Right turns

The result of the rollover index for right turns is shown in Figure 4-2. According to Figure 4-2, the crowned roundabout reduced the truck lateral stability more than the baseline (constant 2% outward cross-slope). This was mainly because the left side of the roadway was higher than the right side for the baseline case; thus, when the truck performed a right turn, the outward roadway cross-section (to the passenger's side) countered the centrifugal accelerations at the CG, reduced the body roll, and improved the truck stability. For the

crowned roundabout, the left edge of the inner two-thirds of the roadway was lower than its right edge. When the truck straddled to make a right turn, its left wheels ran on the inner part of the roadway, thus increasing the tendency to lean to the left side and reducing lateral stability.

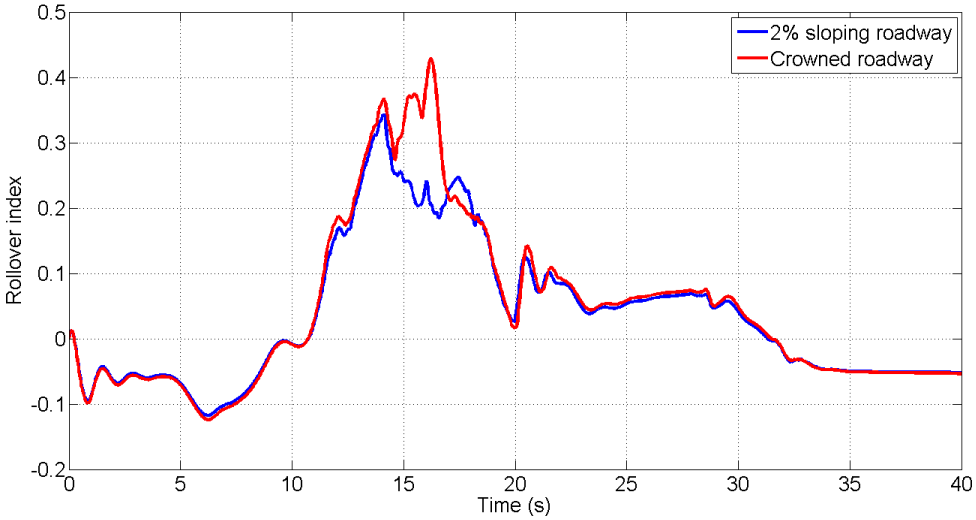

Figure 4-2. Effect of circulatory roadway cross-sections on truck rollover index (right turn, 180-ft two-lane roundabout).

4.3.2 Through-movements

The result of the rollover index for through-movements is shown in Figure 4-3. When trucks performed through-movements through a roundabout following the left-lane path, the crowned circulatory roadway provided better truck roll stability, indicated by the smaller maximum RI (red line) shown in Figure 4-3(a). However, Figure 4-3(b) shows that when a right-lane path was followed, the crowned circulatory roadway resulted in a great maximum RI. This was because the inner two-thirds of the crowned roadway had a 2% inward cross-slope, whereas the outer one-third section had a 2% outward cross-slope. When a truck entered the roundabout in the middle of the right lane, it would shift to the left side and occupy both lanes to perform the first right turn, where the truck ran on the inner section with an inward cross-slope. However, when it shifted back to the right edge to start circulating the central island, it would travel back to the outer section with an outward cross-slope. Such quick opposite road excitation resulted in a rocking motion that increased the likelihood of truck rollover, as indicated by the greater maximum RI shown

by the red line at t=20s. For the cases where the apron path was followed, the crowned roadway was more favored for decreasing the rollover likelihood, which reduced the maximum RI from 0.8 to 0.7.

It should be noted that for the sloping-roadway case, the truck had better lateral stability when it approached the roundabout from the right lane rather than the left lane. A crowned roundabout, however, provided the opposite results. Even though the left lane had a smaller radius than the right lane, the 2% inward cross-slope of the inner two-thirds of the roundabout was much favored for counterbalancing the centrifugal force.

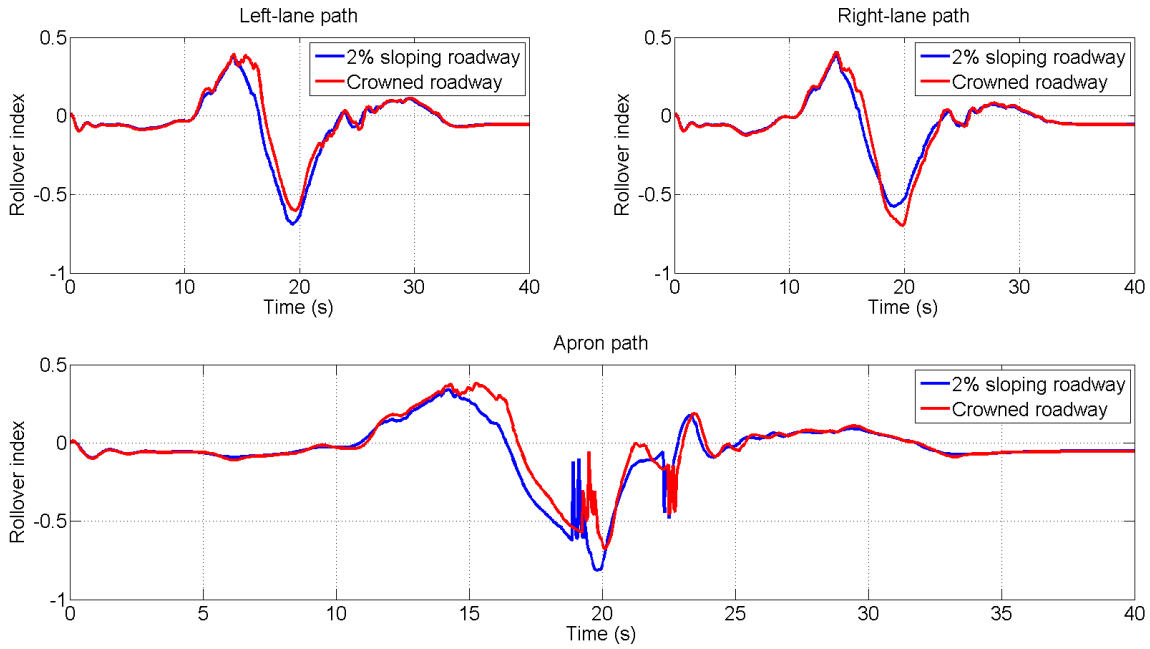

Figure 4-3. Effect of circulatory roadway cross-sections on truck rollover index (through-movements, 180-ft two-lane roundabout).

4.3.3 Left turns

The result of the rollover index for through-movements is shown in Figure 4-4. The left-turn cases presented a similar trend as that for the through-movements cases. The crowned circulatory roadway could reduce the likelihood of truck rollover with both paths, compared to the 2% sloping roadway. It is noted that the WB-67 semi-truck experienced a strong likelihood of rollover when traveling on the 2% sloping roadway and following the apron path at 15 mph because the RIs exceeded 0.9 at t=20s.

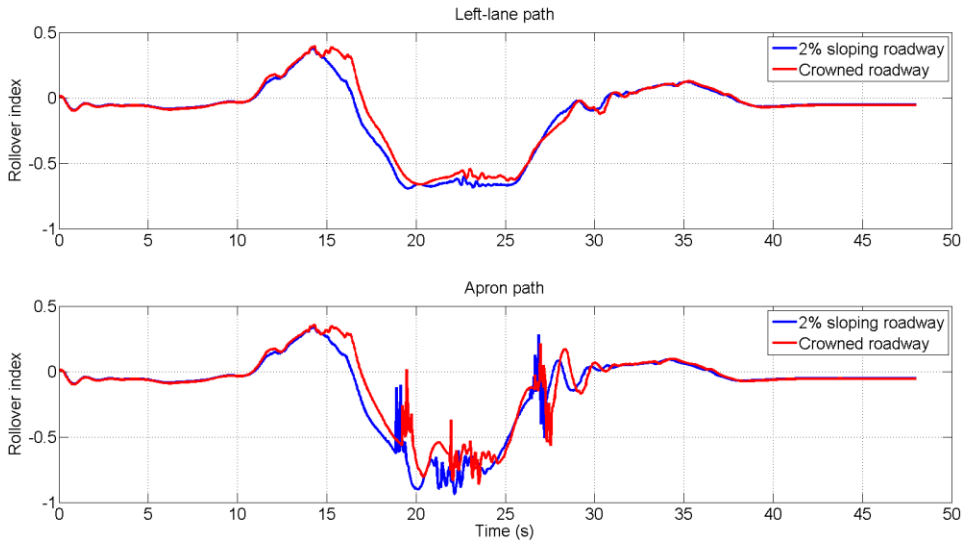

Figure 4-4. Effect of circulatory roadway cross-sections on truck rollover index (left turn, 180-ft two-lane roundabout).

4.4 Effect of Roundabout Tilt on Truck Roll Stability in Roundabouts

In this test, the entire roundabout was tilted at four constant angles to determine the effect of a tilted slope on truck stability. Tilt was with respect to the approaching roadway. Positive tilt indicated that, from the perspective of a driver on the approaching roadway, the entire roundabout was tilted down to the right, i.e., 'outward' toward the roadway's right shoulder. Negative slope indicates that the roadway was tilted, from the perspective of a driver on the approaching roadway, down to the left, i.e., 'inward' toward the road's centerline, as shown in Figure 3-7. The baseline WB-67 semi-truck with a full load was applied in this test. The cases simulated are included in Table 4-2. All dimensions not shown are unchanged within the set of single-lane and two-lane cases (see Table 3-10 for details). In order to reduce the redundancy, only the left-lane path was applied for through-movements and left turns because this is the most common path that a truck driver would follow, according to consultation with an experienced truck test driver.

Table 4-2. Cases for evaluating the roundabout tilt on truck roll stability.

Case #	Roundabout ICD (ft)	Movement	Percent Tilt (slope)*
13	140	Right turn	+4
14	140	Through	+4
15	140	Left turn	+4
16	140	Right turn	+2
17	140	Through	+2
18	140	Left turn	+2
19	140	Right turn	-4
20	140	Through	-4
21	140	Left turn	-4
22	140	Right turn	-2
23	140	Through	-2
24	140	Left turn	-2
25	180	Right turn	+4
26	180	Through (left)	+4
27	180	Left turn	+4
28	180	Right turn	+2
29	180	Through (left)	+2
30	180	Left turn	+2
31	180	Right turn	-4
32	180	Through (left)	-4
33	180	Left turn	-4
34	180	Right turn	-2
35	180	Through (left)	-2
36	180	Left turn	-2
* “+" indicates outward tilt and “-“ indicates inward tilt			

4.4.1 Right turns

The results of the rollover index for right turns are shown in Figure 4-5 and Figure 4-6, for a single-lane roundabout and a two-lane roundabout, respectively. Figure 4-5 and Figure 4-6 show that the RI—and therefore, the likelihood of truck rollover—increased as the roundabout tilt decreased, indicating that tilting the roundabout outward had a stabilizing effect for right-turn movements. This was because tilting the roundabout outward resulted in the left edge higher than the right edge, from the perspective of the driver facing the roundabout. Therefore, the higher left edge could better counter the centrifugal force when the truck performed right turns.

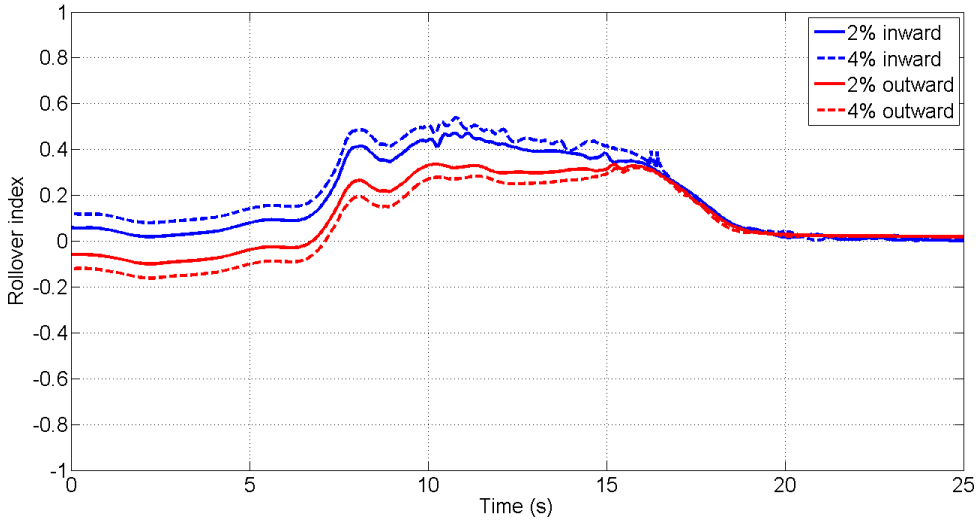

Figure 4-5. Effect of roundabout tilt on truck rollover index (right turn, 140-ft single-lane roundabout).

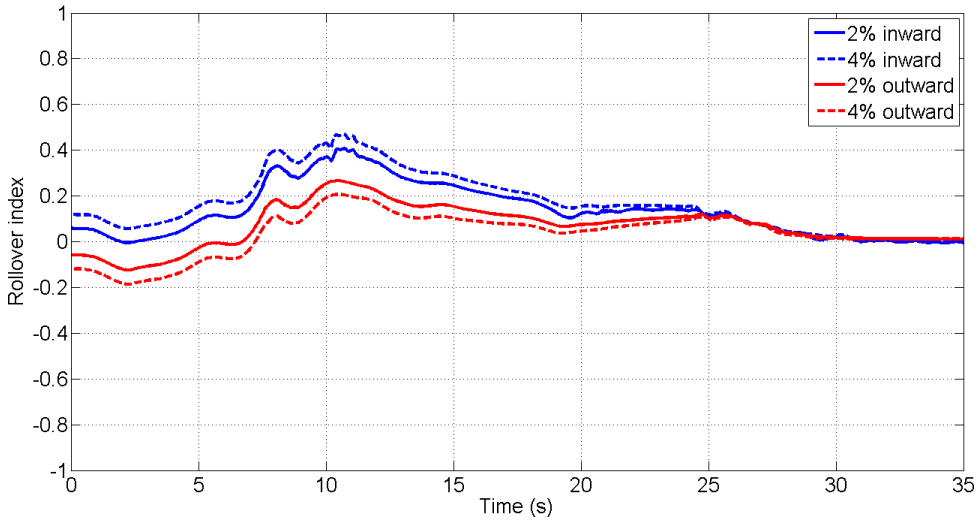

Figure 4-6. Effect of roundabout tilt on truck rollover index (right turn, 180-ft two-lane roundabout).

4.4.2 Through-movements

The results of the rollover index for through-movements are shown in Figure 4-7 and Figure 4-8, for a single-lane roundabout and a two-lane roundabout, respectively.

Figure 4-7 and Figure 4-8 indicate that at the roundabout entry and exit, a more negative/inward tilt increased RI. The opposite was true when the truck was in the roundabout, where a more negative/inward tilt decreased rollover index. For the single-lane roundabout (Figure 4-7), all maximum RIs occurred while the truck was on the

circulatory roadway inside the roundabout, and not at the entrance or exit. Thus, for the single-lane roundabout, a negative/inward tilt was less likely to cause rollover. For the two-lane roundabout (Figure 4-8), maximum RIs also occurred while the truck was on the circulatory roadway inside the roundabout, again suggesting that a negative/inward tilt is preferable.

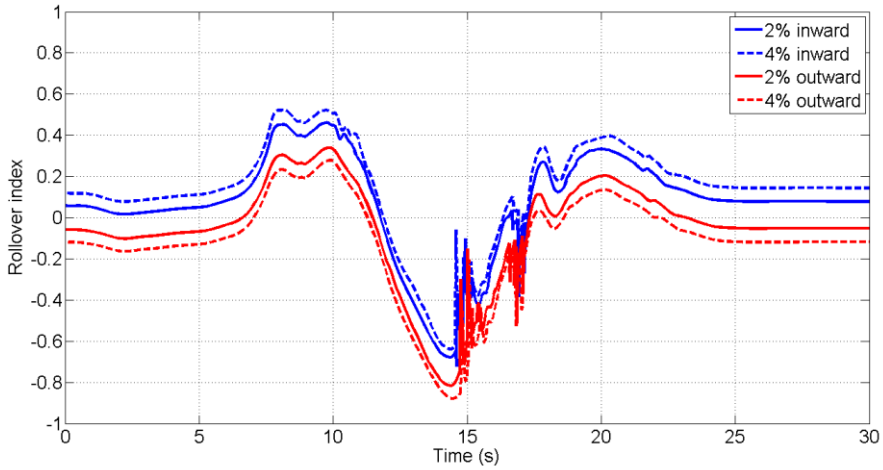

Figure 4-7. Effect of roundabout tilt on truck rollover index (through-movement, 140-ft single-lane roundabout).

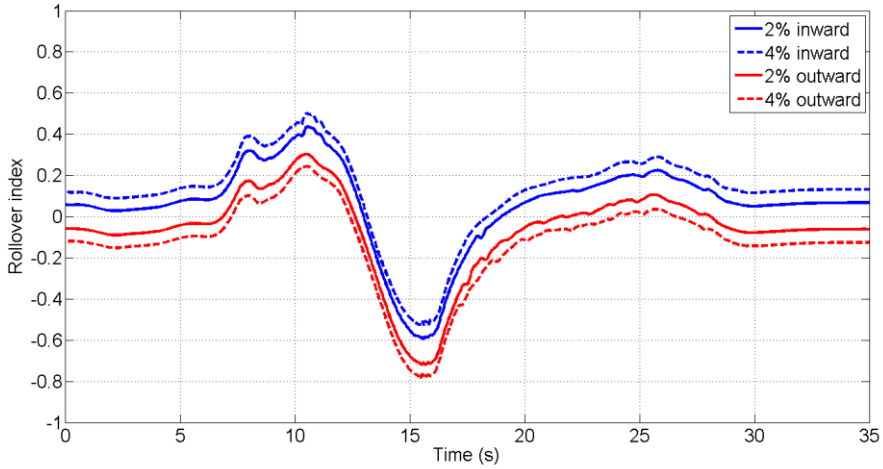

Figure 4-8. Effect of roundabout tilt on truck rollover index (through-movement, 180-ft two-lane roundabout).

4.4.3 Left turns

The results of the rollover index for left turns are shown in Figure 4-9 and Figure 4-10, for a single-lane roundabout and a two-lane roundabout, respectively.

The results in Figure 4-9 and Figure 4-10 have similar trends as those in Figure 4-7 and Figure 4-8. Inward and outward tilting had opposite effects at various parts of the roundabout, i.e., at the entry and exit versus in the roundabout. For the smaller roundabout, inward tilting resulted in lower peaks, to barely keep them below the rollover limit. The outward tilt resulted in maximum RI exceeding 0.9 and the truck risking rollover. As shown in Figure 4-10, for the larger roundabout, a small moderate inward tilt resulted in a good balance between the truck's lateral dynamics at both points of entry and exit, as well as in the roundabout, similar to what was discussed for the through-movement case.

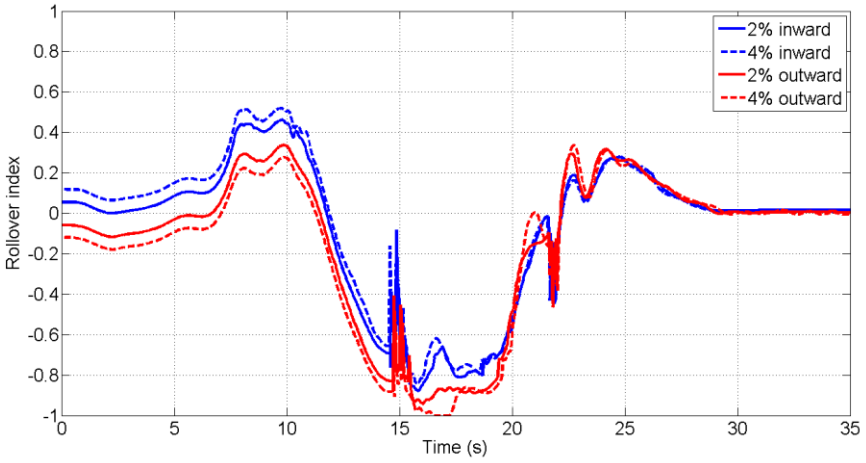

Figure 4-9. Effect of roundabout tilt on truck rollover index (left turn, 140-ft single-lane roundabout).

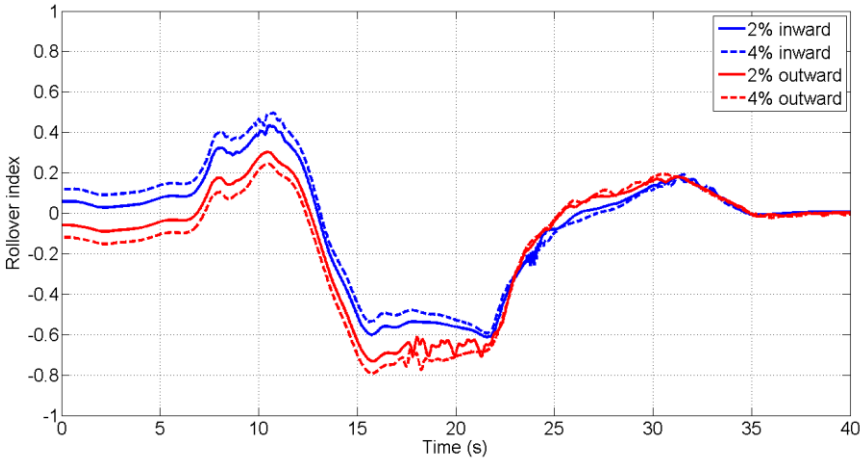

Figure 4-10. Effect of roundabout tilt on truck rollover index (left turn, 180-ft two-lane roundabout).

4.5 Effect of Truck Configuration on Truck Roll Stability in Roundabouts

In this test, four different truck configurations, a single-unit truck, a WB-67 semi-truck, a 28-ft double trailer, and a 40-ft double trailer, were modeled to evaluate their roll dynamics when driving through the baseline 180-ft two-lane roundabout. Each truck entered the roundabout at 20 mph, then slowed down to 15 mph and followed the same path. The cases considered are summarized in Table 4-3.

Table 4-3. Cases for evaluating different truck configurations on truck roll stability.

Case #	Roundabout ICD (ft)	Truck configuration	Maneuver
37	140	Single-unit	Right turn
38	140	Single-unit	Through
39	140	Single-unit	Left turn
40	140	28-ft double	Right turn
41	140	28-ft double	Through
42	140	28-ft double	Left turn
43	140	40-ft double	Right turn
44	140	40-ft double	Through
45	140	40-ft double	Left turn
46	180	Single-unit	Right turn
47	180	Single-unit	Through (right)
48	180	Single-unit	Through (left)
49	180	Single-unit	Left turn
50	180	28-ft double	Right turn
51	180	28-ft double	Through (right)
52	180	28-ft double	Through (left)
53	180	28-ft double	Through (Apron)
54	180	28-ft double	Left turn
55	180	28-ft double	Left turn (Apron)
56	180	40-ft double	Right turn
57	180	40-ft double	Through (right)
58	180	40-ft double	Through (left)
59	180	40-ft double	Left turn

4.5.1 Right turns

The results of rollover index for right turns are shown in Figure 4-11 and Figure 4-12. Figure 4-11 and Figure 4-12 show that all trucks had positive RIs during the right-turn movement, indicating that the loads were transferred to the left side due to the centrifugal force. Vehicles experienced two small RI peaks during the movement, introduced by side-

to-side elevation changes in the transition area. Single-lane roundabouts resulted in greater RIs than the two-lane roundabout, because the latter one had a larger ICD as well as a greater entry radius.

The 28-ft double trailers experienced a slightly larger maximum RI both in the single-lane and multilane roundabouts, followed by the 40-ft double trailers. The single-unit truck had the best roll stability. In general, all trucks had similar roll stability and could safely perform right turns in the scenarios considered here.

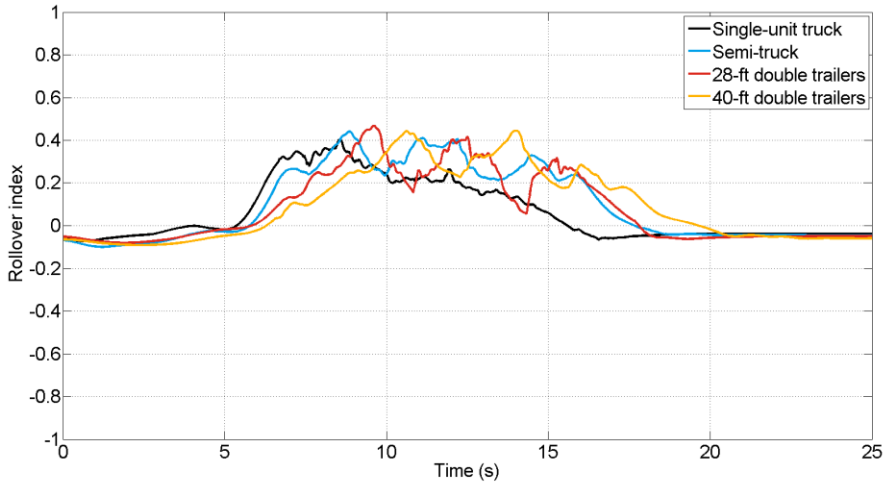

Figure 4-11. Effect of truck configuration on truck rollover index (right turn, 140-ft single-lane roundabout).

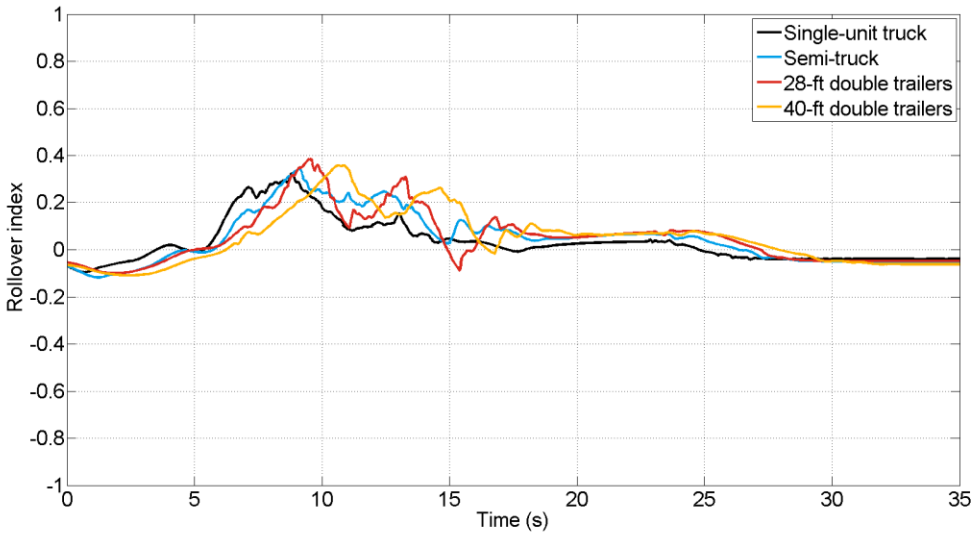

Figure 4-12. Effect of truck configuration on truck rollover index (right turn, 180-ft two-lane roundabout).

4.5.2 Through-movements

The results of rollover index for through-movements are shown in Figure 4-13 and Figure 4-14.

Figure 4-13 shows that the single-unit truck and the 28-ft double trailers exhibited a similar trend, whereas the WB-67 semi-truck encountered the truck apron at t = 13 s, and left at t = 16 s, both resulting in a rapid change of vertical load on both sides of the truck, shown by RI spikes. The 40-ft double trailers also traveled on an apron, however, they experienced a lower likelihood of rollover than the semi-truck. This was because the double-trailer arrangement had two hitch connections that made it more flexible. Additionally, the rear trailer of the 40-ft doubles traveled at a lower speed than the semi-trailer when circulating the roundabout, due to the longer overall wheelbase, and therefore experienced smaller lateral accelerations and less lateral load transfers. Furthermore, the flexibility of the double-trailer arrangement allowed the 28-ft double trailers to not necessarily require a truck apron to accommodate the off-tracking, thereby significantly reducing the risk of rollover, although it was overall slightly longer than the WB-67 semi-truck.

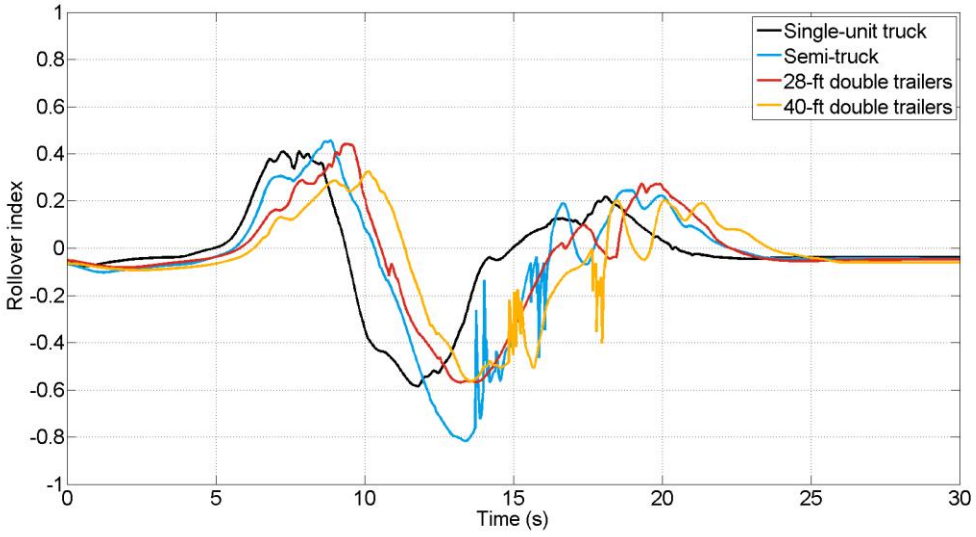

Figure 4-13. Effect of truck configuration on truck rollover index (through-movements, 140-ft single-lane roundabout).

Three different paths were simulated for trucks performing through-movements in the 180-ft two-lane roundabout, as shown in Figure 4-14. In Figure 4-14(a), it was assumed that

trucks approached from the left lane, and then occupied both lanes to travel through the roundabouts. The results of this case are similar to the single-lane case, except that the WB-67 semi-truck did not necessarily need the truck apron to accommodate its off-tracking. In Figure 4-14(b), trucks approached from the right lane and then also occupied both lanes. Results show that in this scenario, all four trucks could travel through the roundabout without using truck aprons. Figure 4-14(a) and (b) indicate that the single-unit truck and the 28-ft double trailers experienced similar and better roll dynamics. The WB-67 semi-truck obtained the largest maximum RI among all truck configurations considered here. In addition, Figure 4-14(a) and (b) also show that trucks generally had better roll stability when traveling in the right lane than in the left lane. Figure 4-14(c) shows the results of the semi-truck and the 28-ft double trailers following the apron path. In general, the 28-ft double trailers had better roll stability than the semi-truck in this case. It is noted that the 28-ft double trailers experienced a large RI spike around t=17s, when the rear trailer's left wheels were falling off the truck apron. At this moment, there were no vertical forces on the left wheels ($F_{z\_left} = 0$), resulting in a peak RI that equaled -1, as indicated by Equation 5-1. However, the semi-truck had tandem wheels on the semi-trailer, compared to the 28-ft double trailers that only had a single axle on each trailer. Therefore, this phenomenon was not observed in the semi-truck case. Since the 28-ft double trailers only exhibited the peak RI momentarily (less than 200 ms), it did not increase the risk of rollover to the truck. The single-unit truck was not simulated with the apron path because it had a short wheelbase and a relatively smaller off-tracking that did not require accommodation of the truck apron. The 40-ft double trailers were not considered either because drivers always take full advantage of the entire width of roadway to insure that the trailer will not traverse the central island when driving a truck with such a long overall length.

Regarding through-movements in roundabouts, generally, the single-unit truck had better roll stability than the other trucks, followed by the 28-ft double trailers. The WB-67 semi-truck and the 40-ft double trailers posed a higher risk of rollover.

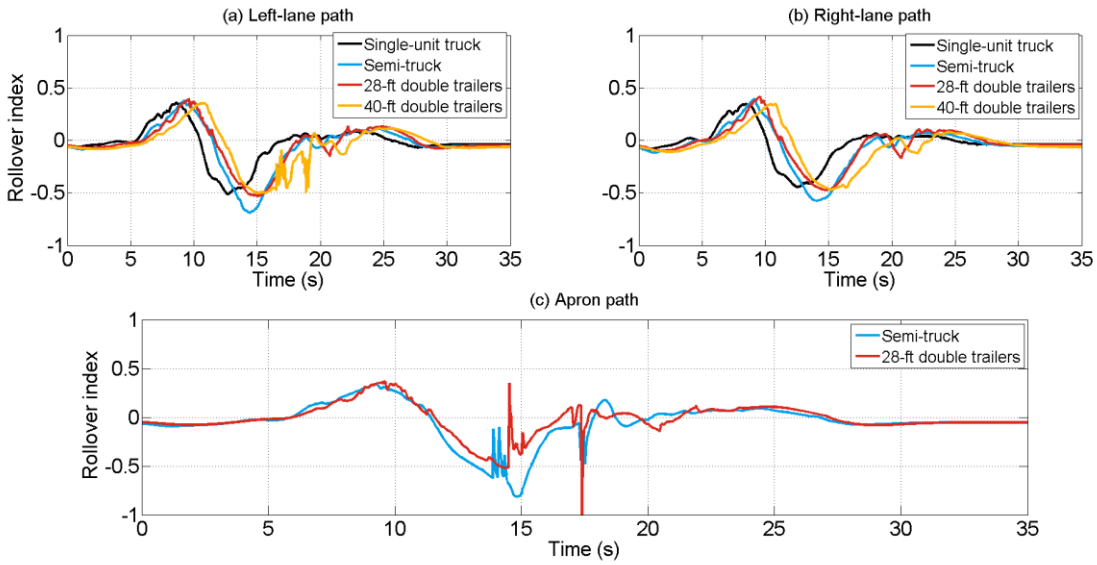

Figure 4-14. Effect of truck configuration on truck rollover index (through-movement, 180-ft two-lane roundabout): (a) left-lane path; (b) right-lane path; (c) apron path.

4.5.3 Left turn

The results of the rollover index for left turns are shown in Figure 4-15 and Figure 4-16. The WB-67 semi-truck traveled on the truck apron between t=14s and t=23s, experiencing transient dynamics shown by RI spikes. In addition, it also exhibited the highest risk of rollover with a maximum RI almost reaching 1.0, followed by the 40-ft double trailers that also had a maximum RI over 0.8, indicating that both of them traveled through this roundabout with a strong likelihood of rollover. The maximum RI for the 28-ft double trailers did not exceed 0.8, and the truck apron was not used due to the shorter trailers and flexible arrangement. The single-unit truck again had the best roll stability compared to the other three truck configurations.

Figure 4-16 shows the results of trucks performing left turns in the 180-ft two-lane roundabout. In Figure 4-16(a), all trucks approached from the left lane, and then occupied both lanes to travel through the roundabout. In this scenario, only the 40-ft double trailers needed a truck apron to accommodate the large off-tracking, shown by RI spikes around t=17s and t=23s. Again, the single-unit truck exhibited the best roll stability, followed by the 28-ft double trailers. The WB-67 semi-truck and the 40-ft double trailers had a similar maximum RI, but the 40-ft doubles experienced extra rocking motions introduced by traveling on the truck apron.

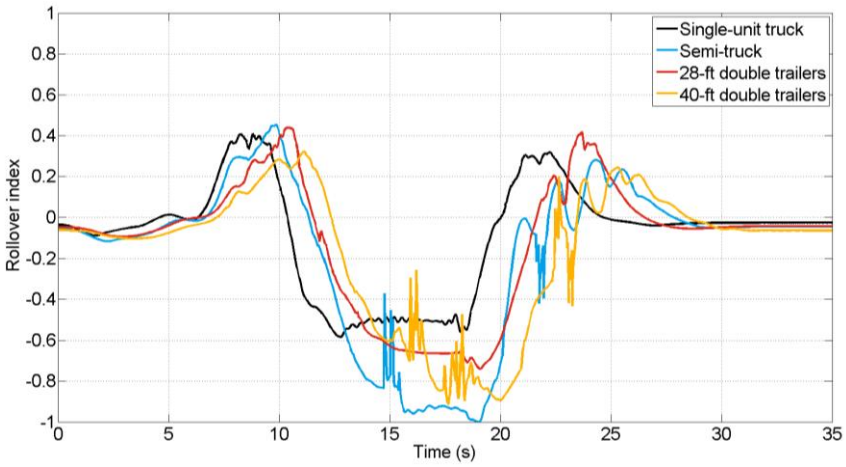

Figure 4-15. Effect of truck configuration on truck rollover index (left turns, 140-ft single-lane roundabout).

Figure 4-16(b) shows that when the semi-truck and the 28-ft double trailers used a truck apron to perform a left turn in the two-lane roundabout, they both experienced greater RIs than those in Figure 4-16(a), especially for the WB-67 semi-truck whose maximum RI increased from 0.69 to 0.93. This phenomenon indicates that traveling on a truck apron can significantly increase the risk of rollover because (1) the overshoot in transient response introduced by bouncing up onto the truck apron and back down can result in a lateral acceleration that exceeds the truck's rollover threshold, and (2) the apron's vertical elevation, as well as the 2% outward cross-slope, make the truck lean more to the outside of the turn, resulting in further lateral load transfer in steady-state response when circulating the roundabout.

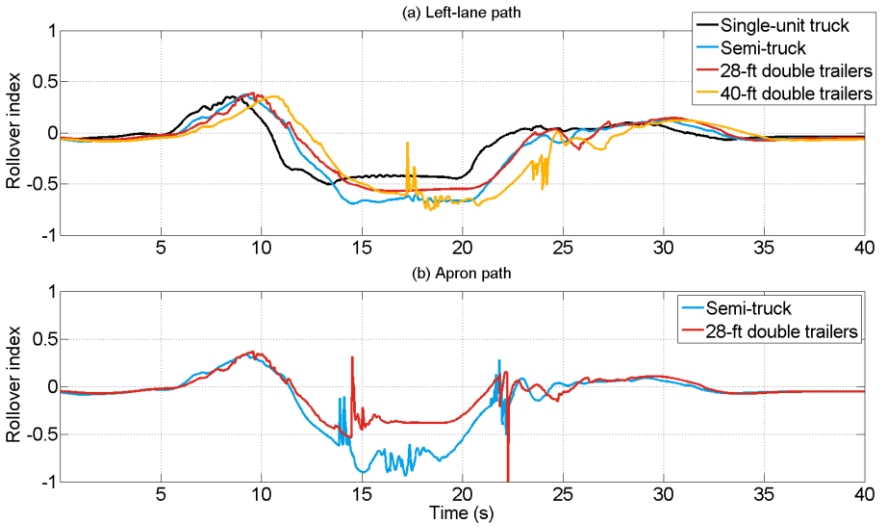

Figure 4-16. Effect of truck configuration on truck rollover index (left turn, 180-ft two-lane roundabout): (a) left-lane path; (b) apron path.

4.6 Effect of Truck Apron Geometry on Truck Roll Stability in Roundabouts

This test evaluated the effect of truck apron geometry on truck rollover likelihood in roundabouts. Based on the results of previous simulation runs, the likelihood of truck rollover could increase considerably when traveling on a truck apron. Therefore, two main geometric parameters of truck aprons were studied to learn their effect on truck roll stability in roundabouts, which included the cross-slope and height of a truck apron, as shown in Figure 4-17. The apron's cross-slope was varied from 0% (no cross-slope) to 6%, and the height was changed from 0 to 3 in. The baseline WB-67 semi-truck was assigned to perform a left-turn movement in the 180-ft two-lane roundabout, where the truck stayed in the left lane and used the apron to travel through the roundabout. The cases are included in Table 4-4, and simulation results are shown in Figure 4-18.

Table 4-4. Cases for evaluating truck apron geometry on truck roll stability.

Case #	Roundabout ICD (ft)	Truck apron height	Truck apron cross-slope	Truck	Maneuver
60	180	3 in.	6%	WB-67	Left turn (Apron)
61	180	3 in.	4%	WB-67	Left turn (Apron)
62	180	3 in.	0%	WB-67	Left turn (Apron)
63	180	2 in.	2%	WB-67	Left turn (Apron)
64	180	1 in.	2%	WB-67	Left turn (Apron)
65	180	0 in.	2%	WB-67	Left turn (Apron)

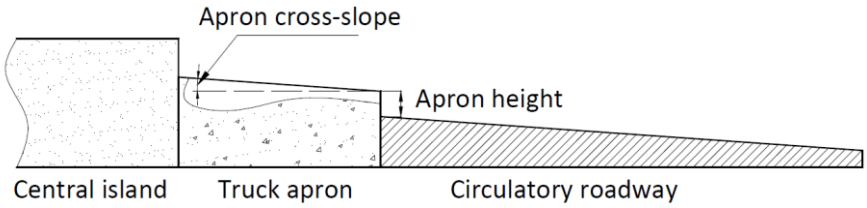

Figure 4-17. Typical roundabout section with a truck apron [21].

Figure 4-18(a) illustrates that different apron cross-slopes resulted in similar roll dynamics to the truck when encountering an apron, indicated by close RIs exhibited by the truck. However, the truck experienced more stable roll dynamics when traveling on and disembarking an apron with a lower slope. In addition, when encountering or disembarking an apron with a taller curb height, the truck experienced a larger side-to-side motion, indicated by larger RI spikes that exceeded 0.8, as shown in Figure 4-18(b).

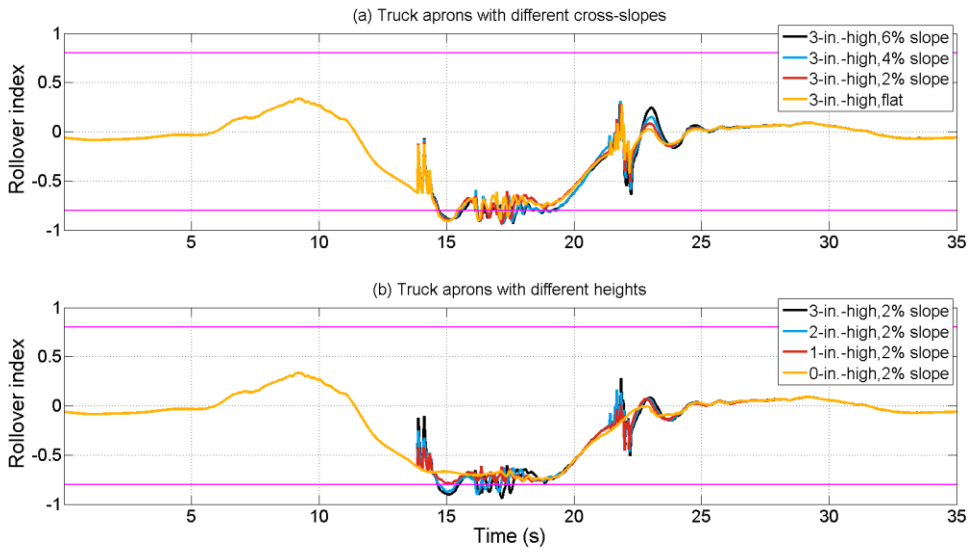

Figure 4-18. Effect of different truck apron geometric parameters on truck rollover index: (a) different cross-slopes; (b) different apron heights.

4.7 Effect of Load Conditions on Truck Roll Stability in Roundabouts

In this test, three load configurations were studied for the WB-67 semi-truck (the baseline vehicle) to determine whether the load would impact truck stability. The baseline truck was evaluated in empty, half-full, and full load conditions, as summarized in Table 4-5. The loads were assumed to be fixed, and no shifting loads were considered.

Table 4-5. Cases for evaluating different load conditions on truck roll stability.

Case #	Roundabout ICD (ft)	Truck Configuration	Load condition	Maneuver
66	140	WB-67	Empty	Right turn
67	140	WB-67	Empty	Through
68	140	WB-67	Empty	Left turn
69	140	WB-67	Half	Right turn
70	140	WB-67	Half	Through
71	140	WB-67	Half	Left turn
72	180	WB-67	Empty	Right turn
73	180	WB-67	Empty	Through (right)
74	180	WB-67	Empty	Through (left)
75	180	WB-67	Empty	Through (apron)
76	180	WB-67	Empty	Left turn
77	180	WB-67	Empty	Left turn (apron)
78	180	WB-67	Half	Right turn
79	180	WB-67	Half	Through (right)
80	180	WB-67	Half	Through (left)

81	180	WB-67	Half	Through (apron)
82	180	WB-67	Half	Left turn
83	180	WB-67	Half	Left turn (apron)

4.7.1 Right turns

The results of the rollover index for right turns in the 140-ft single-lane roundabout and the 180-ft two-lane roundabout are shown in Figure 4-19 and Figure 4-20, respectively.

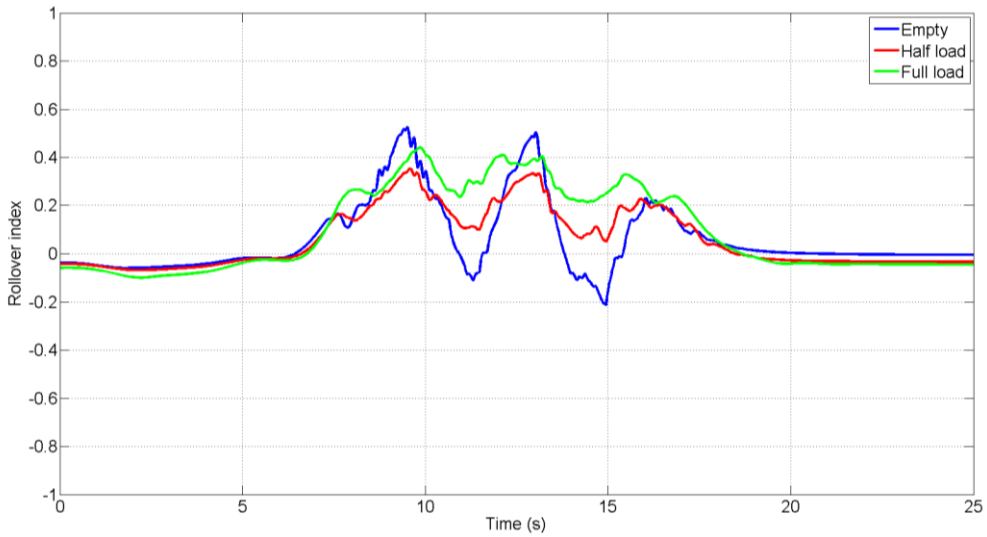

Figure 4-19. Effect of different load conditions on truck rollover index (right turn, 140-ft single-lane roundabout).

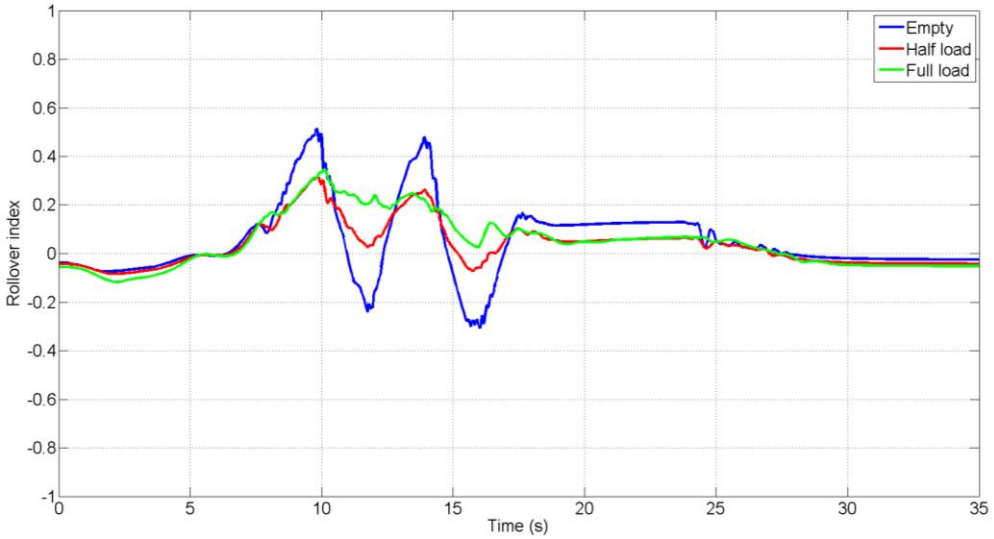

Figure 4-20. Effect of different load conditions on truck rollover index (right turn, 180-ft two-lane roundabout).

Figure 4-19 and Figure 4-20 show that the half-full truck had the lowest RI for both the single-lane and two-lane roundabouts, and surprisingly, the empty truck had the highest RI. The lighter axle load for the empty truck resulted in a smaller denominator in Equation 5-1. Therefore, a larger RI occurred for the side-to-side weight transfer that occurred due to lateral accelerations at the truck's CG. Another way to think of this phenomenon is by considering that a lighter axle has less vertical load holding it down against the road, and therefore it could be more easily unloaded. A heavier axle load, such as the fully-loaded truck, is more heavily loaded against the road and requires more unloading before it reaches zero wheel loads.

The peaks in Figure 4-19 and Figure 4-20 happened during the transition from one steering configuration (roadway curvature) to another, when the truck changed from turning left to turning right and vice versa. The rapid change in roadway elevation at the left edge of the roadway at curvature transitions contributed significantly to the RI peaks. For instance, in roundabouts with 180-ft ICDs, the left edge of the roadway changed from 0 to 6 in. in elevation within 30 ft of travel. Such a rapid change in roadway geometry acted like a lateral impulse force, which in turn acted as a large lateral force at the CG, resulting in proportionally large lateral accelerations, wheel unloading, and RIs. The higher CG for the fully-loaded truck resulted in a somewhat larger RI, as compared with the half-full truck.

The half-full truck's configuration optimized the load on the wheelbase and the mass and position of the truck's CG to create a condition with the lowest maximum RI.

4.7.2 Through-movements

The results of the rollover index for through movements in the 140-ft single-lane roundabout and the 180-ft two-lane roundabout are shown in Figure 4-21 and Figure 4-22, respectively.

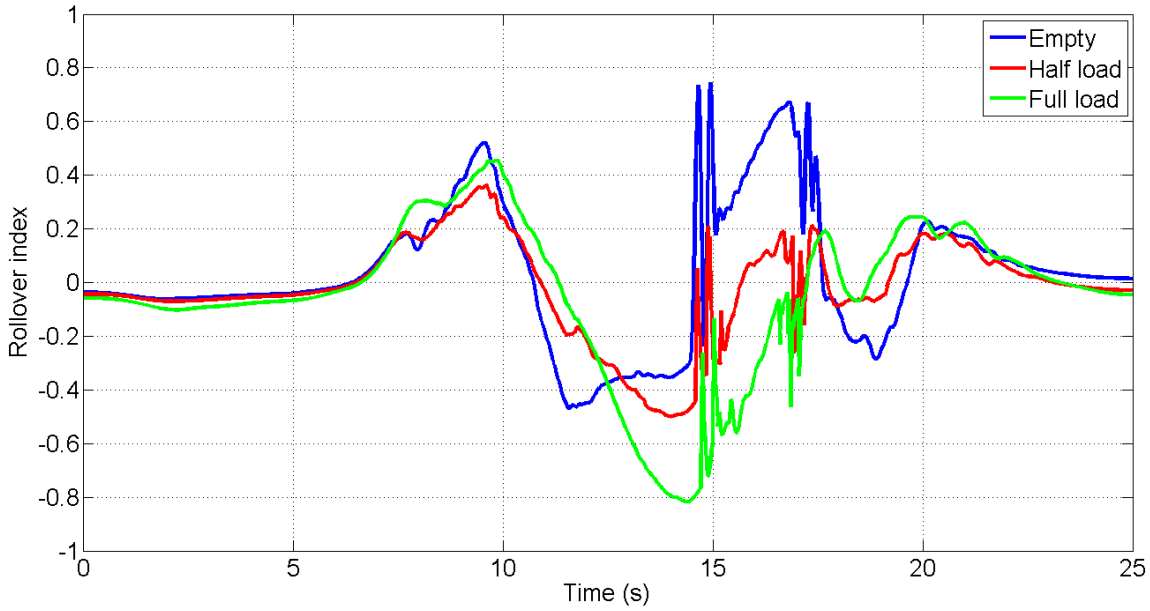

Figure 4-21. Effect of different load conditions on truck rollover index (through-movement, 140-ft single-lane roundabout).

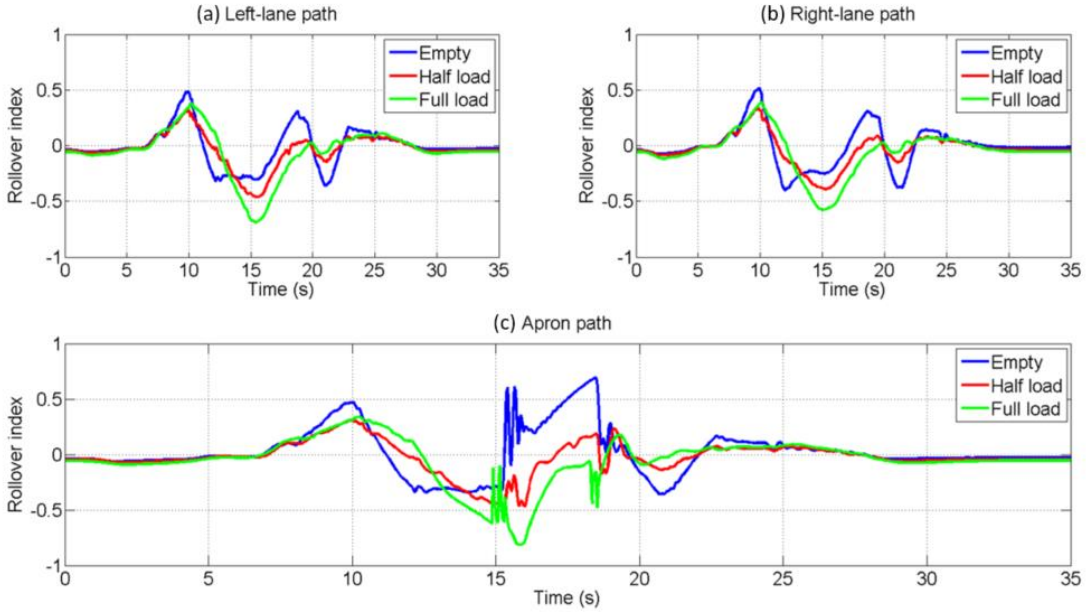

Figure 4-22. Effect of different load conditions on truck rollover index (through-movement, 180-ft two-lane roundabout): (a) left-lane path; (b) right-lane path; (c) apron path.

Figure 4-21 shows that, for through-movements in the single-lane roundabout, the full truck exhibited the highest RI, followed by the empty truck. This was because the empty truck had significantly less axle loads to hold it against the ground. Therefore, it was more sensitive to the road input, indicated by the RI peaks that occurred when the truck was traveling through the road side-to-side elevation transition area (t=8s to t=10s, and t=20s

to t=22s), as well as when encountering the truck apron (t=15s). The half-full truck exhibited a maximum RI of 0.5, indicating it could safely travel through the roundabout. However, the full-load truck's maximum RI reached 0.8 for a reasonably prolonged time (longer than 200 ms), which posed a high risk of rollover.

Figure 4-22 shows the results for through-movements in the two-lane roundabout. The left-lane-path and right-lane-path cases had similar trends as those in the right-turn cases, as shown in Figure 4-22(a) and (b), respectively. The empty truck presented higher RIs during transient response, and lower RIs during steady-state response. The apron-path cases exhibited a similar trend as those in Figure 4-21.

4.7.3 Left turns

The results of the rollover index for left turns in the 140-ft single-lane roundabout and 180-ft two-lane roundabout are shown in Figure 4-23 and Figure 4-24, respectively.

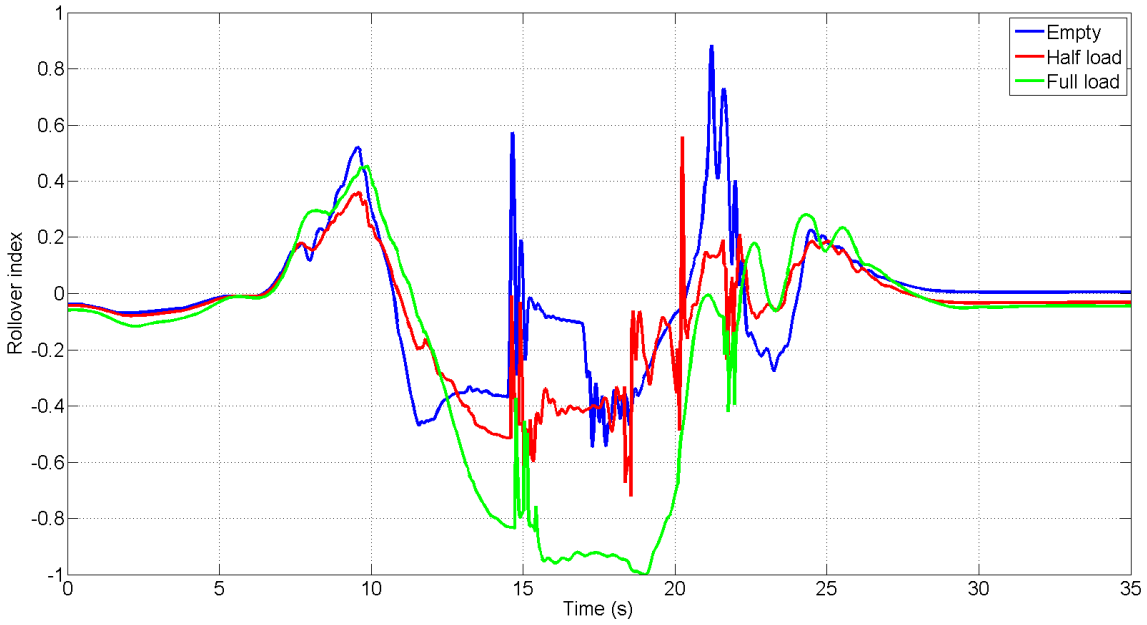

Figure 4-23. Effect of different load conditions on truck rollover index (left turn, 140-ft single-lane roundabout).

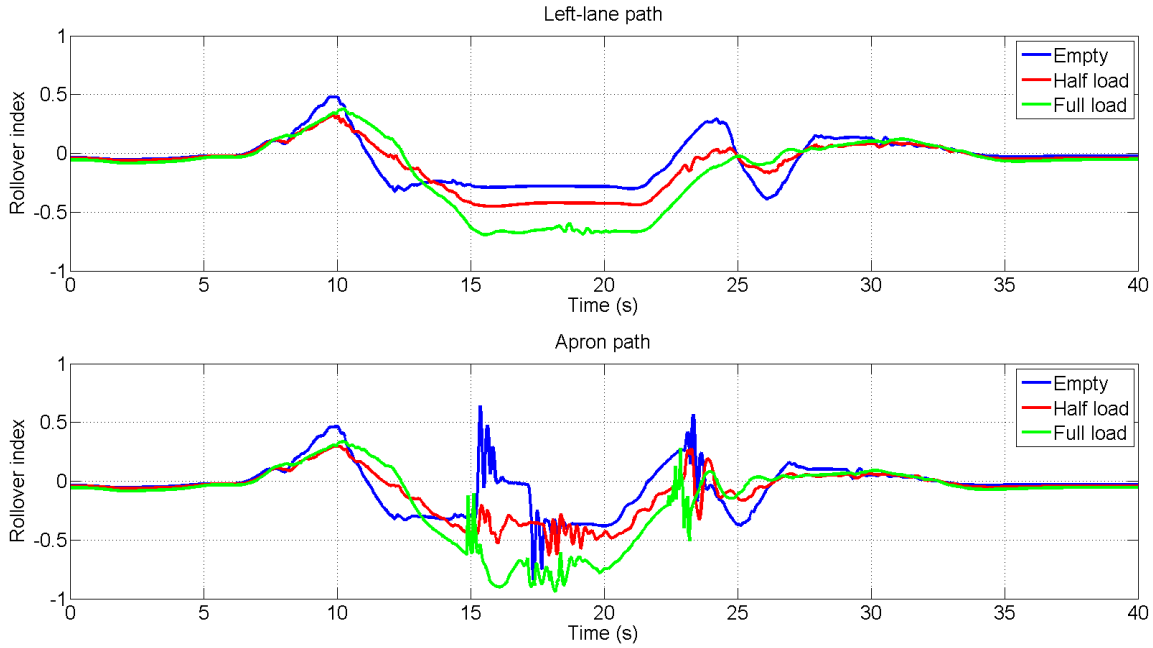

Figure 4-24. Effect of different load conditions on truck rollover index (left turn, 180-ft two-lane roundabout): (a) left-lane path; (b) apron path.

The results in Figure 4-23 and Figure 4-24 are similar in trend to those for through-movements. The empty truck exhibited large RI spikes during transient response to the steering maneuver, rapid road side-to-side elevation change, and truck apron. The full-load truck experienced a strong risk of rollover when performing a left turn using the truck apron, both in the single-lane and two-lane roundabouts. The half-load truck exhibited a maximum RI of 0.6 in the single-lane roundabout, and 0.7 in the two-lane roundabout when following the apron path, indicating that it could travel through these roundabouts safely. All three trucks could stably perform a left turn using the left-lane path through the 180-ft two-lane roundabout.

4.8 Case Study Summary

The results of all five tests are summarized in this section. Maximum RI is used to indicate the strongest truck rollover likelihood during the maneuver in each case. A zero RI represents a perfectly weight-balanced vehicle. A vehicle with an RI lower than 0.8 is capable of traveling through a roundabout and maintaining stability. If maximum RI exceeds 0.8 for a prolonged time, such as 200 ms, the vehicle has a strong likelihood of rollover.

4.8.1 Effect of Circulatory Roadway Cross-section on Truck Roll Stability in Roundabouts

The effect of two circulatory roadway cross-sections on truck roll stability was evaluated in Section 4.3, including a 2% sloping roadway and crowned roadway. The maximum RIs for each case in a 180-ft two-lane roundabout are shown in Figure 4-25.

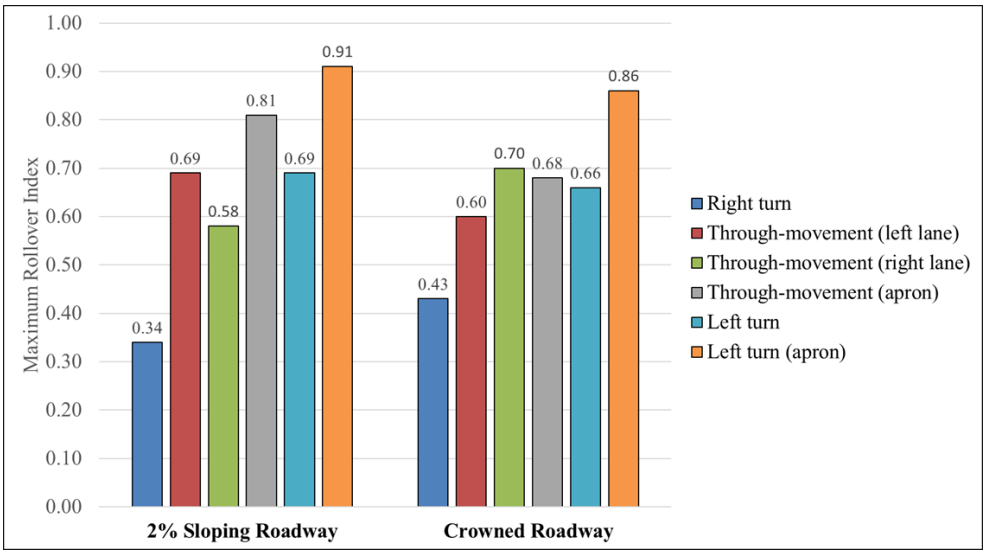

Figure 4-25. Effect of circulatory roadway cross-sections on maximum truck rollover index in a 180-ft two-lane roundabout.

According to Figure 4-25, for right-turn movements, the crowned cross-section caused the truck to have relatively less lateral stability than the sloping cross-section. This occurred because for the crowned roundabout, the left edge of the inner two-thirds of the roadway was lower than the right edge. When the truck occupied the lanes to make a right turn, its left wheels ran on the inner, lower part of the roadway, increasing the truck's tendency to lean to the left side and thereby reducing its lateral stability. However, the RIs for both the sloping and crowned roundabout were low, indicating a low likelihood of rollover.

For the through-movements and left-turns, generally the crowned cross-section had a smaller maximum RI and lower likelihood of rollover than the sloping cross-section. The only exception appeared when trucks followed the right-lane path to perform through-movements. This occurred because the inner two-thirds of the crowned roadway had a 2% inward cross-slope, whereas the outer one-third section had a 2% outward cross-slope. When a truck entered the roundabout in the middle of the right lane, it shifted to the left side and occupied both lanes to perform the first right turn, where the truck ran on the inner

section with an inward cross-slope. However, when it shifted back to the right edge to start circulating the central island, it needed to travel back to the outer section with an outward cross-slope. Such quick opposite road excitation resulted in a rocking motion that increased the RI.

When the trailer rear tires moved onto the truck apron (denoted by '(apron)' in Figure 4-25's legend), the RI was significantly higher than when the truck did not move onto the truck apron. This was mainly because the apron's outward slope, as well as the curb height, caused the truck to lean to the outside in the direction of the centrifugal forces against the trailer, and was also due to transient dynamics caused by the truck moving onto and off of the apron. If the truck did not straddle lanes to make a through-movement or left turn, the crowned roadway resulted in a lower likelihood of rollover than the 2% sloping roadway.

4.8.2 Effect of Roundabout Tilt on Truck Roll Stability in Roundabouts

The entire roundabout was tilted at four separate constant slopes to evaluate the effect of tilted slopes on truck stability in Section 4.4. The maximum RIs for the tilted-slope cases are shown in Figure 4-26 and Figure 4-27 for the 140-ft single-lane and 180-ft two-lane roundabouts, respectively.

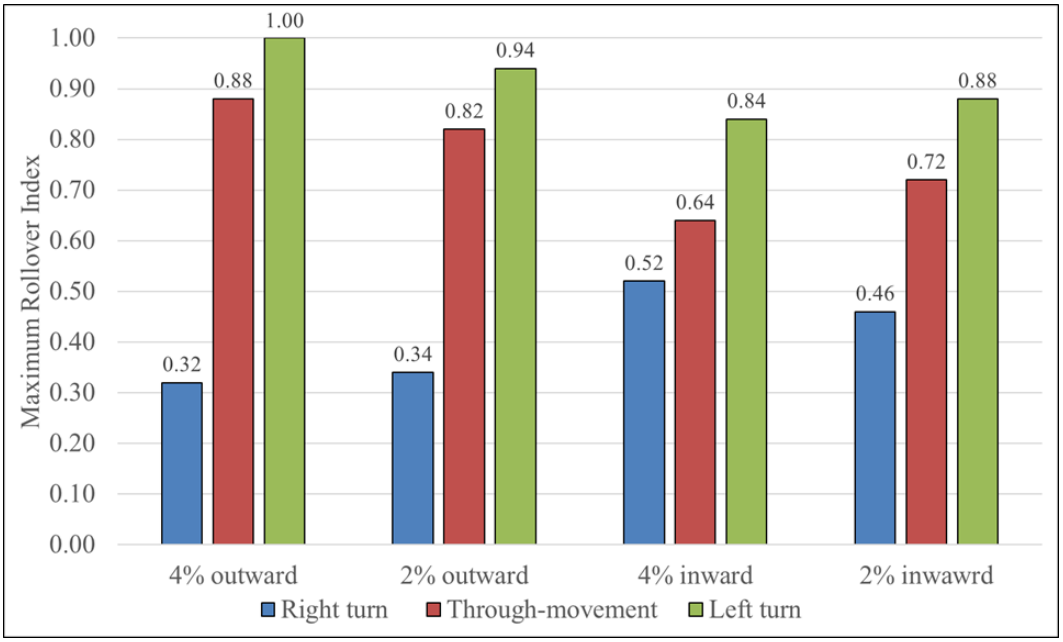

Figure 4-26. Effect of roundabout tilt on maximum truck rollover index in a 140-ft single-lane roundabout.

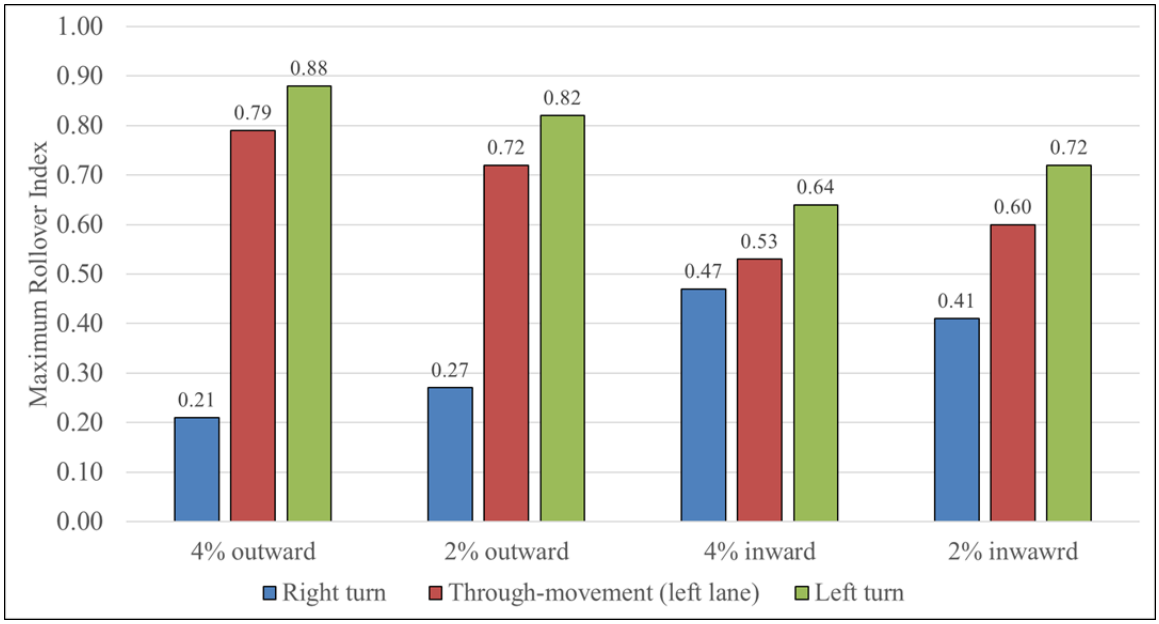

Figure 4-27. Effect of roundabout tilt on maximum truck rollover index in a 180-ft two-lane roundabout.

Figure 4-26 and Figure 4-27 indicate that for right turns, the positive (outward) tilted slopes resulted in better truck lateral stability than negative (inward) tilted slopes. The opposite effect of tilt occurred for through-movements and left turns. At the roundabout entry and exit, negative (inward) tilt increased RI, but in the circulatory roadway, negative (inward) tilt reduced RI. This outcome presents a challenge in terms of designing a roundabout. A positive (outward) tilt would reduce rollover index at the entry and exit, but a negative (inward) tilt would reduce RI in the circulatory roadway. For through-movements and left turns, the RI peaks in the circulating roadway were larger than those at the entry and exit, so moderately tilting the roundabout negatively (inward) would increase truck lateral stability in the areas where it experienced the highest RI. Several elements interact with roundabout tilt to affect truck lateral dynamics, but in general, negative (inward) tilting resulted in better truck lateral stability.

4.8.3 Effect of Truck Configuration on Truck Roll Stability in Roundabouts

Four common truck configurations were modeled, and their roll stability in roundabouts was evaluated in Section 4.5. The maximum RIs for trucks in a 140-ft single-lane and a 180-ft two-lane roundabout are shown in Figure 4-28 and Figure 4-29, respectively.

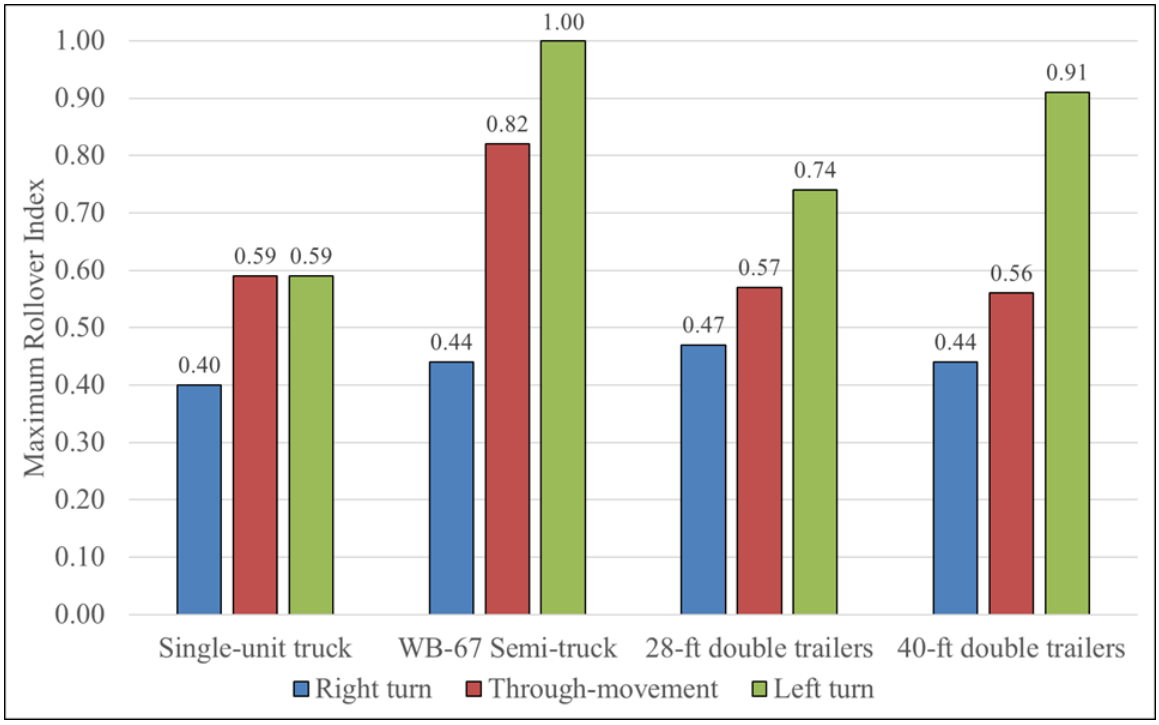

Figure 4-28. Effect of truck configuration on maximum truck rollover index in a 140-ft single-lane roundabout.

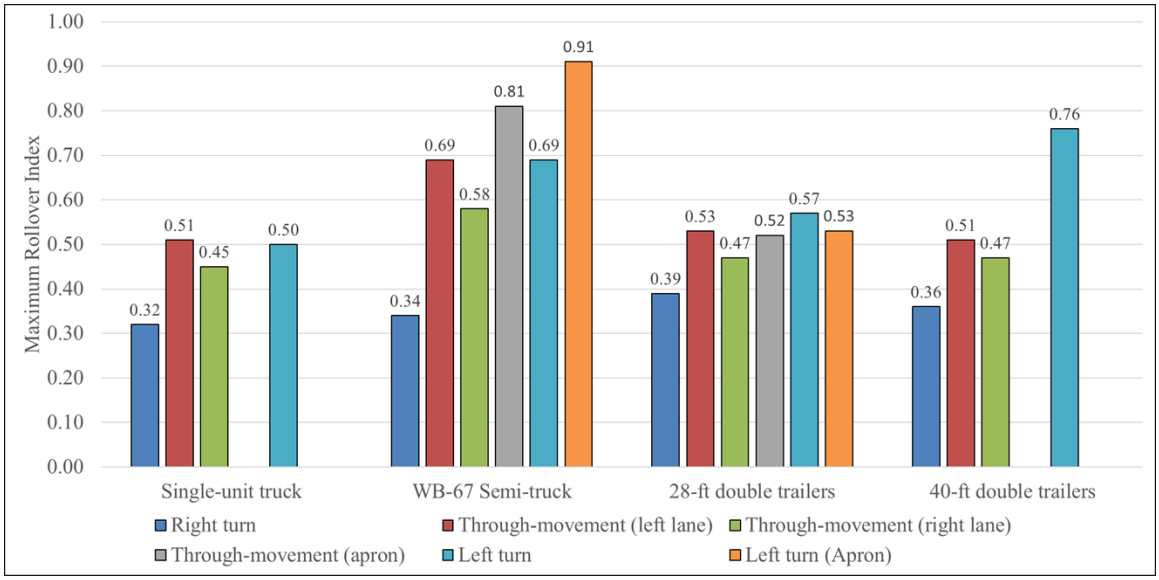

Figure 4-29. Effect of truck configuration on maximum truck rollover index in a 180-ft two-lane roundabout.

According to Figure 4-28 and Figure 4-29, a single-unit truck was more stable than the other three configurations: a WB-67 semi-truck, a 28-ft double trailer, and a 40-ft double trailer, because its maximum RI was always below 0.6. Even though a 28-ft double trailer was longer than a WB-67 semi-truck, each of the trailers was shorter than the semi-truck's

single trailer, and the hitch connection between them allowed the double-trailer configuration to better conform to the roundabout. Additionally, the longer wheelbase and additional hitch connection meant that the double-trailer configuration's second trailer circulated at a lower speed than the semi-truck's trailer, resulting in lower lateral accelerations. Therefore, the 28-ft double trailer exhibited the second-best roll stability in roundabouts. Although the 40-ft double trailer also had double-trailer configuration, the long wheelbase required it to use a truck apron for performing left turns in both single-lane and two-lane roundabouts when following the left-lane path. Therefore, it exhibited high maximum RIs in the single-lane roundabout (0.91) and two-lane roundabout (0.76). The WB-67 semi-truck was more likely to exhibit the greatest maximum RI, indicating the strongest likelihood of rollover, compared to the other three configurations.

4.8.4 Effect of Truck Apron Geometry on Truck Roll Stability in Roundabouts

Two truck apron geometries, the apron curb height and apron cross-slope, were changed from the baseline model to evaluate their effect on truck roll stability in a 180-ft two-lane roundabout in Section 4.6. The maximum RIs for each case are shown in Figure 4-30.

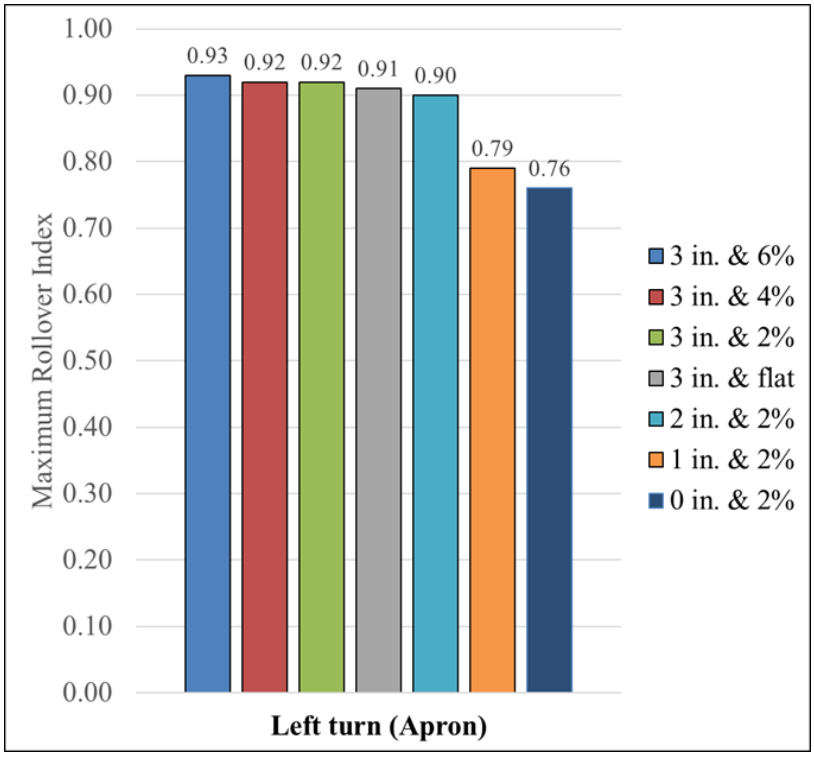

Figure 4-30. Effect of truck apron geometry on maximum truck rollover index in a 180-ft two-lane roundabout.

Figure 4-30 indicates that the trucks exhibited similar maximum RIs when encountering truck aprons with cross-slopes from 6% to flat. However, a lower truck apron curb height could reasonably increase the truck roll stability in roundabouts, in terms of reducing maximum RIs. To be specific, the maximum RI was attenuated from 0.92 (baseline truck apron) to 0.79 when the apron curb height was reduced from 3 in. to 1 in.

4.8.5 Effect of Load Condition on Truck Roll Stability in Roundabouts

Three load conditions were applied to the baseline WB-67 semi-truck to evaluate the effect of load conditions on truck roll stability in roundabouts. The maximum RIs for each load condition are shown in Figure 4-31 and Figure 4-32 for a 140-ft single-lane and 180-ft two-lane roundabout, respectively.

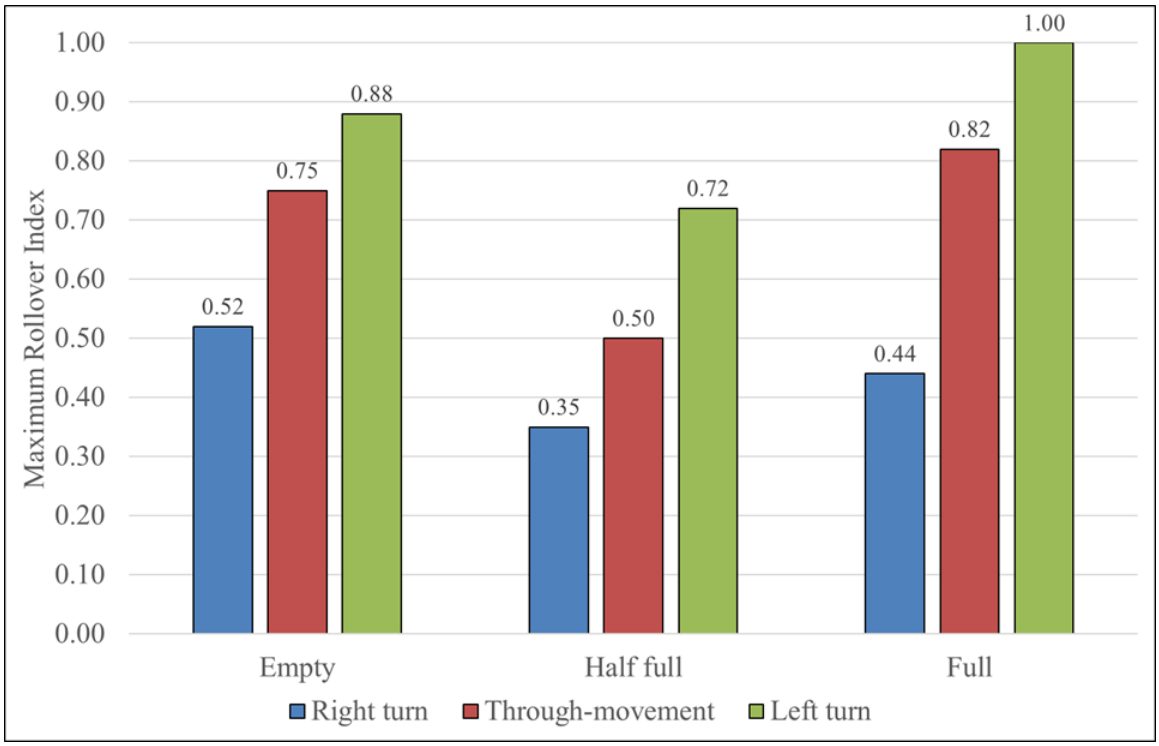

Figure 4-31. Effect of load condition on maximum truck rollover index in a 140-ft single-lane roundabout.

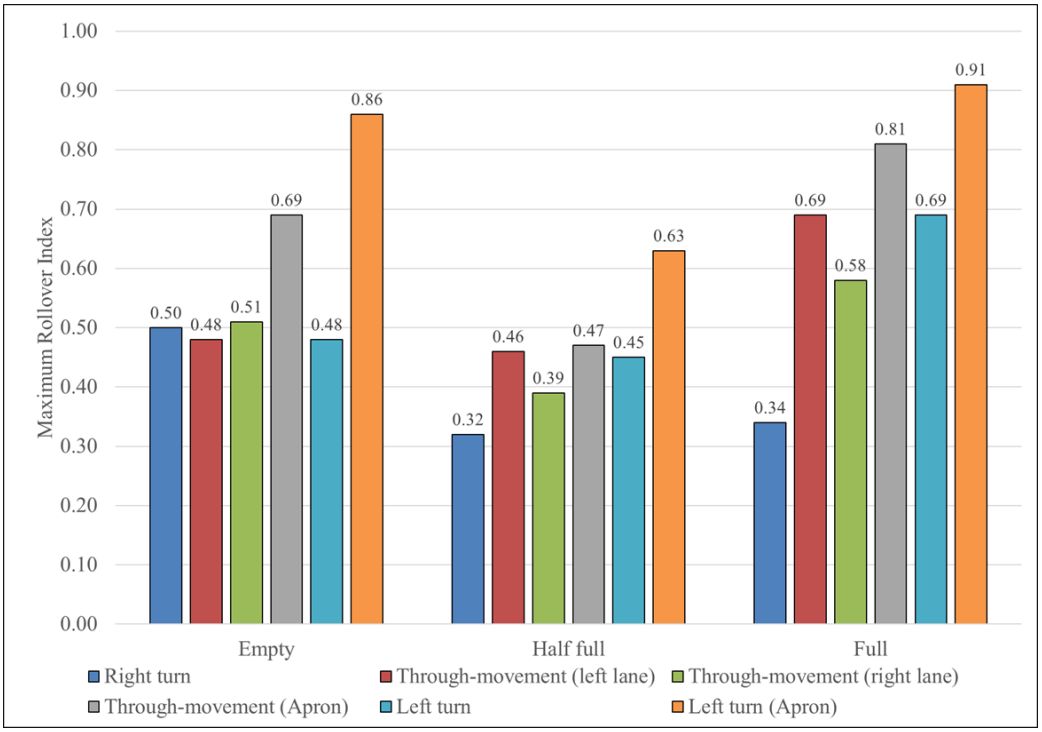

Figure 4-32. Effect of load condition on maximum truck rollover index in a 180-ft two-lane roundabout.

Figure 4-31 and Figure 4-32 both show that the half-load truck presented the best roll stability in roundabouts, indicated by the smallest maximum RI it exhibited in each case, compared to the other load conditions. The empty truck showed higher maximum RIs than the half-load truck because the empty truck had lower inertia to hold it down against the ground, compared to the half-load and full-load trucks. Therefore, it was more sensitive to the dynamic road input, such as the rapid changes in side-to-side road elevation or encountering/leaving a truck apron, resulting in RI spikes as shown in Figure 4-21 to Figure 4-24. Even though these RI spikes experienced by the empty trucks had large values that even exceeded the limit of 0.8, they occurred in a short period of time (less than 200ms) during the transient dynamics, which did not necessarily mean the empty truck experienced strong likelihood of rollover. Based on our experience, in general, the risk of rollover increases significantly when RI exceeds 0.8 for any prolonged period, such as 200 ms. In addition, the fifth-wheel coupling between the tractor and trailer allows very limited roll freedom (~±1°). Hence, the tractor can provide a resistant roll moment in the opposite direction of the trailer's roll motion. Obviously, an empty trailer requires a relatively smaller roll moment from the tractor to hold it from rolling over.

The full-load truck exhibited greater maximum RIs than the other truck configurations when performing through-movements and left turns in both the single-lane and two-lane roundabouts because it had a heavier cargo and a higher CG. Although the empty truck had larger maximum RIs for right turns than the full-load truck, they were all under 0.52, indicating safe maneuvers through roundabouts. In summary, the full-load truck, as perhaps is intuitively clear, posed a higher risk of rollover than the half-load and empty trucks.

Chapter 5 – Overview of Truck Dynamics in High-speed Driving Conditions

This chapter provides an overview of the dynamics of Class 8 heavy trucks and their roll stability at high speeds, particularly for trucks with double trailers. An introduction on typical Class 8 articulated trucks is given. The dynamic stability issues of trucks with double trailers are then reviewed, followed by a discussion about dynamic elements that affect double-trailer stability. A summary is provided at the end of the chapter.

5.1 Introduction of Class 8 Trucks

As introduced in Section 2.1, a Class 8 truck is defined as a truck that has a gross weight rating greater than 33,000 lb. For a Class 8 truck in an articulated configuration, it is normally composed of a lead unit, and one or multiple trailing unit(s). The lead unit is at the front of the configuration, possesses one or more steering axles, and normally provides power to move the entire vehicle combination. Trailing units, which are commonly known as trailers, can be categorized into two main classes: full trailers and semitrailers. A full trailer possesses both front and rear running gears, and a pintle hitch coupling is normally used to tow a full trailer and provide steering input. On the contrary, a semitrailer only possesses rear running gear, indicating that it requires the towing unit to provide vertical support when traveling or parking. Such support can be provided by a tractor, or a converter dolly that "converts" the semitrailer into a full trailer. A semitrailer commonly uses a kingpin to connect to a fifth-wheel coupling installed on the towing unit, which provides towing force and steering input to the semitrailer. An articulated heavy truck could have one or multiple semitrailers or full trailers. The conventional WB-67 semi-trucks (a tractor and a 53-ft box van trailer), which are also known as 53-footers, are the most common Class 8 trucks operated for highway freight transport in the United States. Most existing studies on heavy truck dynamics are focused on WB-67 semi-trucks due to the vast volume of these vehicles. However, Class 8 trucks in double-trailer configurations are becoming more and more favored by freight carriers for operational efficiency, and there are relatively few in-depth studies that have been conducted on the dynamics and stability of trucks with double trailers.

There are three common configurations for Class 8 trucks with double trailers: A-train, B-train, and C-train. The A-train consists of a tractor, two semi-trailers, and a converter dolly that "converts" one of the semi-trailers to a full-trailer, as shown in Figure 5-1. Fifth-wheel couplings are employed to connect the tractor and the front trailer, as well as the converter dolly and the rear trailer. The front trailer and the dolly are coupled with a pintle hitch coupling. A converter dolly with such a coupling mechanism is called an "A-dolly," as shown in Figure 5-2. There are also "B-dolly" and "C-dolly" configurations that have different coupling mechanisms compared with A-dollies, which have been introduced in Section 2.1.

Figure 5-1. An example of a 28-ft A-train double.

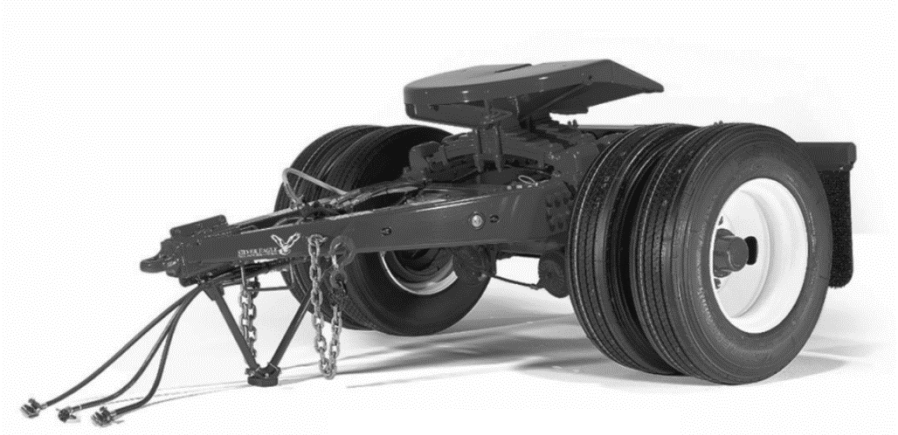

Figure 5-2. An example of A-dollies commonly used in trucks with multi-trailers. (http://glasvangreatdane.com/products/converter_dollies/, accessed August 2017)

In the Surface Transportation Assistance Act (STAA) of 1982, Congress extended the Federal interest to length issues and to highways beyond the Interstate System by requiring all States to permit the operation of 48-foot long semitrailers and twin-trailer combinations

with trailing units to 28-ft long on the Interstate System and on other non-Interstate, Federal-aid, primary system highways to be designated by the Secretary of Transportation [13]. Therefore, trucks with double 28-ft trailers are also referred to as "STAA Doubles" in some documents. After the STAA of 1982 was enacted, trucks with double 28-ft trailers were permitted to be operated in 14 Eastern States from Maine to Florida. In 2000, it was reported that STAA doubles represent approximately 2.5 percent of all truck combinations [13].

A-train trucks, especially those that have dual 28-ft trailers, are commonly operated in Eastern States for freight transport. These 28-ft A-train doubles have many advantages compared with trucks with 53-ft trailers. For example, a 28-ft A-train double has two shorter trailers and three DOF in yaw motion due to additional couplings between the dolly and trailers, as compared to a tractor with a 53-ft trailer. Therefore, a 28-ft A-train double is more flexible and can better negotiate tighter curves in urban areas than a single 53-ft trailer. More importantly, A-train doubles have also better logistic adaptability and efficiency because of the two trailers. For instance, if Location A needs to send one trailer to Location B and another trailer to Location C while Location B also wants to send one trailer to Location C, the company can just send one truck from A to B, drop one trailer, pick up the other one, and then head for C. In this case, the truck does not necessarily have to wait for loading or unloading at Location B, and thus obtains better efficiency.

5.2 Dynamic Stability Issues of Trucks with Double Trailers

The additional couplings and extra trailer bring many benefits to A-train doubles, but unfortunately, they tend to cause stability problems at the same time. One of the most well-known issues is "Rearward Amplification," which generally means the lateral accelerations experienced by the last trailer are higher than that for the tractor. This phenomenon normally occurs when trucks with multiple trailers travel at high speeds and perform a quick steering maneuver, such as those applied in obstacle-avoidance scenarios.

The rearward amplification can lead to severe traffic accidents. The large lateral forces experienced by the rear trailer can result in excessive roll moments that roll over the entire truck. In addition, rearward amplification also leads to aggressive lateral motion on the

rear trailer, especially when traveling on low-friction surfaces. This swing motion of the rear trailer could result in collisions with other vehicles in adjacent lanes or could trigger jackknifing accidents. Rollover and jackknifing are the two types of accidents commonly experienced by heavy trucks that cause high fatality rates and property damage.

Besides the inherent dynamic stability issues mentioned above, the driver's performance is also an important factor that affects heavy truck safety. For a single-unit vehicle like normal passenger cars, the driver could directly receive feedback from the vehicle and react accordingly when that sensing an unstable situation is about to happen. For semi-trucks, the fifth-wheel coupling between the tractor and the semitrailer can transfer the trailer's roll motion to the tractor and therefore could be sensed by the driver. However, the pintle hitch coupling used in an A-train double cannot transfer any moment from dolly to front trailer. Thus, the driver cannot sense any roll motion of the rear trailer without checking rearview mirrors, and before the rear trailer experiences a strong likelihood of rollover. In addition, even though the pintle hitch coupling is capable of transferring lateral and longitudinal forces to the front trailer in theory, these forces are applied to the front trailer first, and what the driver could sense is the response of the front trailer through a fifth-wheel coupling. Therefore, the driver of an A-train double cannot directly sense the roll or yaw motion of the rear trailer and react correctly when an unstable situation is about to occur. Considering that the rear trailer is the least stable unit of an A-train double, and the use of 28-ft A-train doubles is increasing, it is necessary for vehicle engineers and researchers to dig deeper into the dynamics of A-train doubles and find ways to enhance their stability. It is noted that the pintle coupling will lockup and prevent further relative roll motion between the drawbar and pintle hook when the angle is over ~20 degrees. However, tractors and trailers that are commonly operated in the U.S. would experience a strong likelihood of rollover with a roll angle greater than 10 degrees. Therefore, the pintle coupling would not transfer any relative roll motion between the dolly and front trailer until a rollover event happens.

5.3 Dynamic Elements that Affect the Stability of Trucks with Double Trailers

This section introduces identified elements that can be modified to increase the stability of trucks in the A-train configuration. There are other dynamic factors that can affect A-train double stability, such as traveling speed, fifth-wheel locations, trailer CG locations, etc. However, this section is focused on dynamic elements particularly pertaining to the A-train configuration, as well as on external stability enhancement systems that could be potentially applied to A-train doubles.

5.3.1 Pintle Coupling

A pintle coupling that is commonly used on trucks with an A-train configuration consists of two parts–a pintle hook at the front of the converter dolly and a drawbar at the end of the trailer–as shown in Figure 5-3.

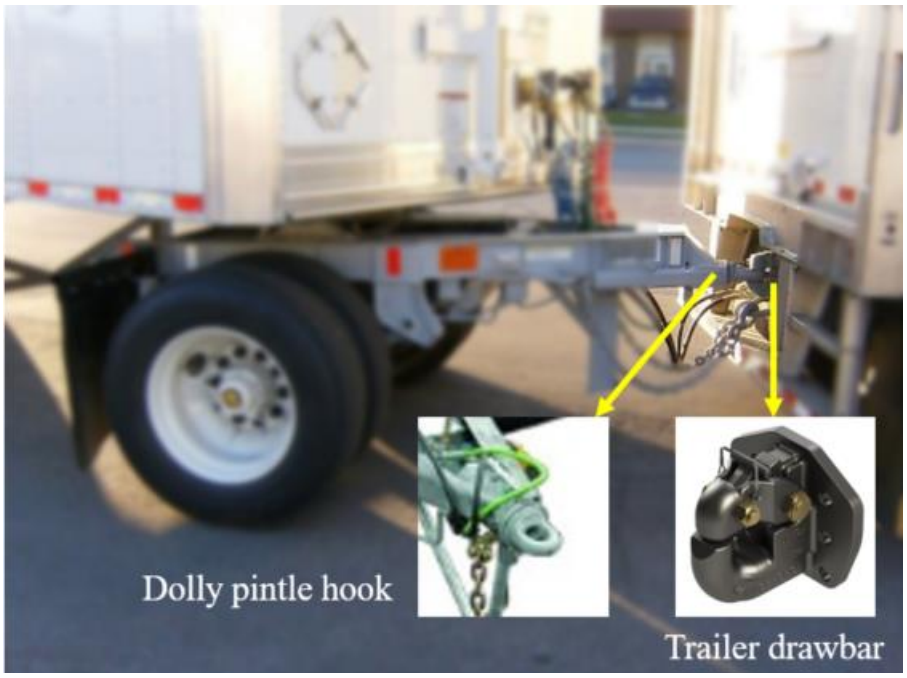

Figure 5-3. An example of pintle couplings commonly applied to trucks in an A-train configuration.

As discussed before, using an A-dolly to connect two trailers results in two additional degrees of freedom (DOF) and makes the entire truck have three DOF in yaw plane. The additional DOF in yaw plane contribute to the rearward amplification effect, especially when rapid-steering maneuvers are performed. Moreover, the pintle coupling cannot

transfer rotational motion between two adjacent vehicle units due to the free-play between the pintle hook and drawbar. Therefore, the rear trailer of an A-train double cannot receive a stabilizing effect from the front trailer when it experiences aggressive roll motion, compared to fifth-wheel couplings that only allow a relative roll angle of ~2 degrees between two adjacent units.

Previous studies ([12] and [60]) have indicated that A-dollies considerably reduced the stability of trucks with double trailers at high speeds, and different configurations for double trailers and converter dollies have been designed and applied to solve this issue [10]. Figure 5-4 shows a B-train double that is also commonly operated in North America. Trucks in B-train configuration do not use a converter dolly to connect two trailers. Instead, the front trailer of a B-train double has an extended chassis with a fifth-wheel plate attached to the end. A B-train double has three vehicle units and two DOF for yaw motion, which is one vehicle unit and one DOF less than an A-train double. In addition, two fifth-wheels couplings are used to connect the three vehicle units where roll moment could be transferred between adjacent units. This would increase truck roll stability because the rear trailer could receive a stabilizing effect from the front trailer. In general, B-train doubles have better directional stability than A-train doubles. However, the two trailers in a B-train configuration are not interchangeable due to the front trailer's extended chassis with a fifth-wheel plate, and a B-train double also results in larger off-tracking that makes it less flexible for negotiating local roads with tight turns. These disadvantages of B-train doubles considerably increase logistical issues and thus limit their usage within freight carriers.

Figure 5-4. An example of a B-train double. (http://www.1-87vehicles.org/photo609/volvo_vt64t800_b-train_chalut.php, accessed August 2017)

Figure 5-5 shows an alternative configuration for converter dollies. This so-called "C-dolly" is similar to an A-dolly but it has two drawbars, compared to an A-dolly that has one. The application of a C-dolly can eliminate one DOF from yaw motion and provide roll moment transfer to a certain extent. Therefore, a C-train double has two DOF for yaw motion, and the front trailer could provide a stabilizing effect to the rear trailer while keeping the two trailers interchangeable. However, based on the feedback from both logistics companies and truck drivers, hooking up an A-train double already requires more skill and experience from a driver than hooking up a tractor to a semitrailer. Unfortunately, the dual-drawbar coupling of C-dollies demands even more skill to connect it to a trailer. Therefore, logistics companies are concerned that operating C-train doubles would require extensive driver training and increase the risk of faulty trailer-dolly connection.

Figure 5-5. An example of a C-dolly. (http://itec-inc.com/dolly/c-dolly.html, accessed August 2017)

There are other innovative designs for converter dollies, such as a forced steer dolly, A-dolly with a lockable drawbar, A-dolly with an additional linkage attached directly from trailer to trailer, etc. [8]. These dolly designs are mainly focused on improving the dynamic performance of multi-trailer vehicles. However, they have not been widely applied due to the price, maintenance cost, or the skill required for drivers to correctly connect them to a trailer.

5.3.2 Trailers with Different Load Combinations

The dual-trailer configuration in an A-train double can result in four load combinations, since each trailer could be loaded independently. The four combinations are empty-front with empty-rear, loaded-front with empty-rear, empty-front with loaded-rear, and loaded-

front with loaded-rear. Different load combinations may lead to different directional stability. This is because an A-train double behaves as a three-DOF mechanical system with dampers and springs in yaw plane, where different inertial parameters will change the damping effect of the system and therefore affect the stability.

Hazemoto [26] studied the effect of different load combinations on a tractor with two 24-ft double trailers, concluding that for all four load permutations mentioned above. The configuration of loaded-front with empty-rear resulted in the best stability, followed by empty-front with empty-rear, whereas the empty-front with loaded-rear led to the worst stability. Such conclusions have also been drawn and commonly practiced by fleet operators based on empirical knowledge. However, they might not hold true when the truck is equipped with a brake-based electronic stability control (ESC) system. This is because such systems are more effective with a heavier axle load, and thus the order of how those four load combinations affect truck stability may change.

5.3.3 Electronic Stability Enhancement Systems

There are two types of electronic stability enhancement systems that are commonly equipped on heavy trucks. The first one is tractor-based Electronic Stability Control (ESC) systems. An ESC system continuously monitors truck dynamics by measuring air spring pressure, yaw rate, lateral acceleration, steering wheel angle, etc. The air spring pressure is for estimating truck load and determining the activation threshold from an embedded look-up table. The yaw rate and lateral acceleration are used to evaluate the truck lateral dynamic situation and compare it with the activation threshold. The steering wheel input is necessary for better predicting the driver's behavior. When a threshold is exceeded and the ESC system decides to engage, it normally cuts off throttle first, and then applies brakes to the tractor wheels. Some ESC systems would brake all wheels to achieve the best speed reduction, whereas other systems would selectively brake certain wheels, such as those on the outside of the turn, to generate a counter-yaw moment while decreasing the speed at the same time.

The other system commonly equipped on trailers is normally referred to as the Roll Stability Control (RSC) system. This system is similar to an ESC system but does not have

the ability to measure steering or throttle input. In general, different RSC systems monitor similar vehicle information, but their methods of engagement can vary significantly. For example, some RSC systems designed for double-trailer configurations can share information between the units on two trailers. More specifically, when the unit on the front trailer senses a rollover risk, it warns the unit on the rear so that the two units can apply brakes to all trailer axles together for better speed reduction. For other RSC systems, the front and rear units might not be able to communicate with each other, but they apply different algorithms or strategies (i.e. monitoring of the magnitude or changing rate of lateral accelerations) for determining when is the best time to engage and how the brakes be applied.

Unfortunately, there are very few studies discussing ESC and RSC control algorithms, due to the fact that they are often proprietary to manufacturers. Some studies applied simplified ESC or RSC control algorithms in their simulations, such as activating the system when lateral accelerations exceed a certain value. However, it is known for a fact that commercial ESC or RSC systems currently available in the market are far more complicated. For instance, these systems normally include embedded look-up tables that were derived based on extensive field tests.

Starting in 2015, NHTSA requires that all truck tractors and certain large buses with a GVWR greater than 11,793 kg (26,000 lb) be equipped with an ESC system [3]. This regulation was determined based on the results of a series of field tests conducted by NHTSA [57, 58]. However, the test trucks applied in these programs were all in single-trailer configurations. Thus, it is necessary to further examine how the regulated tractor-based ESC and potential trailer-based RSC systems would behave on trucks with double trailers.

5.3.4 Pneumatic Suspension Systems

For passenger cars, suspension systems mainly affect vehicle ride comfort and handling. However, for heavy trucks, the effect of suspension systems on truck roll stability is also a significant factor that needs to be considered. Most of the trucks operated in the United States are equipped with pneumatic suspensions on both tractors and trailers. Stock

pneumatic suspensions normally have one or two airbags installed at each end of an axle. These airbags are connected by hoses in series with equal pressures. The stock configuration only uses one leveling valve to supply or purge air for all airbags in order to maintain the truck at a constant ride height despite how much load is applied, which is cost-efficient and requires the least maintenance work. Unfortunately, this configuration is not favored for truck roll stability.

When a vehicle is turning, ideally the stiffness of the inside suspension should be decreased while the outside should be increased in order to attenuate vehicle body roll. The changing of stiffness for pneumatic suspensions can be achieved by charging or discharging airbags. For common stock pneumatic suspension systems, the airbags on the left and right sides are interconnected, and hence they tend to have equal pressures all the time. When the inside airbags are compressed during cornering, the air would be pushed out to the other side to main the same pressures, which reduces the stiffness of the inside airbags. Therefore, stock pneumatic suspensions are not favored for preventing trucks from rollovers.

Many active or semi-active anti-roll suspension systems have been designed and tested. One of them is called "Balanced Pneumatic Suspension System," as introduced in Section 2.4.4. This system employs two leveling valves to independently control left and right airbags, where the inside airbags will be charged to gain larger stiffness when the truck is turning, and meanwhile the outside airbags will be discharged to reduce stiffness. This mechanism tends to actively reduce the truck body roll by bringing it back to a balanced position during cornering, and therefore the truck roll stability can be enhanced. This balanced pneumatic suspension system has been thoroughly studied in [68].

Chapter 6 – Simulation-based Directional Dynamics Analysis of 28-ft A-train Doubles

This chapter provides the development of mathematical models of 28-ft A-train doubles in yaw-roll plane for studying the mechanics that govern the directional dynamics of A-train trucks. The same truck is also modeled in TruckSim, and the simulation results are used to validate the mathematical models. Parametric analyses are conducted based on the mathematical model in order to investigate the effect of identified parameters on rearward amplification.

6.1 Mathematical Vehicle Models

A typical 28-ft A-train double that is commonly operated by logistics companies for highway cargo transport in the North America is selected here, as shown in Figure 6-1. This truck combination consists of one three-axle tractor, two single-axle van box trailers, and one single-axle converter dolly ("A-Dolly").

Figure 6-1. A typical 28-ft A-train double that is commonly operated in the United States. (https://www.flickr.com/photos/scottash/15096687894, accessed August 2017)

Two models are developed for studying the directional dynamics of the truck. First, a five-DOF handling dynamics model is created in yaw plane to derive vehicle lateral accelerations and articulation angles with certain steering inputs. The lateral accelerations are then input to a single-DOF model in roll-plane to investigate the roll dynamics of each vehicle unit. The development of these two models is detailed in the following sections.

6.1.1 Yaw-Plane Model

A "bicycle-with-three-unicycles" configuration with five DOF is developed to model the handling dynamics of the 28-ft A-train double in yaw plane, shown in Figure 6-2 and Figure 6-3. This model is similar to that in [25], but state-space representation and ISO coordinate systems are applied here, where the x-axis points forward, the y-axis points to the left, and the z-axis points upward. The nomenclature is included in Table 6-1.

Some assumptions are made for simplicity, including:

- All angles are sufficiently small
- Constant forward speed
- No lateral or longitudinal load transfer
- No roll or pitch motion
- No suspension or steering compliance effects
- No aerodynamics
- No rotational constraints or resistance at all couplings
- Constant cornering stiffness for all tires
- The total lateral force generated on a certain axle is calculated by multiplying the number of wheels on this axle and the lateral force generated on one wheel
- Flat road surface

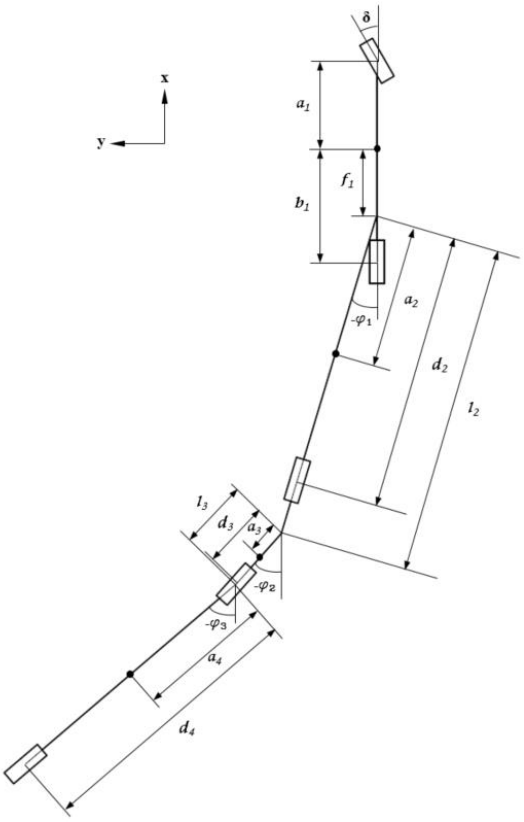

Figure 6-2. The handling dynamics model for an A-train double.

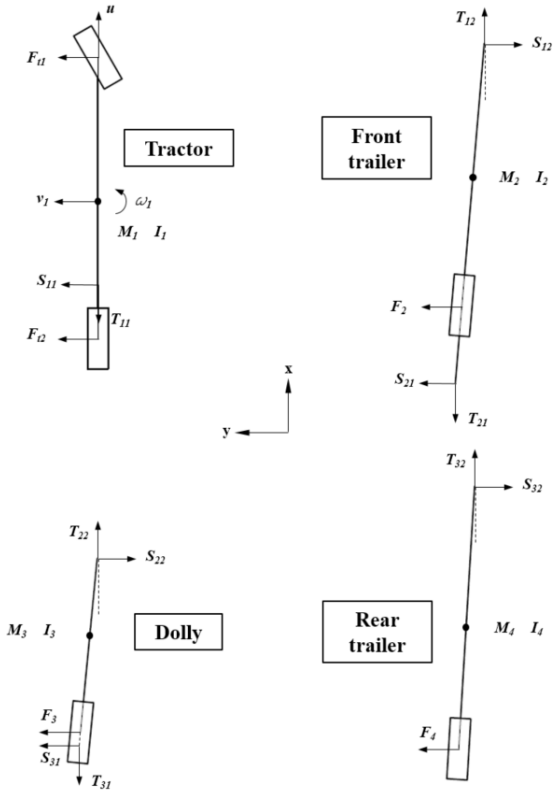

Figure 6-3. The free-body diagram of each individual vehicle unit model.

Table 6-1. Nomenclature for the handling dynamics model.

Variable	Definition	Variable	Definition
a_1	Distance between tractor CG location and steering axle	S_{11}	Lateral force on tractor fifth-wheel plate
b_1	Distance between tractor CG location and rear axle	T_{11}	Longitudinal force on tractor fifth-wheel plate
f_1	Distance between tractor CG location and tractor fifth-wheel	M_2	Front trailer mass
a_2	Distance between front trailer kingpin and front trailer CG location	I_2	Front trailer yaw inertia
d_2	Distance between front trailer kingpin and front trailer axle	F_2	Lateral force on front trailer axle
l_2	Distance between front trailer kingpin and front trailer drawbar	S_{12}	Lateral force on front trailer kingpin
a_3	Distance between dolly pintle hook and dolly CG location	T_{12}	Longitudinal force on front trailer kingpin
d_3	Distance between dolly pintle hook and dolly axle	S_{21}	Lateral force on front trailer drawbar
l_3	Distance between dolly pintle hook and dolly fifth-wheel	T_{21}	Longitudinal force on front trailer drawbar
a_4	Distance between rear trailer kingpin and rear trailer CG location	M_3	Dolly mass
d_2	Distance between rear trailer kingpin and rear trailer axle	I_3	Dolly yaw inertia
δ	Steering angle	F_3	Lateral force on dolly axle
φ_1	Articulation angle between tractor and front trailer	T_{22}	Lateral force on dolly pintle hook
φ_2	Articulation angle between front trailer and dolly	S_{22}	Longitudinal force on dolly pintle hook
φ_3	Articulation angle between dolly and rear trailer	T_{31}	Lateral force on dolly fifth-wheel plate
u	Tractor longitudinal speed	S_{31}	Longitudinal force on dolly fifth-wheel
v_1	Tractor lateral speed	M_4	Rear trailer mass
ω_1	Tractor yaw rate	I_4	Rear trailer yaw inertia
M_1	Tractor mass	F_4	Lateral force on rear trailer axle
I_1	Tractor yaw inertia	T_{32}	Lateral force on rear trailer kingpin
F_{t1}	Lateral force on tractor steering axle	S_{32}	Longitudinal force on rear trailer kingpin
F_{t2}	Lateral force on tractor rear axle		

The lateral motion of the tractor is described by lateral velocity and yaw rate, and the motion of the trailers and dolly are determined based on their articulating motion with respect to the tractor. For the tractor, its traveling speed is given by:

$$V = u\hat{\imath} + v_1\hat{\jmath} \tag{6-1}$$

where $\hat{\imath}$ and $\hat{\jmath}$ are unit vectors attached to the vehicle body on the x- and y-axis, respectively. The longitudinal and lateral accelerations can be derived by taking the derivatives of both sides of the equation with respect to time, which yields:

$$\frac{dV}{dt} = \dot{u}\hat{\imath} + u\dot{\hat{\imath}} + \dot{v}_1\hat{\jmath} + v\dot{\hat{\jmath}} \tag{6-2}$$

Considering $\dot{\hat{\imath}} = \omega_1\hat{\jmath}$ and $\dot{\hat{\jmath}} = -\omega_1\hat{\imath}$, Equation. 6-2 can be written as:

$$\frac{dV}{dt} = \dot{u}\hat{\imath} + u\omega_1\hat{\jmath} + \dot{v}_1\hat{\jmath} - v_1\omega_1\hat{\imath}$$

$$\frac{dV}{dt} = (\dot{u} - v_1\omega_1)\hat{\imath} + (\dot{v}_1 + u\omega_1)\hat{\jmath} \tag{6-3}$$

Therefore, the lateral acceleration on the tractor can be calculated as:

$$a_{y_1} = \dot{v}_1 + u\omega_1 \tag{6-4}$$

Similarly, the lateral accelerations for the trailers and the dolly are derived as follows:

$$\text{Front trailer:}\quad a_{y2} = \dot{v}_1 + u\omega_1 - (f_1 + a_2)\dot{\omega}_1 - d_2\ddot{\varphi}_1 \tag{6-5}$$

$$\text{Dolly:}\quad a_{y3} = \dot{v}_1 + u\omega_1 - (f_1 + l_2 + a_3)\dot{\omega}_1 - l_2\ddot{\varphi}_1 - a_3\ddot{\varphi}_2 \tag{6-6}$$

$$\text{Rear trailer:}\quad a_{y4} = \dot{v}_1 + u\omega_1 - (f_1 + l_2 + l_3 + a_4)\dot{\omega}_1 - l_2\ddot{\varphi}_1 - l_3\ddot{\varphi}_2 - a_4\ddot{\varphi}_3 \tag{6-7}$$

Based on Newton's Second Law, the equations of motion (EOM) for the tractor can be derived by summing all forces and moments applied to it, which yields:

$$M_1 a_{y1} = F_{t1} + F_{t2} - S_{11} \tag{6-8}$$

$$I_1\dot{\omega}_1 = F_{t1}a_1 - S_{11}f_1 - F_{t2}b_1 \tag{6-9}$$

The lateral motion of the front trailer is represented by its relative articulating motion with respect to the tractor. Therefore, the EOM of the front trailer is given by:

$$T_{12} + F_2(-\varphi_1) + T_{21} = 0 \tag{6-10}$$

$$M_2 a_{y2} = S_{12} + F_2 + S_{21} \tag{6-11}$$

$$I_1(\dot{\omega}_1 + \ddot{\varphi}_1) = S_{12}a_2 + T_{12}(-\varphi_1)a_2 - F_2(d_2 - a_2) - T_{21}(-\varphi_1)(l_2 - a_2) - S_{21}(l_2 - a_2) \tag{6-12}$$

Similarly, the lateral motion of the dolly and rear trailer are also determined by their relative articulating motion to the tractor. Their EMO are obtained as:

$$T_{22} + F_3(-\varphi_2) + T_{31} = 0 \tag{6-13}$$

$$M_3 a_{y3} = S_{22} + F_3 + S_{31} \tag{6-14}$$

$$I_2(\dot{\omega}_1 + \ddot{\varphi}_2) = S_{22}a_3 + T_{22}(-\varphi_2)a_3 - F_3(d_3 - a_3) - T_{31}(-\varphi_2)(l_3 - a_3) - S_{31}(l_3 - a_3) \tag{6-15}$$

$$T_{32} + F_4(-\varphi_3) = 0 \tag{6-16}$$

$$M_4[\dot{v}_1 + u\omega_1 - (f_1 + l_2 + l_3 + a_4)\dot{\omega}_1 - l_2\ddot{\varphi}_1 - l_3\ddot{\varphi}_2 - a_4\ddot{\varphi}_3] = F_3 + S_{32} \tag{6-17}$$

$$I_4(\dot{\omega}_1 + \ddot{\varphi}_3) = T_{32}(-\varphi_3)a_4 + S_{32}a_4 - (d_4 - a_4)F_4 \tag{6-18}$$

All the forces and their corresponding reaction forces at couplings are assumed to have the same magnitude but opposite directions, represented by:

$$\left.\begin{array}{l} T_{11} + T_{12} = 0 \\ S_{12} + S_{11} = 0 \\ T_{21} + T_{22} = 0 \\ S_{21} + S_{22} = 0 \\ T_{31} + T_{32} = 0 \\ S_{31} + S_{32} = 0 \end{array}\right\} \tag{6-19}$$

The lateral tire forces are assumed to be proportional to slip angles. In other words, constant cornering stiffness is applied in this study. Therefore, the lateral force on each tire is given by:

$$\left.\begin{array}{l} F_{t1} = \alpha_{t1} C_F \\ F_{t2} = \alpha_{t2} C_R \\ F_i = \alpha_i C_T \ \ (i = 2,3,4) \end{array}\right\} \qquad (6-20)$$

where α_{t1}, α_{t2}, α_2, α_3, and α_4 represent tire slip angles on the tractor front axle, tractor rear axle, front trailer axle, dolly axle, and rear trailer axle, respectively; C_F, C_R, and C_T denote the combined cornering stiffness for the tractor front axle, tractor rear axle, and the axles on all trailing units where they share the same value. The slip angle on each tire is calculated by:

$$\text{Tractor front tire slip angle: } \alpha_{t1} = \delta - \frac{v_1 + a_1\omega_1}{u} \qquad (6-21)$$

$$\text{Tractor rear tire slip angle: } \alpha_{t2} = \frac{b_1\omega_1 - v_1}{u} \qquad (6-22)$$

$$\text{Front trailer tire slip angle: } \alpha_2 = \varphi_1 - \frac{v_1 - (f_1 + d_2)\omega_1 - d_2\dot{\varphi}_1}{u} \qquad (6-23)$$

$$\text{Dolly tire slip angle: } \alpha_3 = \varphi_2 - \frac{v_1 - (f_1 + l_2 + d_3)\omega_1 - l_2\dot{\varphi}_1 - d_3\dot{\varphi}_2}{u} \qquad (6-24)$$

$$\text{Rear trailer tire slip angle: } \alpha_4 = \varphi_3 - \frac{v_1 - (f_1 + l_2 + l_3 + d_4)\omega_1 - l_2\dot{\varphi}_1 - l_3\dot{\varphi}_2 - d_4\dot{\varphi}_3}{u} \qquad (6-25)$$

Therefore, the comprehensive EOM that determine the lateral motion of the 28-ft A-train double are derived in matrix notation by integrating Equations 6-1 to 6-25, which yields:

$$PX = Q\dot{X} + R\delta \qquad (6-26)$$

where

$$X = [v \quad \omega \quad \varphi_1 \quad \dot{\varphi}_1 \quad \varphi_2 \quad \dot{\varphi}_2 \quad \varphi_3 \quad \dot{\varphi}_3]^T$$

$$\dot{X} = [\dot{v} \quad \dot{\omega} \quad \dot{\varphi}_1 \quad \ddot{\varphi}_1 \quad \dot{\varphi}_2 \quad \ddot{\varphi}_2 \quad \dot{\varphi}_3 \quad \ddot{\varphi}_3]^T$$

$$R = [C_F \quad C_F(a_1 + f_1) \quad 0 \quad 0 \quad 0 \quad 0 \quad 0 \quad 0]^T$$

The details of matrices P and Q are provided in Appendix B. The State-Space representation of this vehicle system can hence be obtained as follows:

$$\left.\begin{array}{l} \dot{X} = \boldsymbol{A}X + \boldsymbol{B}u \\ Y = \boldsymbol{C}X + \boldsymbol{D}u \end{array}\right\} \qquad (6-27)$$

where

$$X = [v \quad \omega \quad \varphi_1 \quad \dot{\varphi}_1 \quad \varphi_2 \quad \dot{\varphi}_2 \quad \varphi_3 \quad \dot{\varphi}_3]^T$$

$$\dot{X} = [\dot{v} \quad \dot{\omega} \quad \dot{\varphi}_1 \quad \ddot{\varphi}_1 \quad \dot{\varphi}_2 \quad \ddot{\varphi}_2 \quad \dot{\varphi}_3 \quad \ddot{\varphi}_3]^T$$

$$Y = [v \quad \dot{v} \quad \omega \quad \dot{\omega} \quad \varphi_1 \quad \ddot{\varphi}_1 \quad \varphi_2 \quad \ddot{\varphi}_2 \quad \varphi_3 \quad \ddot{\varphi}_3]^T$$

$$u = \delta$$

The details of matrices $\boldsymbol{A}, \boldsymbol{B}, \boldsymbol{C}$, and $\boldsymbol{D}$ are included in Appendix B as well.

6.1.2 Roll-Plane Model

A simplified single-DOF roll model is developed to study the roll dynamics of each vehicle unit in the 28-ft A-train double, as shown in Figure 6-4. It is assumed that (1) the sprung mass rolls with respect to a roll center; (2) the axle inertia and roll motion are neglected; (3) the roll angle is sufficiently small, where $sin\theta = \theta$ and $cos\theta = 1$; and (4) the roll dynamics of each vehicle unit are independent.

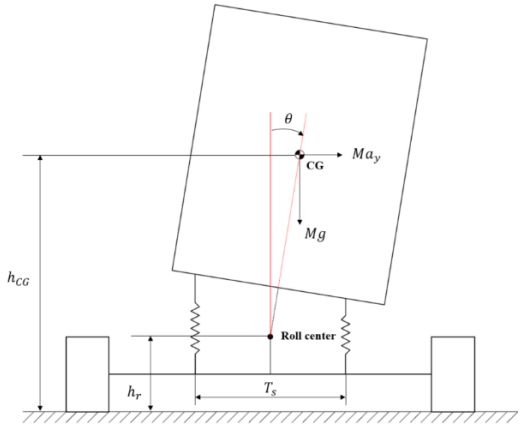

Figure 6-4. The simplified single-DOF roll model.

By applying Newton's Second Law for moments at the roll center, the EOM that governs the roll motion are given by:

$$Ma_y(h_{CG} - h_r) + Mg(h_{CG} - h_r)\theta = \frac{1}{2}K_s T_s^2 \theta \qquad (6-28)$$

where

M = Sprung mass

a_y = Lateral acceleration

h_{CG} = Sprung mass CG height

h_r = Roll center height

θ = Sprung mass roll angle

K_s = Suspension spring stiffness

T_S = Lateral displacement between two springs

The values of all variables applied in both the yaw- and roll-plane models can be found in Appendix B.

6.2 TruckSim Vehicle Model

A vehicle model for the 28-ft A-train double is developed in TruckSim and is used to validate the mathematical models. The tractor model has one steering axle with two tires, and two tandem drive axles both with dual tires, as shown in Figure 6-5. A fifth-wheel coupling is used to connect it to the front trailer.

Figure 6-5. The 6×4 tractor model in TruckSim.

Both the 28-ft semitrailer and the converter dolly have a single-axle with dual tires. A pintle hitch coupling is employed to connect the front trailer and the converter dolly, and a fifth-wheel coupling is used between the dolly and the rear trailer. The complete truck model is shown in Figure 6-6. The parameters used in the TruckSim model are kept the same as those for the mathematical model.

Figure 6-6. The complete 28-ft A-train double model developed in TruckSim.

6.3 Mathematical Model Validation

Two maneuvers are applied to the mathematical models and the TruckSim model. The first one is a ramp-steering maneuver where the steering input increases linearly from 0 to 4 degrees in one second, as shown in Figure 6-7. It is noted that this steering angle is directly input to the steering tire rather than the steering wheel operated by a driver.

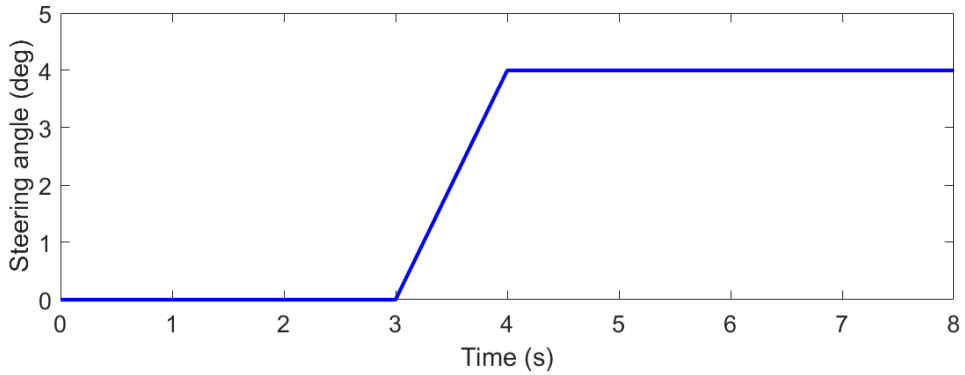

Figure 6-7. Ramp steering input applied to the mathematical and TruckSim models.

Lateral acceleration, articulation angle, and roll angle results are selected for comparing the simulation results derived from the mathematical and TruckSim models. Figure 6-8 and Figure 6-9 provide the comparison of lateral accelerations and articulation angles derived from the two models, respectively. In general, the lateral accelerations of all three vehicle units calculated from the mathematical model follow similar trends as those from the TruckSim model. However, the mathematical model results in faster responses than the TruckSim model in all three cases. This is because some damping effects are neglected in the mathematical model, such as those resulting from steering compliance, etc.

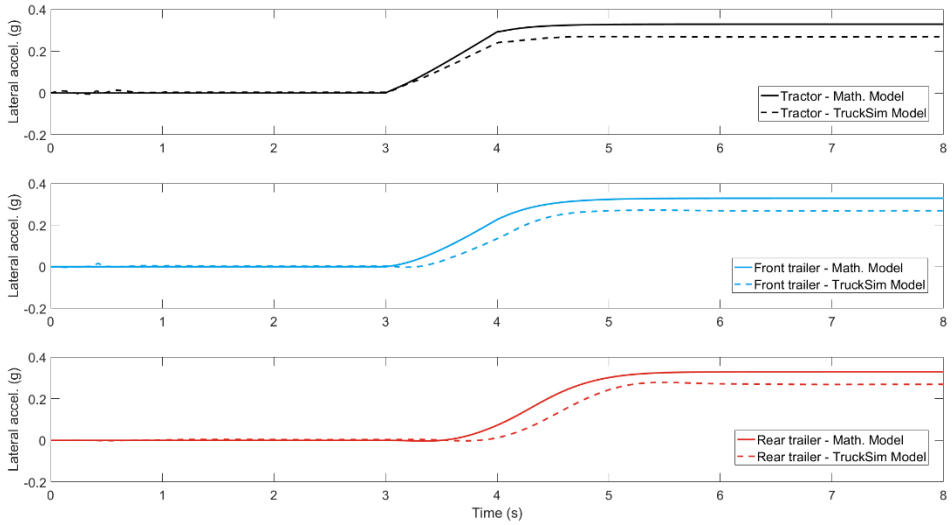

Figure 6-8. Comparison of lateral accelerations derived from the mathematical and TruckSim models with the ramp-steering input.

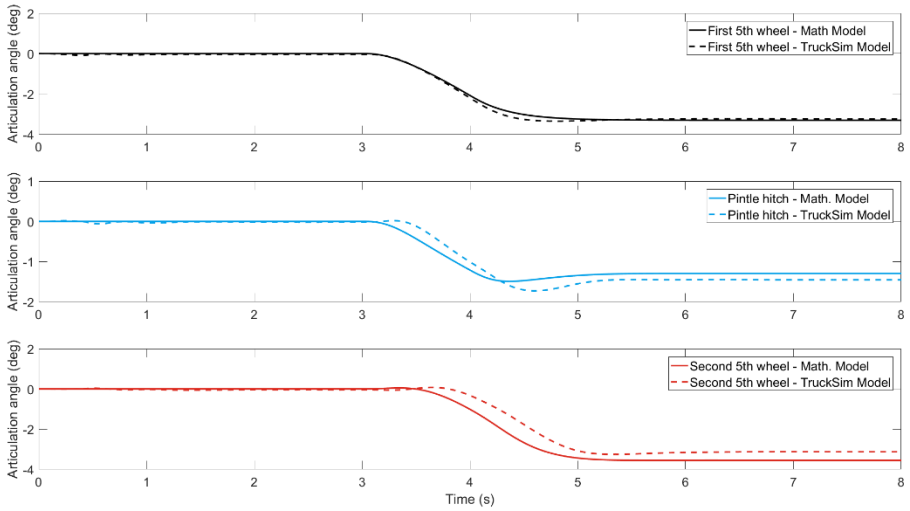

Figure 6-9. Comparison of articulation angles derived from the mathematical and TruckSim models with the ramp-steering maneuver.

The comparison of roll angles is shown in Figure 6-10. Again, the mathematical model results in similar but faster responses than the TruckSim model. A larger disagreement is observed when comparing rear trailer angles. This is because the front trailer in the TruckSim model can receive anti-roll moment from the tractor, and thus it experiences smaller roll angles even though the lateral accelerations applied to both trailers are very close. On the contrary, the roll motion of each vehicle unit of the mathematical model is assumed to be independent, where no roll moment can be transferred between adjacent units.

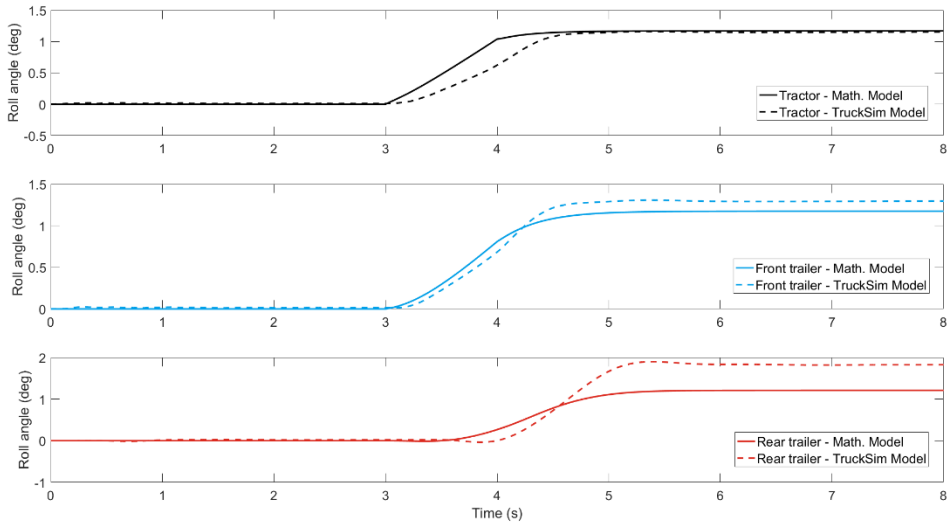

Figure 6-10. Comparison of roll angles derived from the mathematical and TruckSim models with the ramp-steering input.

The other maneuver consists of a 0.25-Hz sinusoid wave with an amplitude of five degrees as the steering input to the steering axle, as shown in Figure 6-11. This maneuver results in more dynamic response to vehicles compared with the ramp-steering input.

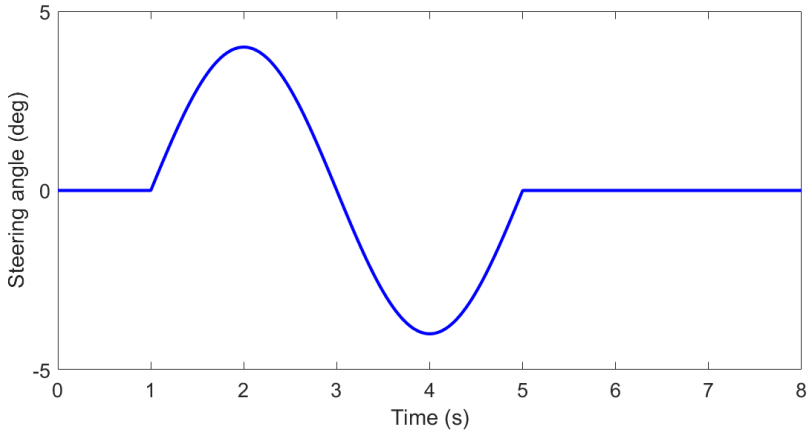

Figure 6-11. 0.25-Hz sinusoid steering input applied to the mathematical and TruckSim models.

The comparison of lateral accelerations, articulation angles, and roll angles derived from the mathematical and TruckSim models are provided in Figure 6-12, Figure 6-13, and Figure 6-14, respectively. Again, the simulation results obtained from the two models share similar trends, but the mathematical model leads to faster responses due to the fact that it considers less damping effect.

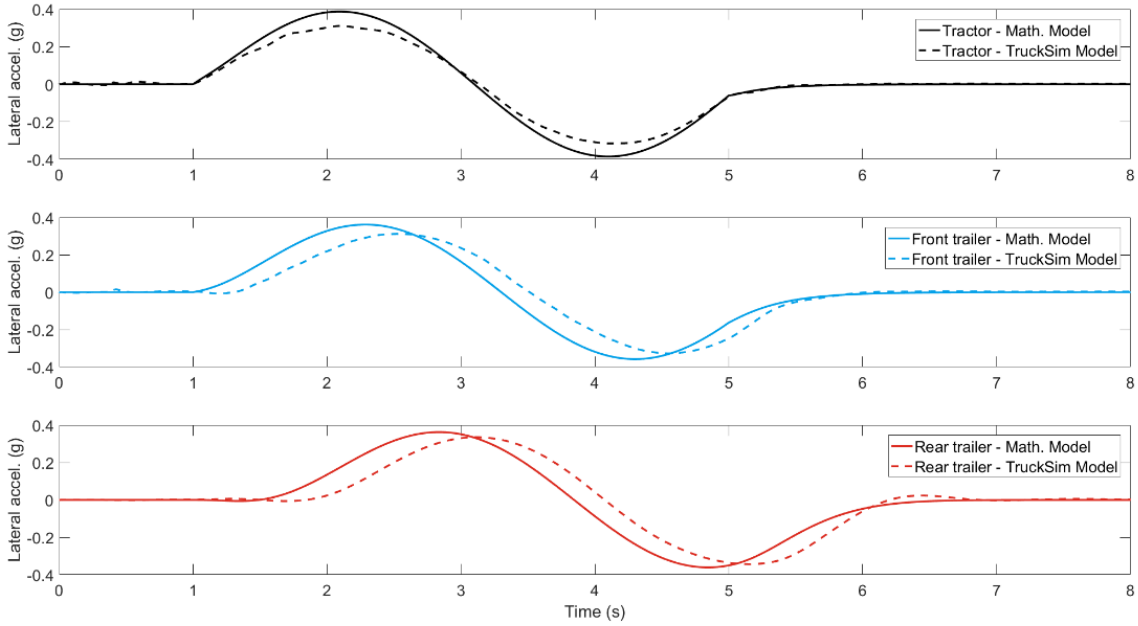

Figure 6-12. Comparison of lateral accelerations derived from the mathematical and TruckSim models with the 0.25-Hz sinusoid input.

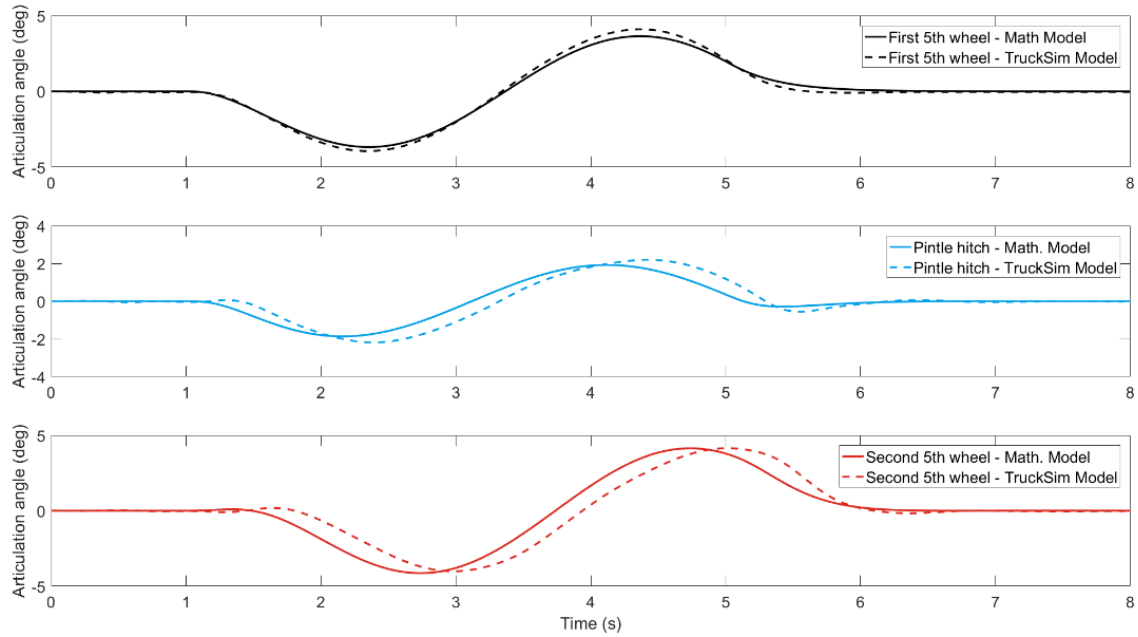

Figure 6-13. Comparison of articulation angles derived from the mathematical and TruckSim models with the 0.25-Hz sinusoid input.

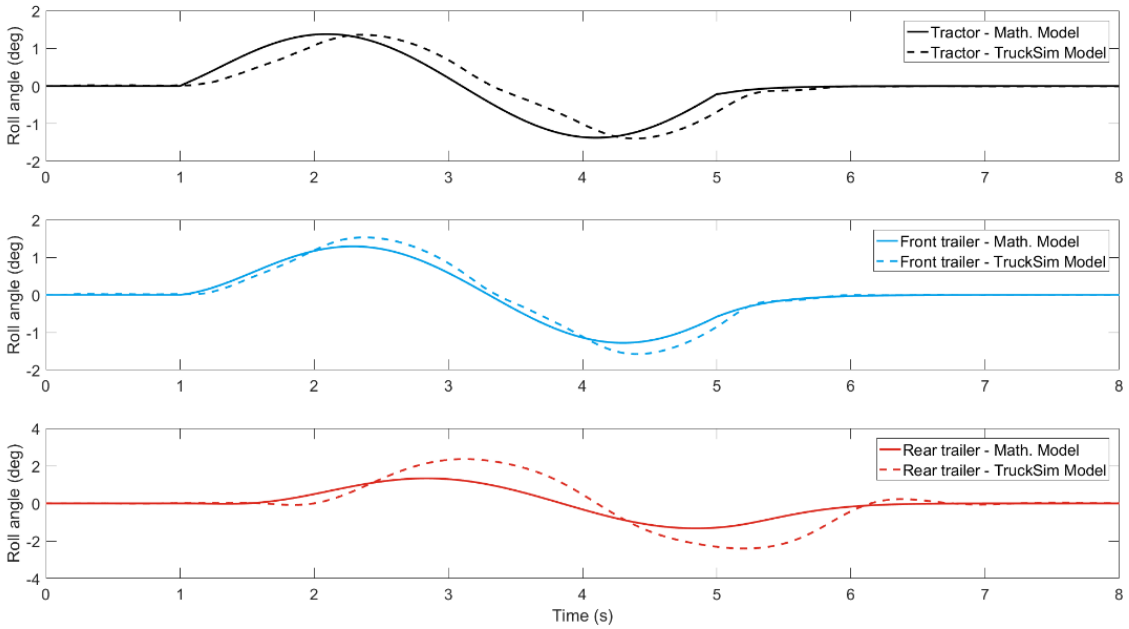

Figure 6-14. Comparison of roll angles derived from the mathematical and TruckSim models with the 0.25-Hz sinusoid input.

In general, the mathematical model is capable of providing reasonably accurate simulation results that capture all necessary characteristics of the directional dynamics for an A-train double. Therefore, the mathematical model can be applied to further study the directional dynamics of 28-ft A-train doubles through parametric analyses.

6.4 28-ft A-train Double Directional Dynamic Analysis

The directional dynamic analysis conducted here is mainly focused on two parameters–traveling speed and trailer load combinations–which are mostly involved with real-world operation. Traveling speed directly determines truck lateral accelerations during cornering, and could also trigger rearward amplification that further increases lateral accelerations on trailing units, especially for the rear trailer, which unfortunately already has the least stability in an A-train configuration. Different trailer load combinations are believed to greatly affect the system dynamics of a truck combination, such as rearward amplification and directional stability. Therefore, parametric analyses are conducted to study the effect of traveling speed and different trailer load combinations on rearward amplification and vehicle system stability.

The 0.25-Hz sinusoid steering input with an amplitude of five degrees is applied to the vehicle model, and the traveling speeds are varied from 40 to 80 mph. Figure 6-15 provides the simulation results of rearward amplification indices versus traveling speeds. The rearward amplification index is defined as the ratio between peak lateral accelerations at the tractor and a trailing unit during a maneuver. It is shown that both the front and rear trailer experience smaller peak lateral accelerations than the tractor at 40 mph, and the indices become larger as the speed increases. The rear trailer index reaches 1 at 45 mph, indicating that the rear trailer would be exposed to larger lateral accelerations than the tractor when the truck travels faster than 45 mph. The front trailer index exceeds 1 at 60 mph, which is 15 mph higher than that of the rear trailer under this scenario. Therefore, the simulation results indicate that the traveling speed plays an important role in triggering rearward amplification phenomenon, and it has a stronger effect on the rear trailer.

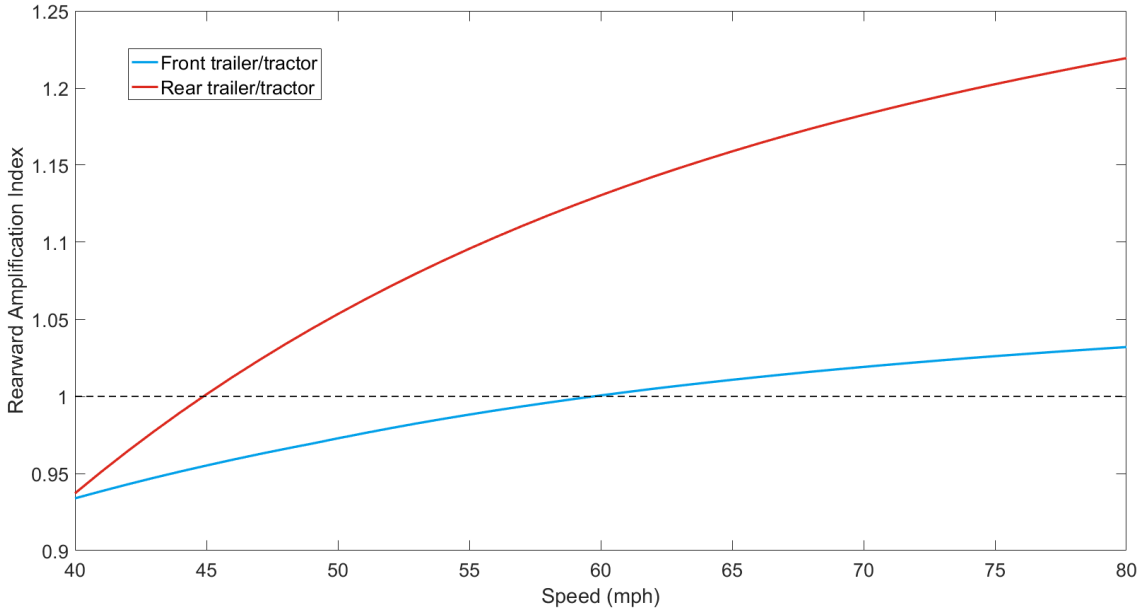

Figure 6-15. Effect of traveling speed on rearward amplification of the 28-ft A-train double.

The eigenvalues of the vehicle systems at different speeds are shown in Figure 6-16. It is obvious that the eigenvalues move towards the positive side of the real axis as the speed varies from 40 to 80 mph, indicating that the truck stability decreases as the speed increases.

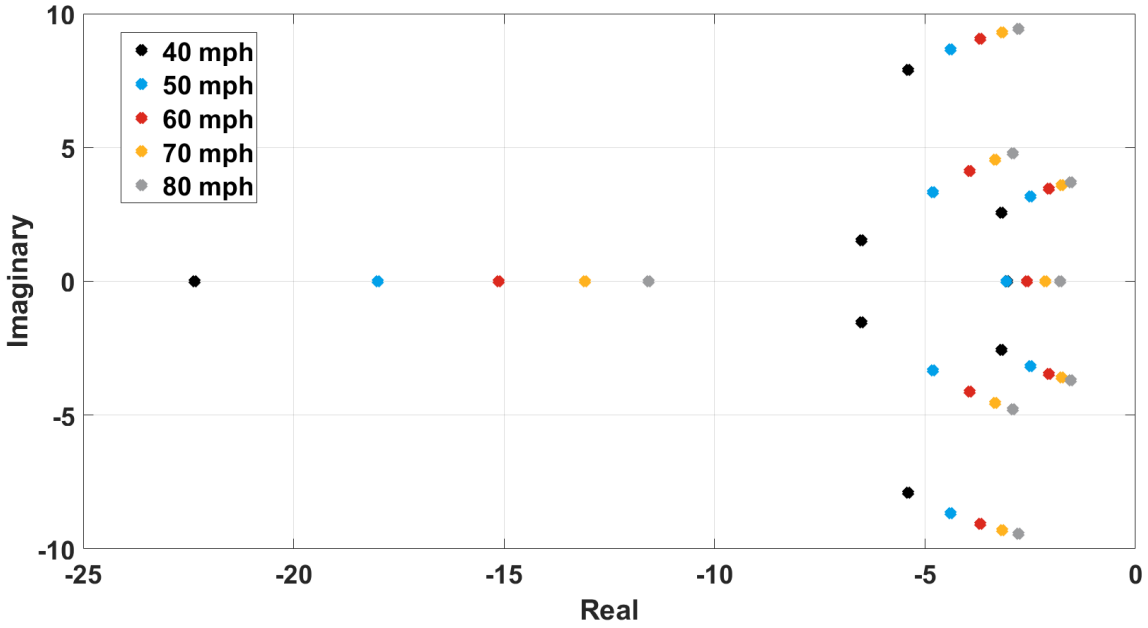

Figure 6-16. Effect of traveling speed on eigenvalues of the vehicle system.

The 0.25-Hz sinusoid steering input is applied again to study the effect of different trailer load combinations on rearward amplification and vehicle stability. The different load combinations are achieved by varying the rear trailer mass and yaw inertia from 40% to 200% of the original values. It is noted that the original mass and inertia parameters of the two trailers are assumed to be the same.

Figure 6-17 illustrates the simulation results of rearward amplification index versus different rear trailer mass ratio. The indices of the rear trailer increase as the mass ratio raises, indicating that a heavier rear trailer leads to a larger rearward amplification index for the rear trailer, whereas the front trailer almost remains unaffected. In this case, the rear trailer starts to experience larger peak lateral accelerations than the tractor when the rear trailer is 1.62 times heavier than the front trailer.

The eigenvalues of the vehicle system with different rear trailer mass ratios are shown in Figure 6-18. The results indicate that eigenvalues of the vehicle system move towards the positive side of the real axis as the rear trailer becomes heavier. In other words, the stability of the truck combination will be lowered with a heavier rear trailer.

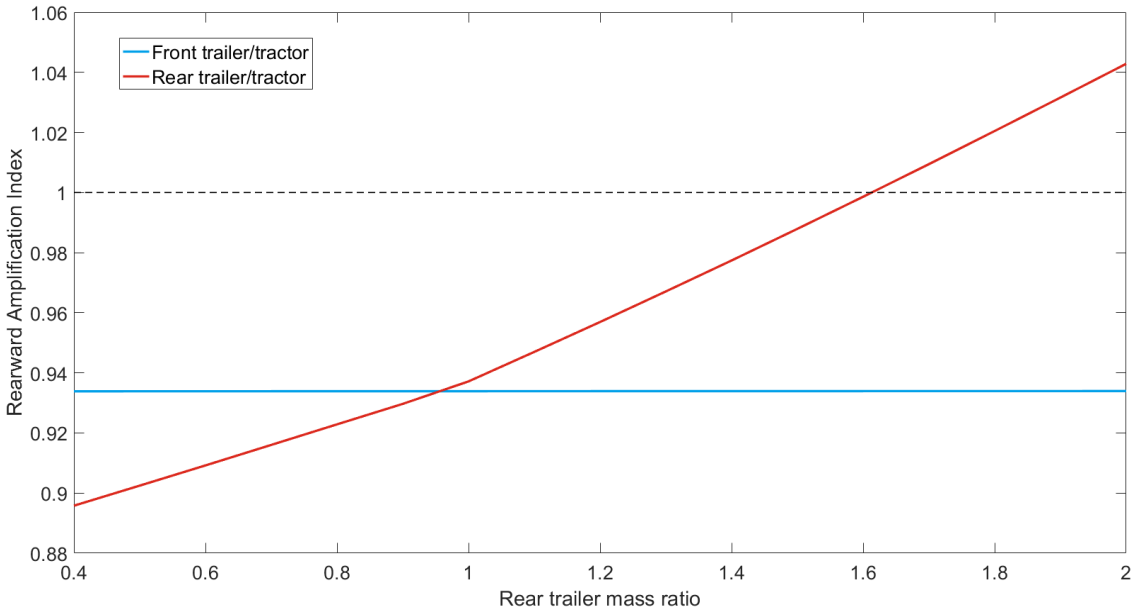

Figure 6-17. Effect of different rear trailer mass ratios on rearward amplification of the 28-ft A-train double.

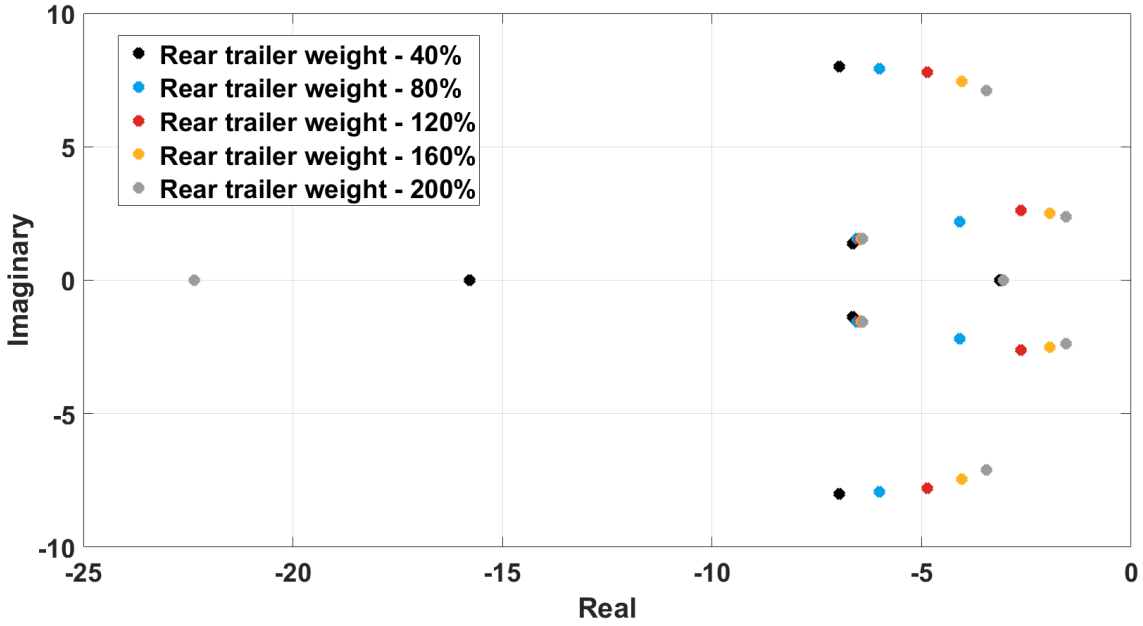

Figure 6-18. Effect of different rear trailer mass ratios on eigenvalues of the vehicle system.

6.5 Summary

This chapter detailed the development of two mathematical models for studying the yaw and roll dynamics of a 28-ft A-train double. The yaw-plane model has five DOF, and the roll-plane model has one DOF. The two mathematical models were validated against a TruckSim model by comparing simulation results of lateral acceleration, articulation angle,

and roll angle, which showed reasonable agreement. Parametric analyses were conducted based on the validated mathematical models to study the effect of traveling speed and different trailer load combinations on rearward amplification and vehicle stability. The simulation results indicate that (1) higher traveling speeds lead to stronger rearward amplification phenomenon for both trailers and therefore lower the vehicle stability; and (2) a heavier rear trailer contributes to greater rearward amplification effect on its own, and also reduces the stability of the entire vehicle system.

Chapter 7 – Testing and Evaluation of Dynamic Stability of 28-ft A-train Doubles with Electronic Stability Control (ESC): Overview, Test Preparation, and Preliminary Tests

As introduced in Chapter 5, 28-ft A-train doubles were permitted to be operated on State roads in the U.S. in 1982. They have been used with increasing frequency due to their operational cost efficiency, dispatching flexibility, and suitability for package carriers that cater to internet commerce. It is reported that in 2000, 28-ft A-train doubles represented approximately 2.5% of all truck combinations in the U.S., with tractor-semitrailer combinations (semi-trucks) accounting for 82% of the truck traffic [13]. Because semi-trucks represent the majority of all truck combinations, most simulation or testing studies of articulated heavy vehicle dynamics are focused on semi-trucks. As for trucks in A-train or other double-trailer configurations, very few studies have been conducted and the analyses have mostly been based on mathematical modeling and simulation [25-27, 38, 40, 59, 69-72]. Even though some of these studies provide great insight into the dynamics and stability of double-trailers, their mathematical models do not accurately simulate all dynamic aspects, mainly due to the system complexities. Therefore, it is necessary to conduct a comprehensive full-scale test on A-train doubles to further investigate their dynamics.

As electronic stability enhancement systems have become standard equipment on all new passenger cars, similar systems have also been employed for heavy commercial vehicles. In 2015, the use of Electronic Stability Control (ESC) systems was mandated for class-8 tractors−of 2017 or later production year−by the Federal Motor Vehicle Safety Administration. The Federal Motor Vehicle Safety Standard 136 (FMVSS 136) requires tractors and certain large buses with a GVWR greater than 11,793 kg (26,000 lb) to be equipped with ESC [3]. This rule was determined based on the results derived from extensive field tests that proved the efficacy and safety benefits of ESC for commercial vehicles. The tests conducted for this rulemaking, however, mainly included tractors with single trailers. With the increasing use of double trailers on the public roads, it is critical to conduct a similar study in which the special dynamics of double trailers are considered.

This chapter provides an overview of the test-based evaluation, followed by the test preparation and preliminary tests conducted in preparation for the final track tests.

7.1 Overview

The two main purposes of this testing-based program include (1) obtaining further understanding of the dynamic stability of 28-ft A-train doubles, and (2) examining how commercially-available electronic stability control systems perform on these trucks in the real world. In order to achieve these purposes, further steps have been taken to bring this program up to a scientific research level, rather than simply following test procedures applied by industry.

The test vehicle was received by the Center for Vehicle Systems and Safety (CVeSS) at Virginia Tech in November 2015, and included two 28-ft drop-frame trailers, one A-dolly, and one 6x4 tractor. The test preparation work was mostly conducted at CVeSS, including mechanical safety structure design and installation, load frame design and installation, structure reinforcement for both trailers, steering robot design and fabrication, test vehicle instrumentation, test maneuver design, and preliminary tests for a system performance check. The final tests were divided into two phases. The Phase I program tested the performance of a dual-module trailer-based roll stability control (RSC) system. In Phase II, the dual-module RSC system was tested again with a tractor-based ESC system, as well as an empty rear trailer. The final tests were all conducted on a professional Vehicle Dynamics Assessment (VDA) pad at Michelin Laurens Proving Ground at South Carolina.

7.1.1 Test Vehicle

The test vehicle is a typical 28-ft A-train double that consists of one tractor, two semitrailers, and one converter dolly (A-dolly). The tractor is a 2004 Volvo VNL 6x4 truck tractor with a total GVWR of 50,000 lb, as shown in Figure 7-1. "6x4" indicates that the tractor has three axles in total, and two of them are drive axles.

Figure 7-1. The tractor used in the 28-ft A-train double.

Figure 7-2 shows the two identical single-axle semitrailers used for testing, which were both manufactured by Kentucky Trailer in 2001. These trailers are 28 ft long, equipped with pneumatic suspensions, and have drop-frames for maximum cargo space volume. The converter dolly was manufactured by Silver Eagle and was also equipped with pneumatic suspensions. More details regarding the tractor and trailers can be found in Appendix C.

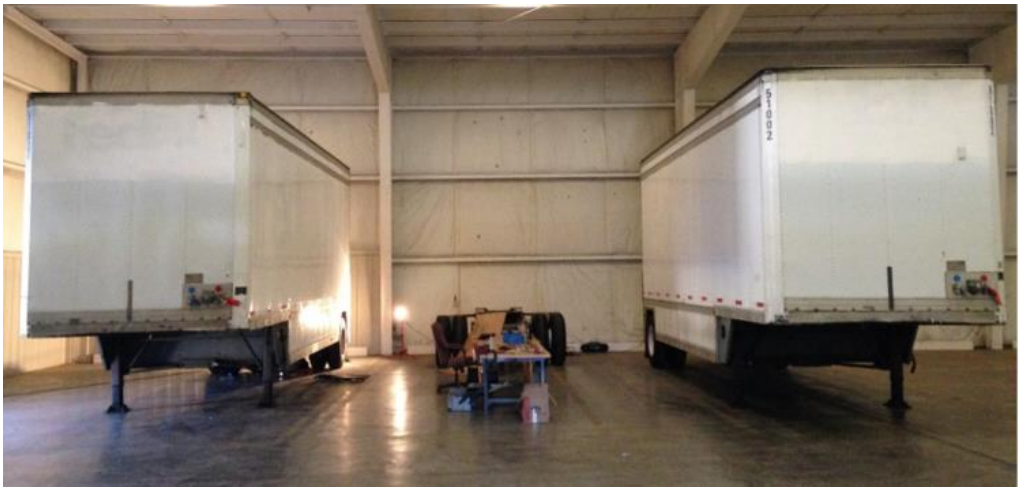

Figure 7-2. Two identical 28-ft drop-frame semitrailers used for testing.

7.1.2 Test Objectives

The main objectives of this testing-based evaluation program are detailed as follows:

- Obtain further and deeper understanding of the real-world dynamic stability of 28-ft A-train double trailers; and
- Evaluate performance of typical commercially-available tractor ESC and trailer RSC systems on 28-ft A-train doubles.

In addition, multiple sub-objectives need to be achieved before the main objectives could be accomplished, which include:

- Design and install mechanical safety structures to the test vehicle for preventing rollover and jackknifing events during dynamic tests;
- Design proper loading mechanism to accurately load the trailers to represent typical real-world load conditions;
- Determine all data that are necessary for conducting comprehensive analyses on truck directional dynamics;
- Design and implement instrumentation to the test vehicle for collecting those data;
- Determine test maneuvers by evaluating existing maneuvers for heavy truck tests, and design new ones, particularly for trucks in the A-train configuration if necessary;
- Develop a steering robot to perform certain test maneuvers that require precise steering input or high repeatability; and
- Define a metric to evaluate the performance of ESC and RSC systems.

7.2 Test Preparation

The following section details the efforts that have been made to prepare for the final track tests, including mechanical safety structures, customized load frame system, steering robot design, test vehicle instrumentation, and test maneuver design, which all serve a vital role in full-scale heavy truck testing. The work was initiated, conducted, and accomplished by CVeSS between November 2015 and June 2016.

7.2.1 Mechanical Safety Structures

Considering the proposed test objectives, the test truck would be operated with aggressive maneuvers where its lateral stability threshold could be exceeded. Therefore, mechanical safety structures are necessary to prevent rollover or jackknifing events during dynamic tests. First, two sets of safety outriggers were designed and installed on the trailers. The CVeSS outrigger provides counterbalance moment once one side contacts the ground, in order to stop further roll motion. The design of the CVeSS outriggers was inspired by the

industry-accepted NHTSA Class 8 tractor/trailer outriggers [73], with the specifications listed as follows:

- Load rating: 11,000 lbf.
- Inboard height: 12 in.
- Transport width: ~102 in. (outboard beams folded)
- Overall width: ~270 in.
- Maximum wheel-to-ground clearance: ~33 in.
- Maximum allowable trailer roll angle: 13 degrees
- Load cell measurement range: 0-200,000 lbf

Load cells were integrated into the outrigger design to provide contact force measurement, as shown in Figure 7-3. A CAD model of the CVeSS outrigger assembly is presented in Figure 7-4, showing that the outrigger assembly was located at the front end of the trailer close to its landing gear, and could perfectly fit the limited space under the drop frame. In addition, the CVeSS outrigger could be folded backwards for highway transport or for passing through common garage gates, as shown in Figure 7-5. The outrigger height could also be adjusted to provide a wide range of allowable trailer body roll, as depicted in Figure 7-6, with the minimum and maximum wheel-to-ground clearance adjustment.

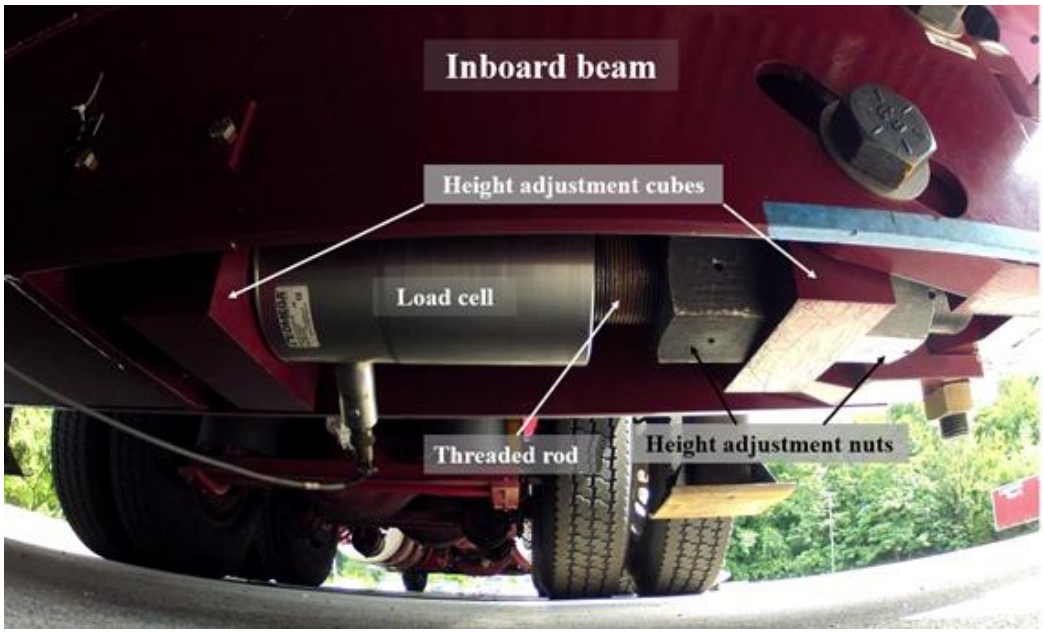

Figure 7-3. The final assembly of outriggers integrated with a load cell for contact force measurement.

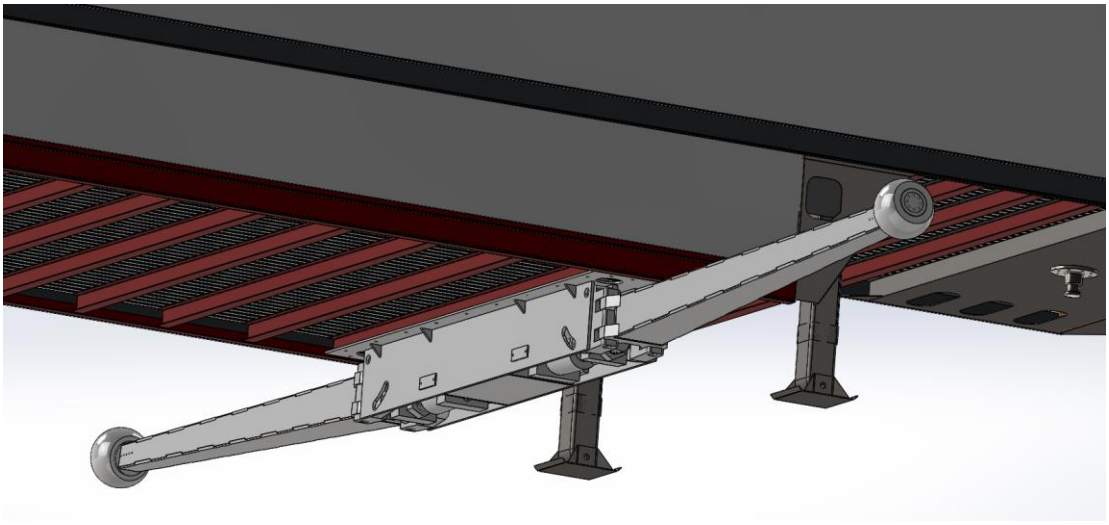

Figure 7-4. The entire CVeSS outrigger assembly is mounted to the trailer frame rails.

(a) (b)

Figure 7-5. Folding setting of the outrigger: (a) the outrigger in testing position, and (b) the outrigger in transport position.

(a) (b)

Figure 7-6. Height setting of the outrigger: (a) no clearance between the wheel and the ground, and (b) maximum wheel height for the testing trailer (~33 in.).

Besides rollover events, the test truck would also be subjected to the risk of jackknifing accidents during aggressive dynamic tests, such as J-turn and Double Lane Change maneuvers. With the safety outriggers already implemented on the trailers to prevent the truck from rolling over, it was also necessary to develop a mechanical system to preserve the test truck from jackknifing. Therefore, an anti-jackknifing system was designed and installed to constrain the maximum articulation angles between adjacent vehicle units.

The CVeSS anti-jackknifing system consisted of mounting pintle hooks, kinetic energy ropes, and metal chains. The mounting pintle hooks were bolted to the tractor and trailer frame as the terminals for attaching ropes and chains. The ropes were used to absorb kinetic energy through elongation when articulation angles exceeded the designed threshold, in order to attenuate further articulation motion. The metal chains served as the reinforcing structure to greatly restrict the maximum allowed articulation angle, in case the kinetic energy ropes became overloaded. Accordingly, the metal chains were installed in parallel with the ropes, and the length of the chains were set such that they would only engage once the ropes reached their maximum lengths.

Since there is only one DOF between the tractor and the front trailer (hereafter referred to as "Trailer A"), the articulation motion is simple and therefore one set of cross ropes and chains is capable of preventing a jackknifing event. However, the articulation motion between Trailer A and the rear trailer (hereafter referred to as "Trailer B") possesses two DOF because they are connected via a converter dolly. Thus, kinematic analysis and simulation were conducted to study the possible jackknifing scenarios, indicating that two types of jackknifing events could occur during the tests, which are referred to as "trailer jackknifing" and "dolly jackknifing," shown in Figure 7-7. Figure 7-7(a) illustrates the trailer jackknifing, where the dolly generally stays in line with Trailer A, but there is a large articulation angle between the dolly and Trailer B. Therefore, the parallel ropes and chains are needed to restrain excessive articulation motion between Trailer A and Trailer B. Figure 7-7(b) shows the dolly jackknifing, where the articulation angle between the two trailers is within a certain allowed threshold. However, they both experience excessive articulation motion with respect to the dolly. Thus, the cross ropes and chains are designed and installed to preserve the truck from such jackknifing events. A more detailed

illustration of the anti-jackknifing systems are provided in Figure 7-8. The final CVeSS anti-jackknifing systems setup for tractor/Trailer-A and Trailer-A/Trailer-B are illustrated in Figure 7-9 and Figure 7-10.

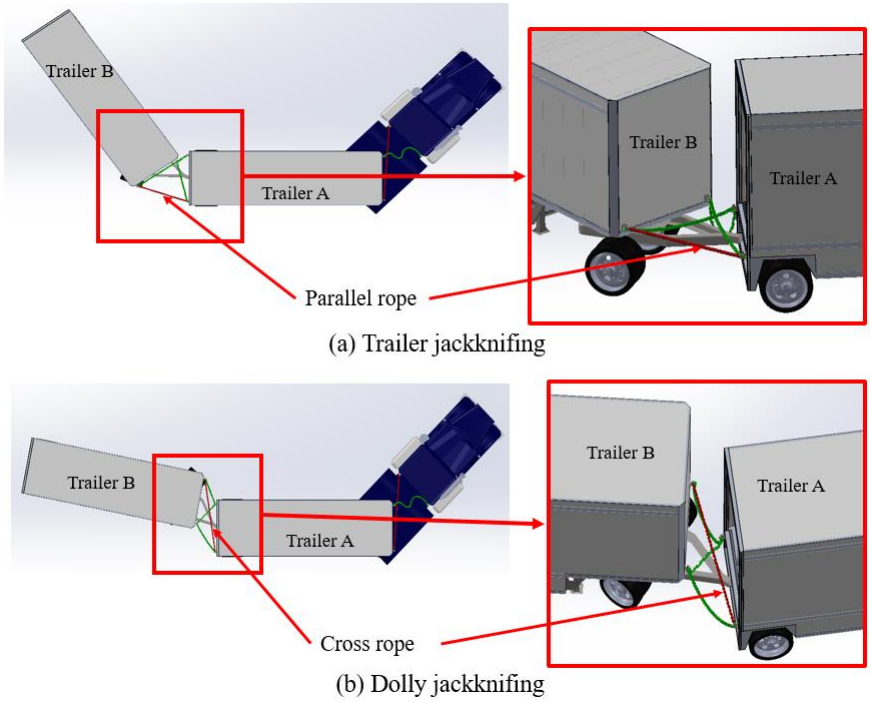

Figure 7-7. Two jackknifing events that could potentially occur between Trailer A and Trailer B during tests: (a) trailer jackknifing, and (b) dolly jackknifing.

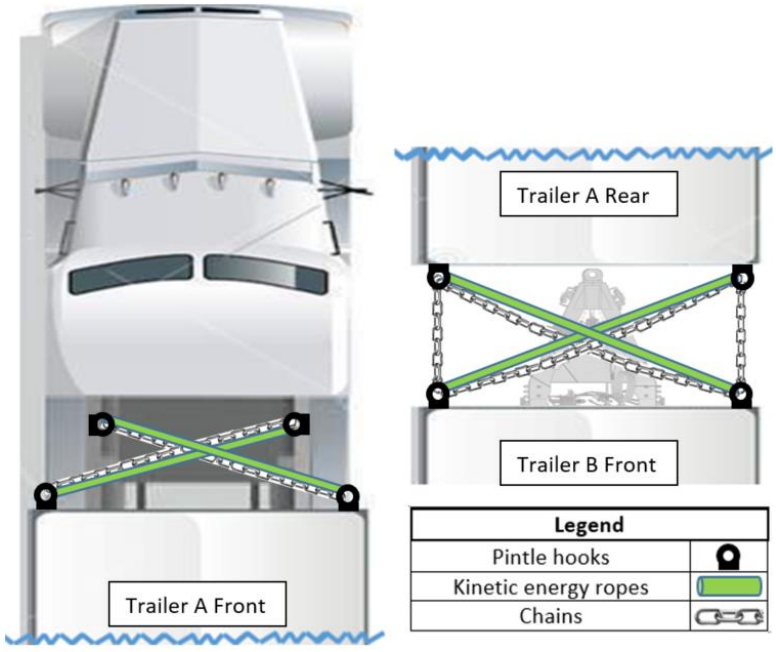

Figure 7-8. The diagram of the CVeSS anti-jackknifing system.

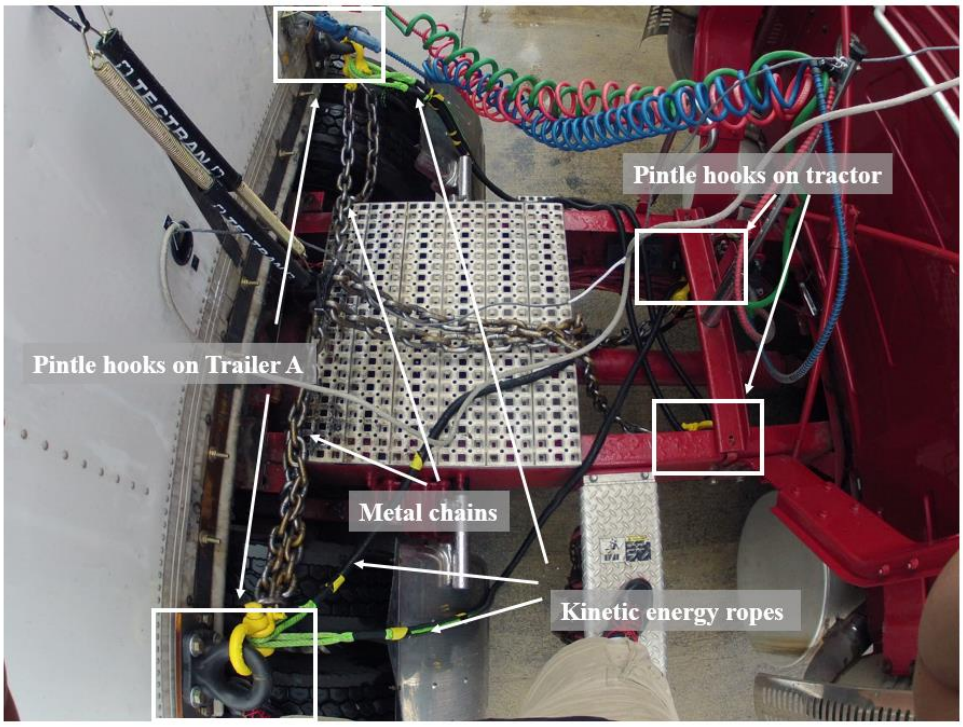

Figure 7-9. The anti-jackknifing system layout for the tractor and Trailer A.

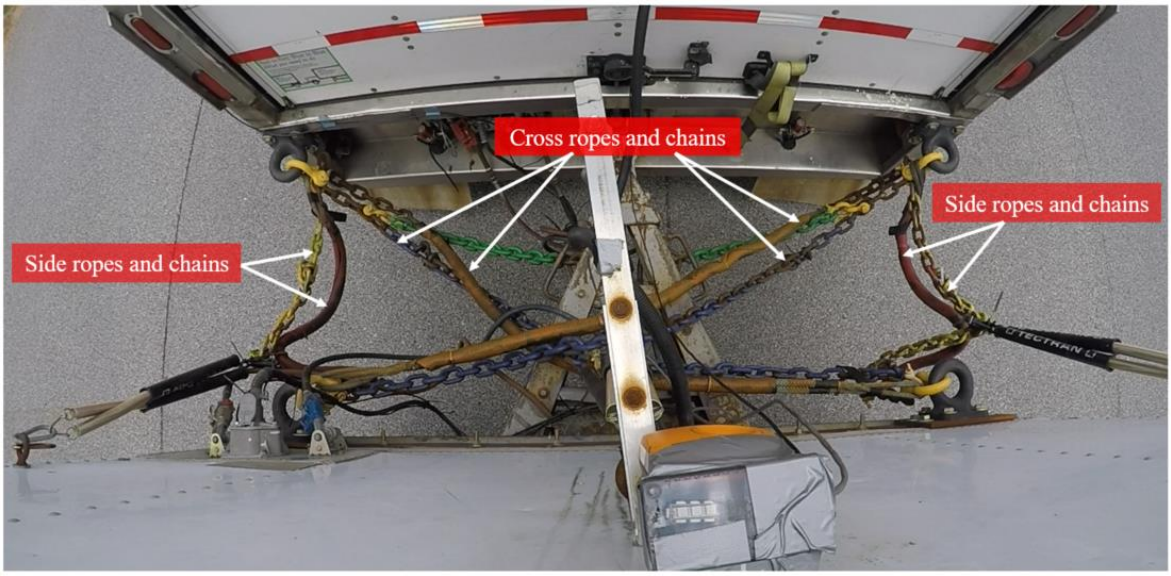

Figure 7-10. The anti-jackknifing system layout between Trailer A and Trailer B.

7.2.2 Customized Load Frame Systems

Customized load frame systems were designed and implemented on two test trailers to replicate typical highway load conditions for 28-ft drop-frame trailers. According to the consultation with a major logistics company, a 28-ft drop-frame trailer typically carries 6,000 lb of cargo load on the highway. This would make the total trailer weight lower than

the GVWR because such trailers are commonly applied to transport cargos with high volume but low weight, such as the packages used for internet commerce. In order to accurately replicate this typical load condition, a comprehensive SolidWorks model of a 28-ft drop-frame trailer was developed, as shown in Figure 7-11. The dimensional parameters were determined based on the measurement of the test trailers. This model considered all the structural details of the trailer, including the rollers inside the trailer used for loading and unloading, the trailer frame rails, the side beams inside the trailer wall, the landing gears, etc. The red rectangle in Figure 7-11 represents the typical load condition, where the trailer is uniformly loaded with 6,000-lb cargo that occupies 75% of the volume inside the trailer. This model was used to determine the trailer CG locations and moments of inertia under typical load conditions.

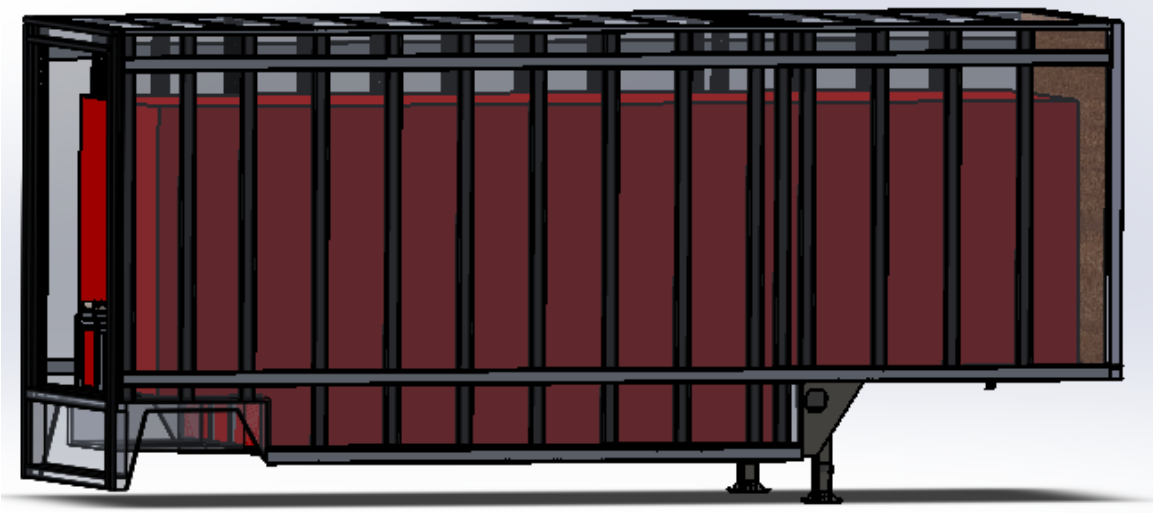

Figure 7-11. The SolidWorks model of a 28-ft drop-frame trailer with typical load conditions.

In order to accurately load the test trailers to obtain similar CG positions and moments of inertia (roll, yaw, and pitch), customized load frames were developed based on a double-layer pallet rack.

Based on the SolidWorks models, the load frame, safety outriggers, and reinforcement structures added approximately 2,600 lb to the trailer sprung mass. Therefore, 68 50-lb sandbags were loaded to the pallet racks (34 on each layer), in order to add 6,000-lb cargo weight to the trailer in total for replicating typical load conditions. The comparison of CG locations and moments of inertia calculated from the trailer model with typical load conditions and those with all the additional mechanical structures are included in Table

7-1. In general, the load frames reasonably replicate the typical load conditions with other additional mechanical structures. The final SolidWorks trailer model is shown in Figure 7-12, and the complete load frame assembly installed in the test trailers is shown in Figure 7-13.

Table 7-1. The comparison of CG locations and moment of inertia calculated from the trailer model with typical load conditions and that with all additional mechanical structures.

	Trailer with typical load	Trailer with load frame	Difference
x_{CG} (in.)*	143.17	136.71	-4.51%
y_{CG} (in.)	0	0	0
z_{CG} (in.)	74.77	73.50	-1.73%
I_{xx} (lbf·in^2)	117,483,779.61	129,412,916.20	10.15%
I_{yy} (lbf·in^2)	533,050,820.79	494,474,275.49	-7.24%
I_{zz} (lbf·in^2)	443,757,613.32	399,924,978.36	-9.88%

* The coordinate origin is located on the ground right underneath the trailer kingpin, where the x-axis points forward, the y-axis points to the driver side, and the z-axis points upward

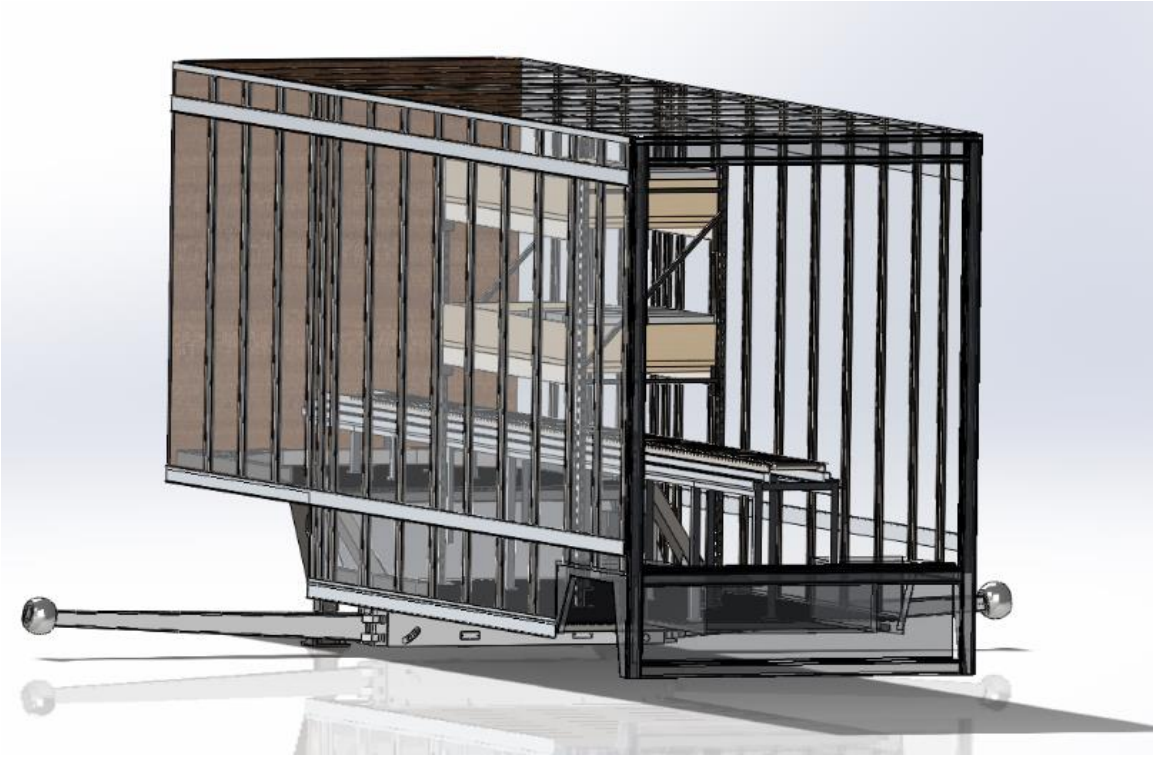

Figure 7-12. The final SolidWorks model of the trailer with all additional mechanical structures including the load frame.

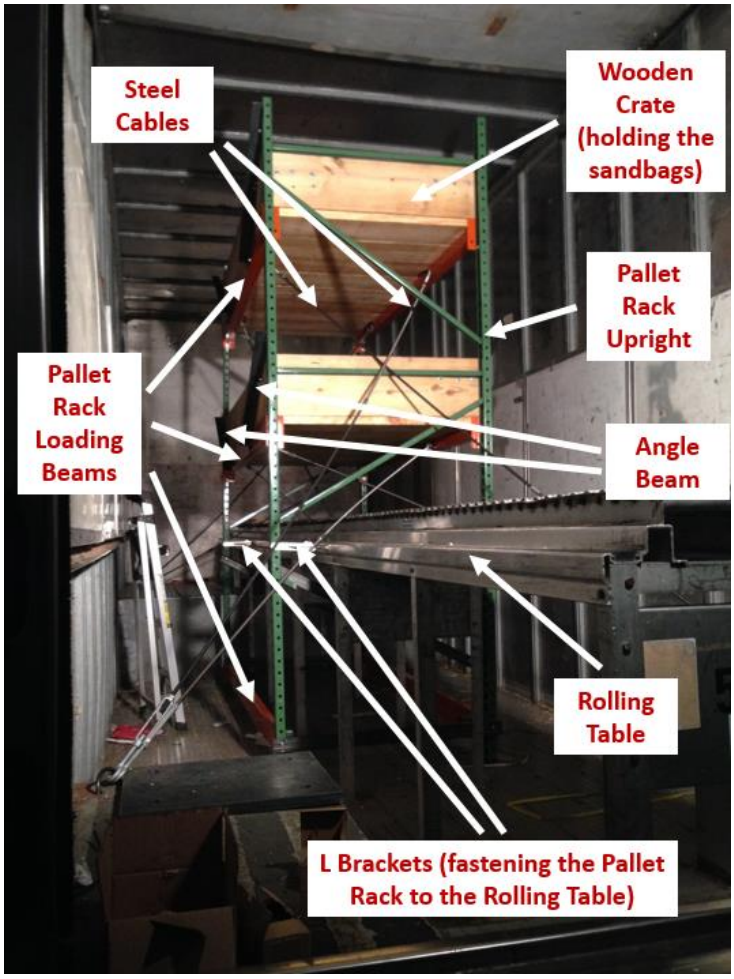

Figure 7-13. The final load frame assembly installed in the test trailers.

7.2.3 Test Vehicle Instrumentation and Steering Robot

An instrumentation and data acquisition (DAQ) plan was specifically designed for the double-trailer directional dynamics tests, which considered the particular double-trailer configuration and critical dynamic parameters that needed to be measured for conducting comprehensive dynamic analyses and evaluating ESC/RSC system performance. The dynamic parameters measured include:

- Tractor lateral acceleration
- Tractor suspension travel
- Tractor airbag pressure
- Tractor travelling speed and path
- Tractor steering wheel angle

- Articulation angle between the tractor and the front trailer
- Front trailer lateral acceleration
- Front trailer outrigger contact force
- Articulation angle between the front trailer and the rear trailer
- Rear trailer suspension travel
- Rear trailer airbag pressure
- Rear trailer tank pressure
- Rear trailer outrigger distance to the ground
- Rear trailer outrigger contact force
- Rear trailer lateral acceleration

The following data were also necessary for evaluating the performance of RSC systems:

- RSC system activation timing
- Brake pressure on the trailer's axle when RSC systems activate

The DAQ system consisted of 29 sensors, 6 cameras, a National Instruments CompactRIO Data Logger, two junction boxes, and power supplies. The two junction boxes were fabricated and installed on two trailers for powering all sensors, and for gathering/transmitting data from the sensors to the CompactRIO housed in the tractor cab. The front junction box connected sensors installed on the front trailer and the tractor, whereas the rear junction box connected sensors mounted on the rear trailer. Two 13-volt Lithium-ion batteries were used to provide a power supply to the CompactRIO and all the sensors. The general diagram of the DAQ system is shown in Figure 7-14.

In addition, six GoPro cameras were mounted to various locations on the test truck to directly capture vehicle dynamic motion, such as outrigger contact and wheel lift, etc. In order to synchronize analog data and video data, an event switch was implemented. This switch controlled six LED lights mounted in front of the cameras to flag key events during tests. When the LED lights were switched on, a voltage signal would be simultaneously sent to the CompactRIO along with the other analog data, and the signal would have stayed on until the LED lights were switched off to mark the end of a test session.

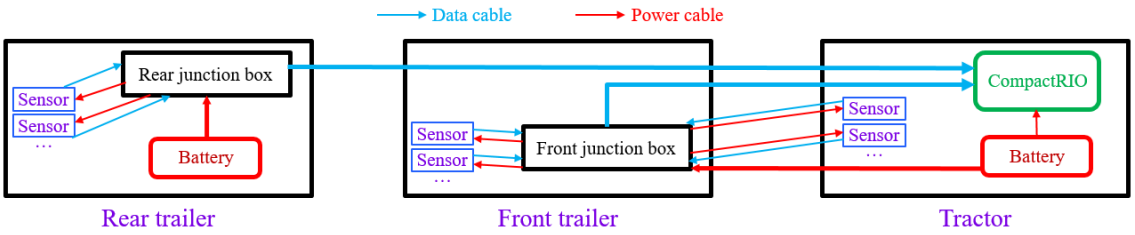

Figure 7-14. Diagram of the data and power flow of the DAQ system.

A steering robot was developed for this testing program, which could execute standard test maneuvers that require precise steering input, and ensure identical test maneuvers can be performed whether they are conducted minutes or weeks apart.

The CVeSS steering robot was specifically designed for Class 8 truck testing. The robot was installed in the engine bay, and applied steering input by controlling the steering column, as shown in Figure 7-15. Such a universal clamp-on design could fit all Class 8 tractors with 1.5-in. steering columns without interfering with the vehicle's safety systems.

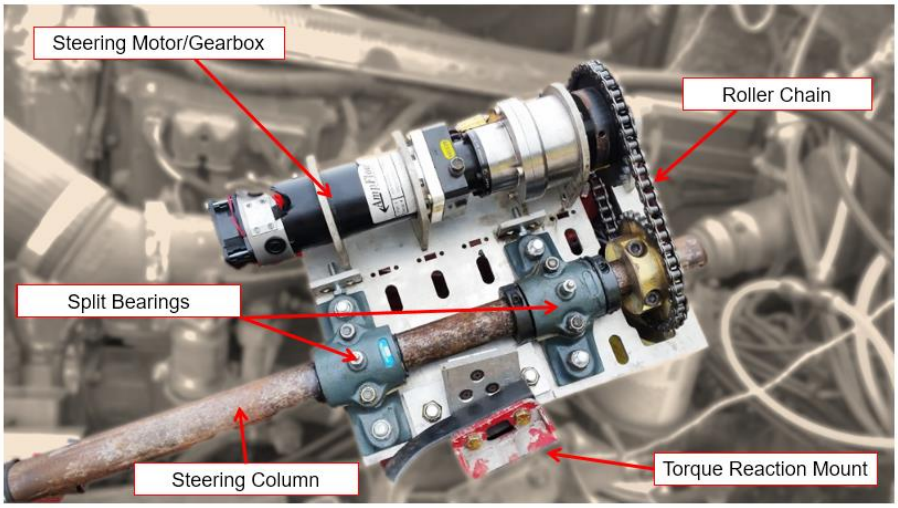

Figure 7-15. The CVeSS steering robot was installed in the engine bay and applied steering input by controlling the steering column.

The controls for the LED lights for the cameras as well as the event flag for the DAQ system were also integrated with the steering robot. Thus, when the steering robot is activated, the LED light would be turned on, and a constant voltage signal would also be sent to the DAQ system immediately to indicate the beginning of a test session. Similarly, when the robot is deactivated, the LED light would be turned off and the constant voltage signal would also be cut off to mark the end of a test session.

7.2.4 Test Maneuver Design

Maneuvers serve a vital role in full-scale vehicle testing due to the fact that different maneuvers could excite the vehicle in different ways. More importantly, an inappropriate maneuver could result in excessive vehicle motion and thus result in significant danger to the test vehicle as well as the testers. A comprehensive literature research was conducted first to evaluate test maneuvers commonly applied for heavy truck testing, and then four maneuvers were selected for this testing program based on its objectives.

7.2.4.1 Class 8 Truck Test Maneuvers Review

Among all the open literature reviewed, three technical reports were found to provide the most in-depth testing-based evaluation of Class 8 truck directional dynamics and stability. The first one was focused on the stability and dynamics of longer combination vehicles conducted by the National Transportation Research Center [74]. In this study, field tests were performed to evaluate the dynamics of a tractor with triple trailers. The test maneuvers applied are summarized in Table 7-2.

Table 7-2. Test maneuvers proposed and performed in [74].

#	Maneuver	Simulated Scenario	Procedure
1	Single Lane Change	Obstacle avoidance	Speed maintained at 45 mph; driver was instructed to travel in the right lane, and then move to the left lane over a distance of 150 ft
2	Gradual Lane Change	Daily highway lane change	Speed maintained at 45 mph; driver was instructed to travel in the right lane, and then move to the left lane over a distance of 400 ft
3	Double Lane Change	Obstacle avoidance	N/A
4	Impulse	To excite the test vehicle with a broad-band input for frequency analysis	This maneuver was actually not performed due to safety concern from the driver

The field tests of this project were conducted on a circular test track with a maximum speed limit of 45 mph. Thus, only lane-change maneuvers could be performed. In addition, the test truck used in this project was not equipped with safety outriggers, which means the truck was not tested well within its stable zone.

In 2011, NHTSA conducted a comprehensive testing project to develop objective performance tests for the evaluation of stability control systems to improve the roll propensity of heavy vehicles [57]. In this project, two Class 8 tractors and a 53-ft dry box van semitrailer were tested in both a lightly- and heavily-loaded condition. In addition, both tractors and the trailer were equipped with a stability control system. The performance test maneuvers performed in this project are summarized in Table 7-3.

Table 7-3. Test Maneuvers performed in [57].

#	Maneuver	Test Setup	Termination Condition
1	Constant Radius Circle with Increasing Velocity	(1) Conducted on the 150-ft and 200-ft radius circle; (2) the driver steered the vehicle to maintain the radius as the vehicle tended to understeer	(1) The driver was no longer able to follow the radius; (2) outrigger contacted the ground
2	J-turn	(1) 150-ft and 200-ft radius; (2) dropped throttle (clutch-in) when entering the start gate; (3) test entrance speed started at 20 mph with an increment of 2 mph	(1) Outrigger contacted the ground; (2) the vehicle was noticeably understeering; (3) stability control brake activated; (4) the test entrance speed reached 50 mph
3	Double Lane Change	(1) Test course setup is shown in Figure 7-16; (2) dropped throttle (clutch-in) when entering the start gate; (3) test entrance speed started at 20 mph with an increment of 2 mph	(1) Outrigger contacted the ground; (2) the vehicle was grossly under- or over-steering; (3) stability control brake activated; (4) the test entrance speed reached 50 mph
4	Slowly Increasing Steer Maneuver (SIS)	(1) Conducted at a constant speed of 30 mph; (2) used steering controller to increase the hand wheel angle at 13.5 degrees/second until a magnitude of 270 degrees was reached; (3) conducted both clockwise and counterclockwise	(1) The maximum hand wheel angle was achieved; (2) the vehicle experienced wheel lift
5	Ramp Steer Maneuver	(1) The entrance speed started at 20 mph with an increment of 2 mph; (2) dropped throttle (clutch-in) when entering the start gate; (3) the hand wheel angle increased at a rate of 175 degrees/second to the maximum angle determined by SIS test results	(1) Outrigger contacted the ground; (2) articulation angle exceeded the limited value; (3) the test entrance speed reached 50 mph

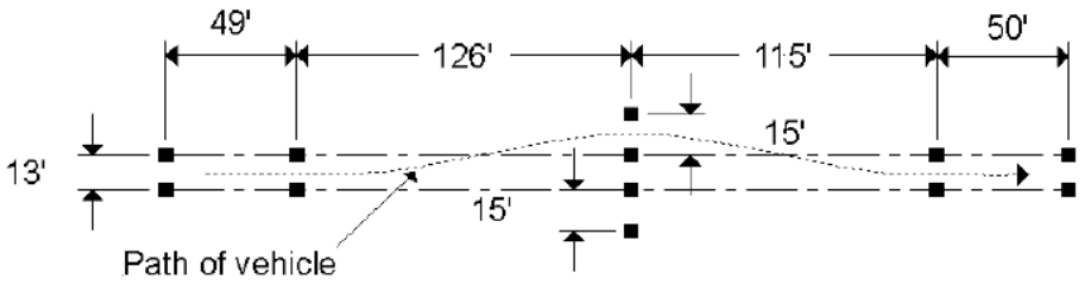

Figure 7-16. NHTSA Double Lange Change course setup [57].

The performance test maneuvers applied in this project required a large testing area and safety equipment, such as safety outriggers and anti-jackknifing structures, as well as a steering controller/robot for SIS and Ramp Steer maneuvers.

NHTSA also published a technical report on the tractor semitrailer stability objective performance test research for yaw stability in 2013 [58]. The objectives of this project were similar to those for the roll stability test project introduced above, but on truck yaw stability. Three Class 8 tractors and four trailers were tested with and without stability control systems. The performance test maneuvers applied in this project are summarized in Table 7-4.

Table 7-4. Test Maneuvers performed in [58].

#	Maneuver	Test Setup	Termination Condition
1	Sine with Dwell and Half-Cycle Sine with Dwell	(1) The generic steering inputs are shown in Figure 7-17; (2) performed at multiple frequencies between 0.3 and 0.7 Hz; (3) two dwell times were tested, 0.5 and 1.0 second; (4) the amplitude of steering angle was determined based on SIS test results	(1) Articulation angle reached 45 degrees or higher; (2) wheel lifted greater than 2 in. for tractor drive axles or trailer axles
2	150-ft Brake-In-Curve Maneuver	(1) The procedure was similar to a 150-ft J-turn maneuver, but a full treadle brake application was made at 100 ft into the arc; (2) the test entrance speed started at 20 mph with an increment of 2 mph	(1) Articulation angle reached 45 degrees or higher; (2) wheel lifted greater than 2 in. for tractor drive axles or trailer axles; (3) test entrance speed of 50 mph achieved
3	Slowly Increasing Steer Maneuver (SIS)	(1) Conducted at a constant speed of 30 mph; (2) used steering controller to increase the hand wheel angle at 13.5 degrees/second until a magnitude of 270	(1) The maximum hand wheel angle was achieved; (2) the

		degrees was reached; (3) conducted both clockwise and counterclockwise	vehicle experienced wheel lift
4	Ramp Steer Maneuver	(1) The entrance speed started at 20 mph with an increment of 2 mph; (2) dropped throttle (clutch-in) when entering the start gate; (3) the hand wheel angle increase at a rate of 175 degrees/second to the maximum angle, which was the average steering wheel angle needed to achieve 0.5 g of lateral acceleration in a 30 mph SIS test	N/A
5	Ramp with Dwell Maneuver	(1) Started with a small constant steering input, then increased the steering wheel magnitude over a 1.0-second interval, held that magnitude for 3.0 seconds, and then returned the steering wheel back to zero over a 1.0-second interval; (2) the initial steering angle was the drive-through angle needed to negotiate a 500-ft radius on the Jennite surface at the maximum drive through speed; (3) the steering wheel angle amplitudes were determined by multiplying a constant (K) integer with a value from 2 to 6 times the characterization drive-through angle rounded to the nearest 90 degrees, and for each test K was increased by 1 until stability control activation occurred	(1) Completed a test at each steering angle increment for the left and right steering directions for each test condition evaluated

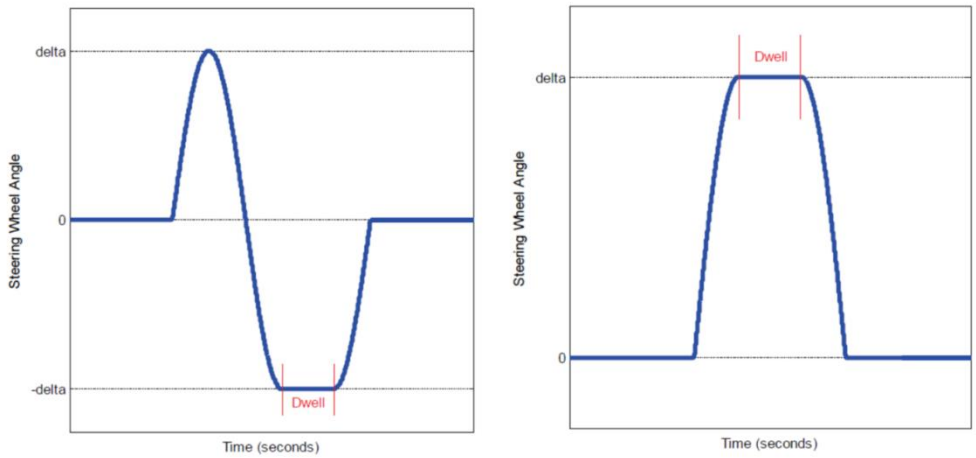

Figure 7-17. The generic profile of (a) Sine with Dwell, and (b) Half-Cycle Sine with Dwell [58].

The performance test maneuvers applied in this project also required a large testing area and safety equipment, such as safety outriggers and anti-jackknifing structures, as well as a steering controller/robot for most maneuvers.

In 2015, NHTSA signed a Federal Motor Vehicle Safety Standards for evaluating electronic Stability Control Systems for Heavy Vehicles–FMVSS 136. This regulation requires electronic stability control (ESC) systems on truck tractor and certain buses with a gross vehicle weight rating of greater than 26,000 lb (11,793 kg). According to the document, SWD and SIS were proposed by NHTSA as the performance tests. However, the two tests were opposed by several heavy truck manufacturers due to the difficulties of performing the tests, such as the testing area requirement, steering controller, etc. Instead, the 150-ft J-turn maneuver was selected as the performance test for an ESC system in FMVSS 136.

7.2.4.2 Proposed Test Maneuvers

According to the literature research, four maneuvers were initially proposed for this test program to comprehensively evaluate the directional dynamics of the 28-ft A-train double, which included:

- 150-ft J-turn Maneuver operated by a human driver
- Double Lane Change (DLC) Maneuver operated by a human driver
- Slowly Increasing Steer (SIS) Maneuver operated by a steering robot
- 0.5-Hz Sine-with-Dwell (SWD) maneuver operated by a steering robot

These performance maneuvers were selected with considerations of including both closed-loop path-following tests (150-ft J-turn, DLC) and open-loop steering input tests (SWD). The path-following tests included the subjective response of a human driver, which closely represents real-world scenarios, while the completely objective open-loop steering tests had high repeatability that could greatly eliminate human influence when comparing the performance of different safety systems with the same maneuver. In addition, both roll and yaw dynamics were condensed when determining the maneuvers. For example, 150-ft J-turn is a standard performance maneuver for evaluating vehicle roll stability, whereas the 0.5-Hz SWD was performed by NHTSA to study the yaw stability of Class 8 trucks.

Considering the fact that these proposed maneuvers have not been tested with trucks in an A-train configuration based on the open literature, preliminary tests are necessary to examine their applicability for this program before applying them for final tests.

7.3 Preliminary Tests

The following section details the preliminary tests conducted at the CVeSS facility and the Michelin Laurens Proving Ground (MLPG) between May and September 2016. The objectives of these preliminary tests included examining the performance of all safety and electronic systems, and looking for any design defects that needed improvement.

7.3.1 Preliminary Laboratory Tests

Eight rounds of preliminary laboratory tests were conducted at the CVeSS facility for examining the performance of mechanical safety structures, the DAQ system, and the steering robot. The details of these tests are introduced in Table 7-5.

Table 7-5. Details of eight sets of preliminary laboratory tests conducted at the CVeSS facility.

Test #	Objective(s)	Finding(s)
1	• Test the integrity of CVeSS outrigger assembly • Derive the ratio between actual outrigger contact force and load cell reading	• The outrigger could provide sufficient support when the trailer wheels on the other side were lifted off the ground • A ratio of 12 was determined and used to describe the relation between actual outrigger contact force and load cell reading
2	Examine the stiffness of the kinetic ropes used in CVeSS anti-jackknifing systems	• The rope managed to withstand a peak tensile force of 8,261 lbf, at an estimated stiffness of 153.97 lbf/in. • The rope met the specification required by the anti-jackknifing systems
3	Examine the functionality of sensors installed on the rear trailer	The rear junction box and all the sensors installed on the rear trailer worked functionally
4	Examine the proposed method of synchronizing analog and video data	The proposed method successfully synchronized analog and video data
5	• Test J-turn maneuvers with the test truck in single-trailer configuration • Examine the performance of a GPS unit on vehicle trajectory and speed recording	• Four sets of 50-ft J-turn tests were successfully conducted • The GPS unit provided good results of vehicle trajectory and speed during the tests
6	• Repeat J-turn maneuvers and also test double-lane-change (DLC)	• Two sets of J-turn and four sets of DLC maneuvers were successfully performed

	maneuvers with the test truck in single-trailer configuration • Examine the performance of a front junction box for data acquisition	• The front junction box functioned well, indicating that the DAQ system had been ready for tests with the double-trailer configuration
7	• Test the truck in double-trailer configuration with constant turning radius and increasing speeds • Examine the DAQ system in full configuration	• A jackknifing accident occurred between the tractor and front trailer during testing (no anti-jackknifing system was installed on this location at the time) • The anti-jackknifing system managed to prevent a jackknifing event between the two trailers • However, it was found that the anti-jackknifing systems needed further reinforcement to provide better performance
8	• Examine the performance of the CVeSS steering robot • Calibrate robot control parameters if needed	• The initial parameters for the steering robot to perform J-turn and DLC tests were obtained • Further tests on a proving ground were found to be needed for performance improvement

The preliminary laboratory tests successfully examined the performance of mechanical safety structures, the DAQ system, and the steering robot. However, further preliminary tests were still necessary after moving to the testing facility due to the fact that the space at the CVeSS facility was limited, and no full-scale maneuvers could be performed.

7.3.2 Preliminary Track Tests

The following section introduces the preliminary track tests conducted at the Michelin Laurens Proving Ground (MLPG) in South Carolina. This facility would also be used for the final tests. MLPG Track 8 served as the testing ground for all full-scale tests conducted in this program, and consists of a 400 ft × 1400 ft asphalt Vehicle Dynamic Assessment (VDA) pad, and a two-mile access loop, as shown in Figure 7-18 and Figure 7-19. The asphalt pad has sufficient space to set up courses for the proposed maneuvers, and the access loop can be used to accelerate the vehicle to reach the target speed.

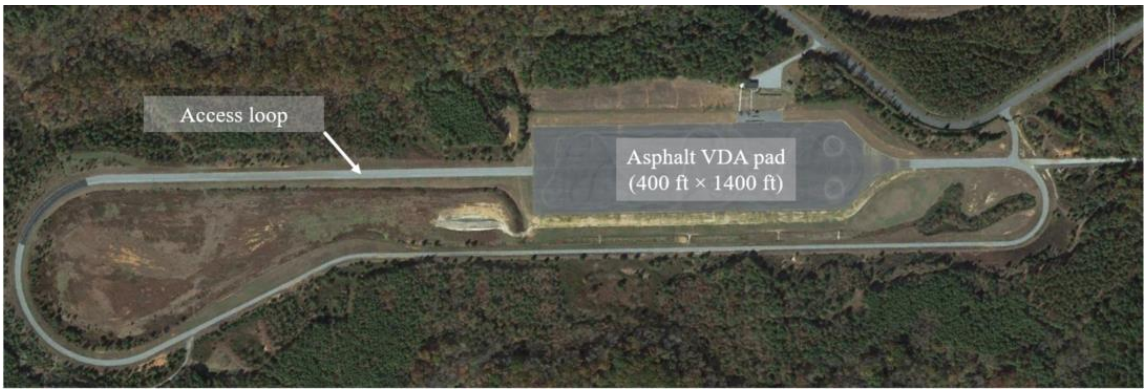

Figure 7-18. Google Earth view of Track 8 area at MLPG (Google Earth image, accessed January 2017).


Figure 7-19. VDA testing area at MLPG Track 8.

The main objectives of the preliminary track tests were to:

- Determine outrigger height;
- Determine length of the ropes and chains for the anti-jackknifing systems;
- Examine the strength and integrity of the outriggers and anti-jackknifing systems through dynamic tests;
- Examine proposed test maneuvers and design new ones if necessary; and
- Test and tune the steering robot, and determine all the parameters needed for the robot-operated maneuvers.

Full-scale driver- and robot-operated J-turn maneuvers were performed first to find the proper outrigger height. The outrigger wheel-to-ground height was eventually set at nine inches from the ground based on the test results. At this height, the outrigger wheels make

contact with the ground, right after the trailer tips up, as shown in Figure 7-20. Then a test-based evaluation was conducted to finalize the configuration of the anti-jackknifing system, where the maximum allowable articulation angles were determined as:

- Tractor/front-trailer: ~33 degrees
- Front-trailer/dolly: ~12.5 degrees
- Front-trailer/rear-trailer: 48 ~ 53 degrees depending on the dolly motion

Figure 7-20. Wheels were lifted when outriggers contacted the ground.

Next, SIS maneuvers were performed by the steering robot in both directions to generate data for determining the steering input for the SWD tests. Specifically, as suggested by NHTSA, the test truck maintained the speed at 30 mph and slowly increased the steering wheel angle at 13.5 degrees per second. The steering wheel angle was documented when the tractor lateral acceleration reached 0.5g, which would be used as the 100% steering input for the SWD tests. The SIS test results are included in Table 7-6. Although the driver had floored the throttle, he was not able to maintain the speed at 30 mph. Therefore, "corrected angles" were estimated, assuming that the steering wheel angle and turning radius had a linear relationship. Since the corrected angles for clockwise and counterclockwise turning were -244.4 and 259.9 degrees, respectively, the team selected 250 degrees as the steering angle input for the SWD tests.

Table 7-6. Steering wheel angles that resulted in 0.5-g tractor lateral acceleration.

Direction	Ay (g)	Steering angle (deg.)	Speed (mph)	Corrected angle (deg.)
Clockwise	-0.5008	-248.5	29.75	-244.4
Counterclockwise	0.5004	268.8	29.50	259.9

With the steering wheel angle input determined, 0.5-Hz SWD tests were then conducted. The SWD steering wheel input started with an amplitude of 30% of 250 degrees as derived from the SIS tests, and increased with an increment of 10% until 100% steering was achieved. Figure 7-21 gives an example of a 0.5-Hz SWD maneuver with 70% to 100% steering wheel input.

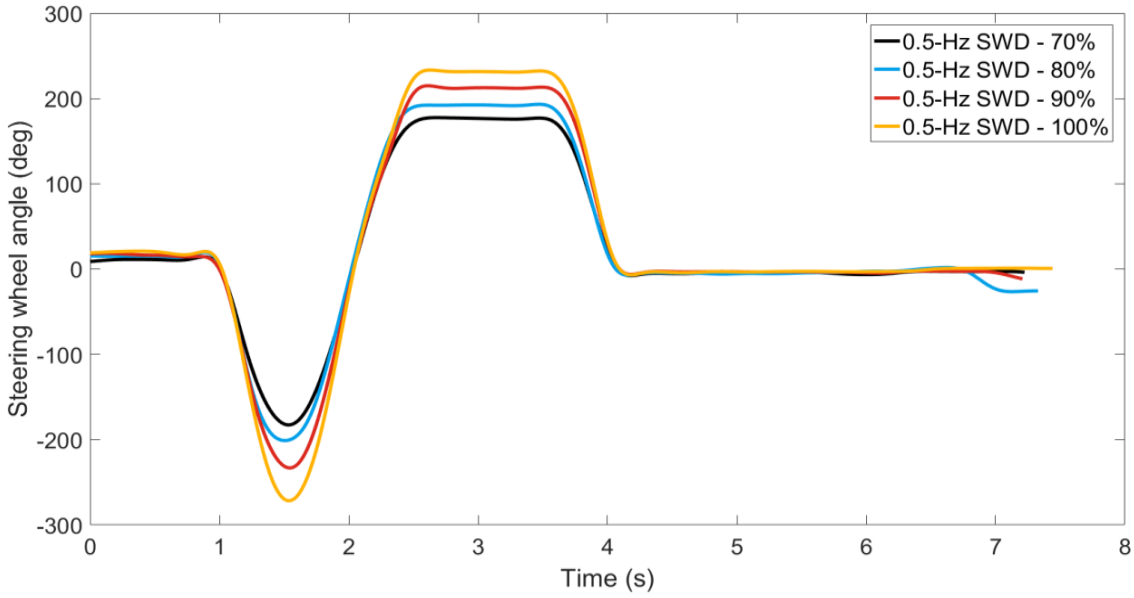

Figure 7-21. 0.5-Hz SWD steering wheel input.

Besides rollover, excessive understeer could also cause problems for a truck. For instance, when a truck performs an obstacle-avoidance maneuver on the highway, excessive understeer could make the trailer hit the obstacle even though the truck does not roll over. This is particularly important for this test program because ESC and RSC systems intend to introduce extra understeer to the truck by applying brakes to implement the control strategy. Therefore, a series of cones were placed 100 ft away from the starting point, representing an obstacle on the road that needed to be avoided. The maneuverability of the truck could be quantified by counting how many cones were hit during the tests. The cone layout is shown in Figure 7-22; 16 cones (one ft apart) were placed to simulate an obstacle that is 15 ft wide. The GPS trajectory of this maneuver is shown in Figure 7-23.

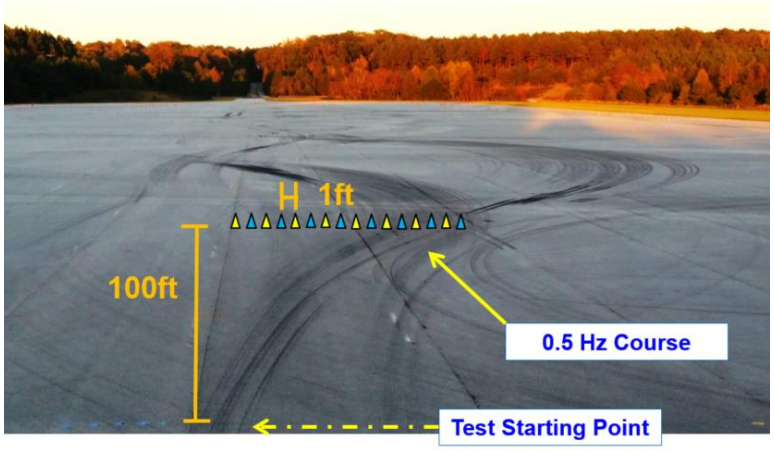

Figure 7-22. Cone layout for 0.5-Hz SWD tests.

The 0.5-Hz SWD results show that the truck experienced passenger-side outrigger contacts at 90% steering (~1,451 lbf on Trailer A, and ~1,512 lbf on Trailer B), and again at 100% steering (1,625 lbf on Trailer A, and 1,546 lbf on Trailer B).

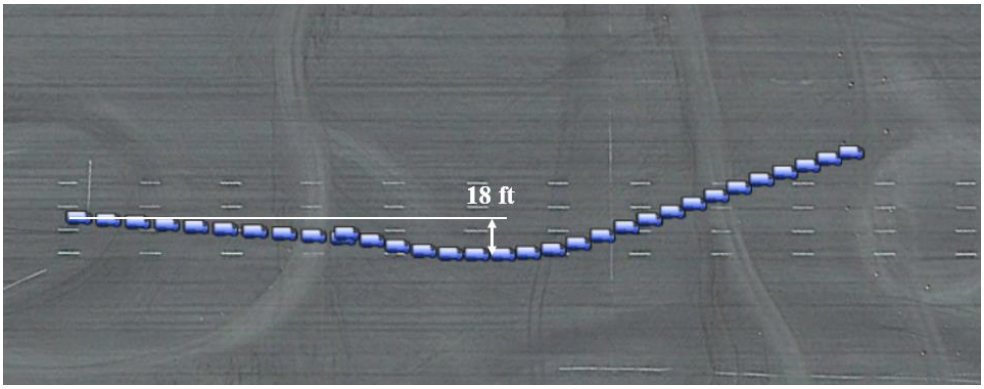

Figure 7-23. Vehicle trajectory of the 0.5-Hz SWD with 90% steering.

Considering that only the passenger-side outriggers made contact during the 0.5-Hz SWD tests, a more dynamic robot-operated maneuver was deemed necessary to excite the test truck in both directions. This could not be achieved by simply increasing the amplitude of the existing 0.5-Hz SWD steering input, due to the fact that it requires turning the steering wheel from 0 to -250 degrees, and then from -250 to 250 degrees in 1.5 seconds to perform the first three-quarters of the 100% 0.5-Hz SWD, which normally pulled 1.33 horsepower (1 horsepower = 550 ft-lbf per second) from the steering robot to perform this maneuver. In other words, the 0.5-Hz SWD maneuver at 100% steering has already reached the capability limit of a human driver, and thus increasing the amplitude would make this

maneuver impractical. Therefore, another SWD maneuver was proposed with the same maximum steering angle amplitude, but the frequency was adjusted to 0.25 Hz and the dwell was also extended to two seconds, as shown in Figure 7-24. A series of cones was again placed to quantify the maneuverability of the truck during these tests, as shown in Figure 7-25; 16 cones were placed 200 ft from the starting point, and the distance between two adjacent cones was 4 ft.

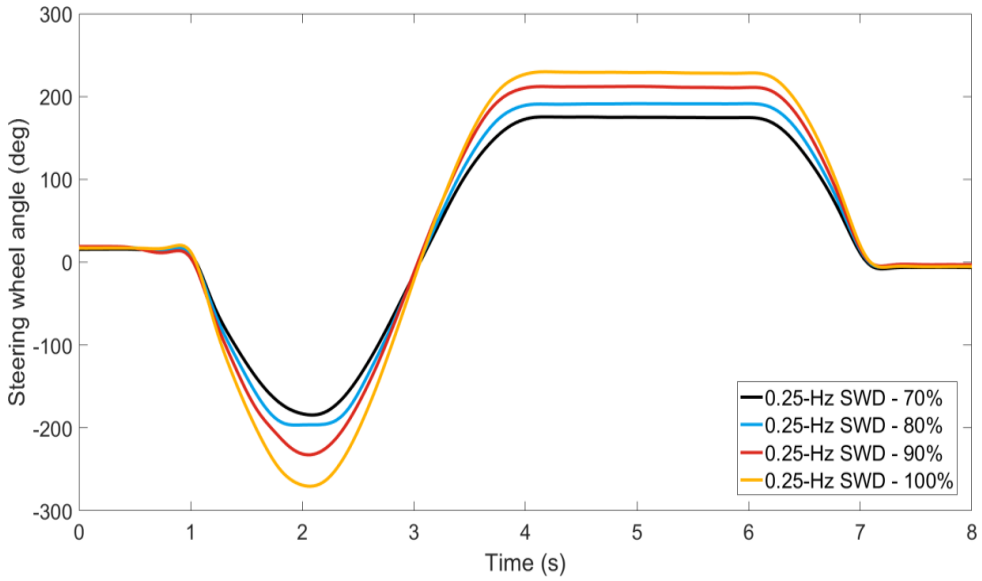

Figure 7-24. Newly-proposed 0.25-Hz SWD maneuvers.

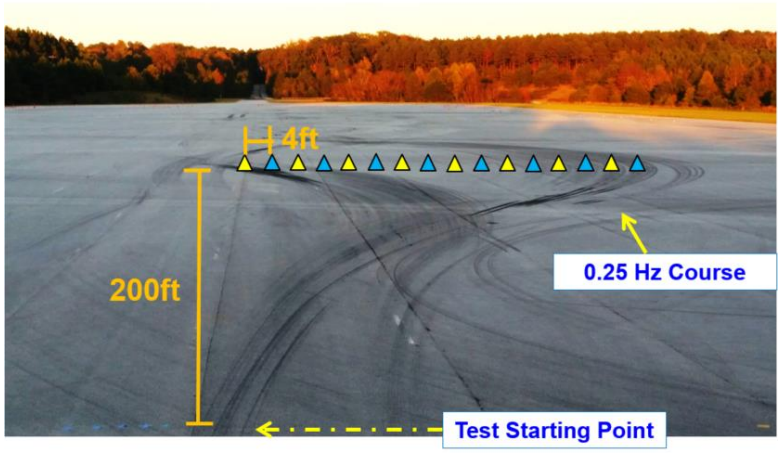

Figure 7-25. Cone layout for 0.25-Hz SWD tests.

The newly-proposed 0.25-Hz SWD maneuvers were also tested during the preliminary track testing. Figure 7-26 compares the data of lateral accelerations collected during a 90% 0.25-Hz SWD test and a 90% 0.5-Hz SWD test. It can be observed that the truck

experienced larger lateral accelerations during the 0.25-Hz SWD test at the first turn (t=2s for 0.5-Hz test, and t=3s for 0.25-Hz test). When the tractor steered back and "dwelt," both Trailer A and Trailer B were subjected to more aggressive dynamics in the 0.25-Hz SWD test, indicated by large lateral acceleration spikes and oscillations (t=6s) resulting from outrigger contacts. The outrigger contact information for these two tests is summarized in Table 7-7, which shows that the 0.25-Hz test resulted in more and heavier peak contact forces for all outriggers, compared to the 0.5-Hz SWD test that only led to outrigger contacts on the passenger side.

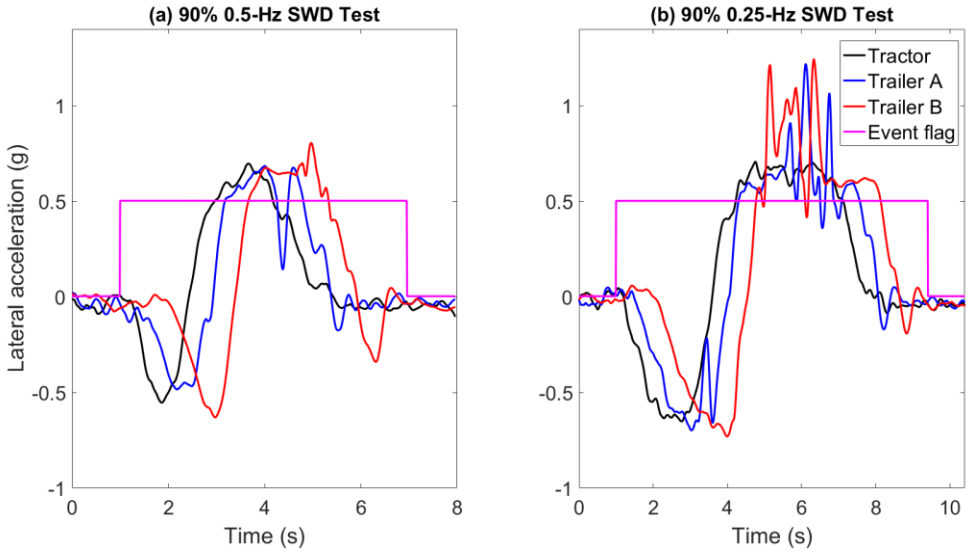

Figure 7-26. Test results comparison between 0.5- and 0.25-Hz SWD tests both at 90% steering.

The vehicle trajectory of a 90% 0.25-Hz SWD test is shown in Figure 7-27. This test maneuver emulates the scenario where a vehicle takes the ramp to exit a highway at an excessive speed.

Table 7-7. Peak outrigger contact force for 0.5- and 0.25-Hz SWD tests both at 90% steering.

Test	Peak Outrigger Contact Force (lbf)			
	Trailer A Dri. side	Trailer A Pas. side	Trailer B Dri. side	Trailer B Pas. side
0.5-Hz SWD 90% Steering	N/A	479.5	N/A	847.1
0.25-Hz SWD 90% Steering	660.3	619.5	487.7	1708.3

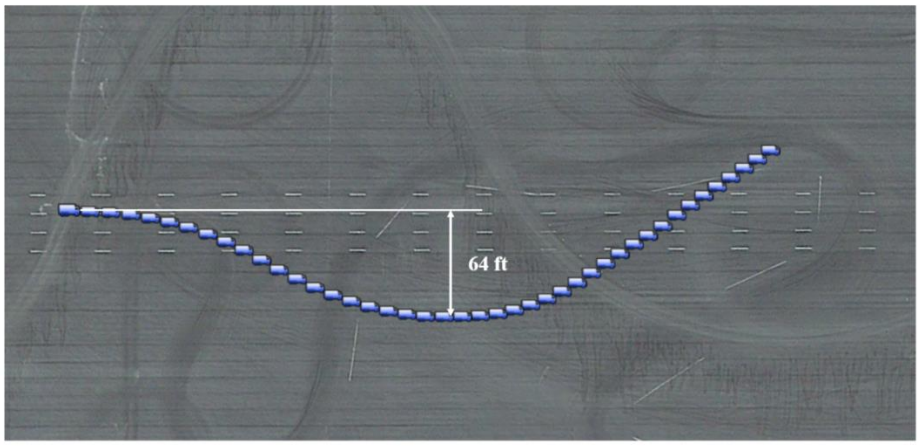

Figure 7-27. Vehicle trajectory of the 0.25-Hz SWD with 90% steering.

After completing the SWD tests, the Double Lane Change (DLC) course was set up according to NHTSA standard, as shown in Figure 7-28. The driver was instructed to approach the start gate at a designated speed, drop throttle (clutch out), and maneuver the truck through the course without hitting any cones.

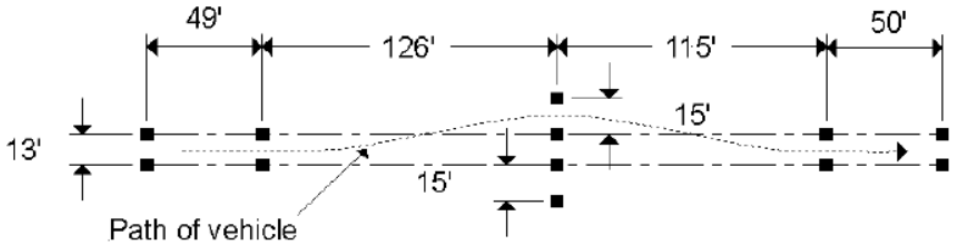

Figure 7-28. NHTSA Double Lane Change Course Setup (ft) [57].

7.4 Finalization of Instrumentation Plan

The initially proposed instrumentation plan was tested through the preliminary tests, and several modifications had been completed either to fix the problems discovered during the tests, or to acquire additional analog or video data found to be important. According to the finalized instrumentation plan, 29 sensors and 6 cameras were applied and installed on the test truck. The comprehensive instrumentation diagram is shown in Figure 7-29, and the sensor specifications can be found in Appendix D. The locations for all the cameras are illustrated in Figure 7-30.

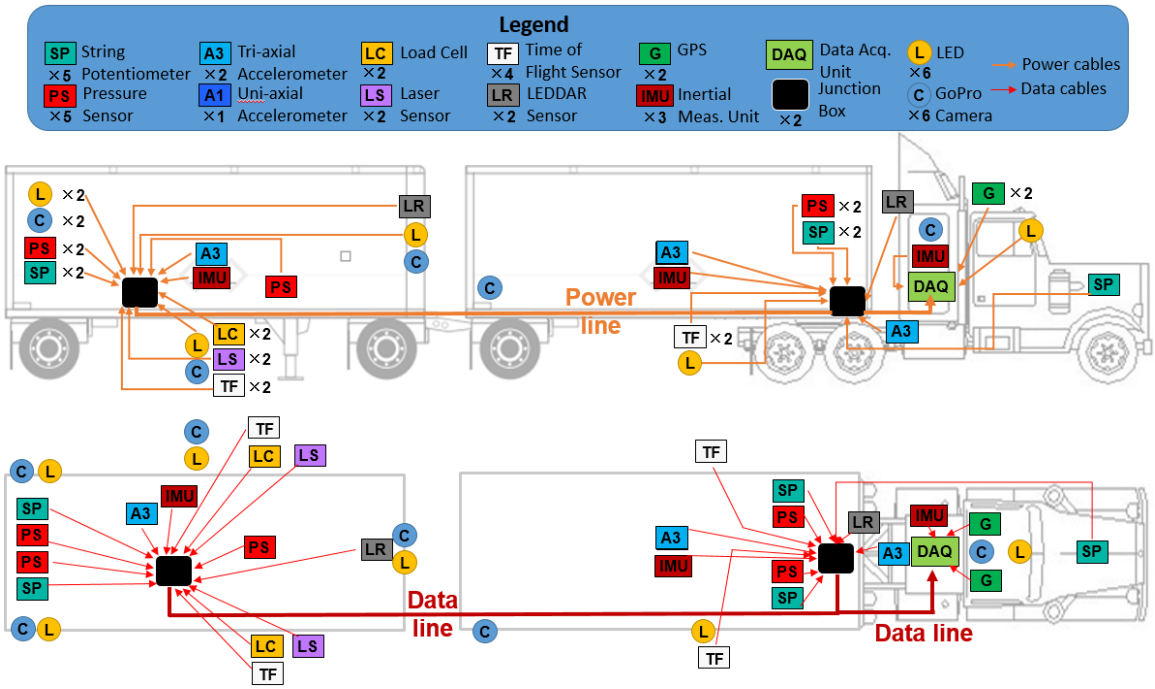

Figure 7-29. Finalized instrumentation diagram.

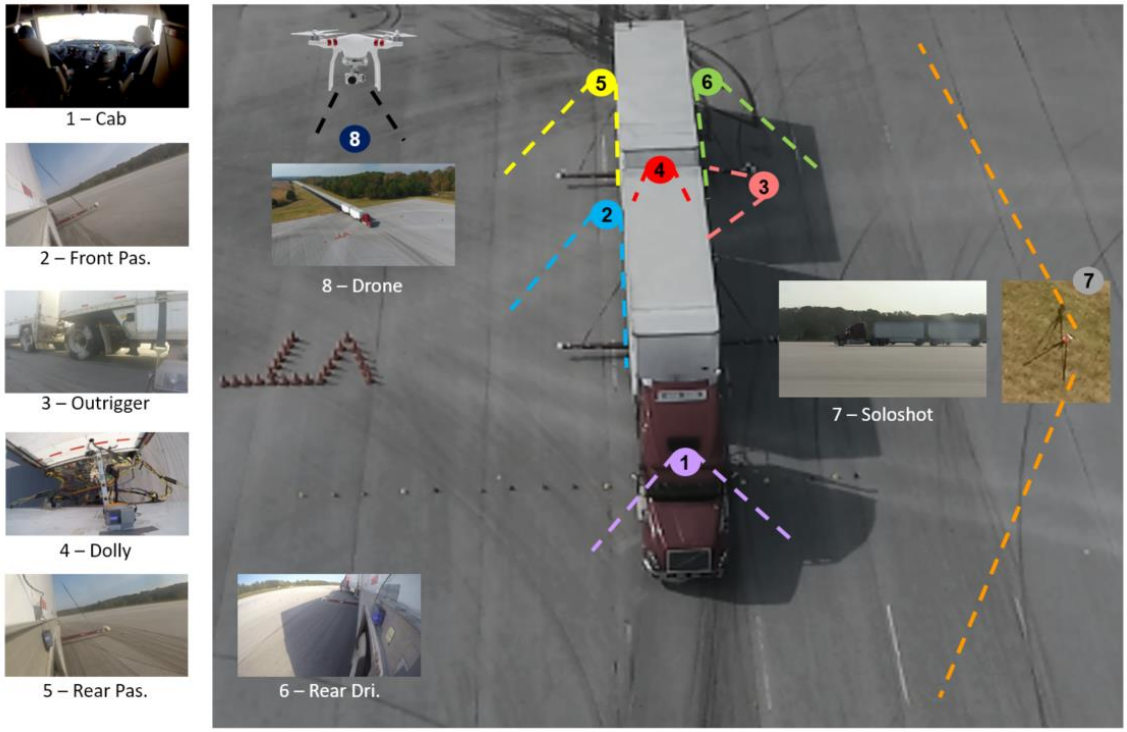

Figure 7-30. Locations and views of all the cameras used during tests.

7.5 Summary

This chapter introduces the preliminary tests conducted at the CVeSS facility and at MLPG. The achievements accomplished during the preliminary tests are summarized as follows:

- Set the outrigger wheel-to-ground height at 9 in. according to the truck dynamic response and safety considerations;
- Conducted test-based evaluation to determine the configuration of the anti-jackknifing system, and set the maximum allowable articulation angles as:
    - Tractor/front trailer: ~33 degrees
    - Front trailer/dolly: ~12.5 degrees
    - Front trailer/rear trailer: 48 ~ 53 degrees depend on the dolly motion
- Examined the strength and integrity of the outriggers and anti-jackknifing systems through dynamic tests;
- Examined the performance of the DAQ system and finalized the instrumentation plan;
- Tested and tuned the steering robot, and determined all the parameters needed for the robot-operated maneuvers;
- Conducted tests on the VDA pad to evaluate all the proposed test maneuvers, and designed and tested new maneuvers for the final tests. The test maneuvers that would be used in the final tests included:
    - 150-ft J-turn
    - Ramp Steer Maneuver (RSM)
    - Slowly Increasing Steer (SIS)
    - Double Lane Change (DLC)
    - 0.5-Hz Sine-with-Dwell (SWD)
    - 0.25-Hz Sine-with-Dwell (SWD)
- The test truck was found to have a higher lateral acceleration threshold (~0.7g) for rollover accidents, compared to that of a typical fully-loaded WB-67 semi-truck (~0.4g).

Chapter 8 – Test Results for a 28-ft A-train Double with Trailer-based Roll Stability Control (RSC) Systems

The details of the tests conducted at the Michelin's Laurens Proving Ground (MLPG) are presented in order to investigate the dynamic stability of a 28-ft A-train double with trailer-based RSC. First, an overview of the tests is provided, including the test objectives, additional test preparation work, finalized test maneuvers, and the test matrix. The corresponding test results and analysis are then discussed. The conclusions drawn from the test results are provided at the end of the chapter.

8.1 Test Overview

8.1.1 RSC System for Evaluation

The RSC system applied in this evaluation employed two 2S2M units for the double trailers (one on each). The "2S2M" indicates that such an RSC unit consists of two wheel speed sensors and two modulators. The function of a wheel speed sensor is indicated by its name−monitoring wheel speed. The modulator in an RSC system serves as an on/off valve for applying brakes when the Electronic Control Unit (ECU) of an RSC system determines that it is necessary. Because this RSC system has two modulators, it is capable of selectively applying brakes to an individual trailer wheel, which is similar to the stability control systems used on passenger cars. In addition, this RSC system has two steps of activation. The first step responds to transient dynamics, where the lateral acceleration has a large increasing rate but a relatively low overall amplitude. On the contrary, the second step responds to steady-state dynamics, where the lateral acceleration has a relatively low increasing rate but a high overall amplitude.

The RSC activation timing data was collected by the DAQ system and synchronized with the other analog data. When the RSC system activates, it sends a constant five-volt signal to the DAQ system. In addition, two pressure transducers were also installed on each trailer to measure the pressure applied to the air brakes. Therefore, both electronic and mechanical signals that indicate RSC activation were recorded.

Unfortunately, more details regarding the control algorithm were unavailable to the test team due to the fact that such information is proprietary to the manufacturer.

8.1.2 Test Maneuvers

As introduced in the previous chapter, six tests maneuvers would be applied in the tests. However, the purpose of the SIS maneuver is to determine the steering wheel input for the SWD tests, which had been accomplished in the preliminary track tests such that there was no need to repeat it. Thus, the five maneuvers that emulate high-speed, highway-driving conditions were performed, which included:

- 150-ft J-turn (J-turn – driver)
- Ramp Steer Maneuver (RSM, or J-turn – robot)
- Slowly Increasing Steer (SIS)
- Double Lane Change (DLC)
- 0.5-Hz Sine-with-Dwell (0.5-Hz SWD)
- 0.25-Hz Sine-with-Dwell (0.25-Hz SWD)

For simplicity, the terms in the parentheses indicate what these maneuvers would be referred to in the following chapters. The trajectory examples of the five maneuvers are shown in Figure 8-1 and Figure 8-2, and more details of these maneuvers will be introduced in the following sections. It is noted that the terminology of maneuvers applied in this dissertation is based on NHTSA's recommendation, some of which may vary from other sources.

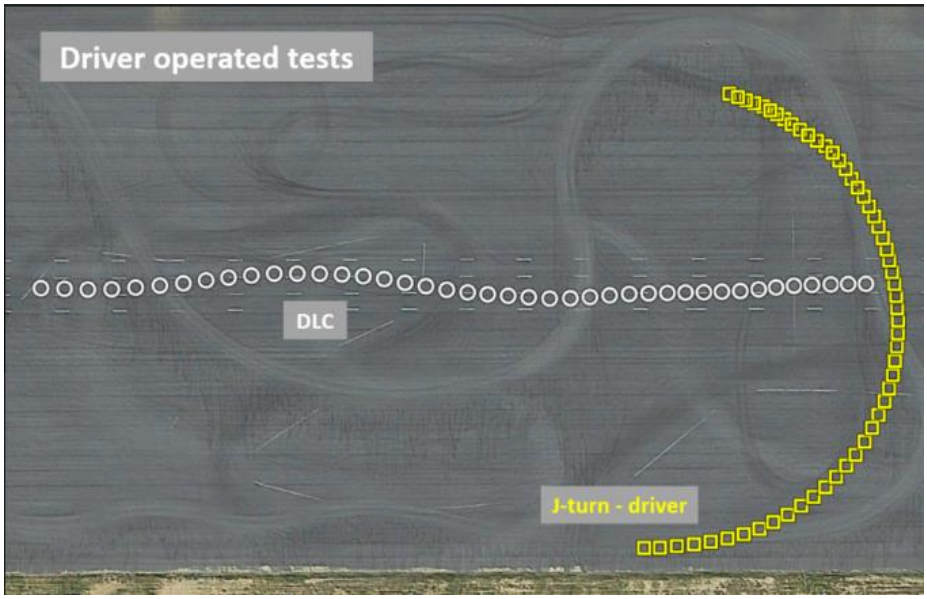

Figure 8-1. GPS trajectories for driver-operated tests.

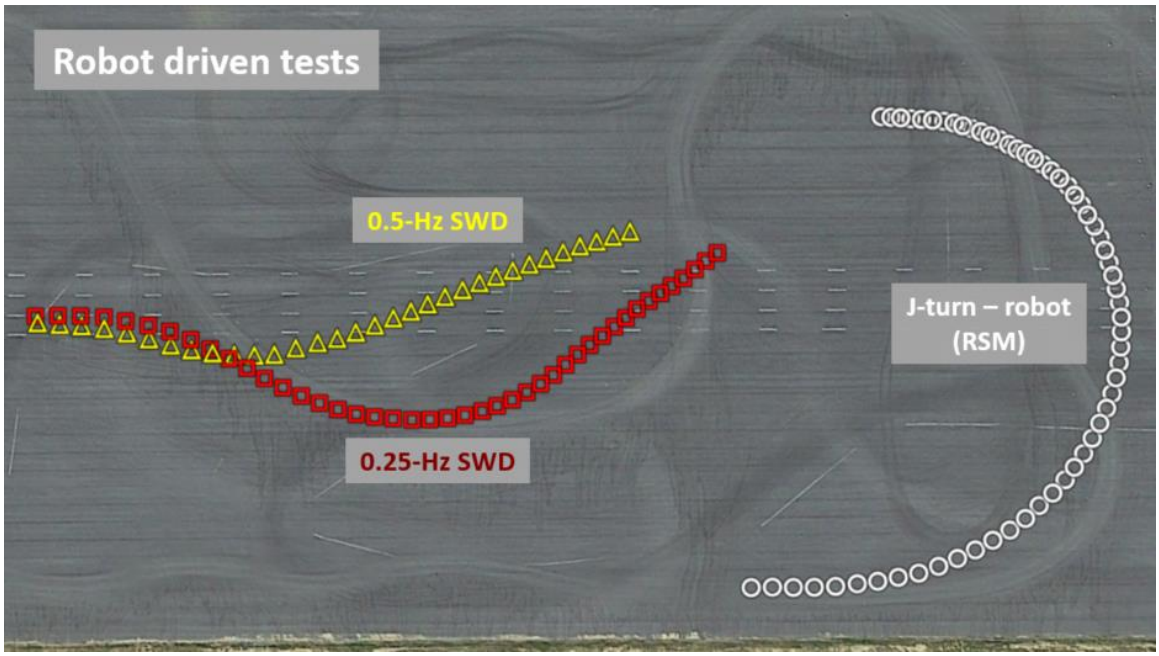

Figure 8-2. GPS trajectories for robot-operated tests.

8.1.2.1 150-ft J-turn Maneuver

The J-turn maneuver applied in the test had a constant radius of 150 ft, and the truck would be operated by a human driver. Figure 8-3 illustrates the course for this maneuver, which simulates a vehicle maneuvering through a curve of 120-180 degrees at high speeds on interstate or local highways. The inner side of the path was marked by cones (indicated by the inner black line) with a radius of 150 ft, and the outer side was also marked by cones (indicated by the outer black line) but with a radius of 162 ft, providing a path width of 12 ft. The ideal trajectory that the truck should follow is indicated by the red dashed line. In practice, the driver approached the starting point, dropped throttle (clutch-out), and steered the truck to stay within the two sets of cones. The entrance speed varied among different tests, but it generally started from 30 mph and increased to the point of failure (rollover). This maneuver will be referred to as "J-turn – driver" in the following chapters.

8.1.2.2 Ramp Steer Maneuver (RSM, J-turn – robot)

Similar to the driver-operated J-turns, the Ramp Steer Maneuver (RSM) also simulates a vehicle negotiating a curve of 120-180 degrees at high speeds on interstate or local highways. However, this maneuver would be performed by a steering robot for highly repeatable steering wheel input. In addition, instead of attempting to keep the truck in the

course, the truck was given a ramp steering input when reaching the starting point. The same steering input was used to run all the tests, as shown in Figure 8-4. Because the steering input profile of the RSM tests is similar to that of the driver-operated J-turns, the RSM will be referred to as "J-turn – robot" in the following chapters, and the results will also be discussed together with the driver-operated J-turn tests.

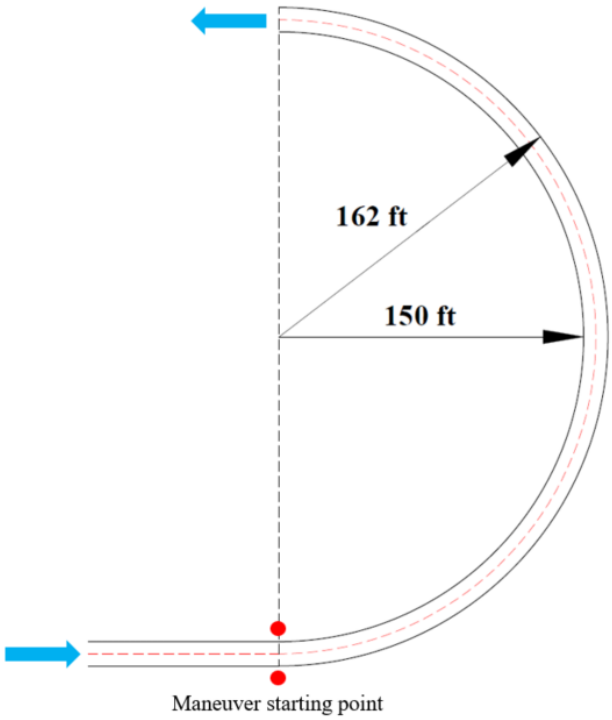

Figure 8-3. The course for the J-turn maneuver with a constant radius of 150 ft.

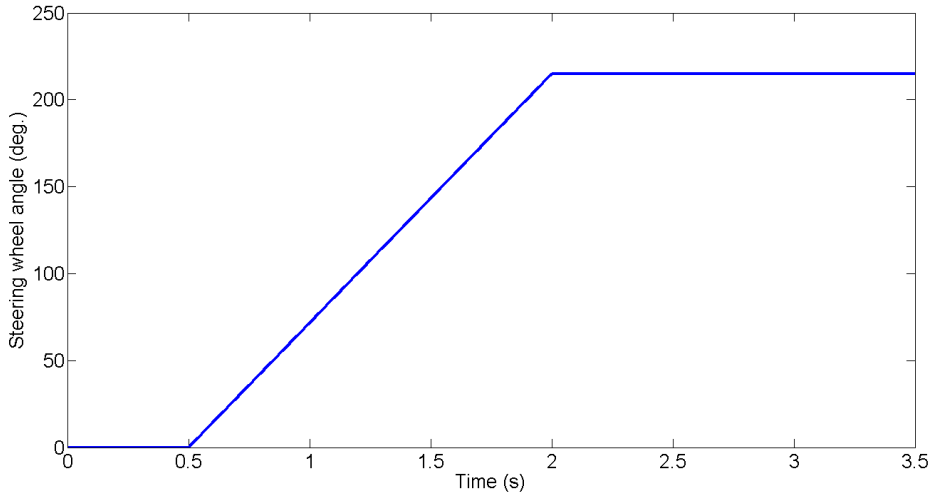

Figure 8-4. Steering wheel input for RSM (J-turn – robot).

8.1.2.3 Double Lane Change (DLC) Maneuver

The DLC maneuver simulates a vehicle performing a high-speed lane change on highways. The course setup is shown in Figure 8-5, which was adopted from NHTSA's recommendation [57].

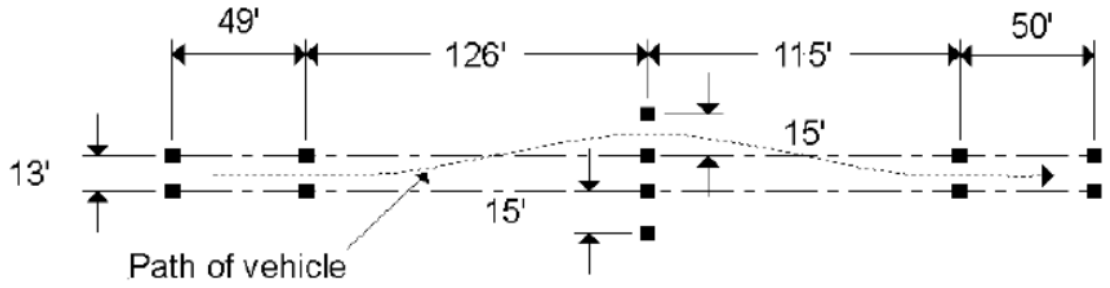

Figure 8-5. DLC maneuver course setup (ft) [57].

The driver was instructed to enter the gate, drop throttle (clutch-out), and steer the truck to follow the path without hitting any cones. The entering speed generally started from 48 mph, and increased to 56 mph with one- or two-mph increments. The driver dropped throttle (clutch-out) immediately after reaching the entering cones.

8.1.2.4 Sine-with-Dwell (SWD) Maneuvers

Two SWD maneuvers would be conducted to evaluate the dynamic stability of the test truck. The first was a 0.5-Hz SWD maneuver, which is proposed by NHTSA as standard to test electronic stability control systems for heavy trucks. This maneuver simulates a truck avoiding an obstacle at high speeds on highways, where the truck should neither roll over nor experience excessive understeer that fails to avoid the obstacle. The 0.5-Hz SWD maneuver consists of a 0.5-Hz sinusoidal steering input, where there is a one-second pause after the third quarter of the sinusoid input is completed. The amplitude of the steering input is determined at 250 degrees (100% steering input) based on the result of SIS tests when a 0.5-g lateral acceleration is experienced by the tractor. The 0.5-Hz SWD steering wheel angle input applied here is shown in Figure 8-6.

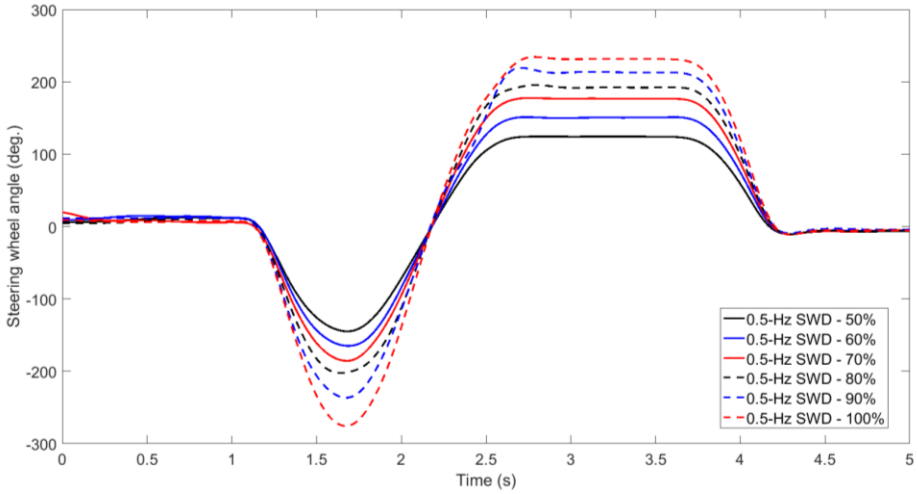

Figure 8-6. Steering wheel angle input for 0.5-Hz SWD tests.

As mentioned before, excessive understeer could also put the truck in danger. In order to qualitatively measure the understeer experienced by the test truck in a 0.5-Hz SWD test, a series of cones were placed 100 ft. away from the starting point at one ft apart, which represented the obstacle on the road that needed to be avoided; 16 cones were placed to represent an obstacle that is 15 ft wide. Therefore, the maneuverability of the truck could be quantified by counting the number of cones that were hit during the tests. The cone layout is shown in Figure 8-7.

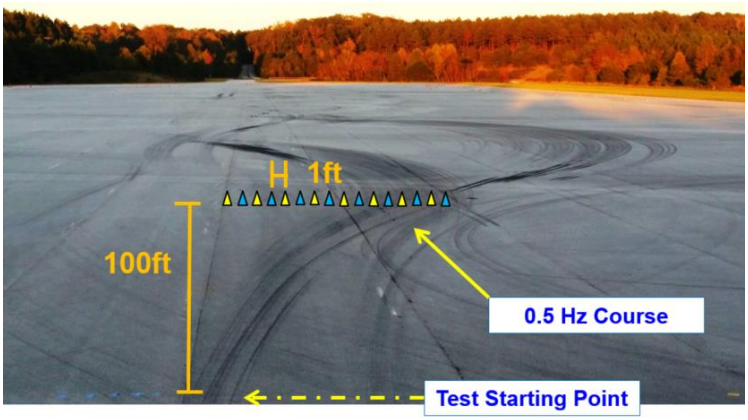

Figure 8-7. Cone layout for 0.5-Hz SWD tests.

In addition to the 0.5-Hz SWD tests as recommended by NHTSA, a new SWD maneuver was designed with 0.25-Hz sinusoidal steering input and a dwell of two seconds (shown in Figure 8-8), which particularly resulted in more aggressive dynamic response to the truck with double trailers. This maneuver simulates a truck taking an exit ramp off the highway at an excessive speed. Similarly, a series of cones was also placed to qualitatively measure

the maneuverability of the truck during these tests, as shown in Figure 8-9; 16 cones were placed 200 ft from the starting point, and the distance between two adjacent cones was 4 ft.

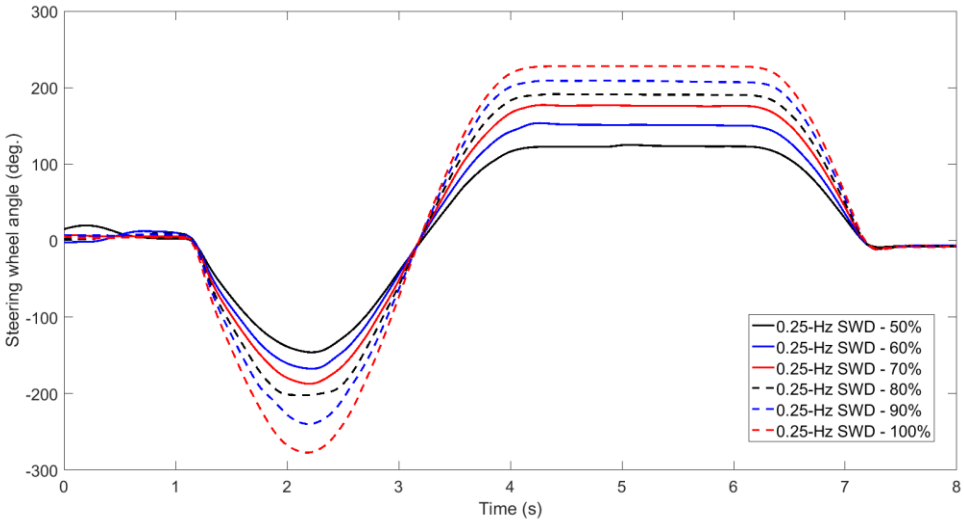

Figure 8-8. Steering wheel angle input for 0.25-Hz SWD tests.

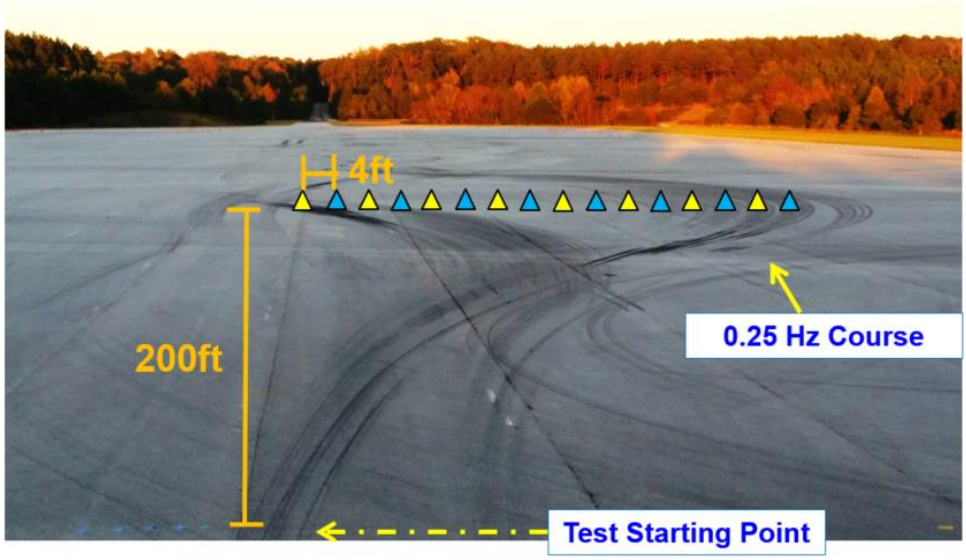

Figure 8-9. Cone layout for 0.25-Hz SWD tests.

8.1.3 Test Matrix

A total of 80 tests were conducted on the VDA testing area at MLPG Track 8 in three test sessions, and the details of the tests are included in Table 8-1.

Table 8-1. Test matrix for evaluating the dynamic stability of a 28-ft A-train double with trailer-based RSC systems.

Date: November 30, 2016 **Weather**: Overcast, 59°/69° **Track surface condition**: Dry							
Test #	**Maneuver**	**RSC**	**Speed (mph)**	**Test #**	**Maneuver**	**RSC**	**Speed (mph)**
1	J-turn - robot	RSC	35	12	J-turn - robot	RSC	41
2	J-turn - robot	RSC	36	13	J-turn - robot	Stock	42
3	J-turn - robot	RSC	37	14	J-turn - robot	RSC	42
4	J-turn - robot	Stock	38	15	J-turn - robot	Stock	42
5	J-turn - robot	RSC	38	16	J-turn - robot	Stock	43
6	J-turn - robot	Stock	39	17	J-turn - robot	RSC	43
7	J-turn - robot	RSC	39	18	J-turn - robot	RSC	43
8	J-turn - robot	Stock	40	19	J-turn - robot	RSC	44
9	J-turn - robot	Stock	40	20	J-turn - robot	RSC	45
10	J-turn - robot	RSC	40	21	J-turn - robot	RSC	46
11	J-turn - robot	Stock	41	22	J-turn - robot	RSC	47
Date: December 1, 2016 **Weather**: Sunny, 41°/60° **Track surface condition**: Dry							
Test #	**Maneuver**	**RSC**	**Steering (%)**	**Test #**	**Maneuver**	**RSC**	**Steering (%)**
1	0.5-Hz SWD	RSC	50	11	0.25-Hz SWD	RSC	50
2	0.5-Hz SWD	RSC	60	12	0.25-Hz SWD	RSC	60
3	0.5-Hz SWD	RSC	70	13	0.25-Hz SWD	RSC	70
4	0.5-Hz SWD	RSC	80	14	0.25-Hz SWD	RSC	80
5	0.5-Hz SWD	RSC	90	15	0.25-Hz SWD	RSC	90
6	0.5-Hz SWD	RSC	100	16	0.25-Hz SWD	RSC	100
7	0.5-Hz SWD	Stock	60	17	0.25-Hz SWD	Stock	60
8	0.5-Hz SWD	Stock	70	18	0.25-Hz SWD	Stock	70
9	0.5-Hz SWD	Stock	80	19	0.25-Hz SWD	Stock	80
10	0.5-Hz SWD	Stock	90	20	0.25-Hz SWD	Stock	90
Test #	**Maneuver**	**RSC**	**Speed (mph)**	**Test #**	**Maneuver**	**RSC**	**Speed (mph)**
1	DLC	RSC	48	9	DLC	RSC	55
2	DLC	RSC	48	10	DLC	RSC	56
3	DLC	RSC	52	11	DLC	RSC	56
4	DLC	RSC	54	12	DLC	Stock	52
5	DLC	RSC	54	13	DLC	Stock	54
6	DLC	RSC	54	14	DLC	Stock	54
7	DLC	RSC	55	15	DLC	Stock	55
8	DLC	RSC	55	16	DLC	Stock	55

Date: December 2, 2016 **Weather**: Sunny, 32°/59° **Track surface condition**: Dry							
Test #	**Maneuver**	**RSC**	**Speed (mph)**	**Test #**	**Maneuver**	**RSC**	**Speed (mph)**
1	J-turn - driver	RSC	30	12	J-turn - driver	Stock	38
2	J-turn - driver	RSC	32	13	J-turn - driver	RSC	38
3	J-turn - driver	RSC	34	14	J-turn - driver	Stock	39
4	J-turn - driver	Stock	36	15	J-turn - driver	RSC	39
5	J-turn - driver	RSC	36	16	J-turn - driver	Stock	39
6	J-turn - driver	Stock	37	17	J-turn - driver	RSC	39
7	J-turn - driver	RSC	37	18	J-turn - driver	Stock	40
8	J-turn - driver	Stock	37	19	J-turn - driver	RSC	40
9	J-turn - driver	RSC	37	20	J-turn - driver	RSC	42
10	J-turn - driver	Stock	38	21	J-turn - driver	Stock	40
11	J-turn - driver	RSC	38	22	J-turn - driver	RSC	41

8.2 Test Results and Analysis

The testing results collected are summarized and analyzed in this section. First, examples are given to introduce the key parameters or data used to assess the truck dynamics, as well as the performance of the RSC system. The test results will then be summarized and analyzed with respect to different maneuvers. The conclusions are provided at the end of the chapter.

8.2.1 Key Parameters and Data Processing Examples

Three metrics were determined to be used for evaluating the truck dynamics and the performance of the RSC system during each test, which are introduced as follows:

- Peak outrigger contact force
- System warning time: the time between RSC activation and the corresponding outrigger contact
- Speed drop: the speed reduction achieved between RSC activation and the corresponding outrigger contact

Besides the three universal metrics for all tests, the number of cones hit during the SWD tests were also used as an additional index specifically for SWD tests in order to evaluate how much understeer was introduced by the RSC systems. However, even though lateral

acceleration data is not required for deriving these four indices, it is a very essential parameter to represent the truck dynamics, and thus the data had been processed as well and used as supporting parameters when necessary. The lateral acceleration results of selected stock tests can be found in Appendix E. Other data, such as articulation angle, tractor or trailer suspension travel, etc., are less relevant to the objectives of this round of tests, but they were all collected during the test as well for potential future studies.

In order to derive the four indices mentioned above, the data needed include: (1) outrigger contact force; (2) RSC activation timing; and (3) speed. Examples are given to illustrate how these data are used to derive the four metrics. First, Figure 8-10 illustrates the activation and deactivation timing of RSC with respect to the lateral accelerations of Trailer B during a 0.25-Hz SWD test at 90% steering. It can be observed that Step 1 activated first (t=2.9s) in response to the fast lateral acceleration increase, and Step 2 also activated ~0.5s later. Step 1 deactivated at t=4.8s, whereas Step 2 maintained engagement until t=8s. This result clearly confirms that Step 1 and Step 2 activation respond to transient and steady-state dynamics, respectively. To be more specific, Step 2 maintained engagement between t=5s and t=8s where the lateral acceleration stayed around 0.6g, while Step 1 deactivated because it did not sense a fast rate of increase in lateral acceleration. It is noted that the large lateral acceleration spikes that occurred around t=5.5s were due to the impact force from the outrigger contacts. In addition, the Step 1 and Step 2 activations are implemented by two RSC modulators that control the same trailer in parallel, which means that the brakes are applied when either one or both steps are activated.

Figure 8-11 shows the definitions of the warning time and the peak outrigger contact force of a contact event on Trailer B. The warning time is defined as the time between the first RSC activation (either Step 1 or Step 2) and the moment of outrigger contact. The peak outrigger contact force is the maximum force that occurred during a contact event.

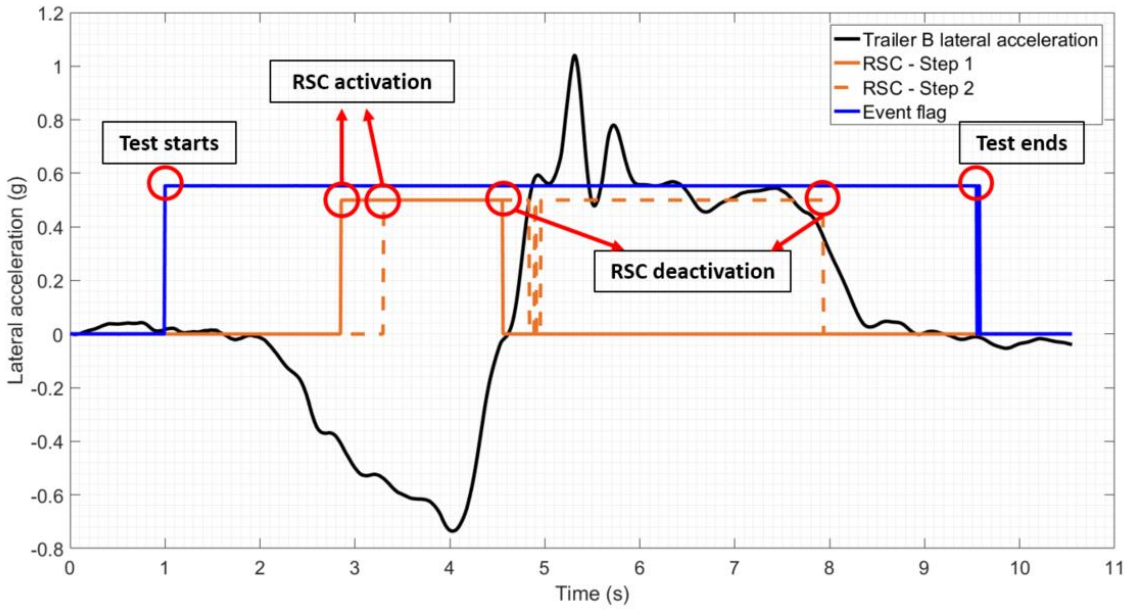

Figure 8-10. Trailer B lateral acceleration and RSC activation for a 0.25-Hz SWD test at 90% steering.

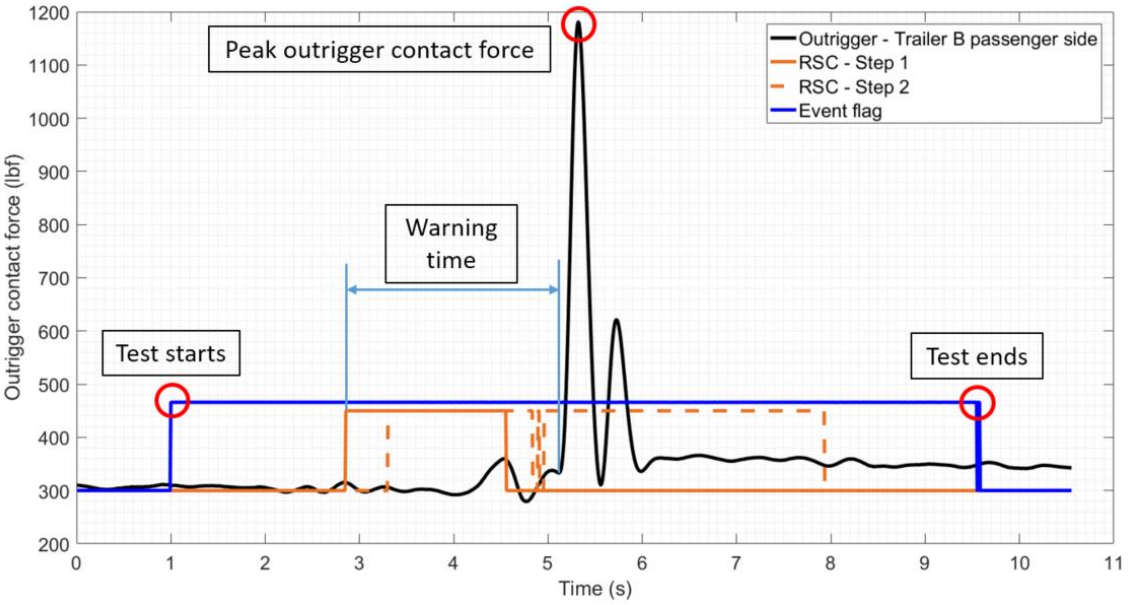

Figure 8-11. Warning time and rear passenger-side outrigger contact force for a 0.25-Hz SWD test at 90% steering.

Figure 8-12 gives a comparison of truck speed reduction in two tests. The first one (black line) is a stock test where no brake was applied during the test, whereas the other one (red line) shows the truck speed profile when the RSC system was equipped. Therefore, speed drop data can be used to evaluate the effectiveness of a certain RSC system.

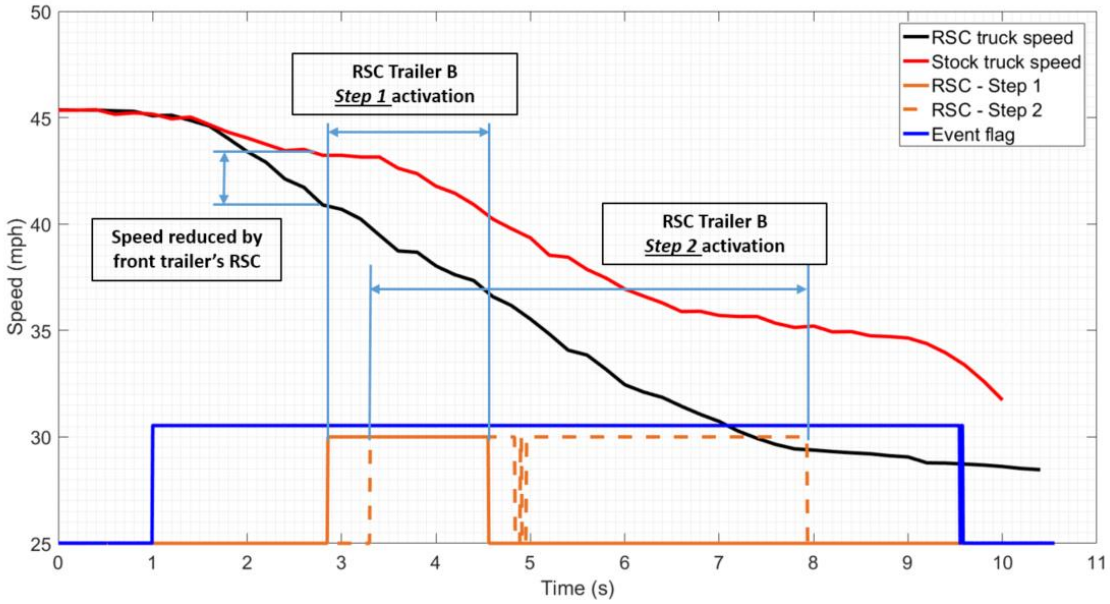

Figure 8-12. The truck speed comparison between the stock and RSC in 0.25-Hz SWD tests at 90% steering.

8.2.2 J-turn Tests

The results of both the driver-operated 150-ft J-turn and the robot-operated J-turn (RSM) maneuvers are presented and analyzed in this section. Figure 8-13 illustrates the peak outrigger contact forces experienced by the test truck during J-turn maneuvers. Only the outrigger on the Trailer A passenger side made contact during the tests, and thus the results on this outrigger are presented. Figure 8-13(a) shows that during the driver-operated J-turn tests, the stock truck started to experience outrigger contact at 38 mph, whereas equipping with the RSC system managed to increase this speed to 39 mph. For the 39- and 40-mph tests, where outrigger contact occurred in both the stock and RSC tests, the RSC system significantly reduced the peak contact forces when compared with the stock tests, indicating that although the RSC system did not completely prevent the trailer from rolling over in these scenarios, it managed to considerably attenuate the severity of the potential rollover accidents. The stock test was not performed at 41 mph due to safety concerns. Figure 8-13(b) summarizes the results of the robot-operated J-turn tests, where the stock tests started to show outrigger contact at 41 mph, and a stronger outrigger contact happened at 42 mph. The RSC system performed better in the robot J-turn tests than in the driver J-turns, since the entrance speed had to be increased to 45 mph to roll over the truck with the RSC system, which was 4 mph higher than the rollover threshold speed for stock tests.

This was because the robot-operated J-turn maneuvers had smoother steering wheel input compared to the driver-operated J-turns, where the driver occasionally needed to "jerk" the steering wheel in order to keep the truck within the lane, and such quick steering input tends to increase the likelihood of rollover. The stock tests were not performed at any speed higher than 42 mph, again due to safety concerns.

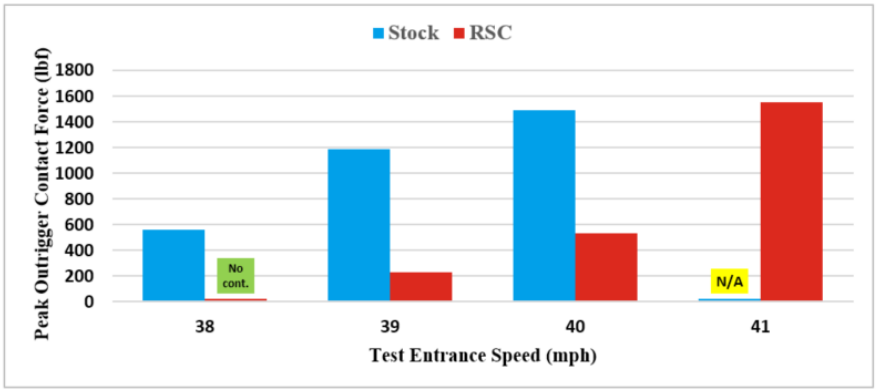

(a) J-turn - Driver

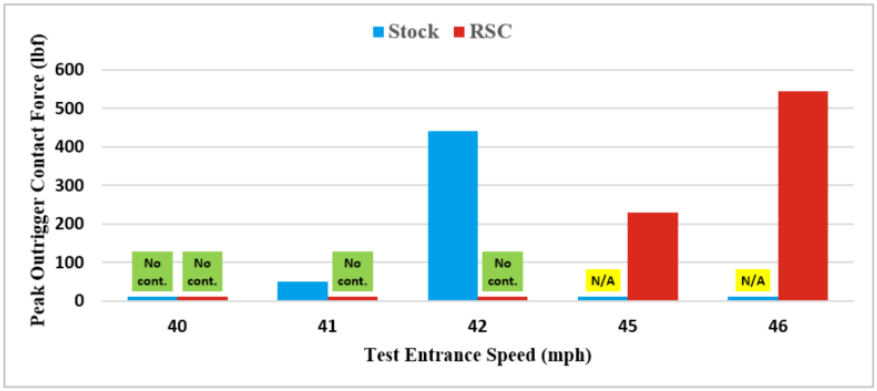

(b) J-turn - Robot

Figure 8-13. Peak outrigger contact forces on Trailer-A passenger side during: (a) J-turn – driver tests, and (b) J-turn – robot tests.

Figure 8-14 shows the results of warning time for the two J-turn tests. A longer warning time indicates that the RSC system has more time to slow down the trailer in order to attenuate the severity of the rollover accident or even completely prevent one. In general, the RSC system could provide at least one second before the outrigger contacted the ground during driver-operated J-turn tests. Similar results are also observed in the robot-operated tests, where the RSC system managed to activate 1.85 and 1.51 seconds before the front trailer rolled over during the 44- and 45-mph tests, respectively.

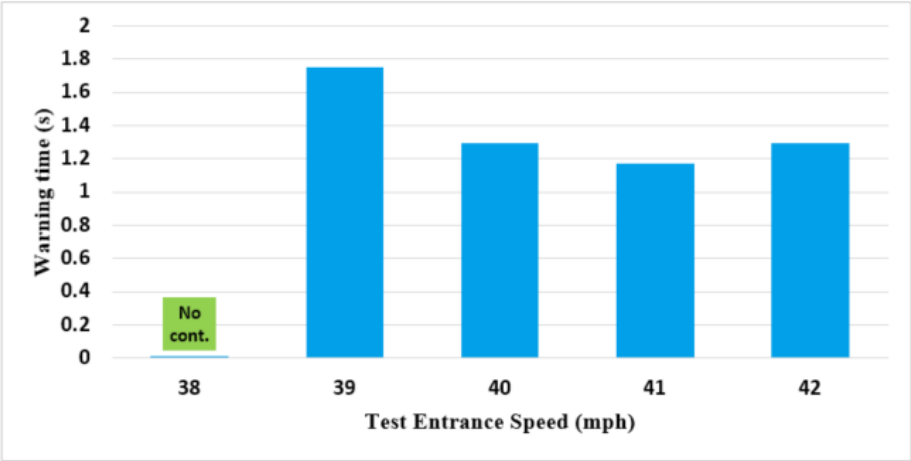

(a) J-turn - Driver

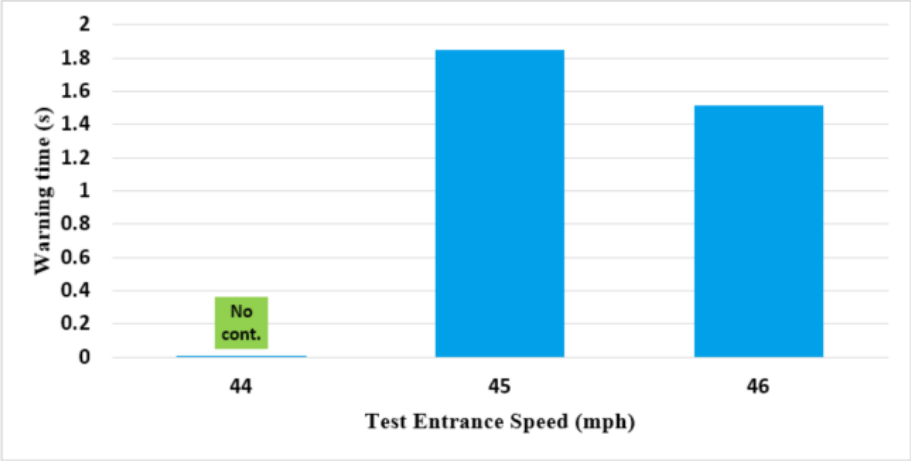

(b) J-turn - Robot

Figure 8-14. Warning time for tests of: (a) J-turn – driver, and (b) J-turn – robot.

Figure 8-15 shows the speed drop achieved during J-turn maneuvers. The speed drop is defined as the speed reduction achieved during the corresponding warning time. Since all the tests were conducted with dropped throttle at the beginning of the test, the speed drop observed during the same period of time in the stock test was also presented as references. Figure 8-15(a) indicates that in the driver-operated J-turn tests, the RSC system managed to provide an addition speed reduction of one mph. It is noted that a one-mph speed reduction might not seem very significant in general, but all these tests were conducted close to the rollover threshold of the test truck and thus, even a speed drop of 0.5 mph could completely prevent a rollover accident. In the robot-operated J-turn tests, larger speed reductions were achieved by the RSC system. More specifically, the RSC managed to reduce the speed by ~4.5 and ~2.9 mph when the front trailer made outrigger contact,

compared with the stock tests at 45 and 46 mph, respectively. In general, the RSC system provided a considerable amount of speed reduction during the J-turn tests.

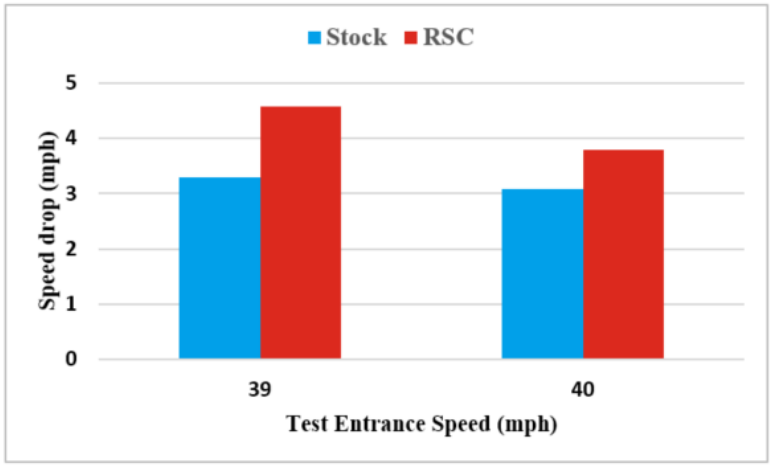

(a) J-turn - Driver

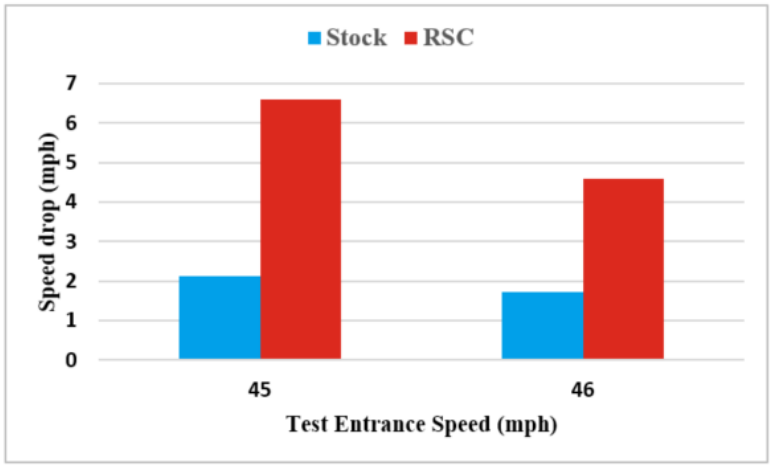

(b) J-turn - Robot

Figure 8-15. Speed drop for tests of (a) J-turn – driver, and (b) J-turn – robot.

8.2.3 SWD Tests

The test results of 0.5- and 0.25-Hz SWD tests are summarized in Table 8-2 and Table 8-3, respectively. The "D" and "P" in the parentheses indicate whether the outrigger contact occurred on the driver or passenger side, respectively. The results presented include warning time, peak outrigger force, and the number of cones hit during the tests. According to Table 8-2 and Table 8-3, most outrigger contacts occurred at 90% and 100% steering for both maneuvers. Hence, the results of 0.5- and 0.25Hz SWD at 90% and 100% test will be further discussed.

Table 8-2. Results of 0.5-Hz SWD tests.

0.5-Hz SWD Tests							
Test #	**RSC configuration**	**Steering (%)**	**Warning time (s)**		**Outrigger force (lbf.)**		**Cones hit**
			Front	**Rear**	**Front**	**Rear**	
1	RSC	0.5	----	----	----	----	4
2	RSC	0.6	----	----	----	----	5
3	RSC	0.7	----	----	----	----	3
4	RSC	0.8	----	----	----	----	2
5	RSC	0.9	1.032(P)	----	338.17(P)	----	1
6	RSC	1	0.96(P)	1.208(P)	850.17(P)	757.67(P)	1
7	Stock	0.6	----	----	----	----	4
8	Stock	0.7	----	----	163.17(P)	----	4
9	Stock	0.8	----	----	----	----	2
10	Stock	0.9	----	----	877.67(P)	1328.67(P)	1

Table 8-3. Results of 0.25-Hz SWD tests.

0.25-Hz SWD Tests							
Test #	**RSC configuration**	**Steering (%)**	**Warning time (s)**		**Outrigger force (lbf.)**		**Cones hit**
			Front	**Rear**	**Front**	**Rear**	
1	RSC	0.5	----	----	----	----	6
2	RSC	0.6	----	----	----	----	5
3	RSC	0.7	----	----	----	----	4.5
4	RSC	0.8	----	----	----	----	2.5
5	RSC	0.9	----	0.360(P)	----	1180.92(P)	1
6	RSC	1	0.504(P)	1.688(D) 0.2(P)	673.58(P)	589.17(D) 1899.42(P)	0
7	Stock	0.6	----	----	----	----	4
8	Stock	0.7	----	----	----	----	3
9	Stock	0.8	----	----	559.42(P)	1277.83(P)	2
10	Stock	0.9	----	----	758.75(D) 1218.00(P)	312.00(D) 2006.17(P)	1

Figure 8-16 provides the results of peak outrigger contact forces experienced by the test truck during 0.5- and 0.25-Hz SWD tests. For the 0.5-Hz SWD tests, only the outriggers on the passenger side of both trailers are shown here because outrigger contact only occurred on this side. Figure 8-16(a) shows that the RSC system managed to reduce the peak contact force on the front trailer by ~79% and completely prevent the rear trailer from rolling over at the 90%-steering test, compared to the stock test with the same steering input. For the 100%-steering tests (Figure 8-16(b)), the RSC system reduced the severity

of the potential rollover accidents, indicated by lower peak contact forces compared with those of the stock test

As for the 0.25-Hz SWD tests, Figure 8-16(c) shows that the RSC system prevented three outrigger contacts during the 0.25-Hz SWD test at 90% steering, whereas all four outriggers made contact during the same stock test. Considering that the outrigger contacts always occurred in a sequence of front driver–rear driver–front passenger–rear passenger, and that the RSC system only allowed the last outrigger to contact (rear trailer passenger side), the system could provide drivers with more time to react after sensing an impending rollover risk. In the 100%-steering tests (Figure 8-16(d)), the RSC system managed to prevent the outrigger on Trailer A's driver side from touching the ground, but the truck would roll over anyway considering the other three outrigger contacts that occurred afterwards.

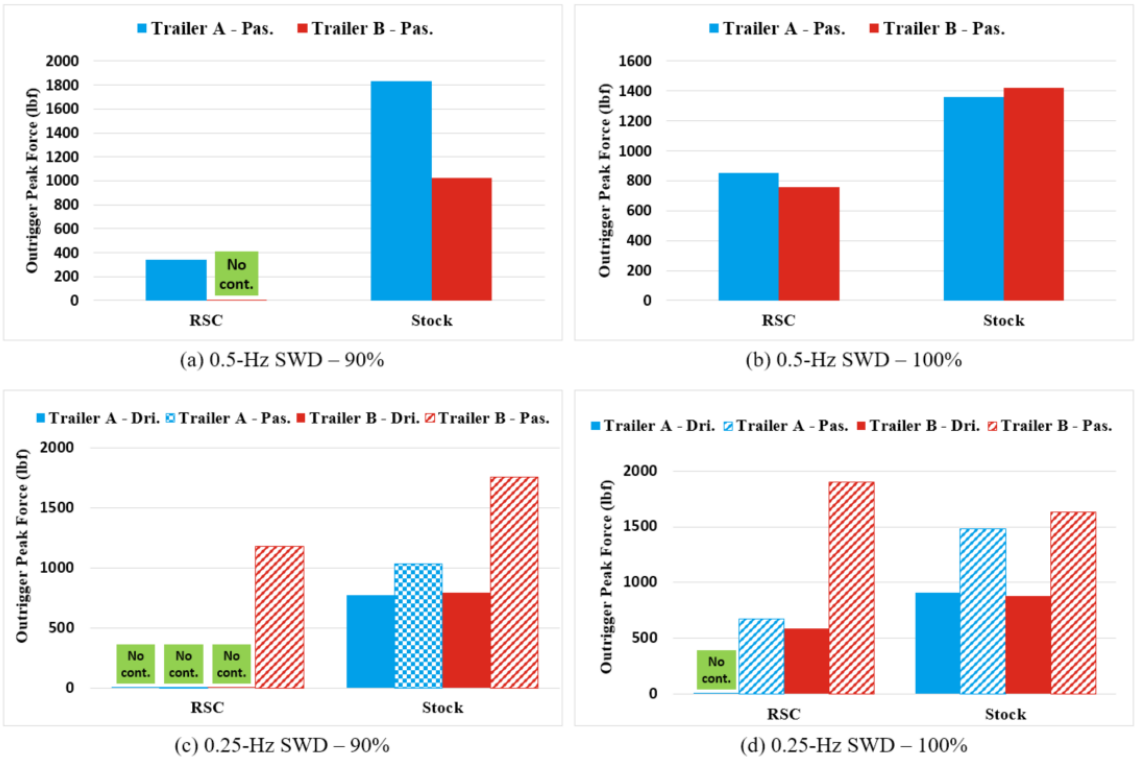

Figure 8-16. Peak outrigger contact forces for tests of (a) 0.5-Hz SWD at 90% steering, (b) 0.5-Hz SWD at 100% steering, (c) 0.25-Hz SWD at 90% steering, and (d) 0.25-Hz SWD at 100% steering.

The results of warning time are shown in Figure 8-17. In general, the RSC system had similar warning time (~1s) before the Trailer A passenger-side outrigger made contact in

the 0.5-Hz SWD tests, and provided an addition 0.2s for the rear outrigger contact during the 100% steering test, as shown in Figure 8-17(a) and (b). For the 0.25-Hz tests at 90% steering, the RSC system provided a warning time of 0.35s before the Trailer B passenger-side outrigger made contact (Figure 8-17(c)). Figure 8-17(d) shows the results for the 0.25-Hz SWD tests at 100% steering, where the RSC system managed to prevent one contact on Trailer A and also provided a larger warning time for the other contact on the driver's side. However, it activated too late before the outrigger on the rear trailer passenger side contacted the ground, which resulted in a large peak contact force, as show in Figure 8-16. In general, the RSC system successfully engaged before the trailer rolled over, indicated by positive warning times.

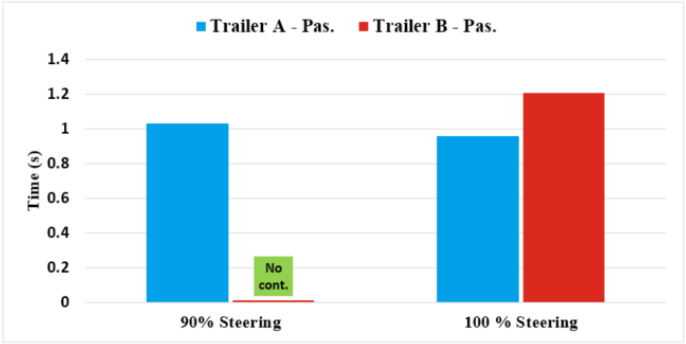

(a) 0.5-Hz SWD

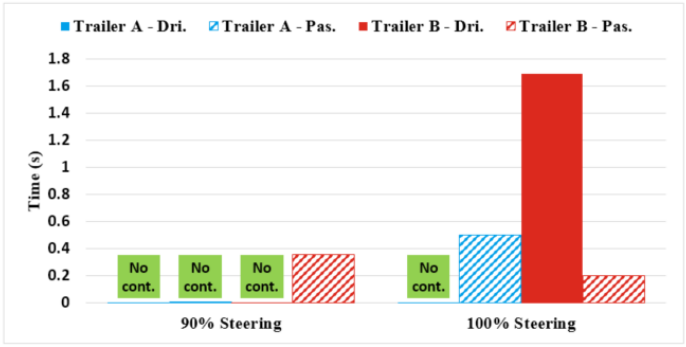

(b) 0.25-Hz SWD

Figure 8-17. Warning time for (a) 0.5-Hz SWD tests, and (b) 0.25-Hz SWD tests.

Figure 8-18 shows the speed drop achieved by the RSC system in the SWD tests. Again, the speed drop is defined as the speed reduction achieved during the corresponding warning time. Since all the tests were conducted with dropped throttle at the beginning of the test, the speed drop observed during the same period of time in the corresponding stock test was also presented as references. For the 0.5-Hz SWD tests (Figure 8-18(a) and (b)), the RSC system could provide an addition speed drop of ~1.5 mph. For the 0.25-Hz SWD tests

(Figure 8-18(c) and (d)), the RSC system managed to reduce the truck speed by 1 and 2.6 mph more than the stock tests during tests at 90% and 100% steering, respectively. Even though these additional speed reductions did not prevent rollover accidents, they could considerably attenuate the severity of the accidents.

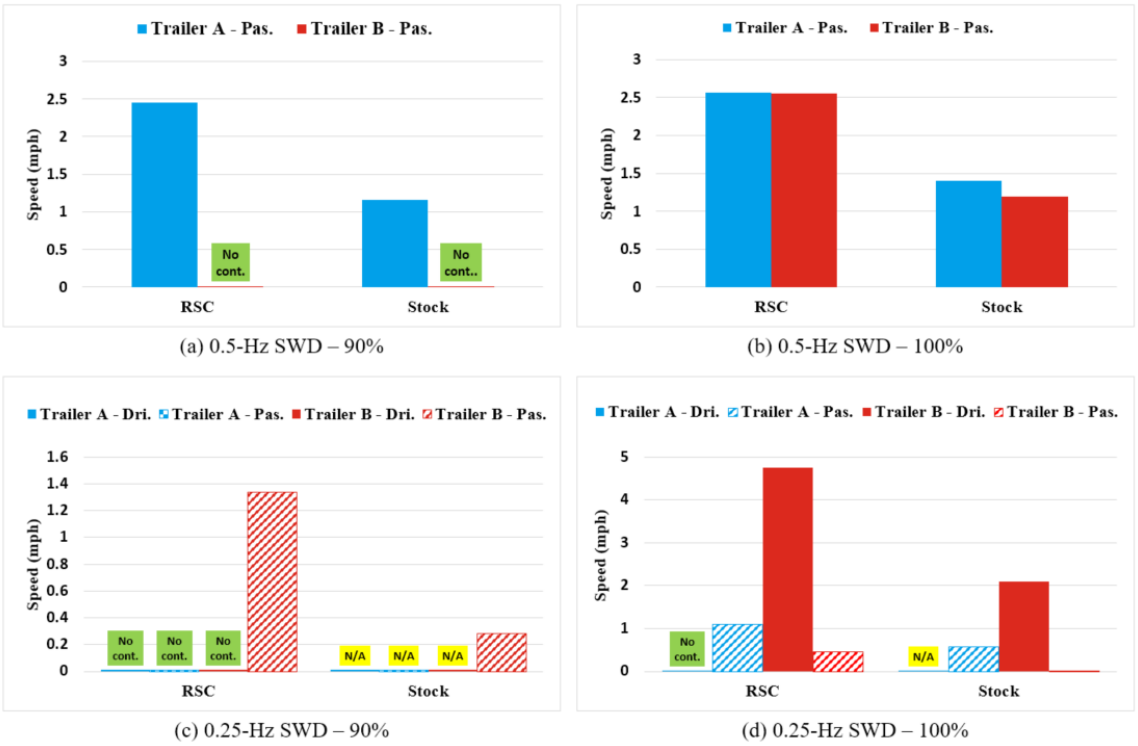

Figure 8-18. Speed drop for tests of (a) 0.5-Hz SWD at 90% steering, (b) 0.5-Hz SWD at 100% steering, (c) 0.25-Hz SWD at 90% steering, and (d) 0.25-Hz SWD at 100% steering.

Figure 8-19 summarizes the number of cones hit during each test, which is proportional to the understeer experienced by the truck in a SWD test. As expected, the RSC system introduced slightly more understeer to the test truck, indicated by the fact that the truck with the RSC system tended to hit more cones during the tests. Because the adjacent cones were 1-ft apart for the 0.5-Hz tests and 4-ft apart for the 0.25-Hz tests, the understeer generally made the truck travel about 1.5 ft towards the inside of the turn at locations of 100 and 200 ft away from the starting point for 0.5- and 0.25-Hz SWD tests, respectively.

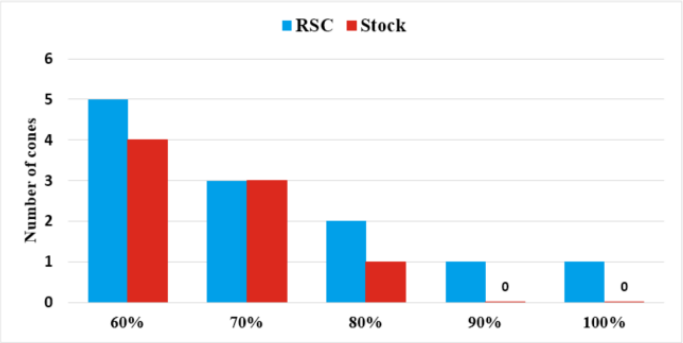

(a) 0.5-Hz SWD

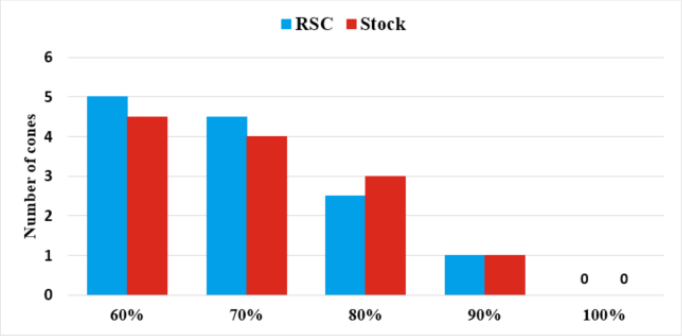

(b) 0.25-Hz SWD

Figure 8-19. Number of cones hit in (a) 0.5-Hz SWD tests, and (d) 0.25-Hz SWD tests.

8.2.4 DLC Tests

The test results of the DLC maneuver are summarized in Table 8-4. The "D" and "P" in the parentheses indicate whether the outrigger contact occurred on the driver or passenger side, respectively.

The peak outrigger contact forces for 54- and 55-mph DLC tests are summarized in Figure 8-20. Considering that the driver needed to maneuver through the course at high speeds, each RSC test was conducted three times for more accurate results. Figure 8-20(a) shows that the truck with the RSC system experienced two outrigger contacts during one test, compared to the stock test that only included one, and lighter contact on the rear trailer passenger side. However, no outrigger contact occurred during the other two 54-mph RSC tests. Similar results are observed in the 55-mph DLC tests (Figure 8-20(b)), where one of the three RSC tests resulted in contact on two outriggers, and the two stock tests both led to a single contact with larger peak forces. The results of the 55-mph DLC tests agreed with those derived from the J-turn and SWD tests. However, the 54-mph DLC test results

are inconsistent with the others, since equipping the RSC system seems to reduce the truck roll stability during test RSC #1.

Table 8-4. Results of DLC tests.

DLC Tests						
Test #	**RSC configuration**	**Speed (mph)**	**Warning time (s)**		**Outrigger force (lbf.)**	
			Front	**Rear**	**Front**	**Rear**
1	RSC	48	----	----	----	----
2	RSC	52	----	----	----	----
3	RSC	54	----	0.672(D) 0.320(P)	----	794.17(D) 2619.08(P)
4	RSC	54	----	----	----	----
5	RSC	54	----	----	----	----
6	RSC	55	----	----	----	----
7	RSC	55	----	----	----	----
8	RSC	55	----	0.864(D) 0.419(P)	----	436.83(D) 393.50(P)
9	RSC	56	----	----	----	----
10	RSC	56	----	----	----	----
11	Stock	52	----	----	----	----
12	Stock	54	----	----	----	1961.50(P)
13	Stock	55	----	----	----	1454.92(P)
14	Stock	55	----	----	----	1094.67(P)

Such contradictory results are observed again when comparing peak contact forces of all RSC tests, as shown in Figure 8-21. The results indicate that the truck equipped with the RSC system experienced more and heavier outrigger contact at lower speeds during the DLC tests. Two potential causes for the contradictory test results were identified. The first is human variance: DLC tests were performed entirely by a test driver, compared to SWD tests where the steering wheel was controlled by a steering robot that could provide highly repeatable input. The driver performed better, which led to smoother truck dynamics as more tests were conducted. For instance, the RSC tests were conducted first with test speed increased from 48 to 56 mph, followed by the stock tests. The driver gradually refined his steering after completing RSC tests at low speeds (i.e. 52, 54 mph), and maneuvered better in the high-speed RSC tests (i.e. 56 mph) as well as the stock tests with smoother steering wheel angle input and lighter outrigger contacts. This explains why the truck experienced

less and lighter outrigger contacts in the stock 54-mph test, compared to those of the first RSC test with the same speed (RSC #1), as shown in Figure 8-20(a).

Initially, it was endeavored to use a steering robot to perform DLC tests for more consistent steering input, but tuning the steering robot for such maneuvers proved to require an extensive amount of track time. This is because a human driver could adjust steering angle input to follow the path when the RSC systems applied brakes to the truck at different speeds, but the steering robot designed and used for this test program is limited in that respect. Some commercially-available steering robots that are equipped with GPS units may have the capability to conduct path-following tests. However, such steering robots are extremely expensive (over $100,000 for each), which is beyond the scope of this study.

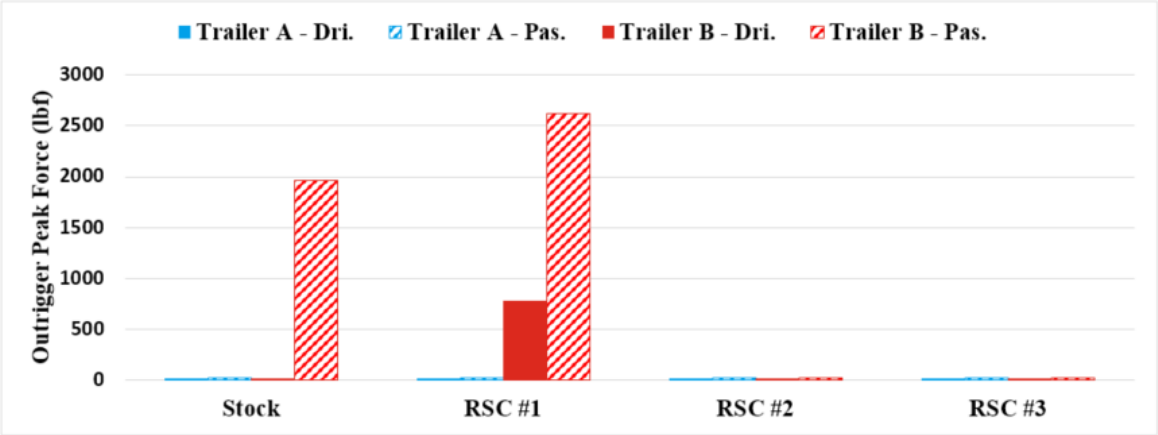

(a) 54-mph DLC tests

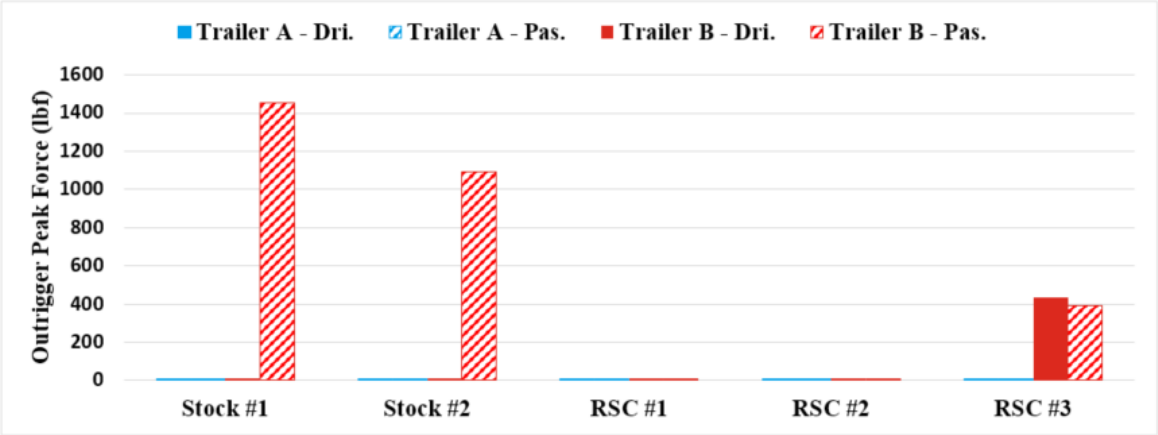

(b) 55-mph DLC tests

Figure 8-20. Results of peak outrigger contact forces for (a) 54-mph DLC tests, and (b) 55-mph DLC tests.

The other potential reason for inconsistent DLC test results is the RSC system self-tuning. The RSC system began to collect truck information as the truck was started. It sensed air suspension pressure to calculate the weight, and applied test pulses to each wheel during cornering to estimate the trailer's CG height. Therefore, more information was collected by the RSC systems as more tests were conducted, and the RSC systems could be re-tuned to obtain more accurate activation threshold and timing. This could contribute to better results for the tests conducted later in the test sequence.

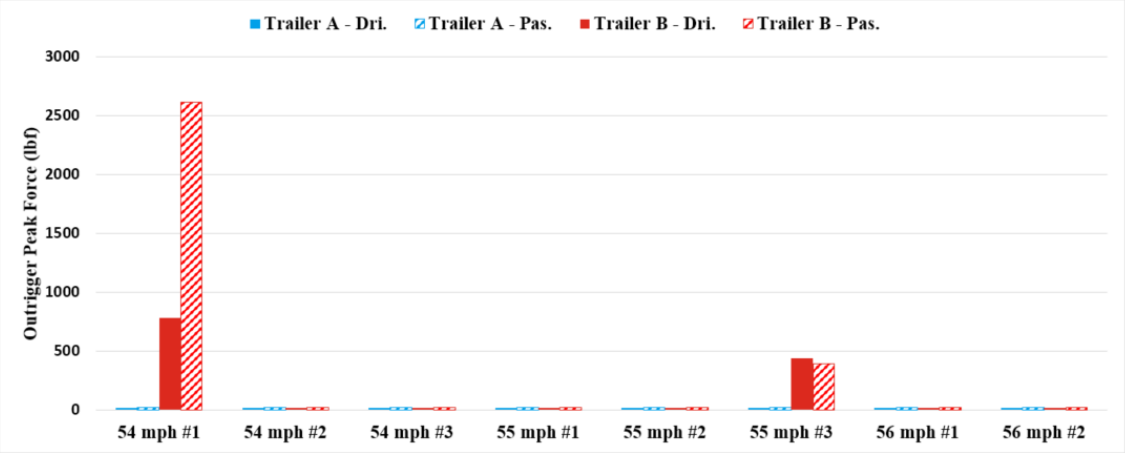

Figure 8-21. Results of peak outrigger contact forces for DLC tests at 54, 55, and 56 mph with the RSC system.

8.3 Conclusions and Summary

This chapter details all the tests that were conducted to evaluate the dynamic stability of a 28-ft A-train double with trailer-based RSC systems. Five maneuvers were performed, including driver-operated J-turns, robot-operated J-turn (RSM), 0.5-Hz SWD, 0.25-Hz SWD, and DLC maneuvers. The results are presented and discussed with respect to the maneuvers, and the conclusions will be summarized in the following sections.

8.3.1 J-turn Maneuvers

Figure 8-22 illustrates the improvement on the peak outrigger contact force achieved by the RSC system, which is defined as how much peak force is reduced in the RSC test compared to the stock test. Figure 8-22(a) shows that the RSC system reduced peak outrigger contact force by 80% and 61% for tests at 39 and 40 mph, respectively. Other test results are not compared here because the stock tests stopped at 40 mph, and the RSC

tests did not result in any outrigger contact during tests with a speed below 39 mph. For the robot-operated J-turn tests (Figure 8-22(b)), the stock test ended at 43 mph, where the RSC tests experienced the first contact at 45 mph, indicating that the RSC system significantly reduced truck rollover likelihood in robot-operated J-turn tests.

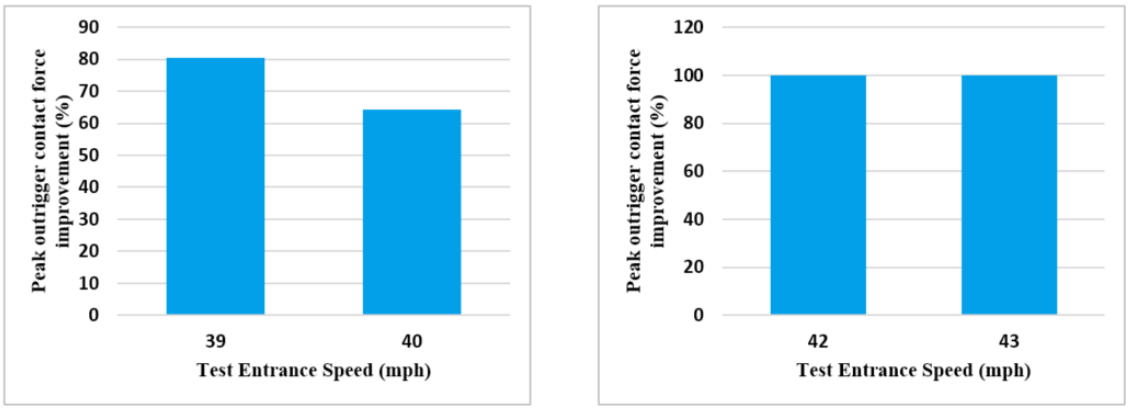

(a) J-turn - Driver (b) J-turn - Robot

Figure 8-22. Peak outrigger contact force improvement achieved by the RSC systems: (a) driver-operated J-turn tests, and (b) robot-operated J-turn tests.

Figure 8-23 illustrates the improvement of speed threshold for triggering rollover events. In the driver-operated J-turn tests, the RSC system managed to improve the rollover speed threshold by ~5%. For the robot-operated J-turn tests, where a more gradual steering input profile was applied, the RSC system could increase the rollover speed by ~15%.

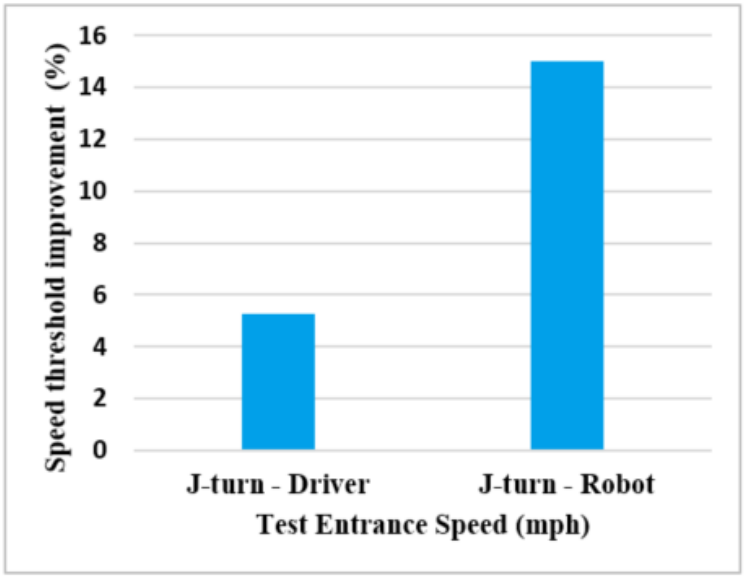

Figure 8-23. Speed threshold improvement compared to the stock test.

In summary, the RSC system applied here could considerably enhance the truck roll stability during the J-turn tests, which increased the truck rollover speed by 5%~15%, and reduced the peak contact force by 61%~80% when rollover accidents occurred.

8.3.2 SWD Maneuvers

Maneuverability improvement is used to evaluate the performance of the RSC system tested here, as shown in Figure 8-24. The maneuverability improvement is defined as how much additional steering an RSC system could provide to the truck without rolling over, compared to stock tests. For instance, if a truck rolls over at 70% steering in stock tests but rolls over at 90% steering in RSC tests, it means that the RSC system could improve the maneuverability because the driver can steer more to avoid an obstacle without rolling over. Figure 8-24 shows that the RSC system could increase the maneuverability of the test truck by ~33.3% in 0.5-Hz SWD tests, and ~11.5% in 0.25-Hz SWD tests. Therefore, the RSC system successfully improved the truck maneuverability, which means the truck equipped with the system could withstand more aggressive steering input without rolling over, compared to the stock truck. Such an improvement could potentially reduce the number of truck rollover accidents triggered by obstacle-avoidance maneuvers or those performed when taking a highway ramp at excessive speeds.

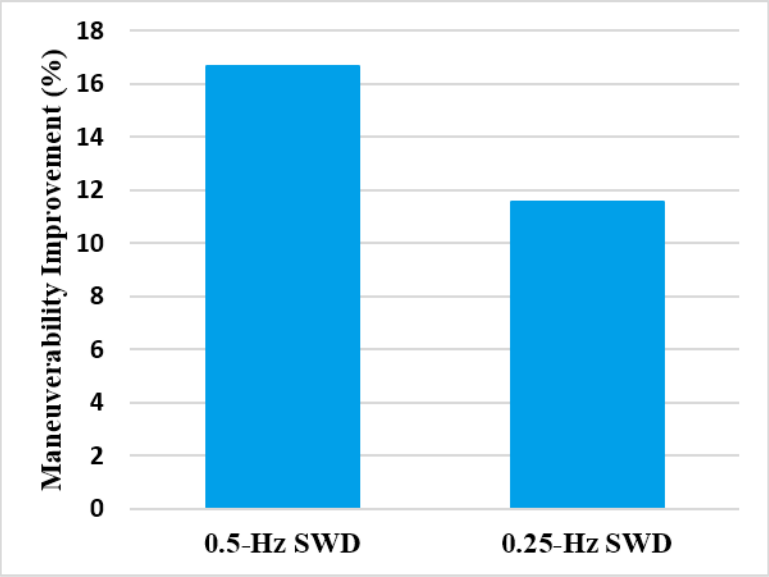

Figure 8-24. Maneuverability improvement for 0.5- and 0.25-Hz SWD tests.

8.3.3 DLC Maneuvers

Contradictory results were observed in the DLC tests, where the test truck experienced fewer outrigger contacts as the test speed increased, exhibiting a trend that the later a test was conducted, the less outrigger contact would result. Two potential reasons have been identified. The first was that the test driver performed better and led to smoother truck dynamics as he practiced more tests. Thus, the driver gradually refined his steering after completing RSC tests at low speeds (i.e. 52, 54 mph), and maneuvered better in the high-speed RSC tests (i.e. 56 mph), as well as the stock tests conducted after the RSC tests. The other potential reason is the RSC system self-tuning function. The RSC system began acquiring truck information once the truck was started. Hence, more information was collected by the RSC systems as more tests were conducted, and the RSC systems could be re-tuned to obtain more accurate activation threshold and timing. This could also contribute to better results for the tests conducted later in the test sequence.

In order to solve this issue, each DLC test should be repeated multiple times, and the test truck should be turned off and on after each test run for rebooting the RSC systems. However, this would significantly increase the number of test runs and also require longer track hours. Therefore, DLC is found not to be ideal for objective tests where different systems should be compared. Instead, it is suggested for system tuning or other subjective tests where the drive feedback is weighed heavily in the evaluation process.

8.3.4 Characteristic Dynamic Behavior of 28-ft A-train Doubles

Besides serving as a platform for the performance evaluation of an RSC system, the 28-ft A-train double employed also exhibited its characteristic dynamic behaviors in the stock tests.

First of all, the rearward amplification phenomenon, which is an inherent property possessed by vehicles with multiple trailing units, was well-substantiated during the tests. For example, Figure 8-25 shows the lateral accelerations experienced by the truck in DLC tests at two different speeds. When the truck started the test at 48 mph, as shown in Figure 8-25(a), the rear trailer exhibited slightly higher peak lateral accelerations at the first steering (t=2-3.5s), and all three units displayed similar peak lateral accelerations during

the other two steerings (t=3.5-5s, and t=6-7s). However, when the test entrance speed was increased to 55 mph, the rearward amplification phenomenon became stronger, and the rear trailer experienced higher peak lateral accelerations than the other two units during each steering. Such excessive lateral accelerations trigger by rearward amplification would not only increase the likelihood of rollover, but also introduce other safety issues. A series of screenshots taken during the 55-mph DLC test are exhibited in Figure 8-26. The maneuver started as in screenshot (1) and ended as in (5). However, as shown in screenshot (6), the rear trailer swung out to the right side after the maneuver had been completed by the driver, due to the excessive lateral accelerations illustrated in Figure 8-25(b) (t=5s). Even though the rear trailer did not roll over in this case, it posed great risks of colliding with other vehicles traveling in the adjacent lane.

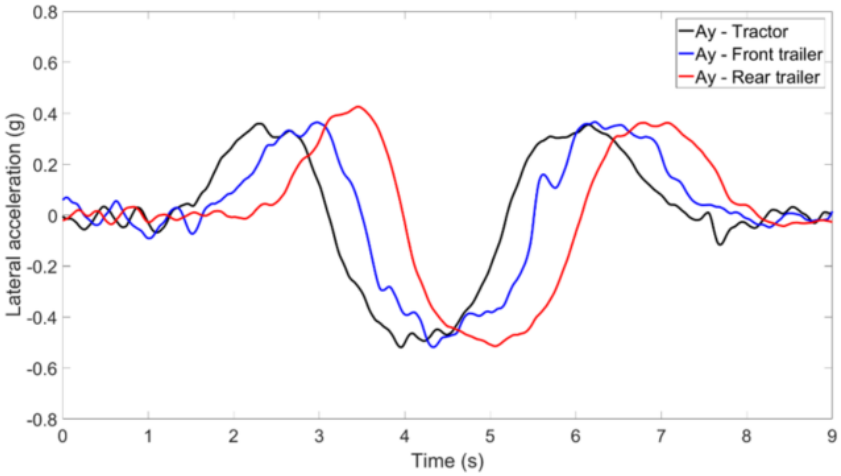

(a) DLC test – 52 mph

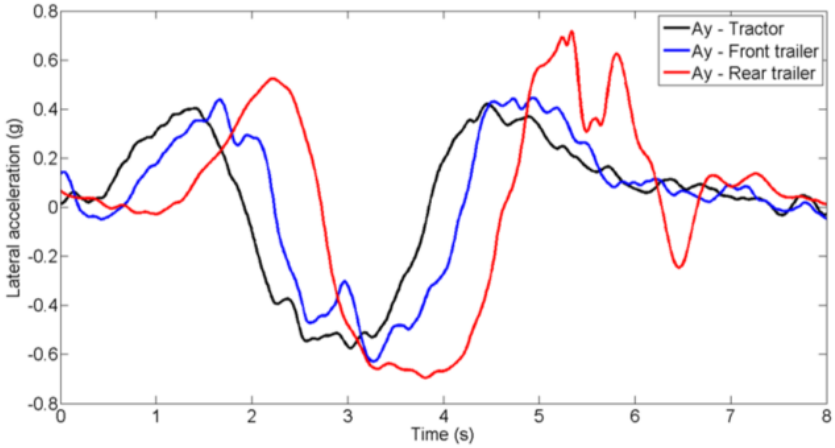

(b) Stock DLC test – 55 mph

Figure 8-25. Lateral acceleration results for DLC tests at 52 and 55 mph.

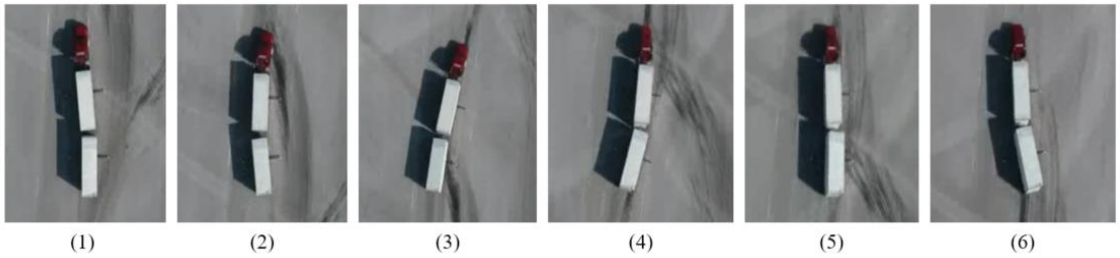

Figure 8-26. A series of screenshots for a 55-mph DLC test.

The other significant dynamic behavior that could potentially lead to safety issues is the considerable delay between the driver's steering input and the rear trailer's response. This behavior was directly experienced by the driver and testers who stayed in the tractor cab during tests, where they felt impact loads transmitted after they thought the test had been completed. For example, even though the steering profile for a 0.25-Hz SWD test had been completed and the steering wheel had returned back to neutral position, the rear trailer experienced another contact ~1s later, as shown in Figure 8-27. Figure 8-27(a) shows that the steering angle went back to zero at t=7.2s, indicating that the robot steering input had been completed. However, Figure 8-27(b) illustrates that Trailer B (rear trailer) experienced an outrigger contact on its passenger side at t=7.9s.

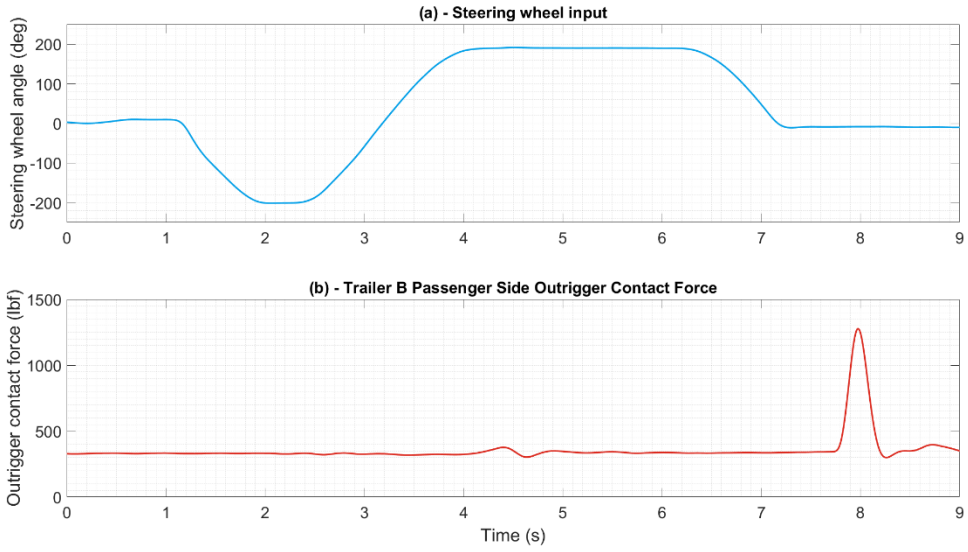

Figure 8-27. Steering wheel input and Trailer B passenger-side outrigger contact force for a 0.25-Hz SWD test at 80% steering.

This delayed response of the rear trailer was also observed in the DLC test shown in Figure 8-26. The rear trailer swung out to the right side after the tractor had exited the testing

course and started to move straightforward. Unlike in the SWD test where the driver could directly feel the contact of the rear trailer, the driver did not realize the excessive lateral motion of the rear trailer during DLC tests until being told. This was because the pintle hitch coupling does not provide constraints for relative yaw motion between two jointed vehicle units.

In summary, the delayed response of the rear trailer poses safety issues to trucks in the A-train configuration. It requires drivers to reasonably predict the rear trailer dynamic response when maneuvering the truck. Otherwise, the rear trailer would have already rolled over or lost control before the driver could physically realize it.

Chapter 9 – Effect of Configuration Changes on the Dynamic Stability of a 28-ft A-train Double

The following chapter details the second set of tests conducted at MLPG, using the same RSC system evaluated in Chapter 8, but with different trailer load configurations, mixed RSC configurations, and a tractor-based ESC system. An overview of the entire test program is provided, followed by the test maneuvers and test matrix. The test results are presented and discussed in three groups, followed with the conclusions drawn from the tests.

9.1 Overview

The objective of this set of tests was to evaluate truck dynamic stability with different rear trailer load conditions and mixed RSC/ESC configurations. The same 2S2M trailer-based RSC system as introduced and applied in the previous test set was employed again. According to the real-world scenarios that are commonly experienced by freight carriers, eight permutations were tested, including:

- RSC on rear trailer only
- RSC on front trailer only
- RSC on both trailers
- Stock (no RSC)
- RSC + ESC (on tractor)
- ESC (tractor only)
- Empty rear trailer + RSC
- Empty rear trailer (no RSC)

The eight permutations were divided into three groups for comparison, as introduced in Table 9-1, and 266 runs were completed in total to test all permutations between March 28 and April 6, 2017 at MLPG. The same VDA pad (MLPG Track 8) was used to perform all the tests.

Table 9-1. Eight permutations were divided into three groups for comparison.

#	Group	Permutation
1	Different Rear Trailer Loading Configurations	Stock (no RSC)
		RSC on both trailers
		Empty rear trailer (no RSC)
		Empty rear trailer + RSC
2	Mixed RSC Configurations	Stock (no RSC)
		RSC on front trailer only
		RSC on rear trailer only
		RSC on both trailers
3	Mixed ESC/RSC Configurations	Stock (no RSC)
		RSC on both trailers
		ESC (tractor only)
		RSC + ESC (on tractor)

9.2 Test Maneuver and Matrix

Four out of five maneuvers used in the previous test set were performed again because the desired permutations required a large number of test runs, but unfortunately the track time was limited. Therefore, the driver-operated J-turn maneuver was excluded since (1) it might require more repeat runs to compensate for human variance, compared to robot-operated tests that have better repeatability; (2) the robot-operated J-turn maneuvers (also known as Ramp-Steering Maneuvers) result in similar dynamics; and (3) the driver-operated Double Lane Change (DLC) maneuvers could be used to analyze RSC performance when a closed-loop path-following steering input is applied. Thus, the four maneuvers used in this set of tests are determined as follows:

- Double Lane Change (DLC) – Human driver
- J-turn with robot – Steering robot
- 0.5-Hz Sine with Dwell (0.5-Hz SWD) – Steering robot
- 0.25-Hz Sine with Dwell (0.25-Hz SWD) – Steering robot

All tests were divided into three blocks/days based on loading conditions and test maneuvers for maximum efficiency. The first block consisted of all tests run with an empty rear trailer. The test team moved all sandbags (~3,400 lb) out of the rear trailer before the tests and put them back after completing the first block of tests. The second block of tests

was conducted with SWD maneuvers, whereas the third and fourth blocks of tests were conducted with robot-operated J-turn and DLC maneuvers, respectively. It is noted that all RSC tests were conducted in a manner such that the RSC system was turned on right before the test started, and turned off after the test was completed, in order to minimize the effect of RSC self-tuning on the test results. The test matrix is shown in Table 9-2.

Table 9-2. Test matrix for examining the effect of configuration changes on the dynamic stability of a 28-ft A-train double.

Date: March 31, 2017 **Weather**: Partly cloudy, 70°, WSW 15-mph wind **Track surface condition**: Dry					
Test #	**Maneuver**	**Rear trailer loading**	**RSC**	**ESC**	**Steering (%)**
1	0.5-Hz SWD	Empty	Both	Off	70
2	0.5-Hz SWD	Empty	Both	Off	80
3	0.5-Hz SWD	Empty	Both	Off	90
4	0.5-Hz SWD	Empty	Both	Off	100
5	0.5-Hz SWD	Empty	Both	Off	70
6	0.5-Hz SWD	Empty	Both	Off	80
7	0.5-Hz SWD	Empty	Both	Off	90
8	0.5-Hz SWD	Empty	Both	Off	100
9	0.5-Hz SWD	Empty	Off	Off	70
10	0.5-Hz SWD	Empty	Off	Off	80
11	0.5-Hz SWD	Empty	Off	Off	90
12	0.5-Hz SWD	Empty	Off	Off	100
Test #	**Maneuver**	**Rear trailer loading**	**RSC**	**ESC**	**Steering (%)**
13	0.25-Hz SWD	Empty	Both	Off	70
14	0.25-Hz SWD	Empty	Both	Off	80
15	0.25-Hz SWD	Empty	Both	Off	90
16	0.25-Hz SWD	Empty	Both	Off	100
17	0.25-Hz SWD	Empty	Off	Off	70
18	0.25-Hz SWD	Empty	Off	Off	80
19	0.25-Hz SWD	Empty	Off	Off	90
20	0.25-Hz SWD	Empty	Off	Off	100
Test #	**Maneuver**	**Rear trailer loading**	**RSC**	**ESC**	**Speed (mph)**
21	DLC	Empty	Both	Off	48
22	DLC	Empty	Both	Off	48
23	DLC	Empty	Both	Off	52
24	DLC	Empty	Both	Off	54
25	DLC	Empty	Both	Off	54
26	DLC	Empty	Both	Off	54

27	DLC	Empty	Both	Off	55
28	DLC	Empty	Both	Off	55
29	DLC	Empty	Both	Off	56
30	DLC	Empty	Both	Off	56
31	DLC	Empty	Both	Off	57
32	DLC	Empty	Both	Off	57
33	DLC	Empty	Both	Off	57
34	DLC	Empty	Both	Off	58
35	DLC	Empty	Both	Off	58
36	DLC	Empty	Both	Off	59
37	DLC	Empty	Both	Off	59
38	DLC	Empty	Both	Off	59
39	DLC	Empty	Both	Off	60
40	DLC	Empty	Both	Off	60
41	DLC	Empty	Both	Off	60
42	DLC	Empty	Off	Off	48
43	DLC	Empty	Off	Off	52
44	DLC	Empty	Off	Off	54
45	DLC	Empty	Off	Off	54
46	DLC	Empty	Off	Off	55
47	DLC	Empty	Off	Off	55
48	DLC	Empty	Off	Off	56
49	DLC	Empty	Off	Off	56
50	DLC	Empty	Off	Off	57
51	DLC	Empty	Off	Off	57
52	DLC	Empty	Off	Off	58
53	DLC	Empty	Off	Off	58
54	DLC	Empty	Off	Off	59
55	DLC	Empty	Off	Off	59
56	DLC	Empty	Off	Off	60
57	DLC	Empty	Off	Off	60
58	DLC	Empty	Off	Off	60
Test #	**Maneuver**	**Rear trailer loading**	**RSC**	**ESC**	**Speed (mph)**
59	J-turn - robot	Empty	Both	Off	38
60	J-turn - robot	Empty	Both	Off	38
61	J-turn - robot	Empty	Off	Off	38
62	J-turn - robot	Empty	Both	Off	39
63	J-turn - robot	Empty	Off	Off	39
64	J-turn - robot	Empty	Both	Off	40
65	J-turn - robot	Empty	Off	Off	40
66	J-turn - robot	Empty	Both	Off	41
67	J-turn - robot	Empty	Off	Off	41
68	J-turn - robot	Empty	Both	Off	42
69	J-turn - robot	Empty	Off	Off	42

70	J-turn - robot	Empty	Both	Off	43
71	J-turn - robot	Empty	Both	Off	44
72	J-turn - robot	Empty	Both	Off	38
73	J-turn - robot	Empty	Both	Off	40
74	J-turn - robot	Empty	off	Off	40
75	J-turn - robot	Empty	Both	Off	41
76	J-turn - robot	Empty	off	Off	41
77	J-turn - robot	Empty	Both	Off	42
78	J-turn - robot	Empty	off	Off	42
79	J-turn - robot	Empty	Both	Off	43
80	J-turn - robot	Empty	Both	Off	44
81	J-turn - robot	Empty	off	Off	43
82	J-turn - robot	Empty	Both	Off	45
83	J-turn - robot	Empty	Both	Off	40

Date: April 2, 2017
Weather: Sunny, 71°, ESE 6-mph wind
Track surface condition: Dry

Test #	Maneuver	Rear trailer loading	RSC	ESC	Steering (%)
1	0.5-Hz SWD	Loaded	Both	Off	70
2	0.5-Hz SWD	Loaded	Both	Off	70
3	0.5-Hz SWD	Loaded	Both	Off	80
4	0.5-Hz SWD	Loaded	Both	Off	90
5	0.5-Hz SWD	Loaded	Both	Off	100
6	0.5-Hz SWD	Loaded	Rear	Off	70
7	0.5-Hz SWD	Loaded	Rear	Off	80
8	0.5-Hz SWD	Loaded	Rear	Off	90
9	0.5-Hz SWD	Loaded	Rear	Off	100
10	0.5-Hz SWD	Loaded	Front	Off	70
11	0.5-Hz SWD	Loaded	Front	Off	80
12	0.5-Hz SWD	Loaded	Front	Off	90
13	0.5-Hz SWD	Loaded	Front	Off	100
14	0.5-Hz SWD	Loaded	Off	Off	70
15	0.5-Hz SWD	Loaded	Off	Off	80
16	0.5-Hz SWD	Loaded	Off	Off	90
17	0.5-Hz SWD	Loaded	Off	Off	100
18	0.5-Hz SWD	Loaded	Both	ESC	70
19	0.5-Hz SWD	Loaded	Both	ESC	80
20	0.5-Hz SWD	Loaded	Both	ESC	90
21	0.5-Hz SWD	Loaded	Both	ESC	90
22	0.5-Hz SWD	Loaded	Both	ESC	100
23	0.5-Hz SWD	Loaded	Off	ESC	70
24	0.5-Hz SWD	Loaded	Off	ESC	80
25	0.5-Hz SWD	Loaded	Off	ESC	90
26	0.5-Hz SWD	Loaded	Off	ESC	100

27	0.25-Hz SWD	Loaded	Both	Off	70
28	0.25-Hz SWD	Loaded	Both	Off	70
29	0.25-Hz SWD	Loaded	Both	Off	70
30	0.25-Hz SWD	Loaded	Both	Off	70
31	0.25-Hz SWD	Loaded	Rear	Off	70
32	0.25-Hz SWD	Loaded	Both	Off	70
33	0.25-Hz SWD	Loaded	Rear	Off	70
34	0.25-Hz SWD	Loaded	Front	Off	70
35	0.25-Hz SWD	Loaded	Off	Off	70
36	0.25-Hz SWD	Loaded	Both	ESC	70
37	0.25-Hz SWD	Loaded	Off	ESC	70
38	0.25-Hz SWD	Loaded	Both	Off	80
39	0.25-Hz SWD	Loaded	Rear	Off	80
40	0.25-Hz SWD	Loaded	Front	Off	80
41	0.25-Hz SWD	Loaded	Off	Off	80
42	0.25-Hz SWD	Loaded	Both	ESC	80
43	0.25-Hz SWD	Loaded	Off	ESC	80
44	0.25-Hz SWD	Loaded	Both	Off	90
45	0.25-Hz SWD	Loaded	Rear	Off	90
46	0.25-Hz SWD	Loaded	Front	Off	90
47	0.25-Hz SWD	Loaded	Off	Off	90
48	0.25-Hz SWD	Loaded	Both	ESC	90
49	0.25-Hz SWD	Loaded	Off	ESC	90
50	0.25-Hz SWD	Loaded	Both	Off	100
51	0.25-Hz SWD	Loaded	Rear	Off	100
52	0.25-Hz SWD	Loaded	Front	Off	100
53	0.25-Hz SWD	Loaded	Both	ESC	100
54	0.25-Hz SWD	Loaded	Off	ESC	100
55	0.25-Hz SWD	Loaded	Off	Off	100

Date: April 4, 2017
Weather: Sunny, 81°, SW 11-mph wind
Track surface condition: Dry

Test #	Maneuver	Rear trailer loading	RSC	ESC	Speed (mph)
1	J-turn - robot	Loaded	Both	ESC	38
2	J-turn - robot	Loaded	Off	Off	38
3	J-turn - robot	Loaded	Off	Off	38
4	J-turn - robot	Loaded	Both	Off	38
5	J-turn - robot	Loaded	Off	ESC	38
6	J-turn - robot	Loaded	Rear	Off	38
7	J-turn - robot	Loaded	Front	Off	38
8	J-turn - robot	Loaded	Both	ESC	39
9	J-turn - robot	Loaded	Off	Off	39
10	J-turn - robot	Loaded	Both	Off	39
11	J-turn - robot	Loaded	Off	ESC	39

12	J-turn - robot	Loaded	Rear	Off	39
13	J-turn - robot	Loaded	Front	Off	39
14	J-turn - robot	Loaded	Both	ESC	40
15	J-turn - robot	Loaded	Off	Off	40
16	J-turn - robot	Loaded	Both	Off	40
17	J-turn - robot	Loaded	Off	ESC	40
18	J-turn - robot	Loaded	Rear	Off	40
19	J-turn - robot	Loaded	Front	Off	40
20	J-turn - robot	Loaded	Both	ESC	41
21	J-turn - robot	Loaded	Off	Off	41
22	J-turn - robot	Loaded	Both	Off	41
23	J-turn - robot	Loaded	Off	ESC	41
24	J-turn - robot	Loaded	Rear	Off	41
25	J-turn - robot	Loaded	Front	Off	41
26	J-turn - robot	Loaded	Both	ESC	42
27	J-turn - robot	Loaded	Off	Off	42
28	J-turn - robot	Loaded	Both	Off	42
29	J-turn - robot	Loaded	Off	ESC	42
30	J-turn - robot	Loaded	Rear	Off	42
31	J-turn - robot	Loaded	Front	Off	42
32	J-turn - robot	Loaded	Both	ESC	43
33	J-turn - robot	Loaded	Off	Off	43
34	J-turn - robot	Loaded	Both	Off	43
35	J-turn - robot	Loaded	Both	Off	43
36	J-turn - robot	Loaded	Off	ESC	43
37	J-turn - robot	Loaded	Rear	Off	43
38	J-turn - robot	Loaded	Front	Off	43
39	J-turn - robot	Loaded	Both	ESC	44
40	J-turn - robot	Loaded	Both	Off	44
41	J-turn - robot	Loaded	Off	ESC	44
42	J-turn - robot	Loaded	Rear	Off	44
43	J-turn - robot	Loaded	Front	Off	44
44	J-turn - robot	Loaded	Both	ESC	45
45	J-turn - robot	Loaded	Both	Off	45
46	J-turn - robot	Loaded	Both	Off	45
47	J-turn - robot	Loaded	Both	Off	45
48	J-turn - robot	Loaded	Off	ESC	45
49	J-turn - robot	Loaded	Rear	Off	45
50	J-turn - robot	Loaded	Front	Off	45
51	J-turn - robot	Loaded	Both	ESC	46
52	J-turn - robot	Loaded	Both	Off	46
53	J-turn - robot	Loaded	Off	ESC	46
54	J-turn - robot	Loaded	Rear	Off	46
55	J-turn - robot	Loaded	Front	Off	46
56	J-turn - robot	Loaded	Both	ESC	47

57	J-turn - robot	Loaded	Both	Off	47
58	J-turn - robot	Loaded	Off	ESC	47
59	J-turn - robot	Loaded	Both	ESC	48
60	J-turn - robot	Loaded	Both	ESC	49
61	J-turn - robot	Loaded	Both	ESC	50
62	J-turn - robot	Loaded	Both	ESC	50
63	J-turn - robot	Loaded	off	Off	41
64	J-turn - robot	Loaded	Both	Off	41
65	J-turn - robot	Loaded	off	Off	42
66	J-turn - robot	Loaded	Both	Off	42
67	J-turn - robot	Loaded	off	Off	43

Date: April 6, 2017
Weather: Sunny, 54°, WSW 17-mph wind
Track surface condition: Dry

Test #	Maneuver	Rear trailer loading	RSC	ESC	Speed (mph)
1	DLC	Loaded	Both	Off	48
2	DLC	Loaded	Both	Off	52
3	DLC	Loaded	Both	Off	54
4	DLC	Loaded	Rear	Off	54
5	DLC	Loaded	Rear	Off	54
6	DLC	Loaded	Front	Off	54
7	DLC	Loaded	Off	Off	54
8	DLC	Loaded	Both	ESC	54
9	DLC	Loaded	Off	ESC	54
10	DLC	Loaded	Both	Off	55
11	DLC	Loaded	Rear	Off	55
12	DLC	Loaded	Front	Off	55
13	DLC	Loaded	Off	Off	55
14	DLC	Loaded	Both	ESC	55
15	DLC	Loaded	Off	ESC	55
16	DLC	Loaded	Both	Off	56
17	DLC	Loaded	Rear	Off	56
18	DLC	Loaded	Front	Off	56
19	DLC	Loaded	Off	Off	56
20	DLC	Loaded	Both	ESC	56
21	DLC	Loaded	Off	ESC	56
22	DLC	Loaded	Both	Off	57
23	DLC	Loaded	Rear	Off	57
24	DLC	Loaded	Front	Off	57
25	DLC	Loaded	Off	Off	57
30	DLC	Loaded	Both	ESC	57
31	DLC	Loaded	Off	ESC	57
32	DLC	Loaded	Both	Off	58
33	DLC	Loaded	Rear	Off	58

34	DLC	Loaded	Front	Off	58
35	DLC	Loaded	Off	Off	58
36	DLC	Loaded	Both	ESC	58
37	DLC	Loaded	Off	ESC	58
38	DLC	Loaded	Both	Off	59
39	DLC	Loaded	Rear	Off	59
40	DLC	Loaded	Front	Off	59
41	DLC	Loaded	Off	Off	59
46	DLC	Loaded	Both	ESC	59
47	DLC	Loaded	Off	ESC	59
48	DLC	Loaded	Both	Off	60
49	DLC	Loaded	Rear	Off	60
50	DLC	Loaded	Front	Off	60
51	DLC	Loaded	Off	Off	60
52	DLC	Loaded	Both	ESC	60
53	DLC	Loaded	Off	ESC	60
54	DLC	Loaded	Both	Off	57
55	DLC	Loaded	Off	Off	57
56	DLC	Loaded	Off	Off	57
57	DLC	Loaded	Rear	Off	58
58	DLC	Loaded	Off	ESC	58
59	DLC	Loaded	Rear	Off	59
60	DLC	Loaded	Off	Off	59
61	DLC	Loaded	Off	ESC	59

9.3 Test Results and Analysis

This chapter presents and discusses the results of tests conducted to evaluate the effect of configuration changes on the dynamic stability of a 28-ft A-train double. 266 test runs were completed in total to evaluate eight desired permutations, which are divided into three different groups for comparison purposes. The testing results are presented and discussed by groups and maneuvers. The lateral acceleration results of selected stock tests can be found in Appendix F.

9.3.1 Different Rear Trailer Load Conditions

The objective of this group of tests was to evaluate how the rear trailer's loading condition affects the truck roll stability and RSC system performance. Four permutations were investigated in this set, including:

- Loaded rear trailer (no RSC)
- Loaded rear trailer + RSC
- Empty rear trailer (no RSC)
- Empty rear trailer + RSC

9.3.1.1 Robot-Operated J-turn Tests

This section evaluates the performance of the RSC systems with different rear trailer loading conditions in robot-operated J-turn tests. The actual test entrance speeds rather than the target entrance speeds are used to represent each test for compensating the driver variance. The results of the time from test start to first RSC activation are shown in Figure 9-1. This metric is used to examine whether an empty rear trailer would change activation timing compared with the loaded rear trailer tests. The results indicate that the activation timing variance is always within 0.05s, and no noticeable difference is observed between the two cases.

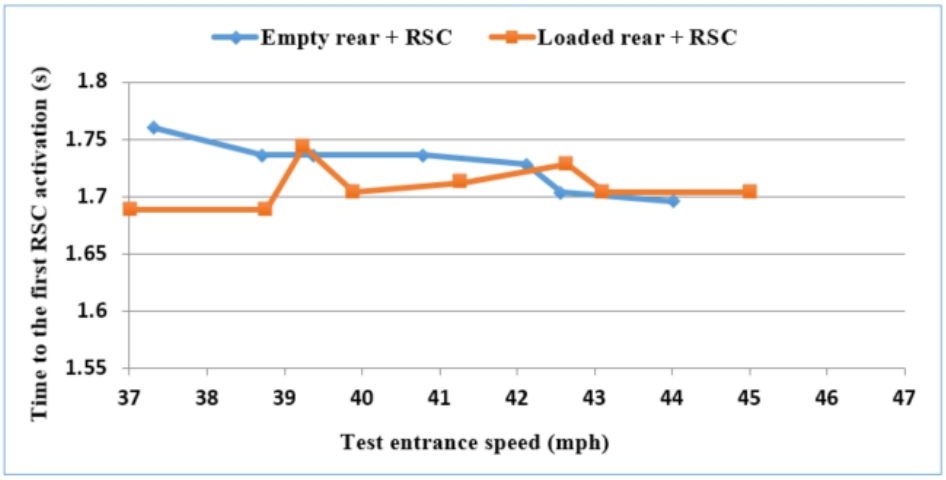

Figure 9-1. Time from test start to the first RSC activation for robot-operated J-turn tests with different rear trailer load conditions.

Figure 9-2 shows the peak outrigger contact forces for the robot-operated J-turn tests. It can be observed that the truck with the empty rear trailer made the first outrigger contact 2.33 mph earlier than the one with a loaded rear trailer, indicating that an empty rear trailer would reduce the truck roll stability when no RSC system is equipped during J-turn tests. For tests with the RSC system, enabling RSC systems increased the rollover speed by 2.88 mph and 3.45 mph for cases with the empty and loaded rear trailer, respectively. In

addition, even though the truck with an empty rear trailer had been equipped with RSC systems, its rollover speed threshold is only ~0.6 mph higher than the stock loaded rear trailer case, and the peak contact forces it experienced were almost three times larger than those in the "loaded rear + RSC" cases. In summary, the empty rear trailer would decrease truck roll stability without RSC systems, and reduce the effectiveness of RSC systems.

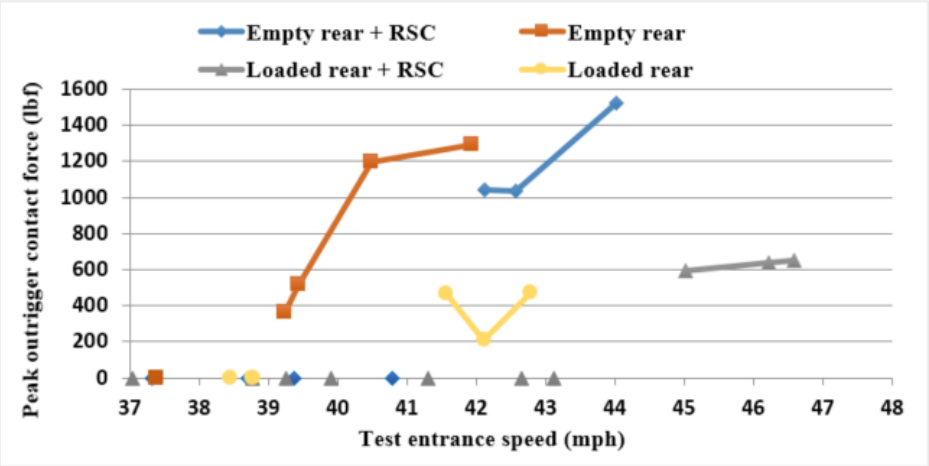

Figure 9-2. Peak outrigger contact force for robot-operated J-turn tests with different rear trailer load conditions.

Figure 9-3 shows the warning time that the RSC system achieved during the tests. Even though the truck with a loaded rear trailer obtained higher rollover speed thresholds, the warning time is similar to those in the empty-rear-with-RSC cases.

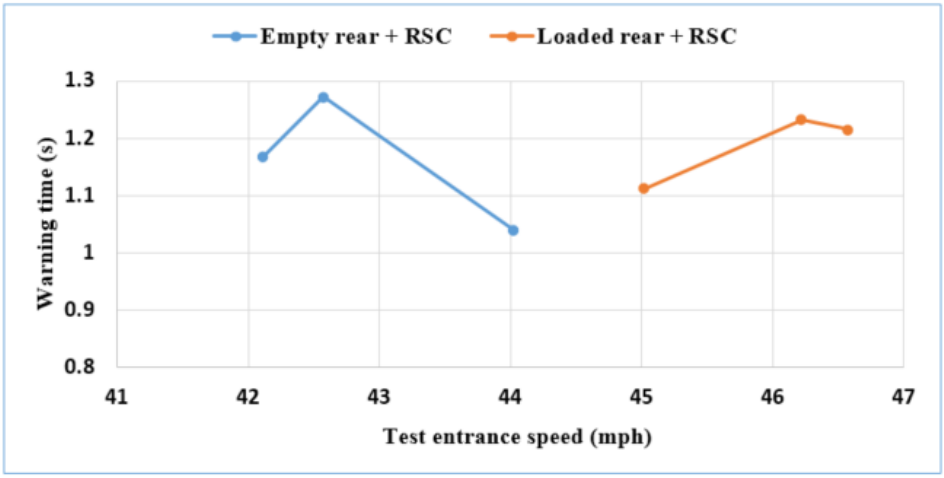

Figure 9-3. Warning time for robot-operated J-turn tests with different rear trailer load conditions.

Figure 9-4 illustrates the articulation angles between the tractor and Trailer A observed three seconds into the test, which normally was the moment when Trailer A experienced

the peak lateral acceleration. The results indicate that the stock truck with an empty rear trailer generally exhibited larger articulation angles, followed by the case where the same truck was equipped with an RSC system; the truck with a loaded rear trailer and RSC system led to the smallest articulation angles. Therefore, an empty rear trailer tended to increase the likelihood of jackknifing events (larger articulation angles). Even when the empty rear trailer was equipped with the RSC system that could attenuate articulation angles, it still led to higher angles than the stock loaded rear trailer case. Again, the truck with a loaded rear trailer and RSC system had better performance in terms of reducing the risk of jackknifing events during the J-turn tests.

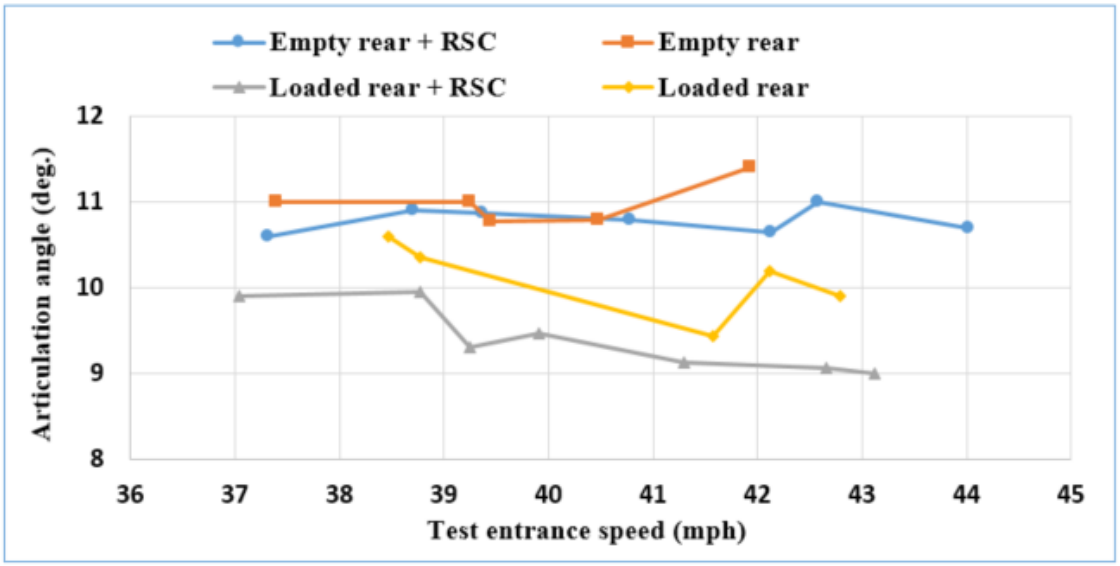

Figure 9-4. Articulation angle between the tractor and Trailer A for robot-operated J-turn tests with different rear trailer load conditions.

Figure 9-5 shows the speed drop achieved from test start to outrigger contact. It can be observed that the RSC system successfully led to more speed drop in both cases. However, with a loaded rear trailer, the RSC system could slow down the truck ~2-mph more due to heavier axle loads and thus better braking effectiveness. As for the stock tests, the empty and loaded rear trailer resulted in similar speed drop.

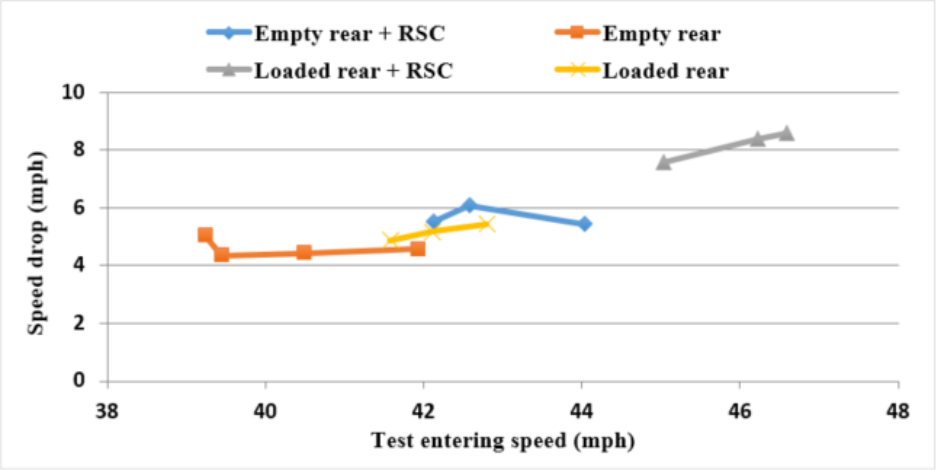

Figure 9-5. Speed drop for robot-operated J-turn tests with different rear trailer load conditions.

9.3.1.2 SWD Tests

The test speed and steering wheel inputs for the SWD maneuvers remained the same as those applied in Chapter 8. Again, two main factors were considered for evaluating the performance of the RSC system, including: (1) whether the truck rolls over during the maneuver (indicated by load cell force), and (2) whether the truck successfully avoids an obstacle, which is qualitatively quantified by the number of cones that the truck hits. The cone layouts for the SWD tests are shown in Figure 8-7 and Figure 8-9. The steering wheel input for the SWD tests in this set of tests began at 70% and was incrementally increased to 100%. Table 9-3 and Table 9-4 provide the results of the outrigger contact force and the number of cones hit during 0.5-Hz and 0.25-Hz SWD tests, respectively. According to the results, rollover events mostly occurred at 90% and 100% steering for both tests. Therefore, the test results of 90% and 100% steering will be further discussed with bar charts.

Figure 9-6 shows the results for time from test start to RSC activation for 0.5-Hz and 0.25-Hz SWD tests at 90% and 100% steering. The entire SWD maneuver is separated into two parts based on the direction of the steering wheel angle input: the truck steers clockwise during the first part, and counterclockwise during the second part, as shown in Figure 8-6. The results indicate that the RSC systems activated at very similar times during the tests. Therefore, the loading condition of the rear trailer did not result in a considerable effect on the RSC system activation timing.

Table 9-3. Results of peak outrigger contact forces and number of cones hit by the truck during 0.5-Hz SWD tests in the loading comparison group.

Group #1 – Different Rear Trailer Loading Configurations							
Test #	**Permutation**	**Steering (%)**	**Outrigger contact force (lbf)**				**Cones hit**
			Front trailer		**Rear trailer**		
			Dri.	**Pas.**	**Dri.**	**Pas.**	
1	Empty rear	70	----	----	----	----	2
2	Empty rear	80	----	----	----	----	0
3	Empty rear	90	----	432.37	----	----	0
4	Empty rear	100	----	1616.41	----	----	0
5	Empty rear + RSC	70	----	----	----	----	1
6	Empty rear + RSC	80	----	----	----	----	0
7	Empty rear + RSC	90	----	----	----	----	0
8	Empty rear + RSC	100	----	946.71	----	----	0
9	Loaded rear	70	----	----	----	----	0
10	Loaded rear	80	----	----	----	----	0
11	Loaded rear	90	----	660.05	----	837.15	0
12	Loaded rear	100	----	2255.43	----	1687.17	0
13	Loaded rear + RSC	70	----	----	----	----	0
14	Loaded rear + RSC	80	----	----	----	----	0
15	Loaded rear + RSC	90	----	----	----	----	0
16	Loaded rear + RSC	100	----	500.08	----	----	0

Table 9-4. Results of outrigger contact forces and number of cones hit by the truck during 0.25-Hz SWD maneuvers in the loading comparison group.

Group #1 – Different Rear Trailer Loading Configurations							
Test #	**Permutation**	**Steering (%)**	**Outrigger contact force (lbf)**				**Cones hit**
			Front trailer		**Rear trailer**		
			Dri.	**Pas.**	**Dri.**	**Pas.**	
1	Empty rear	70	----	----	----	----	2
2	Empty rear	80	530.64	----	----	----	1.5
3	Empty rear	90	909.6	940.4	----	----	0
4	Empty rear	100	1341.8	1349.1	----	----	0
5	Empty rear + RSC	70	----	193.8	----	----	2.5
6	Empty rear + RSC	80	----	----	----	----	1.5
7	Empty rear + RSC	90	----	312.0	----	----	0
8	Empty rear + RSC	100	----	1814.2	----	----	0
9	Loaded rear	70	----	----	----	----	2
10	Loaded rear	80	514.2	508.7	41.6	802.1	0
11	Loaded rear	90	935.0	1225.7	799.6	2052.3	0
12	Loaded rear	100	1399.7	1358.8	1695.2	2193.5	0
13	Loaded rear + RSC	70	----	----	----	----	3.5
14	Loaded rear + RSC	80	----	----	----	----	1.5
15	Loaded rear + RSC	90	----	----	----	----	0
16	Loaded rear + RSC	100	242.0	525.1	190.8	408.2	0

Figure 9-7 shows the results of the peak outrigger contact forces for SWD maneuvers. For 0.5-Hz tests (Figure 9-7(a) and (b)), the truck with the empty rear trailer experienced one outrigger contact on the front trailer's passenger side, compared to two outrigger contacts when the rear trailer was loaded. That was due to the fact that the loaded rear trailer had a higher CG and a lower rollover threshold as compared to the empty rear trailer. Therefore, the loaded rear trailer rolled over at 90% steering, while it also pulled over the front trailer, resulting in a harder outrigger contact on the front trailer. The RSC systems were able to prevent rollover in both cases, indicated by zero outrigger contacts. Similar results are observed for 100% tests, where the test with the loaded rear trailer resulted in more outrigger contacts and higher forces than that with the empty rear trailer. The RSC systems prevented the rear trailer from rolling over in both cases, but it failed to secure the front trailers. The RSC test with the loaded rear trailer resulted in a lower peak contact force because the RSC system achieved a better performance with heaver trailer axle loads.

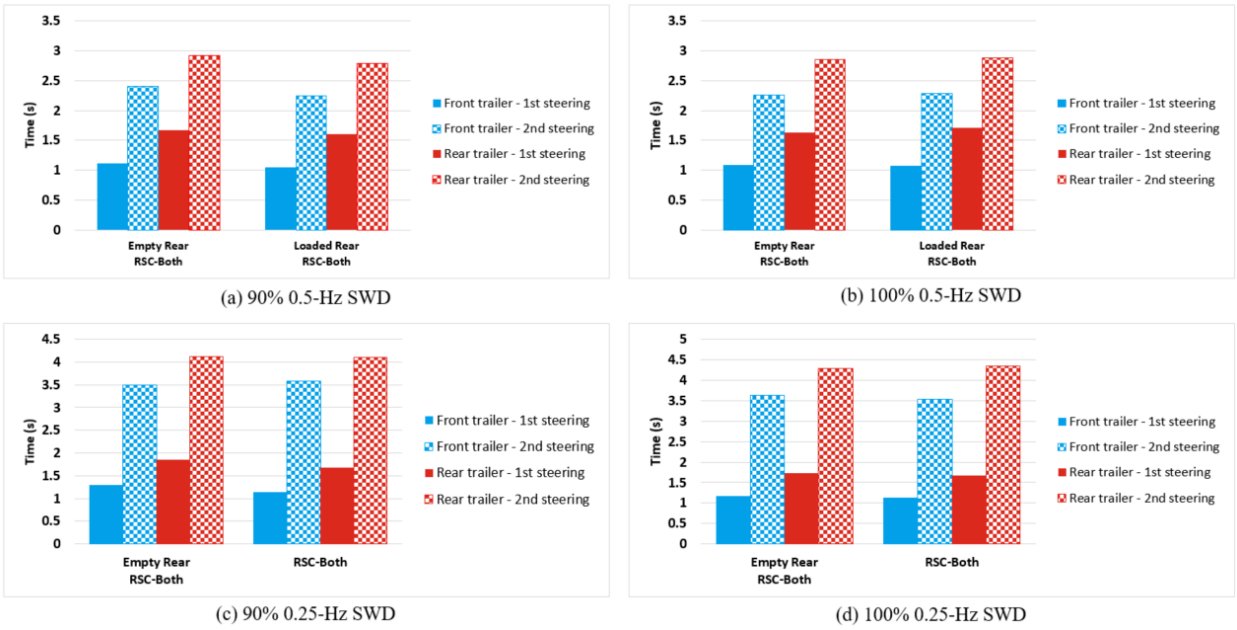

(a) 90% 0.5-Hz SWD

(b) 100% 0.5-Hz SWD

(c) 90% 0.25-Hz SWD

(d) 100% 0.25-Hz SWD

Figure 9-6. Time from test start to RSC activation for tests with different rear trailer load conditions: (a) 90% 0.5-Hz SWD; (b) 100% 0.5-Hz SWD; (c) 90% 0.25-Hz SWD; and (d) 100% 0.25-Hz SWD.

For the 90% 0.25-Hz SWD tests (Figure 9-7(c)), the truck with an empty rear trailer hit two outriggers, unlike the loaded rear trailer that hit all four outriggers. When the truck was equipped with an RSC system, the empty-rear truck hit one outrigger with a peak force over 300 lbf, indicating a strong likelihood of rollover. However, the loaded-rear truck did

not experience any outrigger contact with the RSC systems. The stock 100% 0.25-Hz SWD tests with a loaded rear trailer was aborted slightly earlier before the steering input were completed due to safety concerns, where the truck experienced multiple severe outrigger contacts. Figure 9-7(d) shows that, again, when the truck was equipped with an RSC system, an empty rear trailer could prevent rear outrigger contacts. Even though the truck would roll over when front outriggers contacted in this scenario, fewer outrigger contacts at the rear indicated that the severity of the potential rollover event was reduced. Similar to the 90% tests, the loaded-rear truck exhibited better performance with an RSC system than the one with an empty rear trailer, due to heavier trailer axle loads. Specifically, both trucks would roll over at 100% steering with RSC systems, but the one with a loaded rear trailer had a contact force around 500 lbf, which is nearly 1,000 lbf lighter than the contact experienced by the empty-rear truck. Therefore, the loaded-rear truck would experience a less severe rollover accident in this case.

Based on the peak outrigger contact forces, it could be concluded that a truck with an empty rear trailer has better roll stability than that with a loaded rear trailer when RSC systems are not available. However, when the truck is equipped with an RSC system, it has better roll stability with a loaded rear trailer. This is because RSC systems are more effective with heavier axle loads which could contribute to better braking efficiency.

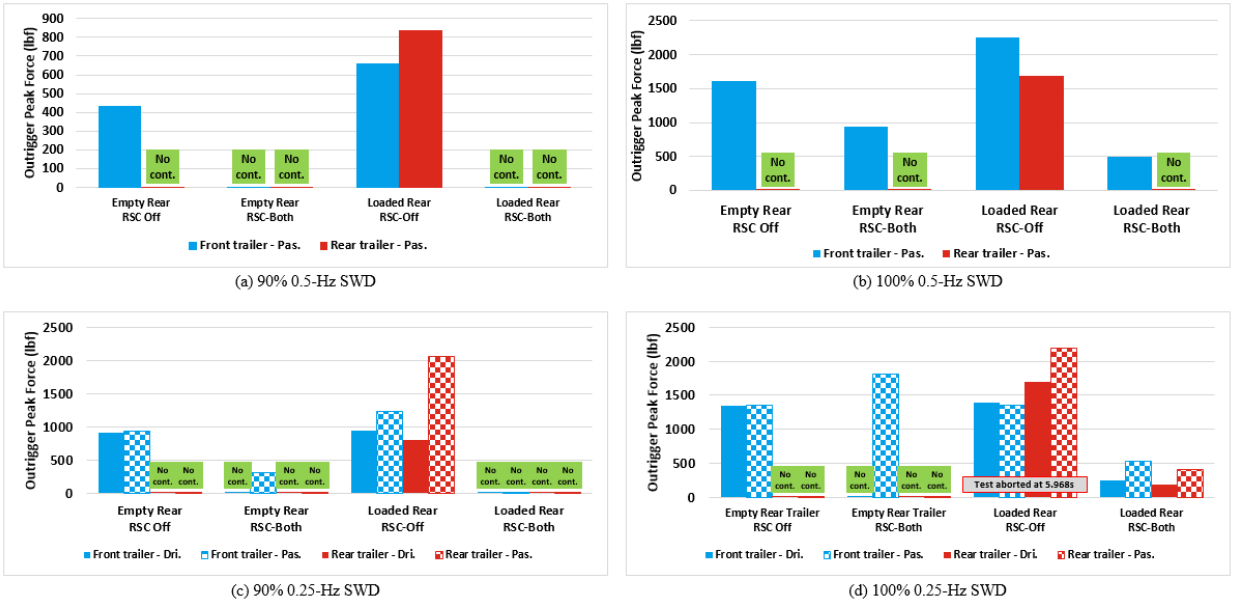

Figure 9-7. Peak outrigger contact forces for tests with different rear trailer load conditions: (a) 90% 0.5-Hz SWD; (b) 100% 0.5-Hz SWD; (c) 90% 0.25-Hz SWD; and (d) 100% 0.25-Hz SWD.

Figure 9-8 shows the speed drop for SWD tests at 90% and 100% steering. In Chapter 8, the speed drop during each test was defined as the speed at RSC activation minus the speed at the moment of outrigger contact. However, in order to compare RSC and stock tests in this set of tests, speed drops are defined as the speed when the test started minus the speed at which an outrigger contact occurs. Figure 9-8(a) indicates that the empty rear trailer did not affect speed drop in 0.5-Hz 90% RSC-off tests. For 0.5-Hz tests at 100% steering, similar results are observed as those for 90% RSC-off tests, but more speed was reduced by the front trailer, as shown in Figure 9-8 (b). In addition, the truck with an empty rear trailer experienced a four-mph speed drop with RSC off, and a five-mph speed drop with RSC on, indicating that the RSC system only provided an additional one-mph speed drop due to the loading condition. However, the RSC system managed to reduce ~3.5 mph with a loaded rear trailer. This indicates that the RSC system is more effective with rear loading in these tests.

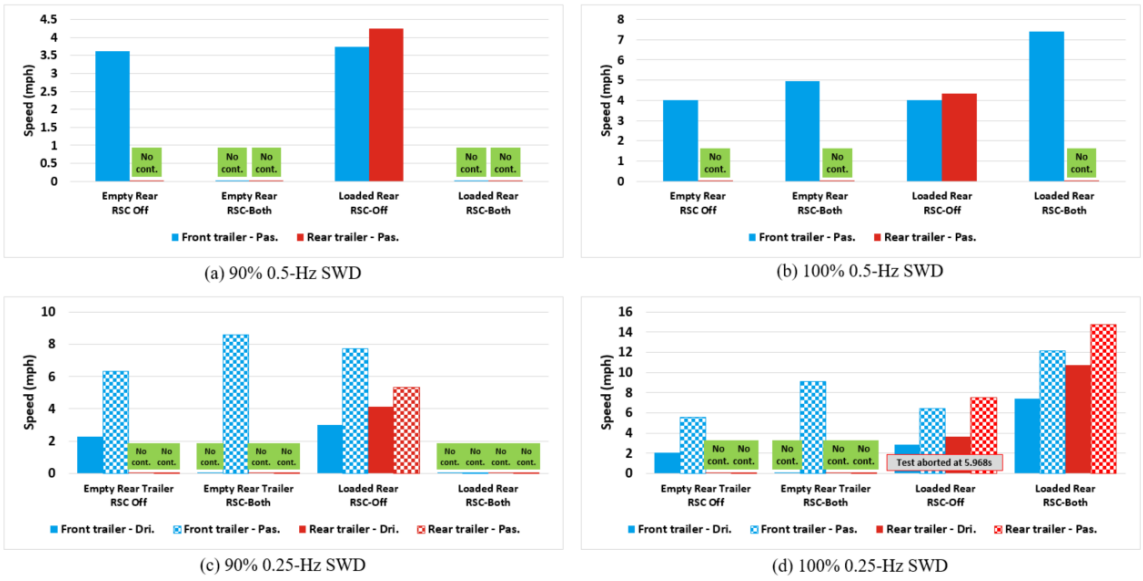

(a) 90% 0.5-Hz SWD

(b) 100% 0.5-Hz SWD

(c) 90% 0.25-Hz SWD

(d) 100% 0.25-Hz SWD

Figure 9-8. Speed drop for tests with different rear trailer load conditions: (a) 90% 0.5-Hz SWD; (b) 100% 0.5-Hz SWD; (c) 90% 0.25-Hz SWD; and (d) 100% 0.25-Hz SWD.

Similar results are observed for the 0.25-Hz SWD tests. Figure 9-8(c) shows that the RSC systems managed to provide an additional two-mph speed drop in the 90% steering test with an empty rear trailer, and completely prevented both trailers from rolling over in the loaded-rear test. For the tests with 100% steering, greater speed drops were achieved in both cases, as shown in Figure 9-8(b). The RSC systems managed to provide extra speed

drop with a loaded rear trailer, compared to the RSC-off test, but they failed to prevent both trailers from rolling over.

Figure 9-9 shows the number of cones that were hit during the 0.25-Hz SWD tests. The results indicate that an empty rear trailer did not introduce additional understeer as it did not hit more cones than the loaded rear trailer configuration. Therefore, the empty rear trailer did not decrease the maneuverability of the truck. The results for the 0.5-Hz SWD tests are not discussed here because, as Table 9-3 shows, the truck only hit cones during two 70% tests and did not hit any cone during other tests.

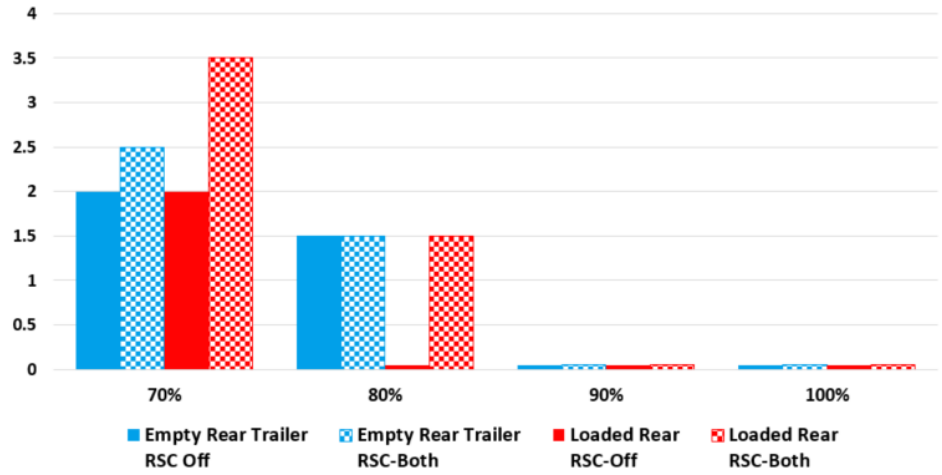

Figure 9-9. Cones hit during tests with different rear trailer load conditions: (a) 90% 0.5-Hz SWD; (b) 100% 0.5-Hz SWD; (c) 90% 0.25-Hz SWD; and (d) 100% 0.25-Hz SWD.

The peak articulation angles are shown in Figure 9-10 and Figure 9-11 for 0.5-Hz and 0.25-Hz SWD tests, respectively. Articulation angles are used to evaluate the likelihood of a jackknifing event that a truck could experience during tests, where a larger angle indicates a stronger risk. Figure 9-10(a) and Figure 9-10(b) indicate that the RSC systems could reduce the articulation angle between the tractor and front trailer, compared to those tests without RSC. The angles between the front and rear trailers showed similar trends in both the 0.5-Hz and 0.25-Hz tests, where the angles increased as the steering percentage increased. It is noted that the team members who stayed in the cab during tests could not clearly tell when an outrigger contacted the ground based on the motion they felt, due to the soft cab suspension and the pintle hitch coupling between the vehicle units. However, team members could feel and observe the tractor yaw motion when the truck oversteered, and they used it to estimate whether the test was safe to proceed or must be aborted. For

example, the 100% 0.25-Hz SWD test with the loaded rear trailer and no RSC system was aborted because the team member experienced excessive yaw motion in the tractor, and therefore decided to terminate the test before the maneuver was completely finished. This event was later confirmed by the articulation angle between the tractor and front trailer, as shown in Figure 9-11(a), where the angle exceeded 30 degrees and the designed anti-jackknifing system started to engage.

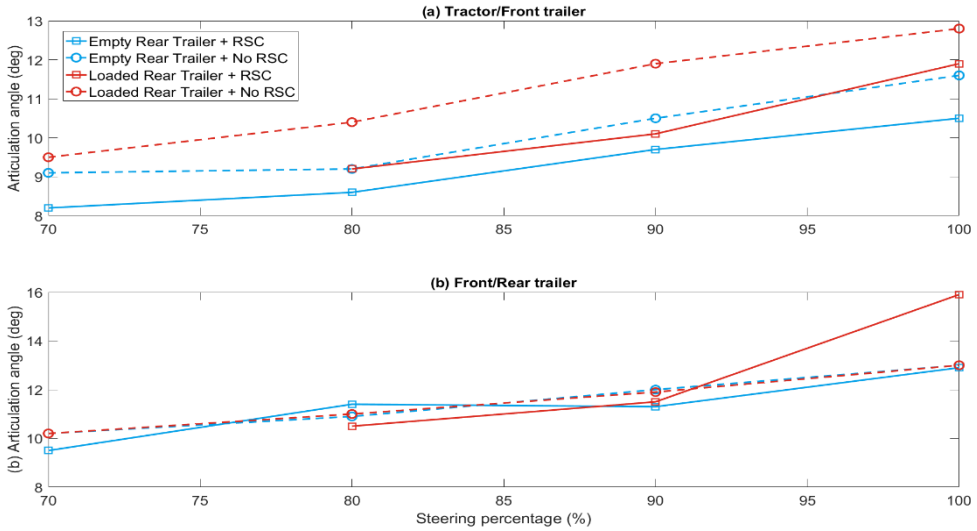

Figure 9-10. Peak articulation angles for 0.5-Hz SWD tests with different rear trailer load conditions: (a) articulation angle between tractor and front trailer; and (b) articulation angle between front and rear trailer.

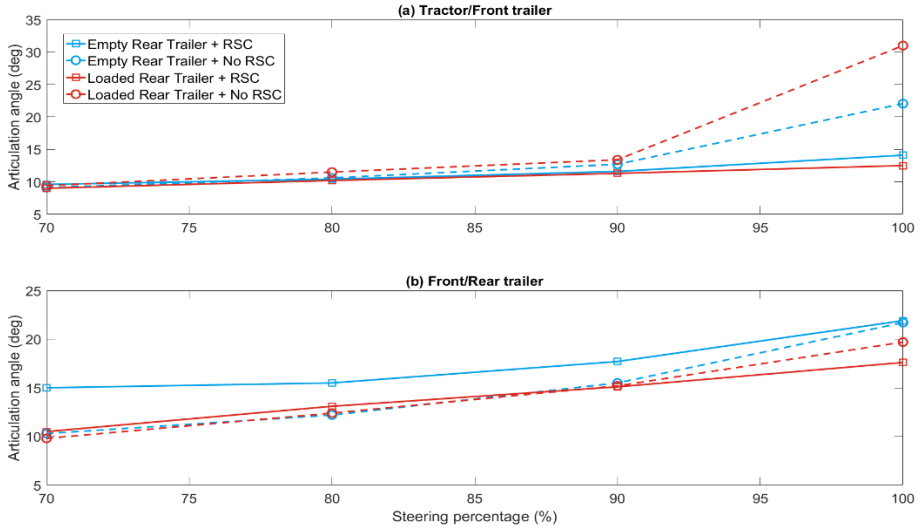

Figure 9-11. Peak articulation angles for 0.25-Hz SWD tests with different rear trailer load conditions: (a) articulation angle between tractor and front trailer; and (b) articulation angle between front and rear trailer.

9.3.1.3 DLC Tests

The peak outrigger contact forces for the DLC tests with different rear trailer loading conditions are summarized in Table 9-5. The results show that the truck with an empty rear trailer experienced a greater number of outrigger contacts on the front trailer's driver side, whereas the truck with a loaded rear trailer mostly hit the rear trailer's outriggers. This indicates that the loaded rear trailer provided a stabilizing effect on the front trailer. When the trailers were equipped with RSC systems, the truck with a loaded rear trailer did not experience any rollover during the tests because the heavier axle load enhanced the performance of the RSC systems, but outrigger contacts were observed for the truck with the empty rear trailer in three tests.

Table 9-5. Results of peak outrigger contact forces for DLC tests in the loading comparison group.

Group #1 – Different Rear Trailer Loading Configurations						
Test #	**Permutation**	**Speed (mph)**	**Outrigger contact force (lbf)**			
			Front trailer		**Rear trailer**	
			Dri.	**Pas.**	**Dri.**	**Pas.**
1	Empty rear	57	----	----	----	----
2	Empty rear	58	2123.7	----	----	----
3	Empty rear	59	620.5	----	----	----
4	Empty rear	60	523.7	----	----	----
5	Empty rear + RSC	57	285.1	----	----	----
6	Empty rear + RSC	58	341.1	----	----	----
7	Empty rear + RSC	59	----	----	----	----
8	Empty rear + RSC	60	1166.1	----	----	76.1
9	Loaded rear	57	----	----	----	1017.3
10	Loaded rear	58	----	----	----	----
11	Loaded rear	59	----	----	----	----
12	Loaded rear	60	----	----	645.0	1846.8
13	Loaded rear + RSC	57	----	----	----	----
14	Loaded rear + RSC	58	----	----	----	----
15	Loaded rear + RSC	59	----	----	----	----
16	Loaded rear + RSC	60	----	----	----	----

Figure 9-12 shows peak articulation angles for tests with different rear trailer loading conditions. In general, the tests with an empty rear trailer exhibit larger articulation angles than those with a loaded rear trailer. In addition, the results also show that RSC systems

could reduce the likelihood of a jackknifing event, indicated by smaller articulation angles compared with the corresponding stock tests.

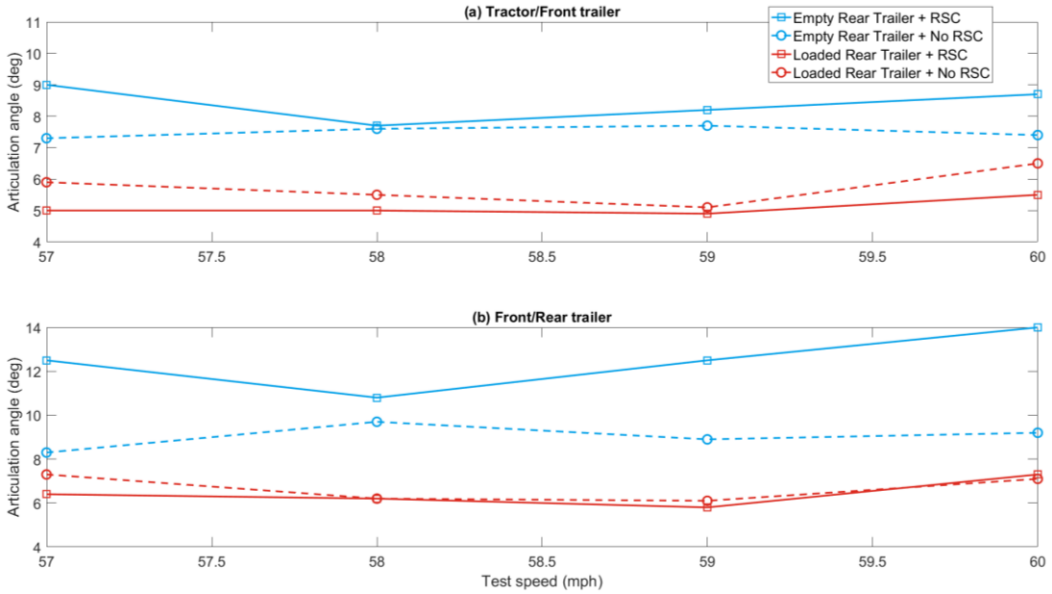

Figure 9-12. Peak articulation angles for DLC tests with different rear trailer load conditions: (a) articulation angle between tractor and front trailer; and (b) articulation angle between front and rear trailer.

9.3.2 Mixed RSC Configurations

The objective of this set of tests is to evaluate how mixed RSC configurations affect the truck roll stability and RSC system performance. Four permutations are investigated in this group, including:

- Stock (no RSC)
- RSC on front trailer only
- RSC on rear trailer only
- RSC on both trailers

9.3.2.1 Robot-Operated J-turn Tests

Figure 9-13 shows the time from test start to the first RSC activation in the robot-operated J-turn tests with entrance speeds from 37 to 46 mph. In general, no clear trend or pattern could be observed from the results. The activation timing difference is always within ~0.05s, and thus it could be concluded that RSC-both and RSC-front had similar first activation timing.

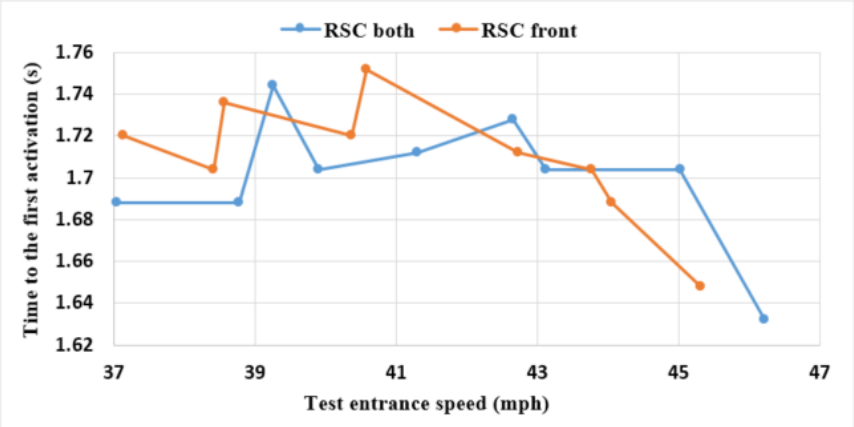

Figure 9-13. Time from test start to the first RSC activation for robot-operated J-turn tests with mixed RSC configurations.

Figure 9-14 shows the results of peak outrigger contact forces (Trailer A passenger side) in the robot-operated J-turn tests with mixed RSC configurations. The stock configuration experienced its first outrigger contact at 41.57 mph, and it was not tested at any speed over 43 mph due to safety concerns. For the RSC-rear configuration, it started to make outrigger contact at 42.33 mph, whereas the RSC-front configuration increased this speed threshold by 1.43 mph and only resulted in a slight contact (~187 lbf). The RSC-both configuration obtained the best performance, which increased the rollover speed to 45 mph.

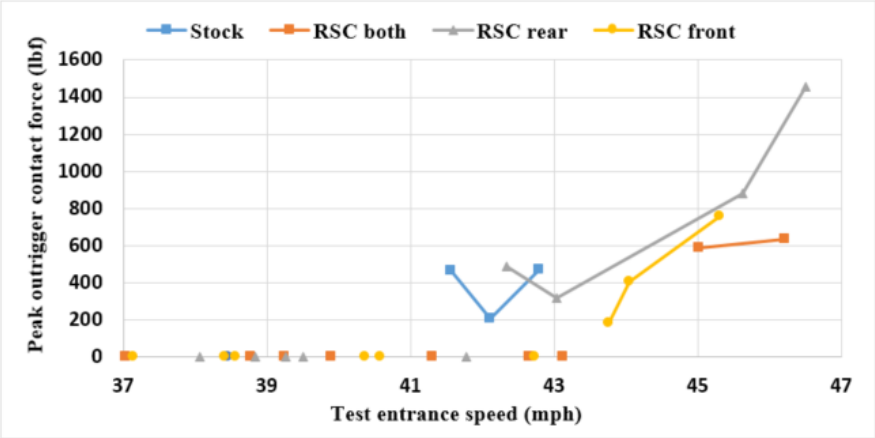

Figure 9-14. Peak outrigger contact force for robot-operated J-turn tests with mixed RSC configurations.

Figure 9-15 shows the warning time that the two RSC configurations achieved during the J-turn tests. RSC-rear is not shown here because the outrigger contact in J-turns almost all happened to the front trailer. Unfortunately, no clear conclusions could be drawn based on the results due to the limited comparable data points. More specifically, the RSC-front

configuration tests stopped at 45.3 mph due to safety concerns, whereas the RSC-both configuration only experienced its first contact at 45 mph. It is noted that almost all outrigger contact happened on the front trailer, and therefore no warning time is available for the RSC-rear configuration.

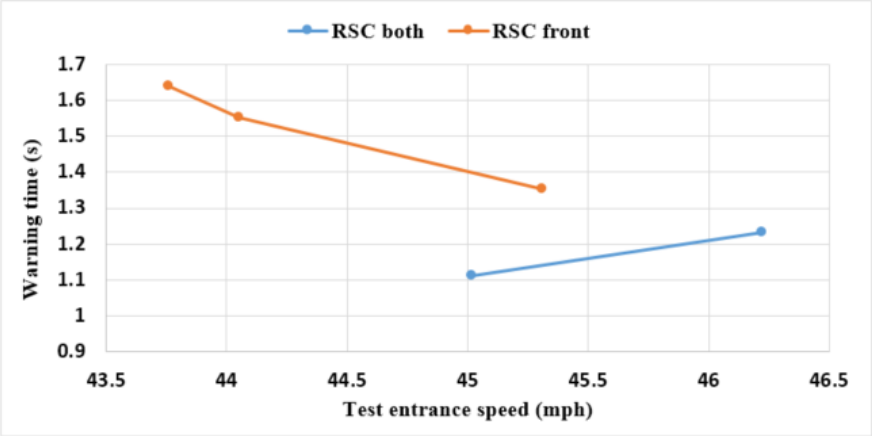

Figure 9-15. Warning time for robot-operated J-turn tests with mixed RSC configurations.

Figure 9-16 shows the results of the articulation angle between the tractor and Trailer A during the robot-operated J-turn tests. It is noted again that the angles shown here are measured three seconds into the test, which was the moment when Trailer A normally experienced the peak lateral acceleration. In general, all configurations led to similar peak articulation angles with variance within one degree. The stock configuration resulted in slightly higher angles, and the RSC-both showed marginally better performance.

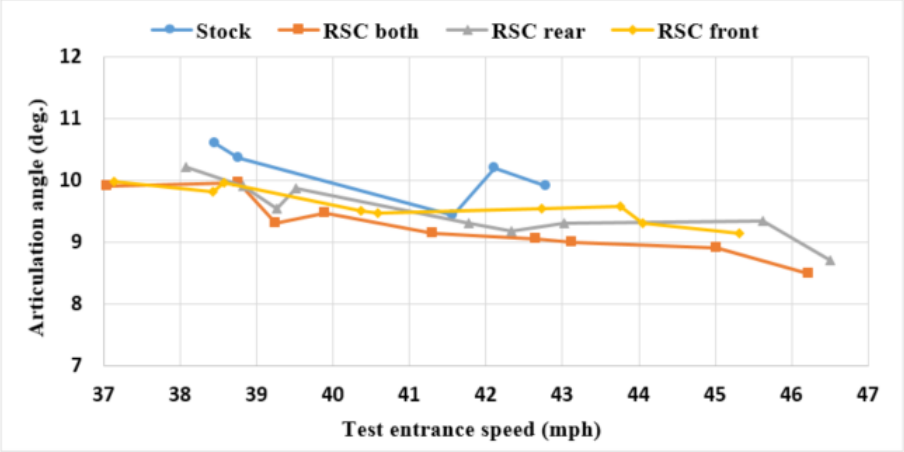

Figure 9-16. Articulation angle between the tractor and Trailer A for robot-operated J-turn tests with mixed RSC configurations.

Figure 9-17 summarizes the speed drop achieved by each configuration from test start to outrigger contact. It can be observed that all RSC configurations managed to provide a considerable amount of speed drop before the outrigger made contact. RSC-rear and RSC-front configurations achieved similar speed reduction at 44 mph, but the RSC-front outperformed the RSC-rear in the other tests. RSC-both tended to provide better speed drop among all configurations.

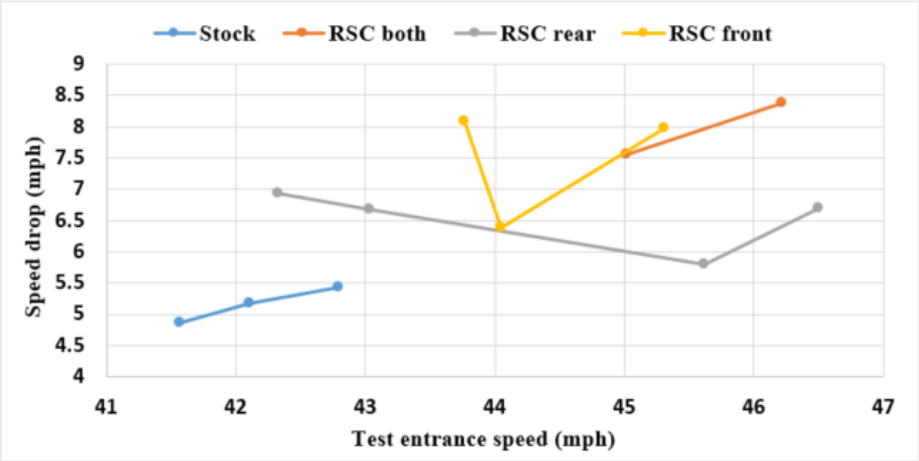

Figure 9-17. Speed drop for robot-operated J-turn tests with mixed RSC configurations.

9.3.2.2 SWD Tests

The peak outrigger contact forces and the number of cones hit during 0.5-Hz and 0.25-Hz SWD tests are summarized in Table 9-6 and Table 9-7, respectively. According to the results, most of the rollover events occurred at 90% and 100% steering in both SWD tests. Hence, the test results of 90% and 100% SWD maneuvers are further examined with bar charts.

Figure 9-18 shows the time from test start to RSC activation for 0.5-Hz and 0.25-Hz SWD tests. The RSC systems demonstrated consistency of activation timing between tests. Specifically, the RSC-front and RSC-rear tests resulted in similar activation times as during the RSC-both tests. This indicates that the activation of one RSC system would not be affected by the system installed on the other trailer in this configuration.

Table 9-6. Results of peak outrigger contact forces and cones for 0.5-Hz SWD tests with mixed RSC configurations.

Group #2 – Mixed RSC Configurations							
Test #	Permutation	Steering (%)	Outrigger contact force (lbf)				Cones hit
			Front trailer		Rear trailer		
			Dri.	Pas.	Dri.	Pas.	
1	Stock (no RSC)	70	----	----	----	----	0
2	Stock (no RSC)	80	----	----	----	----	0
3	Stock (no RSC)	90	----	660.05	----	837.15	0
4	Stock (no RSC)	100	----	2255.43	----	1687.17	0
5	RSC on front only	70	----	----	----	----	0
6	RSC on front only	80	----	----	----	----	0
7	RSC on front only	90	----	----	----	----	0
8	RSC on front only	100	----	540.4	----	1517.3	0
9	RSC on rear only	70	----	----	----	----	0
10	RSC on rear only	80	----	----	----	----	0
11	RSC on rear only	90	----	282.1	----	----	0
12	RSC on rear only	100	----	1110.8	----	402.9	0
13	RSC on both	70	----	----	----	----	0
14	RSC on both	80	----	----	----	----	0
15	RSC on both	90	----	----	----	----	0
16	RSC on both	100	----	500.08	----	----	0

Table 9-7. Results of peak outrigger contact forces and cones for 0.25-Hz SWD tests with mixed RSC configurations.

Group #2 – Mixed RSC Configurations							
Test #	Permutation	Steering (%)	Outrigger contact force (lbf)				Cones hit
			Front trailer		Rear trailer		
			Dri.	Pas.	Dri.	Pas.	
1	Stock (no RSC)	70	----	----	----	----	2
2	Stock (no RSC)	80	514.2	508.7	41.6	802.1	0
3	Stock (no RSC)	90	935.0	1225.7	799.6	2052.3	0
4	Stock (no RSC)	100	1399.7	1358.8	1695.2	2193.5	0
5	RSC on front only	70	----	----	----	----	2
0	RSC on front only	80	----	----	----	295.6	0
7	RSC on front only	90	----	----	----	1601.6	0
8	RSC on front only	100	312.4	----	----	1831.8	0
9	RSC on rear only	70	----	----	----	----	2
10	RSC on rear only	80	----	----	----	----	0
11	RSC on rear only	90	898.4	----	47.7	----	0
12	RSC on rear only	100	1316.4	972.0	1133.0	1295.4	0
13	RSC on both	70	----	----	----	----	3.5
14	RSC on both	80	----	----	----	----	1.5
15	RSC on both	90	----	----	----	----	0
16	RSC on both	100	242.0	525.1	190.8	408.2	0

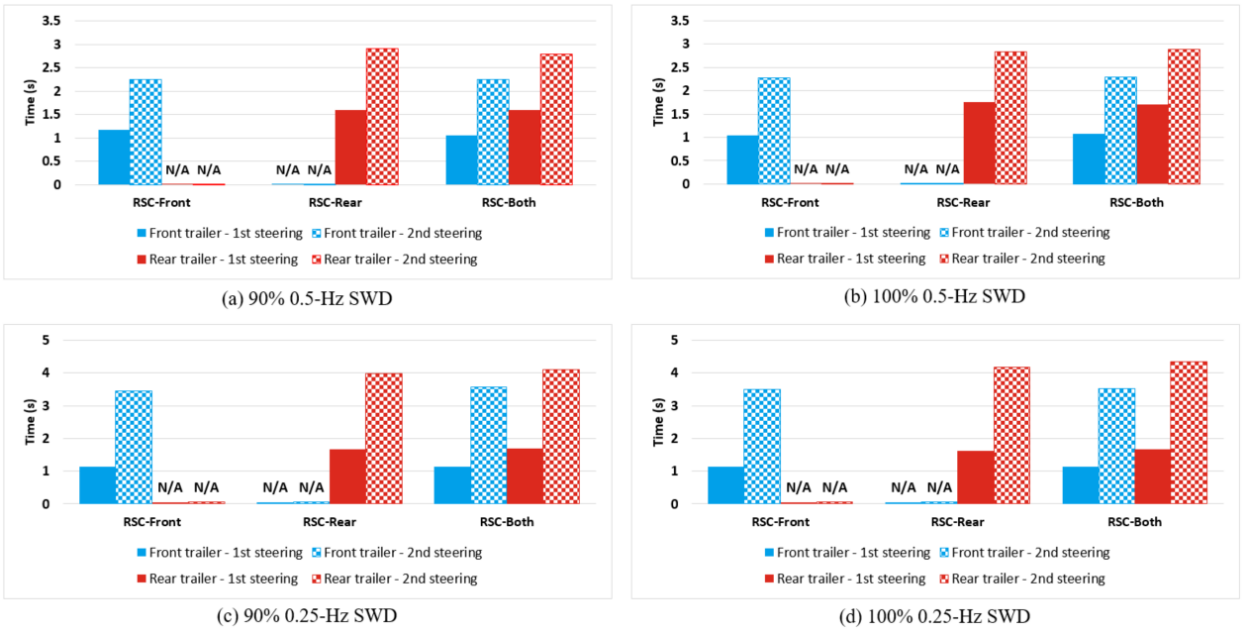

(a) 90% 0.5-Hz SWD

(b) 100% 0.5-Hz SWD

(c) 90% 0.25-Hz SWD

(d) 100% 0.25-Hz SWD

Figure 9-18. Time from test start to RSC activation for tests with mixed RSC configurations: (a) 90% 0.5-Hz SWD; (b) 100% 0.5-Hz SWD; (c) 90% 0.25-Hz SWD; and (d) 100% 0.25-Hz SWD.

Figure 9-19 shows the peak outrigger contact forces for both 0.5-Hz and 0.25-Hz SWD tests with mixed RSC configurations. For the 90% 0.5-Hz test, as shown in Figure 9-19(a), RSC-front and RSC-both configurations both managed to prevent the trailers from rolling over. The RSC-rear configuration resulted in one outrigger contact with a force under 300 lbf, indicating that the truck would experience aggressive roll motion but might not roll over. All RSC configurations performed better than the stock test. For the 100% 0.5-Hz test, Figure 9-19(b) illustrates that the RSC system could reduce the contact force only for the trailer it was equipped to, and best performance was achieved when it was installed on both trailers.

Figure 9-19(c) shows that when an RSC system was only installed on the front trailer, it successfully prevented the front trailer from rolling over, but the rear trailer had a harder outrigger contact. When the RSC system was installed on the rear trailer, the front trailer rolled over and the rear trailer was close to roll, indicated by a small outrigger contact force on the rear trailer driver's side. The rollover could be completely prevented with RSC systems installed on both trailers. For 100% 0.25-Hz SWD tests, as shown in Figure 9-19(d), two out of four outriggers contacted the ground during the RSC-front tests, and one of them was a hard strike. All four outriggers contacted during the RSC-rear tests, but the forces were all smaller than the large hit that occurred during the RSC-front test. When

both trailers were equipped with RSC systems, four outrigger contacts occurred, but two of them were under 300 lbf, and the other two were also less severe.

In general, the test results for the peak outrigger contact forces indicate that installing RSC systems on both trailers provided the best performance. The results of RSC-front and RSC-rear configurations are very close, but installing RSC on the front led to slightly better performance. All RSC tests obtained better results than stock tests, in terms of the number and severity of outrigger contacts.

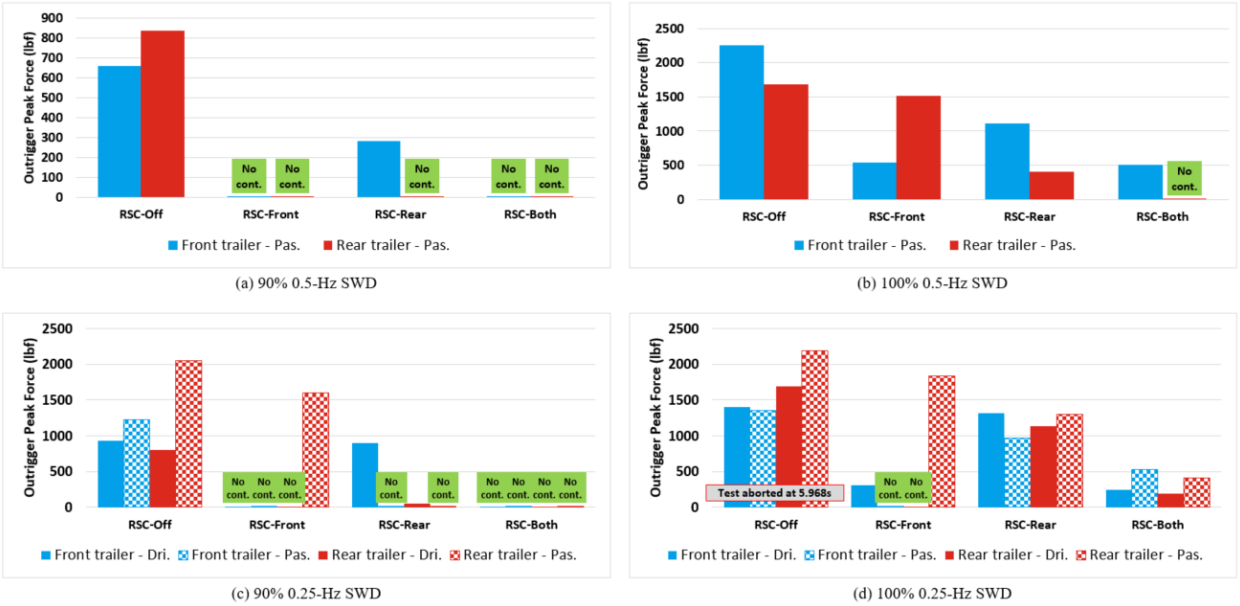

Figure 9-19. Peak outrigger contact forces for tests with mixed RSC configurations: (a) 90% 0.5-Hz SWD; (b) 100% 0.5-Hz SWD; (c) 90% 0.25-Hz SWD; and (d) 100% 0.25-Hz SWD.

Figure 9-20 shows the results of speed drop for both 0.5-Hz and 0.25-Hz SWD tests. In general, the stock tests obtained the least speed drop since no brake was applied in the tests, whereas the largest speed drops were achieved with RSC systems enabled on both trailers. The RSC-front configuration managed to reduce more speed than the RSC-rear configuration.

Figure 9-21 shows the number of cones hit during tests with mixed RSC configurations for the 0.25-Hz SWD tests. The truck hit more cones with the RSC-both configuration than with the other configurations during the tests at 70% and 80% steering, and cleared all the cones during the 90% and 100% steering tests. Therefore, only installing a single RSC

system on either front or rear trailer would not introduce more understeer to the truck, compared to the configuration with RSC enabled on both trailers.

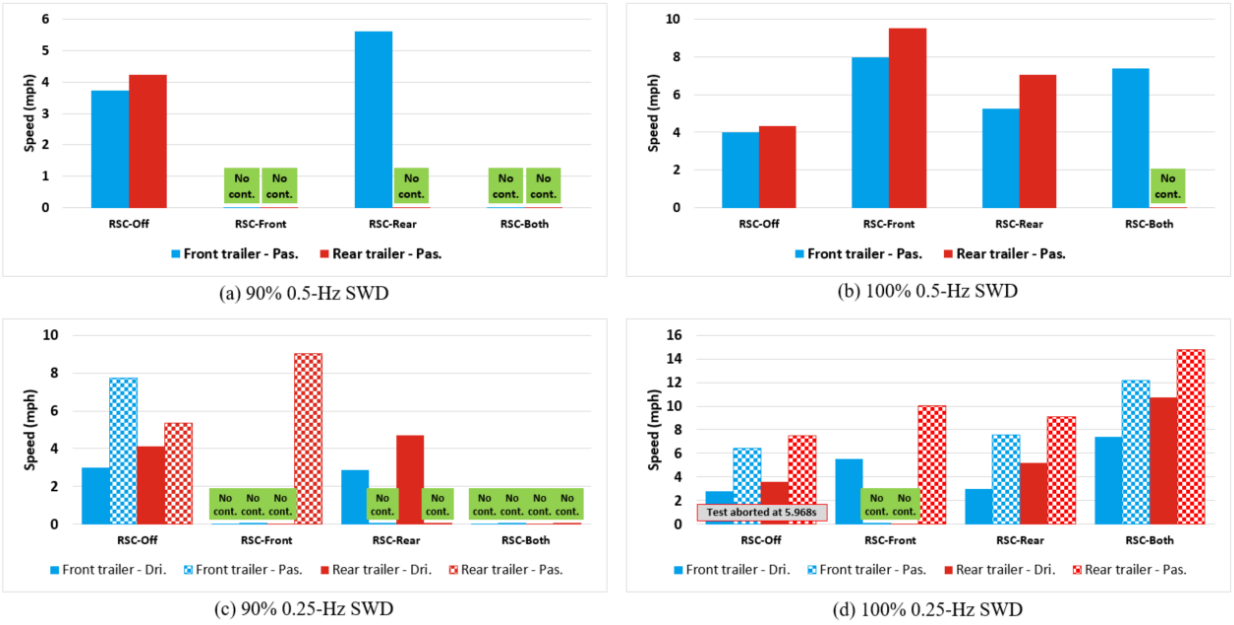

(a) 90% 0.5-Hz SWD

(b) 100% 0.5-Hz SWD

(c) 90% 0.25-Hz SWD

(d) 100% 0.25-Hz SWD

Figure 9-20. Speed drop for tests with mixed RSC configurations: (a) 90% 0.5-Hz SWD; (b) 100% 0.5-Hz SWD; (c) 90% 0.25-Hz SWD; and (d) 100% 0.25-Hz SWD.

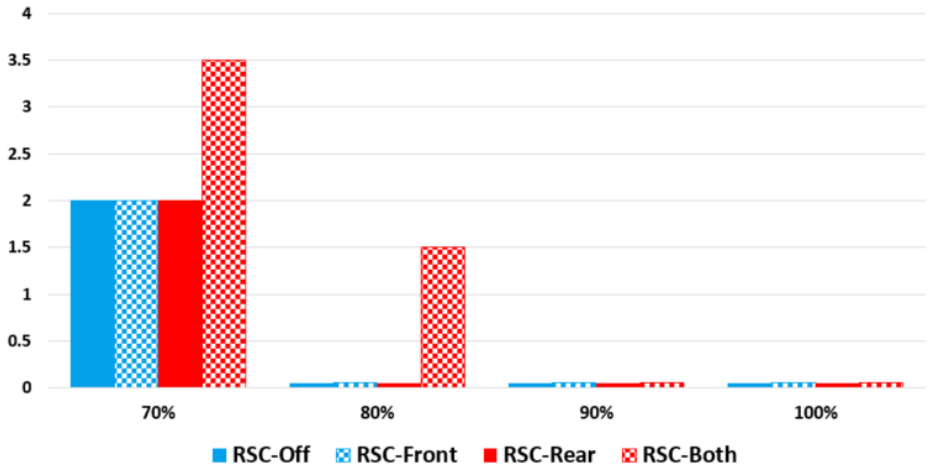

Figure 9-21. Cones hit during tests with mixed RSC configurations: (a) 90% 0.5-Hz SWD; (b) 100% 0.5-Hz SWD; (c) 90% 0.25-Hz SWD; and (d) 100% 0.25-Hz SWD.

Figure 9-22 shows the peak articulation angles for 0.5-Hz SWD tests with mixed RSC configurations. The stock test resulted in larger articulation angles between the tractor and the front trailer, followed by the RSC-rear configuration. This was because only the rear trailer brakes were applied during RSC-rear tests, and therefore it had less effect on stretching the "chain" between the tractor and front trailer, but had more effect between the

front and rear trailer, as shown in Figure 9-22(b). The RSC-both and RSC-front configurations had similar results for tractor-front trailer articulation angles, but RSC-front led to larger angles between the front and rear trailers. This occurred because applying brakes to the front trailer would only make the rear trailer push into the "chain" and therefore resulted in larger articulation angles between the trailers.

Figure 9-23 illustrates that the articulation angle results of the 0.25-Hz SWD tests had a similar trend as those of the 0.5-Hz SWD tests. The only exception is that stock tests resulted in larger angles at all 100% steering tests, compared to the other tests with RSC systems. This was because no braking was applied during stock tests, and therefore the truck experienced more aggressive lateral motion during these tests. The 100% steering maneuver for the 0.25-Hz SWD tests exceeded the yaw stability threshold of the truck without RSC systems. Thus, the truck lost its grip on the tire contact patch during the tests and started to slide, which caused excessive yaw motion indicated by the larger articulation angle (~30 degrees).

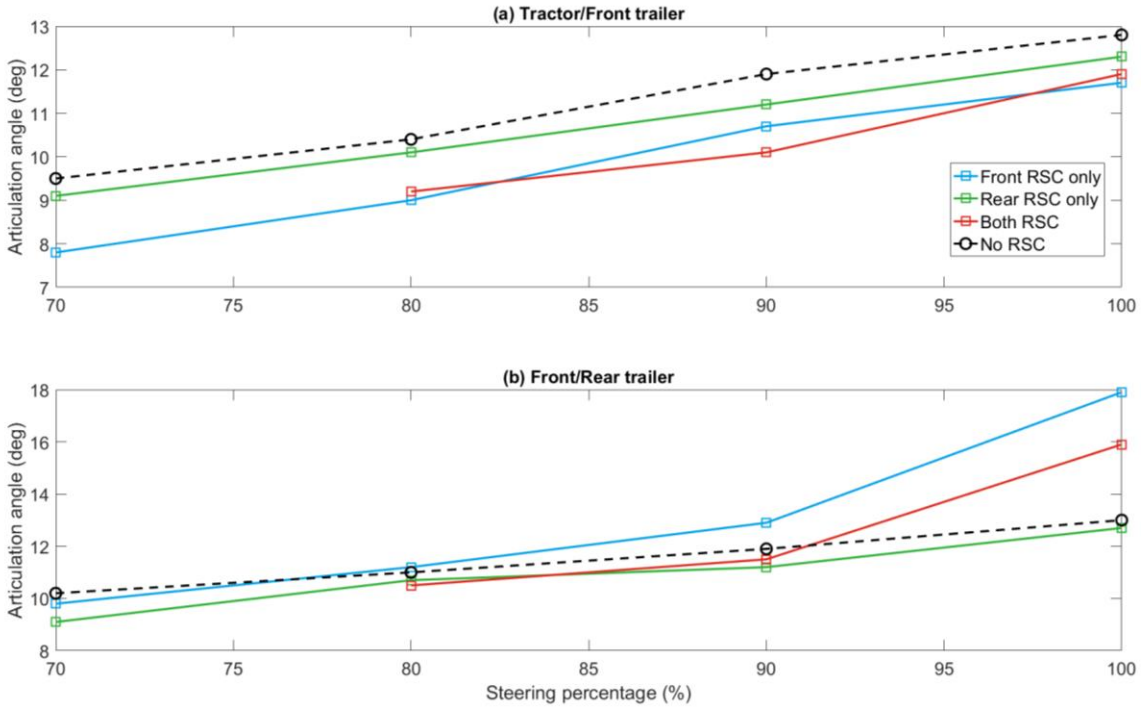

Figure 9-22. Peak articulation angles for 0.5-Hz SWD tests with mixed RSC configurations: (a) articulation angle between tractor and front trailer; and (b) articulation angle between front and rear trailer.

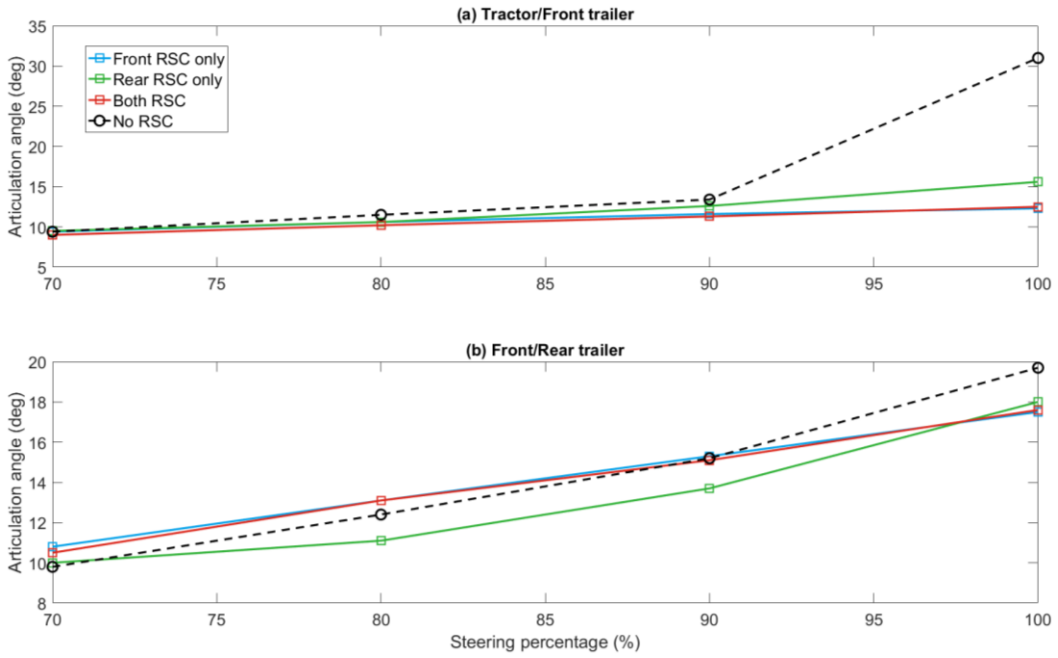

Figure 9-23. Peak articulation angles for 0.25-Hz SWD tests with mixed RSC configurations: (a) articulation angle between tractor and front trailer; and (b) articulation angle between front and rear trailer.

9.3.2.3 DLC Tests

The peak outrigger contact forces for the DLC tests with mixed RSC configurations are summarized in Table 9-8. The results show that installing RSC systems on both trailers completely prevented the truck from rolling over, followed by putting one RSC system on the front trailer, where only one outrigger contacted the ground during the test at 60 mph. When only the rear trailer was equipped with the RSC system, the truck experienced similar outrigger contacts as during the stock tests. Therefore, the findings indicate that if only one RSC unit is available, installing it on the front trailer will result in a better roll stability performance than installing it on the rear.

Figure 9-24 provides articulation angles for the DLC tests with mixed RSC configurations. The RSC-rear configuration resulted in larger articulation angles at both locations (tractor/front trailer and front/rear trailer), whereas equipping both trailers with the RSC systems led to the smallest angles among all configurations. However, the range of angle variation is reasonably small (within two degrees), and thus no major difference is observed.

Table 9-8. Results of peak outrigger contact forces for DLC tests with mixed RSC configurations.

Group #2 – Mixed RSC Configurations						
Test #	Permutation	Speed (mph)	Outrigger contact force (lbf)			
			Front trailer		Rear trailer	
			Dri.	Pas.	Dri.	Pas.
1	Stock (no RSC)	57	----	----	----	1017.3
2	Stock (no RSC)	58	----	----	----	----
3	Stock (no RSC)	59	----	----	----	----
4	Stock (no RSC)	60	----	----	645.0	1846.8
5	RSC on front only	57	----	----	----	----
6	RSC on front only	58	----	----	----	----
7	RSC on front only	59	----	----	----	----
8	RSC on front only	60	----	----	----	922.5
9	RSC on rear only	57	----	----	----	----
10	RSC on rear only	58	----	----	----	----
11	RSC on rear only	59	----	----	----	2871.6
12	RSC on rear only	60	----	----	671.7	2416.5
13	RSC on both	57	----	----	----	----
14	RSC on both	58	----	----	----	----
15	RSC on both	59	----	----	----	----
16	RSC on both	60	----	----	----	----

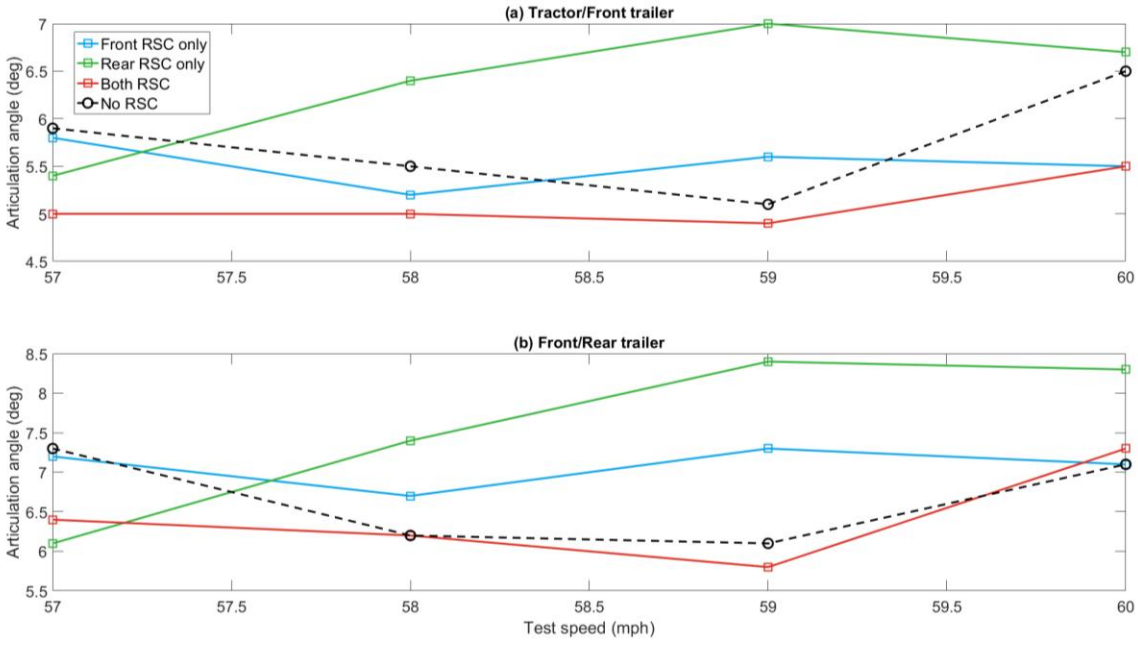

Figure 9-24. Peak articulation angles for DLC tests with mixed RSC configurations: (a) articulation angle between tractor and front trailer; and (b) articulation angle between front and rear trailers.

9.3.3 Mixed ESC/RSC Configurations

The objective of this group of tests is to evaluate the effect of tractor ESC on truck roll stability and RSC system performance. Four permutations are investigated in this group, including:

- Stock (no RSC or ESC)
- RSC only (on both trailers)
- ESC only (on tractor)
- RSC + ESC

9.3.3.1 Robot-Operated J-turn Tests

Figure 9-25 shows the time from test start to the first RSC activation during the robot-operated J-turn tests. For the tests conducted at speeds below 45.5 mph, time to activation for the ESC+RSC configuration was slightly quicker than that for the RSC-only configuration. However, when the test speed was beyond 45.5 mph, opposite results were observed. Considering that the difference between the results of the two configurations is within ~0.05s, it could be concluded that the two configurations had similar performance in terms of activation timing.

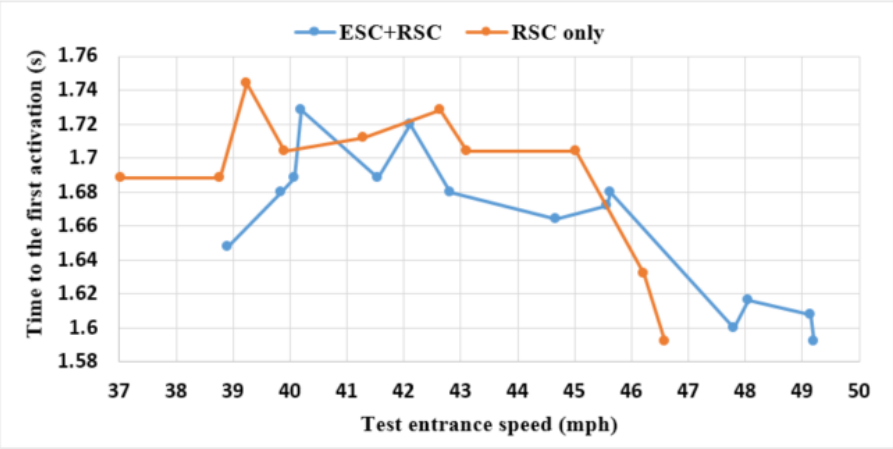

Figure 9-25. Time from test start to the first RSC activation for robot-operated J-turn tests with mixed ESC/RSC configurations.

Figure 9-26 shows the results of peak outrigger contact force for the robot-operated J-turn tests with mixed ESC/RSC configurations. The stock configuration resulted in the first contact at 41.5 mph, and thus, RSC-only, ESC-only, and ESC+RSC configurations

managed to increase the rollover speed by 3.5, 4.9, and 7.64 mph, respectively. Hence, the ESC+RSC configuration demonstrated better performance in terms of increasing rollover speed threshold, followed by the ESC-only configuration.

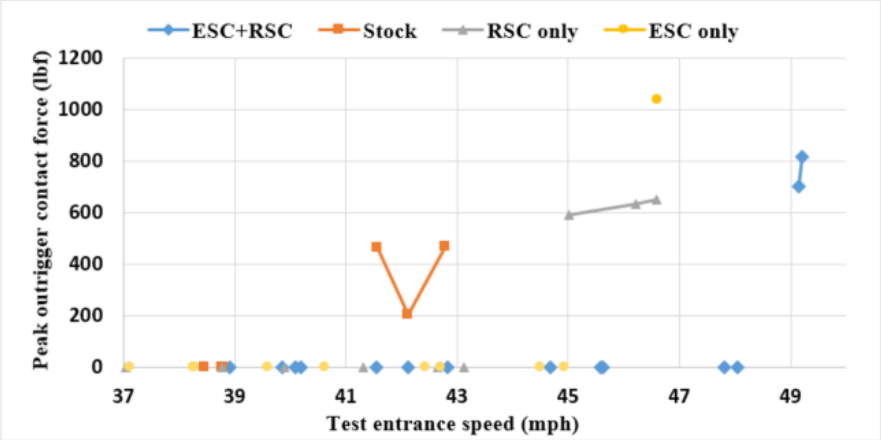

Figure 9-26. Peak outrigger contact force for robot-operated J-turn tests with mixed ESC/RSC configurations.

Results of the warning time for robot-operated J-turn tests with mixed ESC/RSC configurations are shown in Figure 9-27. Both the ESC+RSC and RSC-only configurations managed to activate at least one second before the outrigger contact, and the ESC+RSC provided an additional ~0.34s for warning time than the RSC-only configuration. Unfortunately, no clear conclusions can be drawn based on the comparison between the two configurations due to the fact that the RSC-only test stopped at 46.6 mph for safety concerns, and the ESC+RSC configuration did not experience its first outrigger contact until the speed reached 49.1 mph.

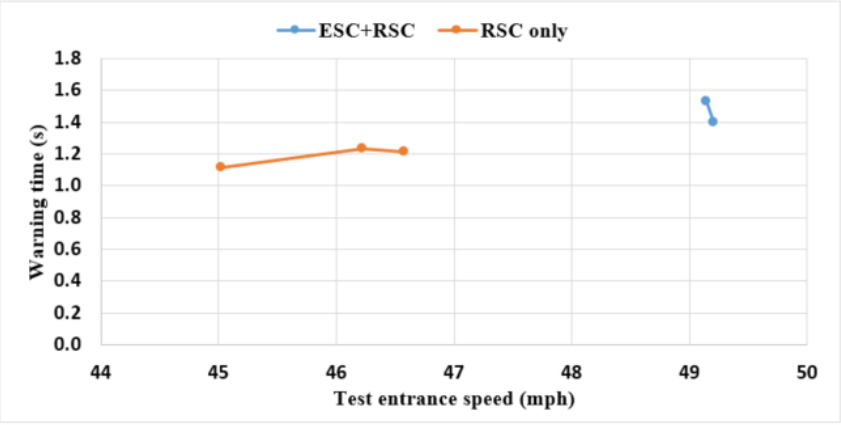

Figure 9-27. Warning time for robot-operated J-turn tests with mixed ESC/RSC configurations.

Figure 9-28 shows the results of peak articulation angles between the tractor and Trailer A for robot-operated J-turn tests with mixed ESC/RSC configurations. It clearly shows that the ESC-only configuration led to larger articulation angles in all cases, indicating a higher risk of jackknifing events. The RSC-only configuration resulted in the least angles in all the tests, which means it provided better yaw motion control. The ESC+RSC and stock test generally exhibited similar articulation motion between the tractor and the front trailer.

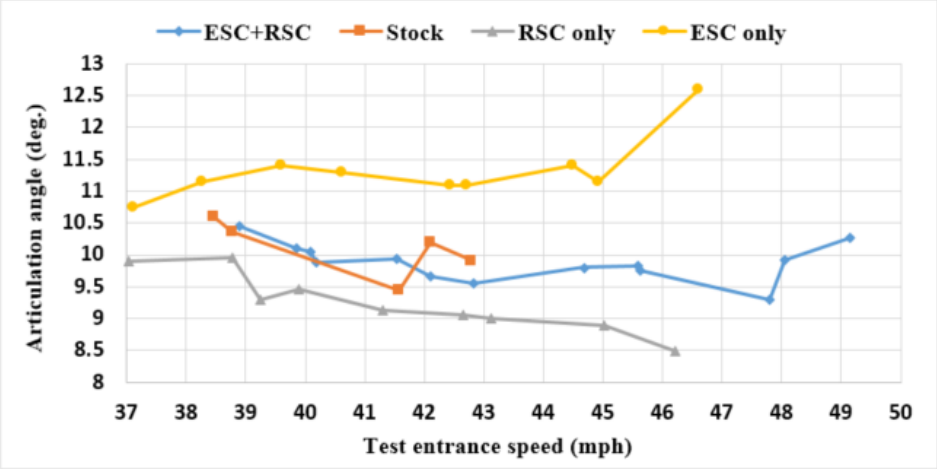

Figure 9-28. Articulation angle between the tractor and Trailer A for robot-operated J-turn tests with mixed ESC/RSC configurations.

Figure 9-29 shows the speed drop achieved by each configuration during the J-turn tests. Again, this speed drop indicates how much speed was reduced between the beginning of the test and the moment of outrigger contact. In general, all the configurations with stability control systems could lead to a speed drop over eight mph. The ESC-only demonstrated better speed reduction effectiveness than the RSC-only configuration in the 46.6-mph test, where the ESC-only provided double speed drop compared with the RSC-only case. This was due to the fact that the tractor used in this program was relatively heavy (20,600 lb) compared with the trailer (15,800 lb), and thus it was likely to skew the results in favor of the ESC system. Unfortunately, no additional conclusions could be drawn in comparing the performance of different configurations due to the limited number of outrigger contacts that happened at similar speeds.

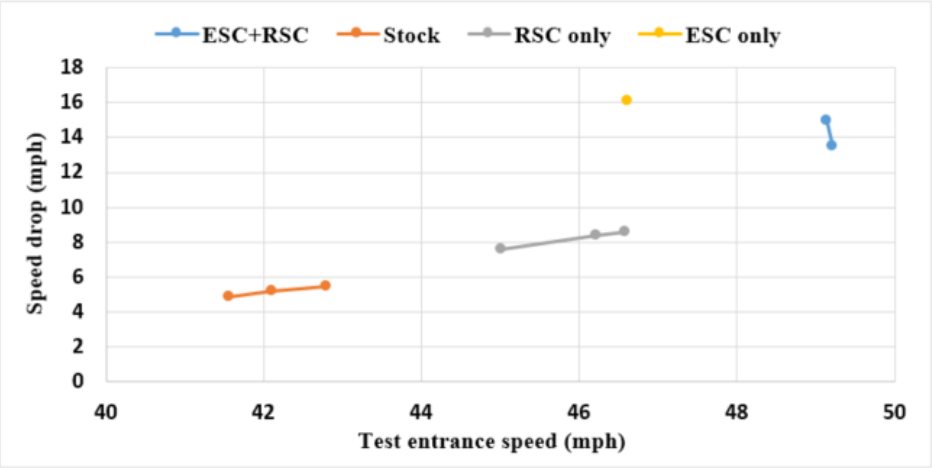

Figure 9-29. Speed drop for robot-operated J-turn tests with mixed ESC/RSC configurations.

9.3.3.2 SWD Tests

The peak outrigger contact forces and cones hit during the 0.5-Hz and 0.25-Hz SWD tests are summarized in Table 9-9 and Table 9-10, respectively. Considering the fact that most of the rollover events occurred at 90% and 100% steering for both SWD tests, the 90% and 100% SWD results are further explored with bar charts.

Table 9-9. Results of peak outrigger contact forces and cones for 0.5-Hz SWD tests with different ESC/RSC configurations.

Group #3 Mixed ESC/RSC Configurations							
Test #	Permutation	Steering (%)	Outrigger contact force (lbf)				Cones hit
			Front trailer		Rear trailer		
			Dri.	Pas.	Dri.	Pas.	
1	Stock (no RSC)	70	----	----	----	----	0
2	Stock (no RSC)	80	----	----	----	----	0
3	Stock (no RSC)	90	----	660.05	----	837.15	0
4	Stock (no RSC)	100	----	2255.43	----	1687.17	0
5	RSC only	70	----	----	----	----	0
6	RSC only	80	----	----	----	----	0
7	RSC only	90	----	----	----	----	0
8	RSC only	100	----	500.08	----	----	0
9	ESC only	70	----	----	----	----	0
10	ESC only	80	----	----	----	----	0
11	ESC only	90	----	----	----	----	0
12	ESC only	100	----	----	----	----	0
13	ESC + RSC	70	----	----	----	----	0
14	ESC + RSC	80	----	----	----	----	0
15	ESC + RSC	90	----	----	----	----	0
16	ESC + RSC	100	----	----	----	----	0

Table 9-10. Results of peak outrigger contact forces and cones for 0.25-Hz SWD tests with different ESC/RSC configurations.

Group #3 Mixed ESC/RSC Configurations							
Test #	**Permutation**	**Steering (%)**	**Outrigger contact force (lbf)**				**Cones hit**
			Front trailer		**Rear trailer**		
			Dri.	**Pas.**	**Dri.**	**Pas.**	
1	Stock (no RSC)	70	----	----	----	----	2
2	Stock (no RSC)	80	514.2	508.7	41.6	802.1	0
3	Stock (no RSC)	90	935.0	1225.7	799.6	2052.3	0
4	Stock (no RSC)	100	1399.7	1358.8	1695.2	2193.5	0
5	RSC only	70	----	----	----	----	3.5
6	RSC only	80	----	----	----	----	1.5
7	RSC only	90	----	----	----	----	0
8	RSC only	100	242.0	525.1	190.8	408.2	0
9	ESC only	70	----	----	----	----	3
10	ESC only	80	----	----	----	----	2.5
11	ESC only	90	417.3	----	----	----	0
12	ESC only	100	1068.7	1143.2	283.4	1080.9	0
13	ESC + RSC	70	----	----	----	----	3.5
14	ESC + RSC	80	----	----	----	----	1
15	ESC + RSC	90	----	----	----	----	2
16	ESC + RSC	100	----	----	----	----	1

Figure 9-30 compares the time from test start to RSC activation for the two RSC permutations. In general, the RSC systems activated at similar moments in the tests when the tractor ESC system was equipped. Therefore, the tractor ESC system did not affect the RSC activation timing in these tests.

Figure 9-31 shows test results of peak outrigger contact forces during 0.5-Hz and 0.25-Hz SWD tests with different ESC/RSC configurations. The tractor ESC system could prevent both trailers from rolling over during 0.5-Hz tests, whereas the RSC systems resulted in an outrigger contact on the front trailer's driver side during the 100% steering test, as shown in Figure 9-31(a) and (b). Two outriggers contacted the ground during the stock tests, indicating the truck would have rolled over in these scenarios without outriggers.

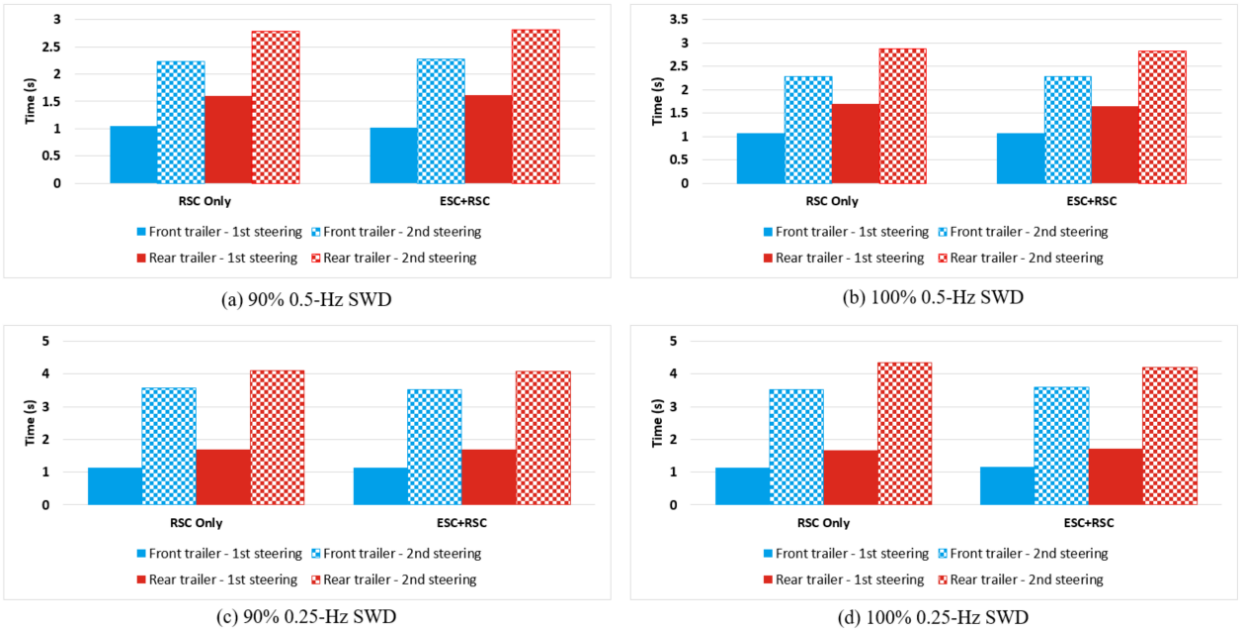

(a) 90% 0.5-Hz SWD

(b) 100% 0.5-Hz SWD

(c) 90% 0.25-Hz SWD

(d) 100% 0.25-Hz SWD

Figure 9-30. Time from test start to RSC activation for tests with different ESC/RSC configurations: (a) 90% 0.5-Hz SWD; (b) 100% 0.5-Hz SWD; (c) 90% 0.25-Hz SWD; and (d) 100% 0.25-Hz SWD.

Figure 9-31(c) indicates that the RSC systems managed to prevent both trailers from rolling over during 90% 0.25-Hz tests, whereas the tractor ESC led to an outrigger contact on the front trailer's driver side. For the 0.25-Hz tests with 100% steering, the "ESC+RSC" configuration managed to prevent both trailers from rolling over. This is the only case where the truck did not roll with this maneuver of all test runs conducted. Neither the RSC system nor the ESC system could single-handedly stop either trailer from rolling over during the tests, but the RSC system resulted in lighter outrigger contacts than the ESC system. This indicates that the RSC system could reduce the severity of this potential rollover event, although it failed to completely prevent it from happening.

In summary, the "RSC+ESC" configuration provided the best performance of all configurations tested in terms of preventing outrigger contact. The tractor ESC system and trailer RSC system obtained similar results. The truck experienced more and harder outrigger contacts without RSC or ESC systems ("RSC-Off" configuration), indicating that severe rollover accidents would have occurred in these scenarios if there were no outriggers installed.

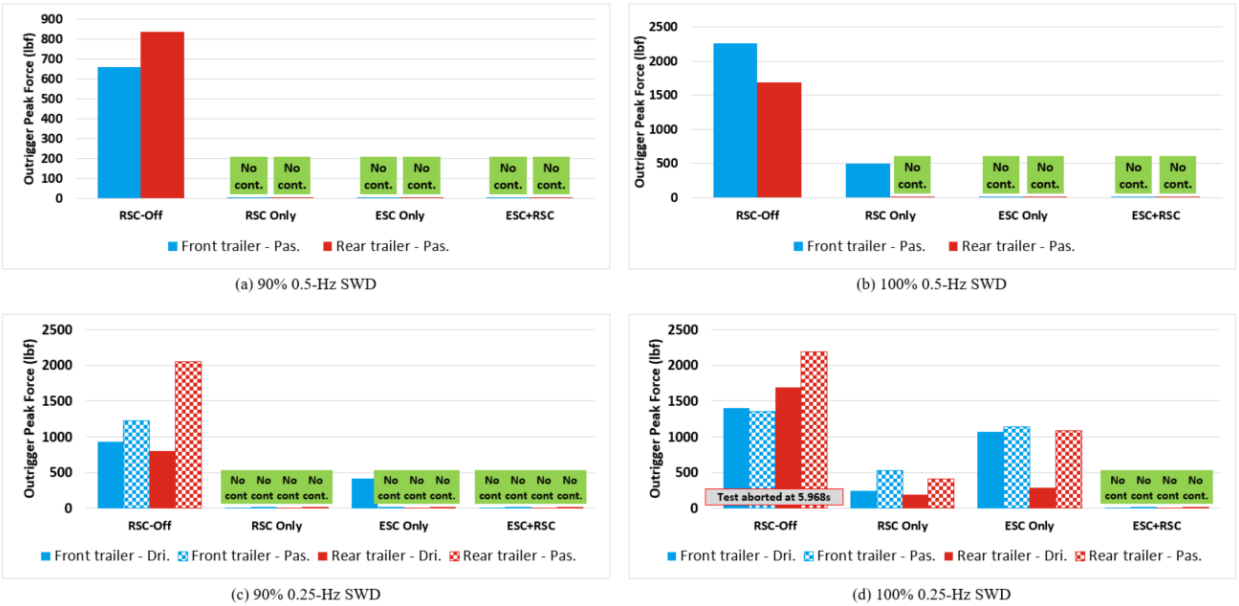

Figure 9-31. Peak outrigger forces for tests with different ESC/RSC configurations: (a) 90% 0.5-Hz SWD; (b) 100% 0.5-Hz SWD; (c) 90% 0.25-Hz SWD; and (d) 100% 0.25-Hz SWD.

Figure 9-32 shows the speed drop results for the 0.5-Hz and 0.25-Hz SWD tests with different ESC/RSC configurations. For the 0.5-Hz SWD tests, RSC systems managed to reduce ~7.5 mph before the front trailer's outrigger contacted the ground, whereas the ESC system successfully prevented all outrigger contacts, as shown in Figure 9-32(a) and (b). Figure 9-32(c) shows that the RSC system stopped the truck from rolling over during the 90% 0.25-Hz test, but the ESC system allowed one outrigger contact on the front trailer's driver side. For the 100% 0.25-Hz SWD test, the ESC system reduced more speed (~6.5 mph) than the RSC system before the front trailer's passenger-side outrigger contacted the ground, but the RSC system reduced more speed before the other three outriggers contacted. In general, the tractor ESC and trailer RSC systems achieved similar performance in terms of how much speed they reduced before outrigger contact. The ESC+RSC configuration should have reduced the most speed of all four configurations since it prevented both trailers from rolling over, but the results cannot be calculated here because the speed drop was defined as how much speed was reduced from test start to outrigger contact.

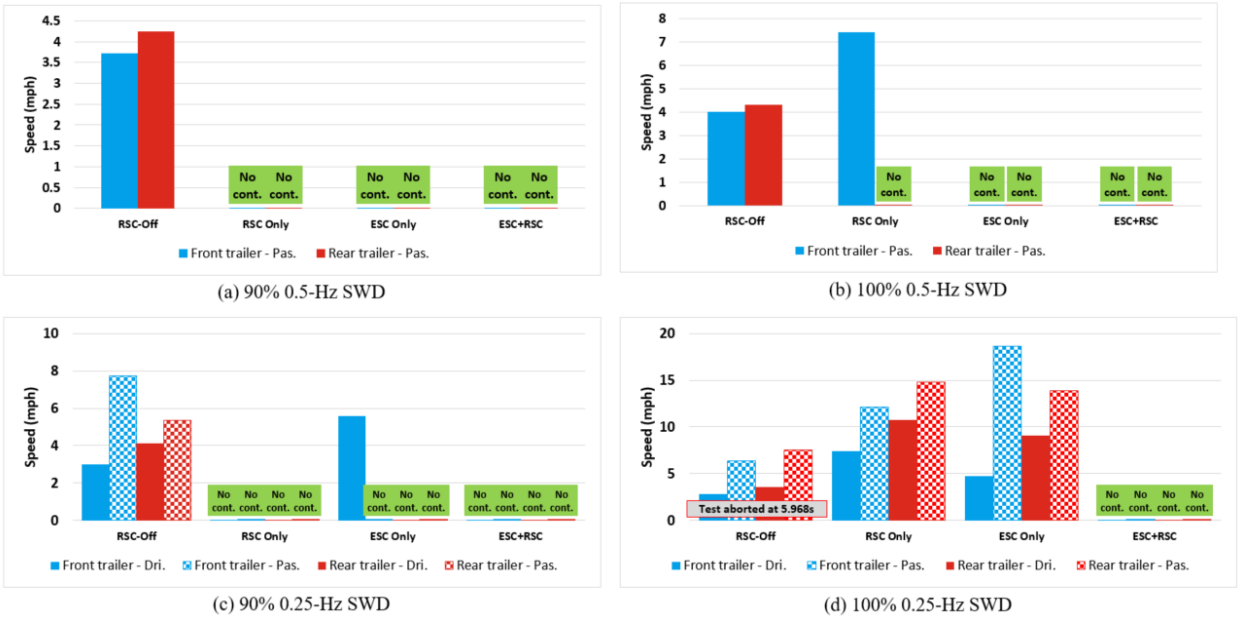

(a) 90% 0.5-Hz SWD

(b) 100% 0.5-Hz SWD

(c) 90% 0.25-Hz SWD

(d) 100% 0.25-Hz SWD

Figure 9-32. Speed drop for tests with different ESC/RSC configurations: (a) 90% 0.5-Hz SWD; (b) 100% 0.5-Hz SWD; (c) 90% 0.25-Hz SWD; and (d) 100% 0.25-Hz SWD.

Figure 9-33 shows the number of cones hit during the 0.5-Hz and 025-Hz SWD tests with different ESC/RSC configurations. The stock tests ("RSC-Off") hit the fewest cones, followed by the RSC tests, and the "ESC+RSC" configuration led to the most cones hit during the tests. This indicates that even though the "ESC+RSC" could successfully prevent a rollover accident, the stability control system introduced an excessive amount of understeer that might force the truck to plow through the obstacle it was trying to avoid. The trailer RSC system hit fewer cones than the tractor ESC system, but they had similar performance in terms of reducing outrigger contacts. Therefore, the RSC system is slightly more favored here than the ESC system.

Figure 9-34 illustrates the maximum articulation angles for the 0.5-Hz SWD tests with different ESC/RSC configurations. The ESC system introduced larger angles between the tractor and front trailer because it slowed down the front of the "chain." Results of the test at 70% steering with the RSC-only are not presented here since the actual test speed was lower than the designed test speed. The stock test resulted in larger front-to-rear-trailer angles due to more aggressive trailer yaw motion.

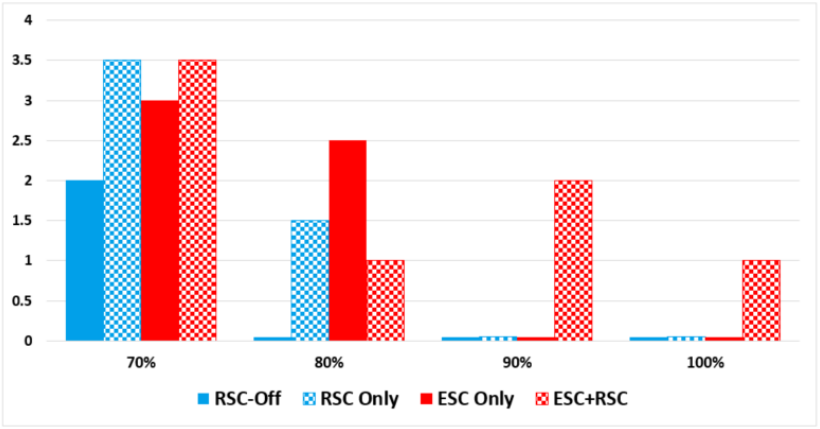

Figure 9-33. Cones hit during tests with different ESC/RSC configurations: (a) 90% 0.5-Hz SWD; (b) 100% 0.5-Hz SWD; (c) 90% 0.25-Hz SWD; and (d) 100% 0.25-Hz SWD.

In summary, the ESC system tended to cause the largest articulation angles of all four configurations tested, indicating a stronger likelihood of jackknifing. The other three configurations generally obtained similar results, but the truck with stock configuration had a slightly higher chance of experiencing larger articulation angles than the other two.

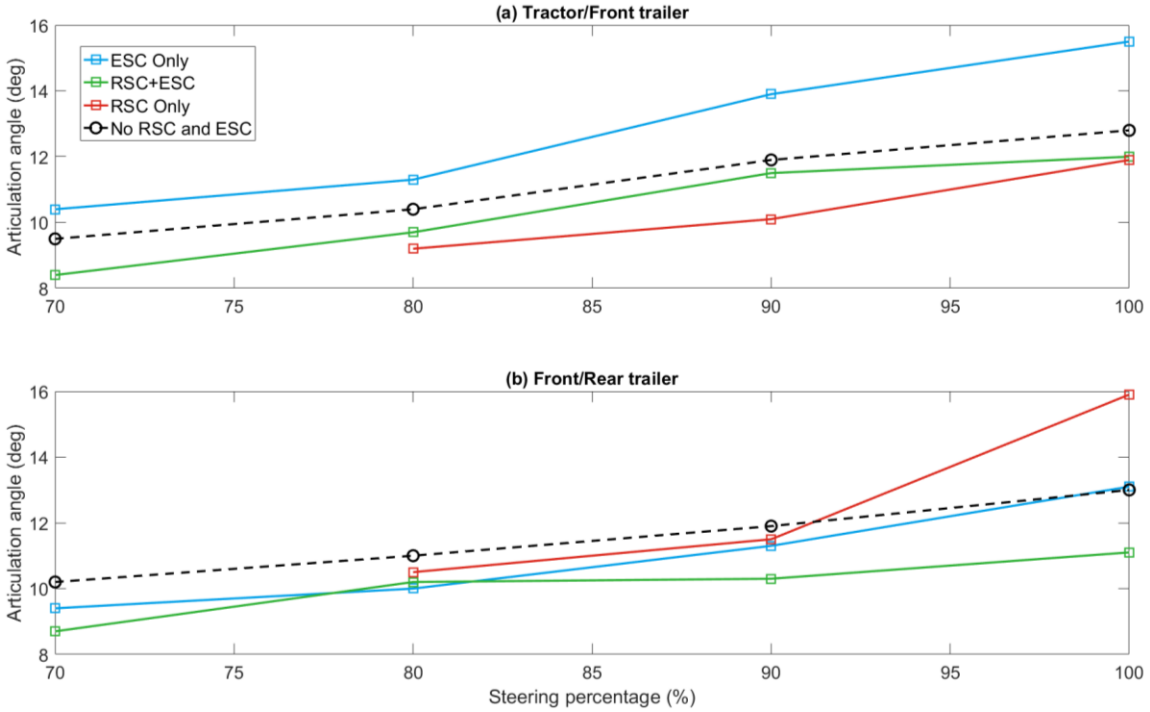

Figure 9-34. Peak articulation angles for 0.5-Hz SWD tests with different ESC/RSC configurations: (a) articulation angle between tractor and front trailer; and (b) articulation angle between front and rear trailer.

Figure 9-35 illustrates articulation angles for the 0.25-Hz SWD tests with different ESC/RSC configurations. The ESC system led to both larger tractor-to-trailer and trailer-

to-trailer angles in most tests, indicating a higher likelihood of jackknifing events. The only exception occurred during the test with 100% steering, where the stock test resulted in a larger tractor-to-trailer articulation angle. This was due to the fact that the steering input was so aggressive that the tractor lost traction and started to oversteer. Otherwise, the "RSC+ESC," "RSC Only," and stock configurations have similar results for both angles.

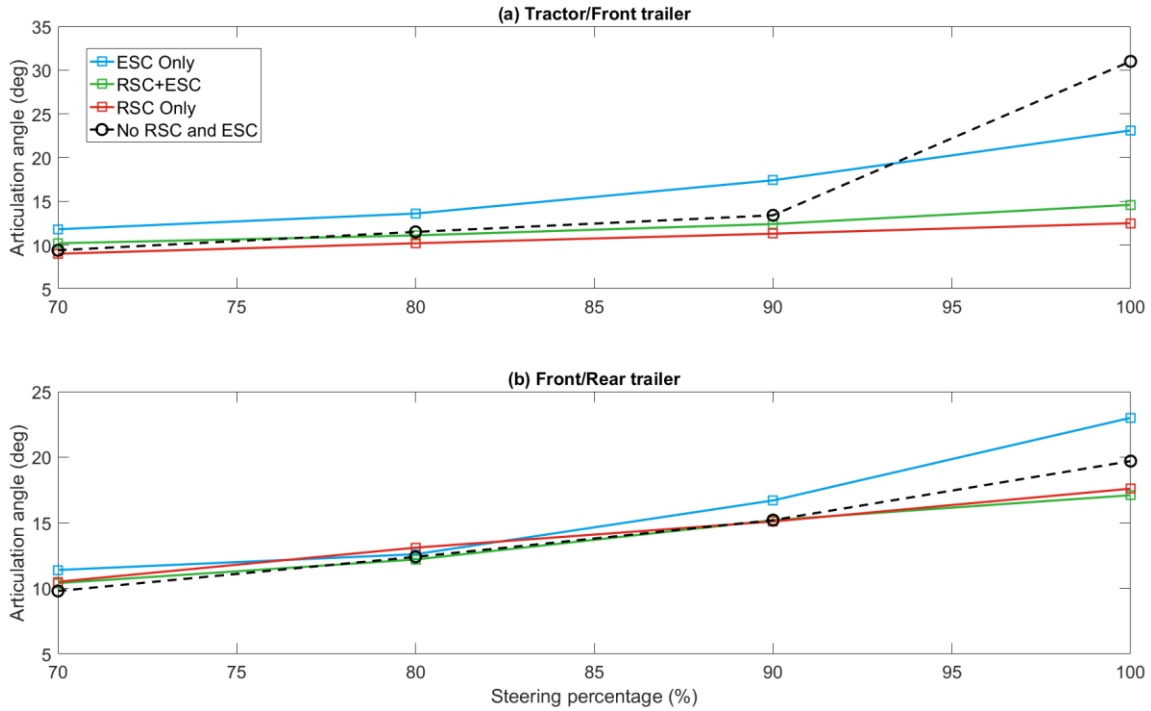

Figure 9-35. Peak articulation angles for 0.25-Hz SWD tests with different ESC/RSC configurations: (a) articulation angle between tractor and front trailer; and (b) articulation angle between front and rear trailer.

9.3.3.3 DLC Tests

The results of the peak outrigger contact forces for the DLC tests are summarized in Table 9-11. The results show that the "RSC-only" and "ESC+RSC" configurations successfully prevented the truck from rolling over during all DLC tests conducted here. The ESC only allowed one outrigger contact at 60 mph.

Figure 9-36 illustrates articulation angles for the DLC tests with different ESC/RSC configurations. The ESC-only tests exhibit larger articulation angles in most cases, which is consistent with the SWD test results. The other three configurations led to similar results, where the difference was normally within one degree.

Table 9-11. Results of peak outrigger contact forces and cones for DLC tests with different ESC/RSC configurations.

Group #3 Mixed ESC/RSC Configurations						
Test #	Permutation	Speed (mph)	Outrigger contact force (lbf)			
			Front trailer		Rear trailer	
			Dri.	Pas.	Dri.	Pas.
1	Stock (no RSC)	57	----	----	----	1017.3
2	Stock (no RSC)	58	----	----	----	----
3	Stock (no RSC)	59	----	----	----	----
4	Stock (no RSC)	60	----	----	645.0	1846.8
5	RSC only	57	----	----	----	----
6	RSC only	58	----	----	----	----
7	RSC only	59	----	----	----	----
8	RSC only	60	----	----	----	----
9	ESC only	57	----	----	----	----
10	ESC only	58	----	----	----	----
11	ESC only	59	----	----	----	----
12	ESC only	60	----	----	----	858.6
13	ESC + RSC	57	----	----	----	----
14	ESC + RSC	58	----	----	----	----
15	ESC + RSC	59	----	----	----	----
16	ESC + RSC	60	----	----	----	----

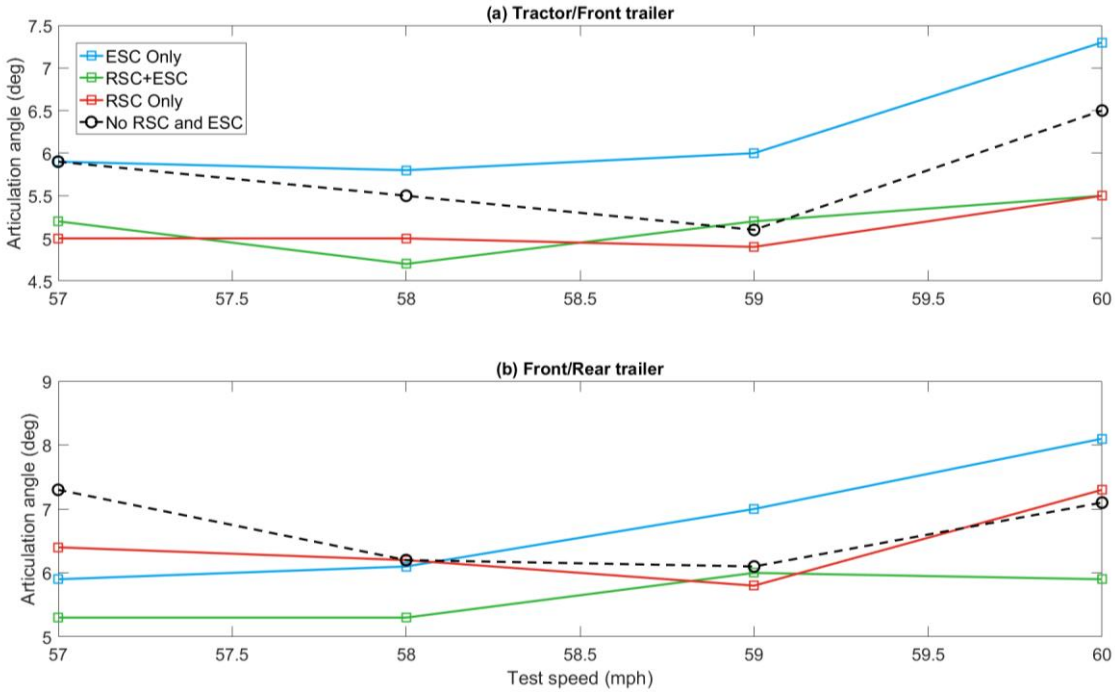

Figure 9-36. Peak articulation angles for DLC tests with different ESC/RSC configurations: (a) articulation angle between tractor and front trailer; and (b) articulation angle between front and rear trailer.

9.4 Conclusions and Summary

This chapter introduced all the tests conducted to examine the effect of configuration changes on the dynamic stability of a 28-ft A-train double. Eight permutations, which were divided into three groups, were tested with four maneuvers, including: robot-operated J-turn, 0.5-Hz SWD, 0.25-Hz SWD, and DLC. The results were presented and discussed with respect to the groups and maneuvers. The conclusions will be summarized in the following sections.

9.4.1 Robot-Operated J-turn Tests

The performance of each configuration is summarized and compared in terms of the speed threshold improved, as shown in Figure 9-37. For the mixed RSC configurations, installing RSC systems on both trailers would achieve the best performance (8.3% improvement), followed by having one RSC unit on the front trailer (6.0% improvement). The ESC+RSC configuration led to the highest speed threshold improvement, which is 18% better than the stock configuration. Even though the ESC-only configuration improved the threshold by 12%, it introduced a significant amount of articulation motion to the truck, which significantly increased the risk of jackknifing events. According to the results, an empty rear trailer would decrease the roll stability of the test truck, indicated by a -5.6% "improvement." Even though the truck was equipped with the RSC systems on both trailers, an empty rear trailer would reduce its improvement to 1.3%, whereas the same RSC systems would achieve 8.3-% improvement with a loaded rear trailer.

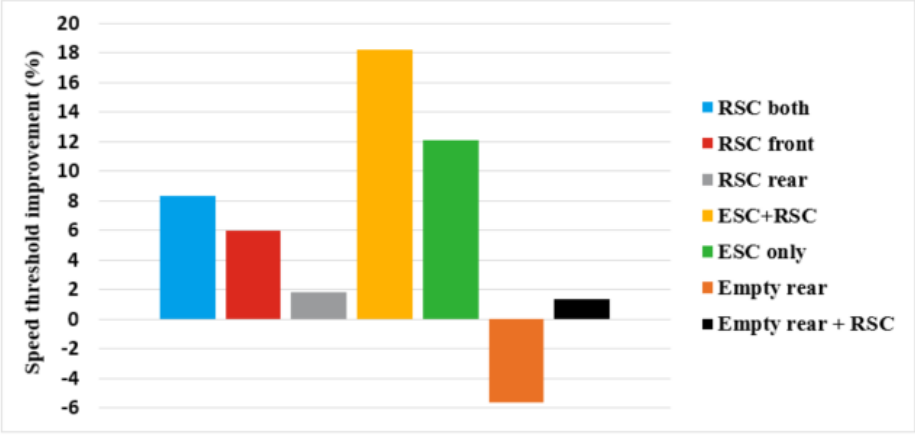

Figure 9-37. Speed threshold improvement achieved by each configuration for the robot-operated J-turn tests.

9.4.2 SWD Tests

Considering that the test truck hit a similar number of cones during both the 0.5- and 0.25-Hz SWD tests in this set of tests, the criterion of maneuverability as applied in Chapter 8 is not applicable here because it would show nothing but very similar performance and some important information would be missed, such as articulation angles. Therefore, the conclusions that were drawn based on the SWD test results are summarized with respect to the groups, which included:

- Different Rear Trailer Load Conditions:
    - Different rear trailer load conditions would not affect the activation timing of the RSC systems;
    - RSC systems achieved better performance in preventing rollover events with a loaded rear trailer, indicated by obtaining higher speed drop and reducing the chance of outrigger contact; and
    - RSC systems could also reduce the risk of jackknifing events during dynamic maneuvers.
- Mixed RSC Configurations:
    - The activation of one RSC system would not be affected by the system installed on the other trailer, except when the unit that activates first manages to significantly reduce the truck rollover tendency before the other unit activates, which is unlikely and never occurred in this test program;
    - If only one RSC unit is available, installing it on the front trailer would achieve better stability control performance;
    - Equipping both trailers with the RSC systems provided the best performance in all mixed RSC configurations; and
    - The RSC-front configuration could better reduce the articulation angles between the tractor and front trailer than the RSC-rear configuration, whereas the latter one could achieve better articulation angle attenuation between the two trailers.

- Mixed ESC/RSC Configurations:
    - The tractor-based ESC system generally did not affect the activation timing of the trailer-based RSC system in the SWD tests;
    - The ESC+RSC configuration resulted in the best performance of preventing outrigger contacts of all the SWD tests conducted. However, it also introduced the most understeer to the truck; and
    - The ESC-only and RSC-only configurations generally obtained similar performance in truck roll stability enhancement, but only installing an ESC on the tractor would greatly increase the likelihood of jackknifing events.

9.4.3 DLC Tests

In Chapter 8, the DLC tests exhibited contradictory results caused by the driver performance variance and RSC system self-tuning. In this set of tests, DLC maneuvers were further tested to evaluate their applicability in such a testing program, where different systems would be compared side by side. In order to solve the issues mentioned above, two procedures were undertaken in the DLC tests, including (1) repeating each DLC multiple times, and (2) turning on the RSC system right before the test started and then turning it off after the test was completed in order to minimize the effect of RSC self-tuning on the test results. However, even though more rational DLC test results were acquired, there is still contradiction in the results. Considering that it was a professional test driver who operated the test truck, and that he had already been familiar with the truck through hundreds of test runs, it could be concluded that DLC maneuvers are not suitable for objective tests where different systems should be compared, especially when the performance difference of the systems is insignificant. Instead, it is suggested that DLC maneuvers be used for system tuning or other subjective tests where the drive feedback is weighed heavily in the evaluation process. If DLC maneuvers are required in objective tests for some reason, then test at each speed should be repeated at least five times while all the other factors remain the same.

9.4.4 Summary

The conclusions drawn from this set of tests can be summarized as follows:

- The RSC systems could improve the truck roll stability without introducing significant additional understeer or jackknifing risk;
- If only one RSC unit is available, installing it on the front trailer would achieve better performance;
- A combination of the tractor-based ESC system and the trailer-based RSC system would greatly improve the truck roll stability, but it would also introduce a considerable amount of understeer to the truck;
- The tractor-based ESC system exhibited similar performance as the trailer-based RSC systems, but the ESC system significantly increased the likelihood of jackknifing events when dynamic maneuvers were performed; and
- An empty rear trailer could decease the roll stability of the 28-ft A-train tested especially with J-turn maneuvers, and it also diminished the performance of the onboard RSC unit.

Chapter 10 – Conclusions and Recommendations

10.1 Summaries and Conclusions

A comprehensive evaluation of roll and yaw stability of Class 8 heavy trucks with single and dual trailers in city and highway conditions was conducted. Commercial vehicles fundamentally behave differently in city driving conditions, such as negotiating a roundabout, than at high speeds during highway driving conditions. In order to closely examine each, this study offered two distinct evaluations of commercial vehicles: 1) low-speed driving roundabouts, representative of city driving; and 2) high-speed lane change and evasive maneuvers, typical of highway driving. The summaries and conclusions of these two studies are provided in the following sections.

10.1.1 Heavy Truck Low-Speed Stability Evolution

Modern roundabouts, which are commonly used in urban settings with increasing frequency, are unfortunately one of those places in cities that bring challenges to heavy truck roll stability. A vehicle needs to negotiate successive tight reverse curves to travel through a roundabout, requiring maneuvers that can result in large lateral accelerations which may then lead to vehicle rollovers. Moreover, some cross-sectional geometric designs of roundabouts, such as the roadway's cross-slope and truck apron, may additionally increase the likelihood of rollover. Therefore, a simulation-based study was conducted in TruckSim to closely examine the effect of geometric parameters of roundabouts, as well as truck load conditions and configurations on roll stability in roundabouts.

In Chapter 3, five truck models were developed in TruckSim, including a single-unit truck, a WB-67 semi-truck, an A-train with two 28-ft trailers, and another A-train with two 40-ft trailers. The WB-67 semi-truck was selected as the baseline truck model since it is the most common truck configuration that is operated on U.S. roads. In addition, five comprehensive roundabout models were also developed, with considerations of inscribed circle diameters (ICD), number of lanes, entry curve radius, exit radius, roadway width, truck apron, crowned roadway, and roundabout tilt. These geometric parameters were all identified as potential factors contributing to heavy truck rollover accidents in roundabouts.

A single-lane roundabout, which had a truck apron and a 2% outward cross-slope on the circulatory roadway, was selected as the baseline roundabout model.

Five potential factors that affect commercial truck roll stability in roundabouts were identified and evaluated, including (1) circulatory roadway cross-section, (2) roundabout tilt, (3) truck configuration, (4) truck apron geometry, and (5) truck load condition. Accordingly, 83 individual cases were designed in total to form a parametric study for evaluating the effects of these factors. This parametric study also considered different maneuvers that could be performed to travel through a single-lane or a multilane roundabout, and each maneuver contained multiple paths that a vehicle could follow to complete the maneuver. All the paths were examined by an experienced truck driver in order to assure they closely replicated real-world scenarios.

In Chapter 6, a parametric study was conducted in TruckSim and a rollover index (RI) was used as the metric to indicate the likelihood of rollover. First, a preliminary case study was completed to compare the roll stability between the tractor and trailer of each truck configuration, where the results indicated that the rearmost trailing unit tended to experience a larger RI than the leading unit. Therefore, the roll stability of each articulated truck configuration was determined to be represented by the rearmost trailer unit.

The effect of circulatory roadway cross-section on truck roll stability was analyzed. For right-turn movements, the crowned cross-section caused the truck to have relatively less lateral stability than the sloping cross-section. This occurred because, for the crowned roundabout, the left edge of the inner two-thirds of the roadway was lower than the right edge. When the truck occupied the lanes to make a right turn, its left wheels ran on the inner, lower part of the roadway, increasing the truck's tendency to lean to the left side and thereby reducing its lateral stability. However, the RIs for both the sloping and crowned roundabout were low, indicating a low likelihood of rollover. For the through-movements and left turns, generally the crowned cross-section had a smaller maximum RI and lower likelihood of rollover than the sloping cross-section. The only exception appeared when trucks followed the right-lane path to perform through-movements. This occurred because the inner two-thirds of the crowned roadway had a 2% inward cross-slope, whereas the outer one-third section had a 2% outward cross-slope. When a truck entered the

roundabout in the middle of the right lane, it shifted to the left side and occupied both lanes to perform the first right turn, where the truck ran on the inner section with an inward cross-slope. However, when it shifted back to the right edge to start circulating the central island, it needed to travel back to the outer section with an outward cross-slope. Such quick opposite road excitation resulted in a rocking motion that increased the RI. When the trailer rear tires moved onto the truck apron, the RI was significantly higher than when the truck did not move onto the truck apron. This was mainly because the apron's outward slope, as well as the curb height, caused the truck to lean to the outside in the direction of the centrifugal forces against the trailer, and was also due to transient dynamics caused by the truck moving onto and off of the apron. If the truck did not straddle lanes to make a through-movement or left turn, the crowned roadway resulted in a lower likelihood of rollover than the 2% sloping roadway.

Next, the effect of roundabout tilt on truck roll stability was studied. For right turns, the positive (outward) tilted slopes resulted in better truck lateral stability than the negative (inward) tilted slopes. The opposite effect of tilt occurred for through-movements and left turns. At the roundabout entry and exit, negative (inward) tilt increased RI, but in the circulatory roadway, negative (inward) tilt reduced RI. This outcome presents a challenge in terms of designing a roundabout. A positive (outward) tilt would reduce the rollover index at the entry and exit, but a negative (inward) tilt would reduce the RI in the circulatory roadway. For through-movements and left turns, the RI peaks in the circulating roadway were larger than those at the entry and exit, so moderately tilting the roundabout negatively (inward) would increase truck lateral stability in the areas where it experienced the highest RI. Several elements interact with roundabout tilt to affect truck lateral dynamics, but in general, negative (inward) tilting resulted in better truck lateral stability.

As for the effect of truck configuration on truck roll stability in roundabouts, a single-unit truck was more stable than the other three configurations−a WB-67 semi-truck, a 28-ft double trailer, and a 40-ft double trailer−because its maximum RI was always below 0.6. Even though a 28-ft double trailer was longer than a WB-67 semi-truck, each of the trailers was shorter than the semi-truck's single trailer, and the hitch connection between them allowed the double-trailer configuration to better conform to the roundabout. Additionally,

the longer wheelbase and additional hitch connection meant that the double-trailer configuration's second trailer circulated at a lower speed than the semi-truck's trailer, resulting in lower lateral accelerations. Therefore, the 28-ft double trailers exhibited the second-best roll stability in roundabouts. Although the 40-ft double trailers also had a double-trailer configuration, the long wheelbase required them to use a truck apron for performing left turns in both single-lane and two-lane roundabouts when following the left-lane path. Therefore, the 28-ft double trailer exhibited high maximum RIs in the single-lane roundabout (0.91) and two-lane roundabout (0.76). The WB-67 semi-truck was more likely to exhibit the greatest maximum RI, indicating the strongest likelihood of rollover, compared to the other three configurations.

The truck apron geometry was also identified as a contributing factor to truck rollover accidents in roundabouts. The results indicate that the trucks exhibited similar maximum RIs when encountering truck aprons with cross-slopes from 6% to flat. However, a lower truck apron curb height could reasonably increase the truck roll stability in roundabouts, in terms of reducing maximum RIs. To be specific, the maximum RI was attenuated from 0.92 (baseline truck apron) to 0.79 when the apron curb height was reduced from 3 in. to 1 in.

Finally, the effect of load condition on truck roll stability in roundabouts was examined. The results indicate that the half-load truck presented the best roll stability in roundabouts, indicated by the smallest maximum RI it exhibited in each case as compared to the other load conditions. The empty truck showed higher maximum RIs than the half-load truck because the empty truck had lower inertia to hold it down against the ground, compared to the half-load and full-load trucks. Therefore, it was more sensitive to the dynamic road input, such as the rapid changes in side-to-side road elevation or encountering/leaving a truck apron, resulting in RI spikes. Even though these RI spikes experienced by the empty trucks had large values that even exceeded the limit of 0.8, they occurred in a short period of time (less than 200ms) during the transient dynamics, which did not necessarily mean the empty truck experienced a strong likelihood of rollover. Based on our experience, in general, the risk of rollover increases significantly when RI exceeds 0.8 for any prolonged period, such as 200 ms. In addition, the fifth-wheel coupling between the tractor and trailer

allows very limited roll freedom (~±1°). Hence, the tractor can provide a resistant roll moment in the opposite direction of the trailer's roll motion. Obviously, an empty trailer requires a relatively smaller roll moment from the tractor to hold it from rolling over.

The full-load truck exhibited greater maximum RIs than the other truck configurations when performing through-movements and left turns in both the single-lane and two-lane roundabouts because it had a heavier cargo and a higher CG. Although the empty truck had larger maximum RIs for right turns than the full-load truck, they were all under 0.52, indicating safe maneuvers through roundabouts. In summary, the full-load truck, as perhaps intuitively clear, posed a higher risk of rollover than the half-load and empty trucks.

10.1.2 Testing and Evaluation of Dynamic Stability of a 28-ft A-train Double and Electronic Stability Control Systems in Highway-driving Conditions

The second study conducted in this dissertation was to evaluate the dynamic stability of a 28-ft A-train double with different electronic stability control systems in highway-driving conditions by testing.

An overview was provided in Chapter 5 to review the critical elements in dynamic stability of a tractor with double trailers in the A-train configuration, where four factors were identified and briefly discussed. Chapter 6 presented the simulation studies conducted to determine the directional dynamics of A-train doubles, based on a five-DOF yaw-plane model and a single-DOF roll-plane model, which were validated against another vehicle model developed in TruckSim. The directional dynamic analyses were then conducted based on the validated mathematical models to investigate the effect of two identified factors–traveling speed and rear trailer load conditions−on rearward amplification and the stability of the vehicle system. Simulation results indicated that the traveling speed significantly affected the truck dynamics and stability. More specifically, higher traveling speeds would 1) increase rearward amplification ratios on both trailers, where the rear trailer's ratio increased faster than that of the front trailer; and 2) also decrease the stability of the vehicle system. As for the rear trailer load conditions, the results suggested that a heavier rear trailer tended to increase its own rearward amplification ratio and also reduced the stability of the entire vehicle system.

Chapter 7 first presented an overview of the test-based studies to examine the dynamic stability of a 28-ft A-train double with electronic stability control systems, followed by the corresponding test preparation work and preliminary tests conducted at the CVeSS facility and MLPG testing track. Findings derived from the preliminary tests included: 1) two types of jackknifing events could potentially occur between the front and rear trailers: "trailer jackknifing" and "dolly jackknifing;" 2) the 28-ft A-train double tested had a higher rollover threshold (~0.7g) compared to that of a typical fully-loaded WB-67 semi-truck (~0.4g); and 3) the proposed testing methodology could successfully excite the truck to exhibit its dynamic characteristics and acquire data that were necessary for conducting comprehensive evaluations of the dynamic stability.

Chapter 11 presented and analyzed the test results of a 28-ft A-train double with trailer-based RSC systems. Five test maneuvers were performed, including driver-operated J-turns, robot-operated J-turns (RSM), 0.5-Hz SWD, 0.25-Hz SWD, and DLC maneuvers.

For the driver-operated J-turn tests, the RSC system managed to reduce the peak outrigger contact force by 80% and 61% for tests at 39 and 40 mph, respectively. It also increased the threshold speed for rollover by ~5%. For the robot-operated J-turn tests, the RSC achieved better performance by increasing the rollover speed to 45 mph, whereas the truck without the RSC system experienced its first outrigger contact event at 41 mph, and the test had to be aborted at 43 mph due to safety concerns. In summary, the RSC system applied here could considerably enhance the truck roll stability during the two J-turn tests, which increased the truck rollover speed by 5%~15%, and reduced the peak contact force by 61%~80% when rollover accidents occurred.

Maneuverability improvement is used to evaluate the performance of the RSC system tested during the SWD tests, which is defined as how much additional steering an RSC system could provide to the truck without rolling over as compared to stock tests. For instance, if a truck rolls over at 70% steering in stock tests but rolls over at 90% steering in RSC tests, it means that the RSC system could improve the maneuverability so that the driver can steer more to avoid an object without rolling over. Results indicated that the RSC system managed to increase the maneuverability of the test truck by ~33.3% in the 0.5-Hz SWD tests and ~11.5% in the 0.25-Hz SWD tests. Therefore, the RSC system

successfully improved the truck maneuverability, which means the truck equipped with the system could withstand more aggressive steering input without rolling over as compared to the stock truck. Such an improvement could potentially reduce the number of truck rollover accidents triggered by obstacle-avoidance maneuvers or those performed when taking a highway ramp at excessive speeds.

Contradictory results were observed in the DLC tests, where the test truck experienced less outrigger contacts as the test speed increased, exhibiting a trend that the later a test was conducted, the less outrigger contact would be experienced. Two potential reasons had been identified. The first was that the test driver performed better and led to smoother truck dynamics as he practiced more tests. Thus, the driver gradually refined his steering after completing the RSC tests at low speeds (i.e. 52, 54 mph), and maneuvered better in the high-speed RSC tests (i.e. 56 mph) as well as the stock tests conducted after the RSC tests. The other potential reason is the RSC system self-tuning function. The RSC system began acquiring truck information after the truck was started. Hence, more information was collected by the RSC systems as more tests were conducted, and the RSC systems could be re-tuned to obtain more accurate activation threshold and timing. This could also contribute to better results for the tests conducted later in the test sequence. In order to solve this issue, each DLC test should be repeated multiple times, and the test truck should be turned off and on after each test run for rebooting the RSC systems. However, this would significantly increase the number of test runs and also require longer track hours. Therefore, DLC is found not to be ideal for objective tests where different systems should be compared. Instead, it is suggested for system tuning or other subjective tests where the driver feedback is weighed heavily in the evaluation process.

Additional characteristic dynamic behavior of trucks in the A-train configuration were also observed. First of all, the rearward amplification phenomenon, which is an inherent property possessed by vehicles with multiple trailing units, was well-substantiated during the SWD and DLC tests. The excessive lateral accelerations triggered by rearward amplification would not only increase the likelihood of rollover, but also introduce other safety issues. For instance, the rear trailer swung out to the outside of the turn during a 55-mph DLC test, shown in Figure 8-26. Even though the rear trailer did not roll over in this

case, it posed great risks of colliding with other vehicles traveling in the adjacent lane. The other significant dynamic behavior that could potentially lead to safety issues is the considerable delay between the driver's steering input and the rear trailer's response. This behavior was directly realized by the driver and testers who stayed in the tractor cab during tests, where they felt impact loads transmitted from the trailer to the tractor after they thought the test had been completed. For instance, the outrigger on the rear trailer passenger side contacted the ground ~1s after the steering profile had been completed during a 0.25-Hz SWD test at 80% steering, as shown in Figure 8-27. This delayed response of the rear trailer was also observed in the DLC test mentioned earlier. The rear trailer swung out to the right side after the tractor had exited the testing course and started to move straightforward. Unlike in the SWD test where the driver could directly feel the contact of the rear trailer, the driver did not realize the excessive lateral motion of the rear trailer during the DLC tests until being told. This was due to the fact that the pintle hitch coupling does not provide constraints for relative yaw motion between two jointed vehicle units. In summary, the delayed response of the rear trailer poses safety issues to trucks in the A-train configuration because it requires drivers to reasonably predict the rear trailer response before maneuvering the truck. Otherwise, the rear trailer would have already rolled over or lost control before the driver could realize it.

Chapter 12 presented and discussed the test results for evaluating the effect of configuration changes on the dynamic stability of a 28-ft A-train double. The same trailer-based RSC system was further tested, together with a tractor-based ESC system and different rear trailer load conditions. Eight proposed permutations were divided into three groups, as summarized in Table 10-1. Four test maneuvers were performed, including robot-operated J-turn, 0.5-Hz SWD, 0.25-Hz SWD, and DLC. The driver-operated J-turn maneuver was not applied in this set of tests due to the limited track time.

The results of the robot-operated J-turn tests indicated that for the mixed RSC configurations, installing RSC systems on both trailers would achieve the best performance (8.3% improvement), followed by having one RSC unit on the front trailer (6.0% improvement). The ESC+RSC configuration led to the highest speed threshold improvement, which is 18% better than the stock configuration. Even though the ESC-

only configuration improved the threshold by 12%, it introduced a significant amount of articulation motion to the truck, which significantly increased the risk of jackknifing events. According to the results, an empty rear trailer would decrease the roll stability of the test truck, indicated by a -5.6% "improvement." Even though the truck was equipped with the RSC systems on both trailers, an empty rear trailer would reduce its improvement to 1.3%, whereas the same RSC systems would achieve an 8.3% improvement with a loaded rear trailer.

Table 10-1. Eight permutations were divided into three groups for comparison.

#	Group	Permutation
1	Different Rear Trailer Loading Configurations	Stock (no RSC)
		RSC on both trailers
		Empty rear trailer (no RSC)
		Empty rear trailer + RSC
2	Mixed RSC Configurations	Stock (no RSC)
		RSC on front trailer only
		RSC on rear trailer only
		RSC on both trailers
3	Mixed ESC/RSC Configurations	Stock (no RSC)
		RSC on both trailers
		ESC (tractor only)
		RSC + ESC (on tractor)

For the 0.5- and 0.25-Hz SWD tests, the conclusions are summarized with respect to the groups, which included:

- Different rear trailer load conditions:
    - Different rear trailer load conditions would not affect the activation timing of the RSC systems;
    - RSC systems achieved better performance in preventing rollover events with a loaded rear trailer, indicated by obtaining higher speed drop and reducing the chance of outrigger contact; and
    - RSC systems could also reduce the risk of jackknifing events during dynamic maneuvers.

- Mixed RSC Configurations:
    - The activation of one RSC system would not be affected by the system installed on the other trailer, except when the unit that activates first manages to significantly reduce the truck rollover tendency before the other unit activates, which is unlikely and never occurred in this test program;
    - If only one RSC unit is available, installing it on the front trailer would achieve better stability control performance;
    - Equipping both trailers with the RSC systems provided the best performance in all mixed RSC configurations; and
    - The RSC-front configuration could better reduce the articulation angles between the tractor and front trailer, whereas the RSC-rear configuration could achieve better attenuation for the articulation angles between the two trailers.
- Mixed ESC/RSC Configurations:
    - The tractor-based ESC system generally did not affect the activation timing of the trailer-based RSC system in the SWD tests;
    - The ESC+RSC configuration resulted in the best performance of preventing outrigger contacts of all the SWD tests conducted. However, it also introduced the most understeer to the truck, as expected; and
    - The ESC-only and RSC-only configurations generally obtained similar performance in truck roll stability enhancement, but installing an ESC only on the tractor would greatly increase the likelihood of jackknifing events.

In Chapter 8, the DLC tests exhibited contradictory results caused by the driver performance variance and RSC system self-tuning. In this set of tests, DLC maneuvers were further tested to evaluate their applicability in such a testing program, where different systems would be compared side by side. In order to solve the issues mentioned above, two procedures were undertaken in the DLC tests, including (1) repeating each DLC multiple times, and (2) turning on the RSC system right before the test started and then turning it off after the test was completed, in order to minimize the effect of RSC self-

tuning on the test results. However, even though more rational DLC test results were acquired, there was still contradiction in the results. Considering that it was a professional test driver who operated the test truck, and that he had already been reasonably familiar with the truck through hundreds of test runs, it could be concluded that DLC maneuvers are not suitable for objective tests where different systems should be compared, especially when the performance differences of the systems are insignificant. Instead, it is suggested that DLC maneuvers be used for system tuning or other subjective tests where the driver feedback is weighed heavily in the evaluation process. If DLC maneuvers are required in objective tests for some reason, the test at each speed should be repeated at least five times while all the other factors remain the same.

The conclusions drawn for the effect of configuration changes on the dynamic stability of 28-ft A-train doubles can be summarized as follows:

- The RSC systems could improve the truck roll stability without introducing significant additional understeer or jackknifing risk;
- If only one RSC unit is available, installing it on the front trailer would achieve better performance;
- A combination of the tractor-based ESC system and the trailer-based RSC system would greatly improve the truck roll stability, but it would also introduce a considerable amount of understeer to the truck;
- The tractor-based ESC system exhibited similar performance as the trailer-based RSC systems, but the ESC system significantly increased the likelihood of jackknifing events when dynamic maneuvers were performed; and
- An empty rear trailer could decrease the roll stability of the 28-ft A-train tested, especially with J-turn maneuvers, and it also diminished the performance of the onboard RSC unit.

10.2 Recommended Future Work

10.2.1 28-ft A-train Double Model Development

The two sets of tests introduced in Chapter 8 and Chapter 9 generated a tremendous amount of data that could be used to validate and improve the mathematical and TruckSim models

introduced in Chapter 6. The validated model could be employed to further study the dynamics of 28-ft A-train doubles with different maneuvers, load conditions, roadway input, etc. This model could also be coupled with other ESC or RSC systems for performance evaluation and system tuning.

10.2.2 RSC System Optimization

According to the test results and on-site observation, it is believed that the performance of the two RSC systems tested in this program could be further optimized. For example, even though the RSC systems managed to activate before outriggers contacted the ground, the lead times they achieved were normally under 2 seconds, and sometimes were even in fractions of a second. Considering that it commonly takes 0.4s for a truck air brake system from building up pressure to applying full brake, a lead time of 2s is deemed not long enough. Therefore, the control strategy or threshold of the RSC system could be further optimized.

10.2.3 Further Analysis of the Articulation motion between Two Trailers

The relative yaw motion, or the articulation motion between the two trailers in an A-train configuration, has two degrees of freedom. Therefore, two types of jackknifing events could happen to an A-train double, which are identified as "trailer jackknifing" and "dolly jackknifing" in this dissertation. This issue was briefly investigated when designing the CVeSS anti-jackknifing systems. However, the complexity behind this phenomenon certainly requires further in-depth studies.

10.2.4 Dynamic Stability Analysis of Class 8 Trucks in Other Configurations

As the 28-ft A-train doubles are becoming more favored by freight carriers, Class 8 trucks in other configurations, such as 33-ft A-train doubles or 28-ft A-train triples, are also being considered by logistics companies to further maximize operational efficiency. Considering that different trailer lengths and an additional trailing unit would considerably affect truck dynamics, the dynamic stability of these trucks with or without RSC/ESC systems should be thoroughly investigated.

References

[1] 2016, "Large Truck and Bus Crash Facts 2014," No. FMCSA-RRA-16-001, Federal Motor Carrier Safety Administration.

[2] Waddell, E., Gingrich, M., and Lenters, M., 2009, "Trucks in Roundabouts: Pitfalls in Design and Operations," ITE Journal, 79.2 (2009), pp.40-45.

[3] National Highway Traffic Safety Administration, 2015, "FMVSS No. 136, Electronic Stability Control Systems for Heavy Vehicles," Docket No. NHTSA-2015-0056, Department of Transportation, Washington, DC.

[4] Fancher, P., and Winkler, C., 2007, "Directional Performance Issues in Evaluation and Design of Articulated Heavy Vehicles," Vehicle System Dynamics, 45(7-8), pp. 607-647.

[5] International Organization for Standardization, 2011, "Road vehicles - Vehicle dynamics and road-holding ability - Vocabulary," No. ISO 8855:2011(E).

[6] 2005, "Ontario Regulation 32/94: Vehicle Configurations," https://www.ontario.ca/laws/regulation/940032

[7] Fancher, P., and Winkler, C., "A Methodology for Measuring Rearward Amplification," Proc. Proceedings: International Technical Conference on the Enhanced Safety of Vehicles, National Highway Traffic Safety Administration, Washington, DC, Vol. 1992, pp. 352-358.

[8] Winkler, C., 1988, "Innovative Dollies: Improving the Dynamic Performance of Multi-Trailer Vehicles," Proc. International Symposium on Heavy Vehicle Weights and Dimensions, pp. 289-313.

[9] Winkler, C., and Fancher, P., 1988, "Directional Dynamics of Multi-Articulated Heavy Trucks Employing Controlled Steering of Dolly Wheels," Vehicle System Dynamics, 17:sup1, pp. 525-540.

[10] Winkler, C., Fancher, P., Carsten, O., Mathew, A., and Dill, P., 1986, "Improving the Dynamic Performance of Multitrailer Vehicles: A Study of Innovative Dollies, Final Report," FHWA/RD-86/162, The University of Michigan Transportation Research Institute, Ann Arbor, MI.

[11] National Center for Statistics & Analysis, 2008, "Motor vehicle traffic crash fatality counts and estimates of people injured for 2007," No. DOT HS 811 034, National Highway Traffic Safety Administration, Washington, DC.

[12] Ervin, R., Fancher, P., and Gillespie, T. D., 1984, “An Overview of the Dynamic Performance Properties of Long Truck Combinations,” UMTRI-84-26, The University of Michigan Transportation Research Institute, Ann Arbor, MI.

[13] 2000, "Comprehensive Truck Size and Weight Study," No. FHWA-PL-00-029, Federal Highway Administration, Washington, DC.

[14] Peng, H., and Eisele, D., 2000, "Vehicle Dynamics Control with Rollover Prevention for Articulated Heavy Trucks," 5th International Symposium on Advanced Vehicle Control, Ann Arbor, MI.

[15] Solmaz, S., Akar, M., and Shorten, R., 2008, "Adaptive Rollover Prevention for Automotive Vehicles with Differential Braking," IFAC Proceedings Volumes, 41(2), pp. 4695-4700.

[16] Winkler, C. B., and Ervin, R., 1999, "Rollover of Heavy Commercial Vehicles," No. UMTRI-99-19, The University of Michigan Transportation Research Institute, Ann Arbor, MI.

[17] 2014, "Large Truck and Bus Crash Facts 2012," No. FMCSA-RRA-14-004, Federal Motor Carrier Safety Administration, Washington, DC.

[18] Rao, S. Y., Jeong, J., Ashby, R. M., Heydinger, G. J., and Guenther, D. A., 2014, "Modeling and Validation of ABS and RSC Control Algorithms for a 6× 4 Tractor and Trailer Models using SIL Simulation," SAE Technical Paper 2014-01-0135.

[19] Gillespie, T. D., 1992, Fundamentals of Vehicle Dynamics, Society of Automotive Engineers, Inc., Warrendale, PA.

[20] Rao, S. Y., 2013, "Development of a Heavy Truck Vehicle Dynamics Model using TruckSim and Model Based Design of ABS and ESC Controllers in Simulink," Master Thesis, The Ohio State University, Columbus, OH.

[21] Hou, Y., Chen, Y., and Ahmadian, M., 2016, "A Simulation-based Study on the Improvement of Semi-truck Roll Stability in Roundabouts," SAE Technical Paper No.2015-01-2741.

[22] Chen, Y., Ahmadian, M., and Peterson, A., 2015, "Pneumatically Balanced Heavy Truck Air Suspensions for Improved Roll Stability," SAE Technical Paper No.2015-01-2749.

[23] Hou, Y., and Ahmadian, M., 2015, "Effects of Commercial Truck Configuration on Roll Stability in Roundabouts," SAE Technical Paper No.2016-01-8038.

[24] Jindra, F., 1963, "Tractor and Semi-Trailer Handling," Automobile Engineer, 53(10), pp. 438-446.

[25] Jindra, F., 1965, "Handling Characteristics of Tractor-Trailer Combinations," SAE Technical Paper No.650720.

[26] Hazemoto, T., 1973, "Analysis of Lateral Stability for Doubles," SAE Technical Paper No.730688.

[27] Mallikarjunarao, C., and Fancher, P., 1978, "Analysis of the Directional Response Characteristics of Double Tankers," SAE Technical Paper No.781064.

[28] Sanyal, A., and Karmakar, R., 1995, "Directional Stability of Truck-Dolly-Trailer System," Vehicle System Dynamics, 24(8), pp. 617-637.

[29] Alexander, L., Donath, M., Hennessey, M., Morellas, V., and Shankwitz, C., 1996, "A Lateral Dynamic Model of a Tractor-Trailer: Experimental Validation," No. MN/RC-97/18, University of Minnesota, Minneapolis, MN.

[30] Verma, M., and Gillespie, T., 1980, "Roll Dynamics of Commercial Vehicles," Vehicle System Dynamics, 9(1), pp. 1-17.

[31] Winkler, C. B., 1998, "Simplified Analysis of the Steady-State Turning of Complex Vehicles," Vehicle System Dynamics, 29(3), pp. 141-180.

[32] Esmailzadeh, E., and Tabarrok, B., 2000, "Directional Response and Yaw Stability of Articulated Log Hauling Trucks," SAE Technical Paper No.2000-01-3478.

[33] Wideberg, J., 2004, "Simplified Method for Evaluation of the Lateral Dynamic Behaviour of a Heavy Vehicle," International Journal of Heavy Vehicle Systems, 11(2), pp. 195-207.

[34] Elhemly, M. A. E., and Fayed, M. A. G., 2011, "Simulation of Tractor Semitrailer Manoeuvre at High Speed Using MATLAB/SIMULINK," International Journal of Heavy Vehicle Systems, 18(4), pp. 341-358.

[35] Tabatabaei, S. H., Zahedi, A., and Khodayari, A., "The Effects of the Cornering Stiffness Variation on Articulated Heavy Vehicle Stability," 2012 IEEE International Conference on Vehicular Electronics and Safety (ICVES 2012), Istanbul, 2012, pp. 78-83.

[36] Morrison, G., 2015, "Combined Emergency Braking and Cornering of Articulated Heavy Vehicles," PhD Dissertation, Department of Engineering, University of Cambridge, Cambridge, UK.

[37] Morrison, G., and Cebon, D., 2017, "Combined Emergency Braking and Turning of Articulated Heavy Vehicles," Vehicle System Dynamics, 55(5), pp. 725-749.

[38] Ervin, R., Francher, P., Gillespie, T., Winkler, C., and Wolfe, A., 1978, "Ad Hoc Study of Certain Safety-Related Aspects of Double-Bottom Tankers," UM-HSRI-78-18-2, The University of Michigan Highway Safety Research Institute, Ann Arbor, MI.

[39] Winkler, C. B., Fancher, P., and MacAdam, C. C., 1983, "Parametric Analysis of Heavy Duty Truck Dynamic Stability", No.DOT HS-806-411, National Highway Traffic Safety Administration, Washington, DC.

[40] Ervin, R. D., and MacAdam, C. C., 1982, "The Dynamic Response of Multiply-Articulated Truck Combinations to Steering Input," No. 0148-7191, SAE Technical Paper.

[41] Fancher, P. S., 1982, "The Transient Directional Response of Full Trailers," SAE Technical Paper No. 820973.

[42] Ei-Gindy, M., Mrad, N., and Tong, X., 2001, "Sensitivity of Rearward Amplification Control of a Truck/Full Trailer to Tyre Cornering Stiffness Variations," Proceedings of the Institution of Mechanical Engineers, Part D: Journal of Automobile Engineering, 215(5), pp. 579-588.

[43] Jin, Z., Zhang, L., Zhang, J., and Khajepour, A., 2016, "Stability and Optimised H∞ Control of Tripped and Untripped Vehicle Rollover," Vehicle System Dynamics, 54(10), pp. 1405-1427.

[44] Zhang, X., Yang, Y., Guo, K., Lv, J., and Peng, T., 2017, "Contour Line of Load Transfer Ratio for Vehicle Rollover Prediction," Vehicle System Dynamics, 2017, pp. 1-16.

[45] Chen, B.-C., and Peng, H., 2005, "Rollover Warning for Articulated Heavy Vehicles Based on a Time-To-Rollover Metric," Journal of Dynamic Systems, Measurement, and Control, 127(3), pp. 406-414.

[46] Chen, C., and Tomizuka, M., 2000, "Lateral Control of Commercial Heavy Vehicles," Vehicle System Dynamics, 33(6), pp. 391-420.

[47] Hyun, D., and Langari, R., 2003, "Modeling to Predict Rollover Threat of Tractor-Semitrailers," Vehicle System Dynamics, 39(6), pp. 401-414.

[48] Dahlberg, E., and Stensson, A., 2005, "The Dynamic Rollover Threshold - A Heavy Truck Sensitivity Study," International Journal of Vehicle Design, 40(1-3), pp. 228-250.

[49] Jo, J.-S., You, S.-H., Joeng, J. Y., Lee, K. I., and Yi, K., 2008, "Vehicle Stability Control System for Enhancing Steerabilty, Lateral Stability, and Roll Stability," International Journal of Automotive Technology, 9(5), pp. 571-576.

[50] Hecker, F., Hurnrnel, S., Jundt, O., Leirnbach, K.-D., Faye, I., and Schramm, H., 1997, "Vehicle Dynamics Control for Commercial Vehicles," SAE Technical Paper No. 973284.

[51] MacAdam, C., Hagan, M., Fancher, P., Winkler, C., Ervin, R., Zhou, J., and Bogard, S., 2000, "Rearward Amplification Suppression (RAMS)," UMTRI-2000-47, The University of Michigan Transportation Research Institute, Ann Arbor, MI.

[52] Lin, R., Cebon, D., and Cole, D., 1994, "An Investigation of Active Roll Control of Heavy Road Vehicles," Vehicle System Dynamics, 23(S1), pp. 308-321.

[53] Sampson, D., and Cebon, D., 1998, "An Investigation of Roll Control System Design for Articulated Heavy Vehicles," Proc. Proc. 4th International Symposium on Advanced Vehicle Control, pp. 311-316.

[54] Sampson, D., McKevitt, G., and Cebon, D., 2000, "The Development of an Active Roll Control System for Heavy Vehicles," Vehicle System Dynamics, 33, pp. 704-715.

[55] Sampson, D. J., and Cebon, D., 2003, "Achievable Roll Stability of Heavy Road Vehicles," Proceedings of the Institution of Mechanical Engineers, Part D: Journal of Automobile Engineering, 217(4), pp. 269-287.

[56] Miege, A. J., and Cebon, D., 2005, "Optimal Roll Control of an Articulated Vehicle: Theory and Model Validation," Vehicle System Dynamics, 43(12), pp. 867-884.

[57] Barickman, F., Elsasser, D., Albrecht, H., Church, J., and Xu, G., 2011, "Tractor Semitrailer Stability Objective Performance Test Research – Roll Stability," No. DOT HS 811 467, National Highway Traffic Safety Administration, Washington, DC.

[58] Elsasser, D., Barickman, F. S., Albrecht, H., Church, J., Xu, G., and Heitz, M., 2013, "Tractor Semitrailer Stability Objective Performance Test Research – Yaw Stability," No. DOT HS 811 734, National Highway Traffic Safety Administration, Washington, DC.

[59] Wang, Q., and He, Y., 2016, "A Study on Single Lane-Change Manoeuvres for Determining Rearward Amplification of Multi-Trailer Articulated Heavy Vehicles with Active Trailer Steering Systems," Vehicle System Dynamics, 54(1), pp. 102-123.

[60] Fancher, P., Ervin, R., Winkler, C., and Gillespie, T., 1986, "A Factbook of the Mechanical Properties of the Components for Single-Unit and Articulated Heavy Trucks, University of Michigan," No. UMTRI-86-12, The University of Michigan Transportation Research Institute, Ann Arbor, MI.

[61] Robinson, B. W., Rodegerdts, L., Scarborough, W., Kittelson, W., Troutbeck, R., Brilon, W., Bondzio, L., Courage, K., Kyte, M., and Mason, J., 2000, "Roundabouts: An Informational Guide," No. NCHRP Report 672, Transportation Research Board of the National Academies, Washington, DC.

[62] Rodegerdts, L., 2007, “Roundabouts in the United States,” No. NCHRP Report 572, Transportation Research Board of the National Academies, Washington, DC.

[63] Rodegerdts, L., Griffin, A., Steyn, H., Ahmadian, M., Hou, Y., and Taheri, M., 2015, "Evaluation of Geometric Parameters that Affect Truck Maneuvering and Stability," No. FHWA-SA-15-073, Federal Highway Administration, Washington, DC.

[64] Cerezo, V., and Gothie, M., 2006, "Heavy Goods Vehicles Accidents on Roundabouts: Parameters of Influence," Proc. 9th International Symposium on Heavy Vehicle Transport Technology, France.

[65] 2001, "A Policy on Geometric Design of Highways and Streets," American Association of State Highway and Transportation Officials, Washington, DC.

[66] 2012, "Trailer Equipment Guide,"C.H. Robinson Worldwide Inc., https://www.chrobinson.com/en-US/-/media/ChRobinson/News-PDF/TruckloadEquipmentGuide.pdf.

[67] 2006, "Minnesota Truck Size and Weight Project - Final Report," Cambridge Systematics Inc., Bethesda, MD.

[68] Chen, Y., 2017, “Modeling, Control, and Design Study of Balanced Pneumatic Suspension for Improved Roll Stability in Heavy Trucks,” PhD Dissertation, Virginia Polytechnic Institute and State University, Blacksburg, VA.

[69] Sharp, R., 1979, "The Steering Responses of Doubles," Vehicle System Dynamics, 8(2-3), pp. 219-224.

[70] de Bruin, D., and Van den Bosch, P., 1999, "Modelling and Control of a Double Articulated Vehicle with Four Steerable Axles," Proceedings of the 1999 American Control Conference (Cat. No. 99CH36251), San Diego, CA, pp. 3250-3254 vol.5.

[71] Aoki, A., Marumo, Y., and Kageyama, I., 2013, "Effects of Multiple Axles on the Lateral Dynamics of Multi-Articulated Vehicles," Vehicle System Dynamics, 51(3), pp. 338-359.

[72] Xu, H., Zhang, Y., Liu, H., Qi, S., and Li, W., 2015, "Effects of Configuration Parameters on Lateral Dynamics of Tractor–Two Trailer Combinations," Advances in Mechanical Engineering, 7(12), pp. 1-9.

[73] Elsasser, D., 2010, "National Highway Traffic Safety Administration’s Class 8 Tractor/Trailer Safety Outrigger," No. DOT HS 811 289, National Highway Traffic Safety Administration, Washington, DC.

[74] Pape, D., Arant, M., Brock, W., Broshears, E., Chitwood, C., Clinansmith, R., Colbert, J., Cutler, M., Hathaway, R., Keil, M., LaClair, T., McAuley, M., Patterson, J., Petrolino, J., Pittro, C., Spezia, A., and Wafer, D., 2011, "U32: Vehicle Stability and Dynamics Longer Combination Vehicles Final Report," No. NTRCI-50-2011-025, National Transportation Research Center Inc., University Transportation Center, Knoxville, TN.

[75] Lyons, R. G., 2012, Understanding Digital Signal Processing (3rd Edition), Pearson Education Inc., Upper Saddle River, NJ.

[76] Placko, D., 2013, Fundamentals of Instrumentation and Measurement, John Wiley & Sons, London, UK.

[77] Mashadi, B., and Mostaghimi, H., 2017, "Vehicle Lift-Off Modelling and a New Rollover Detection Criterion," Vehicle System Dynamics, 55(5), pp. 1-21.

[78] Shangguan, W.-B., Chen, Y., Wang, Q., and Rakheja, S., 2016, "Simulation of a Partly Filled Tank Vehicle Combination in TruckSim and Tank Design Optimisation," International Journal of Heavy Vehicle Systems, 23(3), pp. 264-282.

[79] Tseng, H. E., and Hrovat, D., 2015, "State of the Art Survey: Active and Semi-Active Suspension Control," Vehicle System Dynamics, 53(7), pp. 1034-1062.

[80] Sorge, F., 2015, "On the Sway Stability Improvement of Car–Caravan Systems by Articulated Connections," Vehicle System Dynamics, 53(9), pp. 1349-1372.

[81] Kang, J. Y., Burkett, G., Bennett, D., and Velinsky, S. A., 2015, "Nonlinear Vehicle Dynamics and Trailer Steering Control of the TowPlow, a Steerable Articulated Snowplowing Vehicle System," Journal of Dynamic Systems, Measurement, and Control, 137(8), p. 081005.

[82] Hecker, F., 2014, "Brake-Based Stability Assistance Functions for Commercial Vehicles," Handbook of Driver Assistance Systems: Basic Information, Components and Systems for Active Safety and Comfort, H. Winner, S. Hakuli, F. Lotz, and C. Singer, eds., Springer International Publishing, Cham, pp. 1-20.

[83] Gordon, T., and Lidberg, M., 2015, "Automated Driving and Autonomous Functions on Road Vehicles," Vehicle System Dynamics, 53(7), pp. 958-994.

[84] Chiu, J., and Goswami, A., 2014, "The Critical Hitch Angle for Jackknife Avoidance during Slow Backing Up of Vehicle–Trailer Systems," Vehicle System Dynamics, 52(7), pp. 992-1015.

[85] Barbieri, F. A., de Almeida Lima, V., Garbin, L., and Boaretto, J., 2014, "Rollover Study of a Heavy Truck Combination with Two Different Semi-Trailer Suspension Configurations," SAE Technical Paper No. 2014-36-0025.

[86] Richardson, S., Sandvik, A., Jones, C., Josevski, N., Pok, W. P. T., and Orton, T., 2013, "The Comparative Testing of a Single and Double Ride Height Control Valve Suspension Control Systems," Proc. 23rd International Technical Conference on the Enhanced Safety of Vehicles (ESV), No.13-0292.

[87] Jazar, R. N., 2013, Vehicle Dynamics: Theory and Application, Springer Science & Business Media, Riverdale, NY.

[88] Dahmani, H., Chadli, M., Rabhi, A., and El Hajjaji, A., 2013, "Vehicle Dynamic Estimation with Road Bank Angle Consideration for Rollover Detection: Theoretical and Experimental Studies," Vehicle System Dynamics, 51(12), pp. 1853-1871.

[89] Zong, C., Zhu, T., Wang, C., and Liu, H., 2012, "Multi-Objective Stability Control Algorithm of Heavy Tractor Semi-Trailer Based on Differential Braking," Chinese Journal of Mechanical Engineering, 25(1), pp. 88-97.

[90] Islam, M. M., Ding, X., and He, Y., 2012, "A Closed-Loop Dynamic Simulation-Based Design Method for Articulated Heavy Vehicles with Active Trailer Steering Systems," Vehicle system dynamics, 50(5), pp. 675-697.

[91] Oberoi, D., 2011, "Enhancing Roll Stability and Directional Performance of Articulated Heavy Vehicles Based on Anti-Roll Control and Design Optimization," Master Thesis, University of Ontario Institute of Technology, Oshawa, ON.

[92] Karnopp, D., 2004, Vehicle Stability, CRC Press, New York, NY.

[93] Abe, M., 2015, Vehicle Handling Dynamics: Theory and Application, Butterworth-Heinemann, Oxford, UK.

[94] Currier, P. N., 2011, "A Method for Modeling and Prediction of Ground Vehicle Dynamics and Stability in Autonomous Systems," PhD Dissertation, Virginia Polytechnic Institute and State University, Blacksburg, VA.

[95] Cao, D., Song, X., and Ahmadian, M., 2011, "Editors' Perspectives: Road Vehicle Suspension Design, Dynamics, and Control," Vehicle System Dynamics, 49(1-2), pp. 3-28.

[96] Knight, I., Robinson, T., Robinson, B., Barlow, T., McCrae, I., Odhams, A., Roebuck, R., and Cheng, C., 2010, "The Likely Effects of Permitting Longer Semi-Trailers in the UK: Vehicle Specification, Performance and Safety," No. PPR526, Transport Research Laboratory, Wokinghan, UK.

[97] Khemoudj, O., Imine, H., and Djemai, M., 2010, "Robust Observation of Tractor-Trailer Vertical Forces Using Inverse Model and Numerical Differentiation," SAE International Journal of Materials and Manufacturing, 3(1), pp. 278-289.

[98] Karkee, M., and Steward, B. L., 2010, "Study of the Open and Closed Loop Characteristics of a Tractor and a Single Axle Towed Implement System," Journal of Terramechanics, 47(6), pp. 379-393.

[99] Woodrooffe, J., Blower, D., Gordon, T., Green, P. E., Liu, B., and Sweatman, P., 2009, "Safety Benefits of Stability Control Systems for Tractor-Semitrailers," No. DOT HS 811 205, National Highway Traffic Safety Administration, Washington, DC.

[100] Svenson, A. L., Grygier, P. A., Salaani, M. K., and Heydinger, G. J., 2009, "Validation of Hardware in the Loop (Hil) Simulation for Use in Heavy Truck Stability Control System Effectiveness Research," Proc. 21th International Technical Conference on the Enhanced Safety of Vehicles - (ESV), Stuttgart, Germany, 09–0189.

[101] Solmaz, S., Akar, M., Shorten, R., and Kalkkuhl, J., 2008, "Real-Time Multiple-Model Estimation of Centre of Gravity Position in Automotive Vehicles," Vehicle System Dynamics, 46(9), pp. 763-788.

[102] Inman, D. J., 2014, Engineering vibration (4th Edition), Pearson Education Inc., Upper Saddle River, NJ.

[103] Dorf, R. C., and Bishop, R. H., 2011, Modern Control Systems (10th Edition), Pearson Education Inc., Upper Saddle River, NJ.

[104] Zhu, T., Zong, C., Zheng, H., Tian, C., and Zheng, H., 2007, "Yaw/Roll Stability Modeling and Control of HeavyTractor-SemiTrailer," SAE Technical Paper No. 2007-01-3574.

[105] Isiklar, G., 2007, "Simulation of Complex Articulated Commercial Vehicles for Different Driving Manoeuvres," Master thesis, Eindhoven University of Technology, Eindhoven, The Neitherlands.

[106] Feng, L., He, Y., Bao, Y., and Fang, H., 2005, "Development of Trajectory Model for a Tractor-Implement System for Automated Navigation Applications," 2005 IEEE Instrumentationand Measurement Technology Conference Proceedings, Ottawa, Ont., pp. 1330-1334

[107] Gäfvert, M., and Lindgärde, O., 2004, "A 9-DOF Tractor-Semitrailer Dynamic Handling Model for Advanced Chassis Control Studies," Vehicle System Dynamics, 41(1), pp. 51-82.

[108] Jujnovich, B., and Cebon, D., 2002, "Comparative Performance of Semi-Trailer Steering Systems," Proc. Proceedings of 7th International Symposium on Heavy Vehicle Weights and Dimensions, Delft, The Netherlands, pp. 16-20.

[109] Kang, X., Rakheja, S., and Stiharu, I., 2001, "Effects of Tank Shape on the Roll Dynamic Response of a Partly Filled Tank Vehicle," Vehicle System Dynamics, 35(2), pp. 75-102.

[110] Ma, W.-H., and Peng, H., 1999, "Worst-Case Vehicle Evaluation Methodology – Examples nn Truck Rollover/Jackknifing and Active Yaw Control Systems," Vehicle System Dynamics, 32(4-5), pp. 389-408.

[111] Ranganathan, R., and Yang, Y., 1996, "Impact of Liquid Load Shift on the Braking Characteristics of Partially Filled Tank Vehicles," Vehicle System Dynamics, 26(3), pp. 223-240.

[112] Winkler, C., and Fancher, P., 1988, "Directional Dynamics of Multi-Articulated Heavy Trucks Employing Controlled Steering of Dolly Wheels," Vehicle System Dynamics, 17, pp. 525-540.

[113] Ervin, R. D., 1986, "The Influence of Weights and Dimensions on the Stability And Control of Heavy-Duty Trucks In Canada. Volume II-Appendices. Final Report," NO. UMTRI-86-35/II, The University of Michigan Transportation Research Institute, Ann Arbor, MI.

[114] Kortum, W., and Schiehlen, W., 1985, "General Purpose Vehicle System Dynamics Software Based nn Multibody Formalisms," Vehicle System Dynamics, 14(4-6), pp. 229-263.

[115] Fancher, P. S., 1985, "The Static Stability of Articulated Commercial Vehicles," Vehicle System Dynamics, 14(4-6), pp. 201-227.

Appendix A

This section includes the steering wheel angle and lateral acceleration applied to the baseline WB-67 semi-truck when traveling through the single- and two-lane roundabouts with respect to different movements.

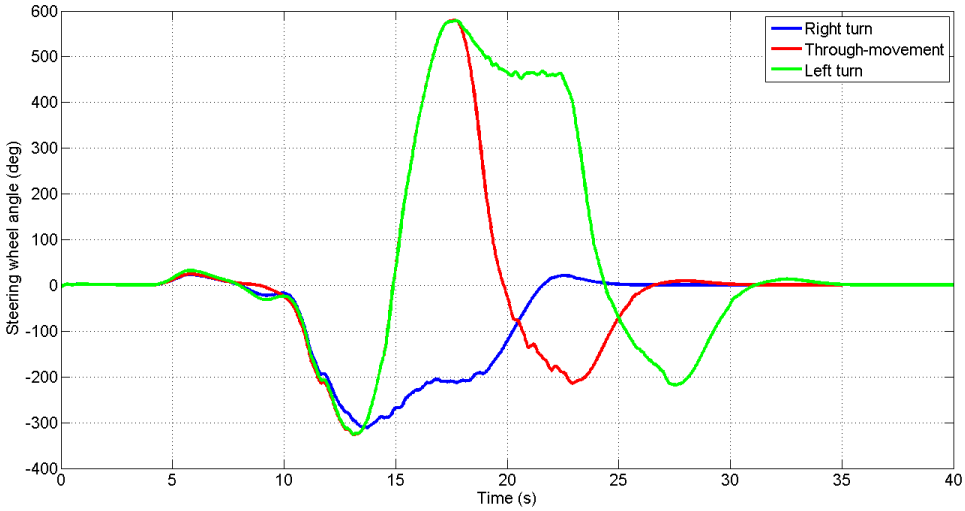

Figure A-1. Steering wheel angle applied to the WB-67 semi-truck when traveling through the 140-ft single-lane roundabout.

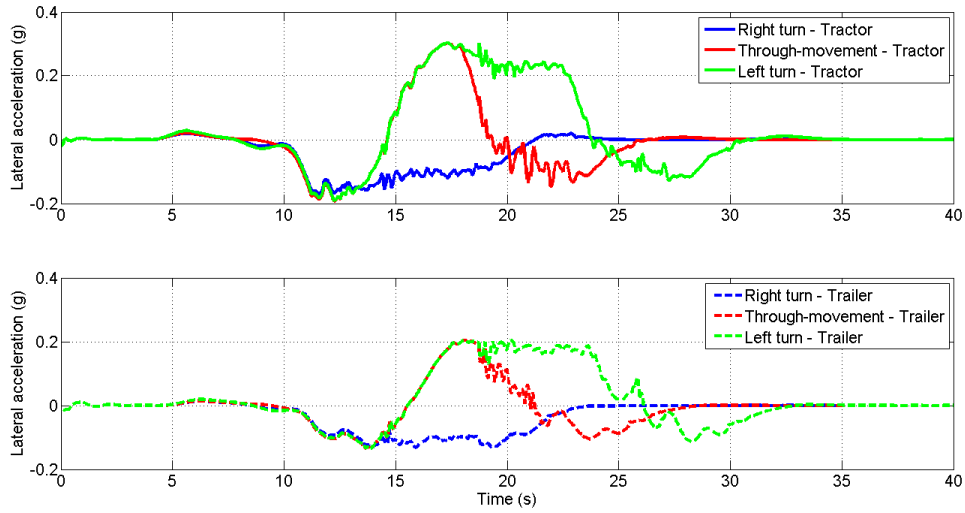

Figure A-2. Lateral acceleration experienced by the WB-67 semi-truck when traveling through the 140-ft single-lane roundabout.

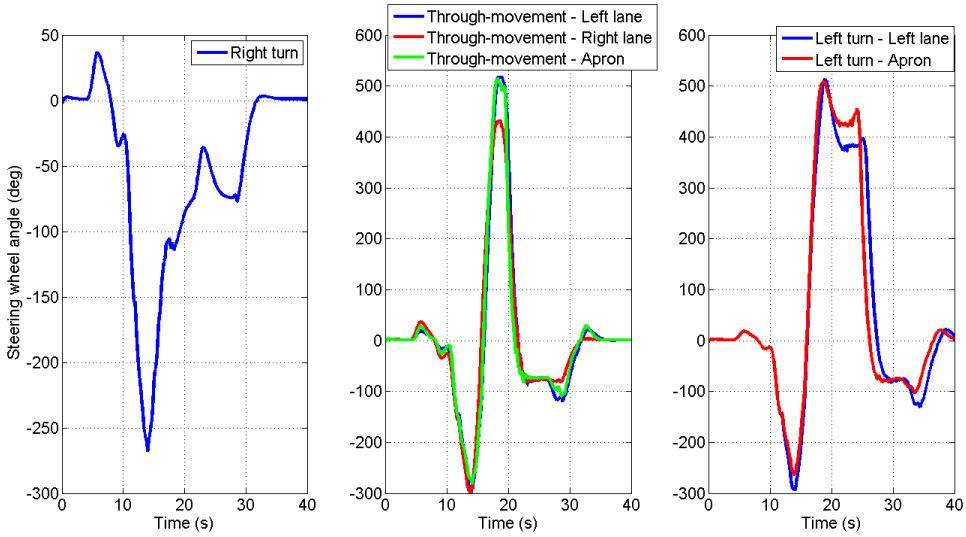

Figure A-3. Steering wheel angle applied to the WB-67 semi-truck when traveling through the 180-ft two-lane roundabout.

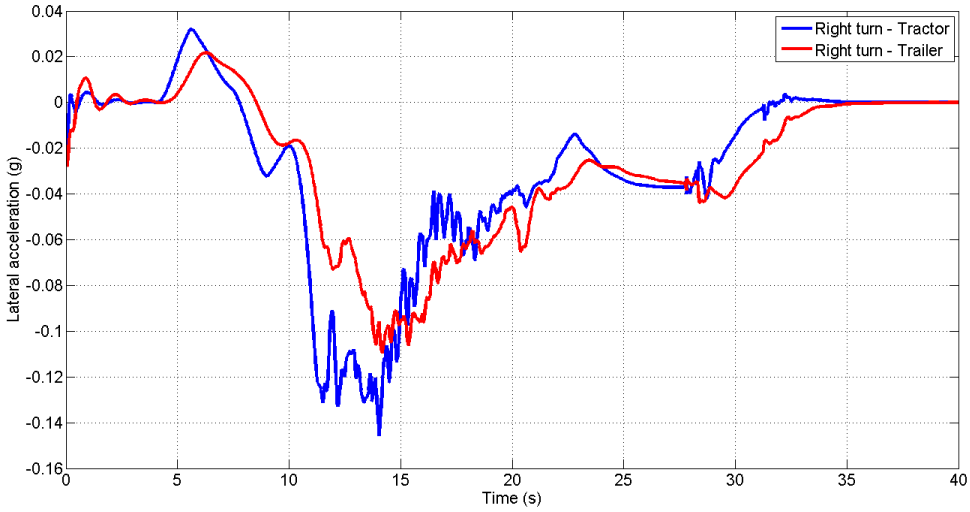

Figure A-4. Lateral acceleration experienced by the WB-67 semi-truck when performing a right turn in the 180-ft two-lane roundabout.

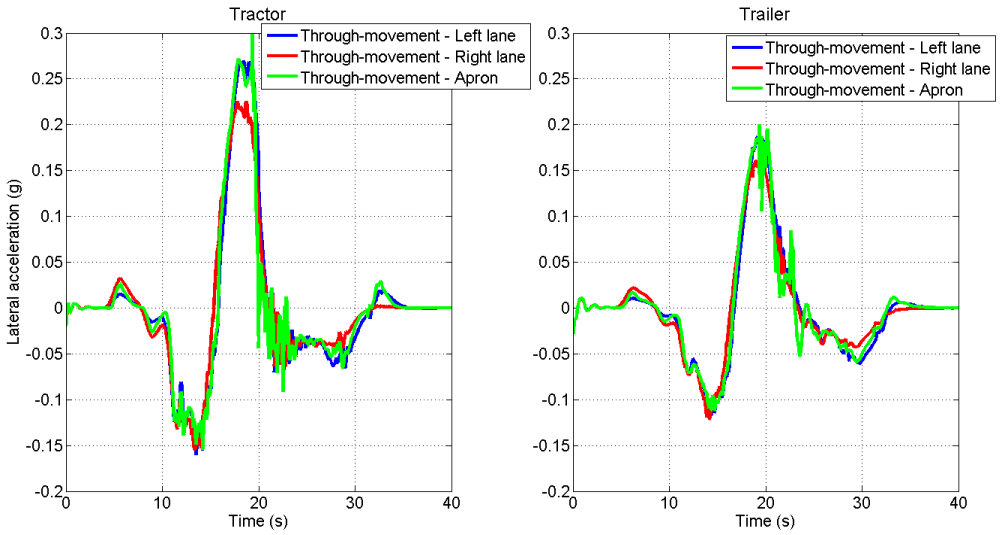

Figure A-5. Lateral acceleration experienced by the WB-67 semi-truck when performing through-movements in the 180-ft two-lane roundabout.

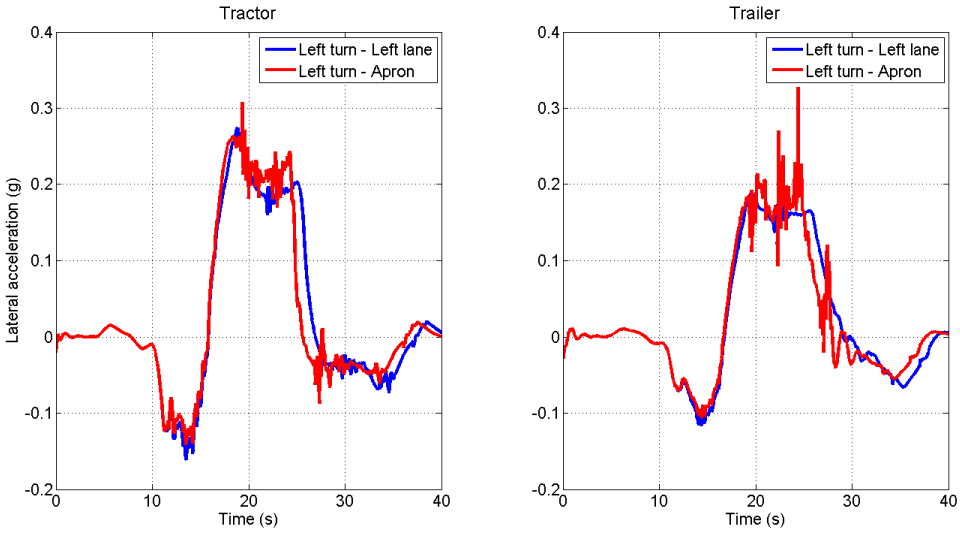

Figure A-6. Lateral acceleration experienced by the WB-67 semi-truck when performing left turns in the 180-ft two-lane roundabout.

Appendix B

This section includes the additional information for the mathematical model of a 28-ft A-train double developed in Chapter 6.

$$P = \begin{bmatrix} M_1 + M_2 + M_3 + M_4 & -M_2' - M_3' - M_4{}' & 0 & -M_2 a_2 - l_2(M_3 + M_4) & 0 & -M_3 a_3 - M_4 d_3 & 0 & -M_4 a_4 \\ M_1 f_1 & I_1 & 0 & 0 & 0 & 0 & 0 & 0 \\ 0 & 0 & 1 & 0 & 0 & 0 & 0 & 0 \\ -M_2 a_2 - l_2(M_3 + M_4) & I_2 + M_2' a_2 + l_2(M_3' + M_4') & 0 & (M_3 + M_4) l_2^2 + M_2 a_2^2 + I_2 & 0 & l_2(M_3 a_3 + M_4 d_3) & 0 & l_2 M_4 a_4 \\ 0 & 0 & 0 & 0 & 1 & 0 & 0 & 0 \\ -M_3 a_3 - M_4 d_3 & I_3 + M_3' a_3 + M_4' d_3 & 0 & l_2(M_3 a_3 + M_4 d_3) & 0 & M_3 a_3^2 + M_4 d_3^2 + I_3 & 0 & M_4 a_4 d_3 \\ 0 & 0 & 0 & 0 & 0 & 0 & 1 & 0 \\ -M_4 a_4 & I_4 + M_4' a_4 & 0 & l_2 M_4 a_4 & 0 & M_4 a_4 d_3 & 0 & M_4 a_4^2 + I_4 \end{bmatrix} \quad (B-1)$$

$$Q = \begin{bmatrix} \frac{-(C_F + C_R + C_{T2} + C_{T3} + C_{T4})}{u} & \frac{C_1' + C_{T1}' + C_{T2}' + C_{T3}{}'}{u} - u(M_1 + M_2 + M_3 + M_4) & C_{T2} & \frac{C_{T2} d_2 + l_2(C_{T3} + C_{T4})}{u} & C_{T3} & \frac{d_3(C_{T3} + C_{T4})}{u} & C_{T4} & \frac{C_{T4} d_4}{u} \\ \frac{C_1' - f_1(C_F + C_R)}{u} & \frac{-(C_F a_1^2 + C_R b_1^2 - C_1' f_1)}{u} - M_1 f_1 u & 0 & 0 & 0 & 0 & 0 & 0 \\ 0 & 0 & 0 & 1 & 0 & 0 & 0 & 0 \\ \frac{C_{T2} d_2 + l_2(C_{T3} + C_{T4})}{u} & u[a_2 + l_2(M_3 + M_4)] - \frac{C_{T1}' d_2 + l_2(C_{T2}' + C_{T3}')}{u} & -C_{T2} d_2 & -\frac{[(C_{T3} + C_{T4}) l_2^2 + C_{T2} d_2^2]}{u} & -C_{T3} l_2 & -\frac{l_2 d_3(C_{T3} + C_{T4})}{u} & -C_{T4} l_2 & -\frac{C_{T4} l_2 d_4}{u} \\ 0 & 0 & 0 & 0 & 1 & 0 & 0 & 0 \\ \frac{d_3(C_{T3} + C_{T4})}{u} & u(M_3 a_3 + M_4 d_3) - \frac{d_3(C_{T2}' + C_{T3}')}{u} & 0 & -\frac{l_2 d_3(C_{T3} + C_{T4})}{u} & -C_{T3} d_3 & -\frac{d_3^2(C_{T3} + C_{T4})}{u} & -C_{T4} d_3 & -\frac{C_{T4} d_3 d_4}{u} \\ 0 & 0 & 0 & 0 & 0 & 0 & 0 & 1 \\ \frac{C_{T4} d_4}{u} & M_4 a_4 u - \frac{C_{T3}' d_4}{u} & 0 & -\frac{C_{T4} l_2 d_4}{u} & 0 & -\frac{C_{T4} d_3 d_4}{u} & -C_{T4} d_4 & -\frac{C_{T4} d_4^2}{u} \end{bmatrix} \quad (B-2)$$

$$\boldsymbol{A = P^{-1} Q} \quad (B-3)$$

$$\boldsymbol{B = P^{-1} R} \quad (B-4)$$

$$\boldsymbol{C} = \begin{bmatrix} 1 & 0 & 0 & 0 & 0 & 0 & 0 & 0 & 0 & 0 \\ A_{11} & A_{12} & A_{13} & A_{14} & A_{15} & A_{16} & A_{17} & A_{18} & A_{19} & A_{110} \\ 0 & 1 & 0 & 0 & 0 & 0 & 0 & 0 & 0 & 0 \\ A_{21} & A_{22} & A_{23} & A_{24} & A_{25} & A_{26} & A_{27} & A_{28} & A_{29} & A_{210} \\ 0 & 0 & 1 & 0 & 0 & 0 & 0 & 0 & 0 & 0 \\ A_{41} & A_{42} & A_{43} & A_{44} & A_{45} & A_{46} & A_{47} & A_{48} & A_{49} & A_{410} \\ 0 & 0 & 0 & 0 & 1 & 0 & 0 & 0 & 0 & 0 \\ A_{61} & A_{62} & A_{63} & A_{64} & A_{65} & A_{66} & A_{67} & A_{68} & A_{69} & A_{610} \\ 0 & 0 & 0 & 0 & 0 & 0 & 0 & 0 & 1 & 0 \\ A_{81} & A_{82} & A_{83} & A_{84} & A_{85} & A_{86} & A_{87} & A_{88} & A_{89} & A_{810} \end{bmatrix} \quad (\mathrm{B}-5)$$

$$\boldsymbol{D} = \begin{bmatrix} 0 \\ B_{21} \\ 0 \\ B_{22} \\ 0 \\ 0 \\ 0 \\ 0 \end{bmatrix} \quad (B-6)$$

The parameters applied in the mathematical models are summarized in Table B-1.

Table B-1. Parameters applied in the mathematical models.

Variable	Value	Unit	Variable	Value	Unit
a_1	118.11	in.	C_R	115,926	lbf/deg.
b_1	110.24	in.	C_2	115,926	lbf/deg.
f_1	0	in.	C_3	115,926	lbf/deg.
a_2	149.61	in.	C_4	77,284	lbf/deg.
d_2	275.59	in.	M_{1_s}	15,873	lb
l_2	303.15	in.	M_{2_s}	15,432	lb
a_3	74.80	in.	M_{4_s}	15,432	lb
d_3	74.80	in.	h_{CG_1}	53.15	in.
l_3	74.80	in.	h_{CG_2}	70.87	in.
a_4	149.61	in.	h_{CG_4}	70.87	in.
d_2	275.59	in.	K_{s_1}	3,426	lbf/in.
M_1	19,842	lb	K_{s_2}	4,568	lbf/in.
I_1	75,177,782	lb-in^2	K_{s_4}	4,568	lbf/in.
M_2	15,873	lb	h_{r_1}	19.69	in.
I_2	109,349,501	lb-in^2	h_{r_2}	19.69	in.
M_3	2,645	lb	h_{r_4}	19.69	in.
I_3	1,025,152	lb-in^2	T_{s_1}	72.83	in.
M_4	15,873	lb	T_{s_2}	76.77	in.
I_4	109,349,501	lb-in^2	T_{s_4}	76.77	in.
C_F	115,926	lbf/deg.			

Appendix C

This section introduces the general information for the test truck.

Table C-1. Tractor general information.

Brand	Volvo
Model Year	2004
Model	VNL
VIN	4V4LC9TK14N37047301
Date of Manufacture	Jan. 2004
ESC Supplier	Bendix

Table C-2. Tractor tire information.

Tire Size	11R22.5	
Tire Brand	Goodyear	
Tire Model	Steer Axle	G661 HSA
	Front Drive Axle	G372 LHD
	Rear Drive Axle	G363
Tire Pressure	105 psi (all tires)	

Table C-3. Tractor gross axle weight rating (GAWR) and gross vehicle weight rating (GVWR) information (Unit: lb).

GAWR			GVWR
Steer Axle	Front Drive Axle	Rear Drive Axle	
12,361	19,000	19,000	50,361

Table C-4. Trailer general information.

Trailer Model	2001 Kentucky
VIN	1KKVD28132L206827
Date of Manufacture	Aug. 2001

Table C-5. Trailer tire information.

Tire Size	295/7R22.5
Tire Brand	Goodyear
Tire Model	G316 (all tires)
Tire Pressure	110 psi (all tires)

Table C-6. Trailer GAWR and GVWR information (Unit: lb).

GAWR	GVWR
20,000	20,000

Appendix D

The specifications and applications of the sensors employed during the tests are summarized in Table D-1.

Table D-1. The specifications and applications of the sensors employed during the tests.

	Sensor type	Brand and model	Measurement range	Supply Voltage	Output type	Label	Application
1	String potentiometer	Uni Measure – VP510-10-NJC	0 – 10 in.	25 V Max.	Analog	SP-3	Suspension travel on driver's side – rear trailer
2	String potentiometer	Uni Measure – VP510-10-NJC	0 – 10 in.	25 V Max.	Analog	SP-4	Suspension travel on passenger's side – rear trailer
3	String potentiometer	Uni Measure – VP510-10-NJC	0 – 10 in.	25 V Max.	Analog	SP-5	Suspension travel on driver's side – tractor
4	String potentiometer	Uni Measure – VP510-10-NJC	0 – 10 in.	25 Volts Max.	Analog	SP-6	Suspension travel on passenger's side – tractor
5	String potentiometer	Uni Measure – HX-P510-15-NJC-N6-L3M	0 – 15 in.	4.9 – 30 VDC	Analog	SP-S	Steering wheel angle
6	Pressure transducer	OMEGA – PX329-200G5V	0 – 200 psi	9 – 30 VDC	Analog	PS-1	Air tank pressure – rear trailer
7	Pressure transducer	OMEGA – PX329-200G5V	0 – 200 psi	9 – 30 VDC	Analog	PS-2	Airbag pressure on driver's side – rear trailer
8	Pressure transducer	OMEGA – PX329-200G5V	0 – 200 psi	9 – 30 VDC	Analog	PS-3	Airbag pressure on passenger's side – rear trailer
9	Pressure transducer	OMEGA – PX329-200G5V	0 – 200 psi	9 – 30 VDC	Analog	PS-4	Airbag pressure on driver's side - tractor
10	Pressure transducer	OMEGA – PX329-200G5V	0 – 200 psi	9 – 30 VDC	Analog	PS-5	Airbag pressure on passenger's side - tractor

11	Load cell	OMEGA – LC714	0 – 200,000 lb.	10 VDC (15 VDC max.)	Analog	LC-1	Outrigger contact force on driver's side – rear trailer
12	Load cell	OMEGA – LC714	0 – 200,000 lb.	10 VDC (15 VDC max.)	Analog	LC-2	Outrigger contact force on passenger's side – rear trailer
13	Laser sensor	Omron ZX1-LD600A86	200 – 1,000 mm (7.87 – 39.37 in.)	30 VDC max.	Analog	LS-1	Outrigger distance to the ground on driver's side – rear trailer
14	Laser sensor	Omron ZX1-LD600A86	200 – 1,000 mm (7.87 – 39.37 in.)	30 VDC max.	Analog	LS-1	Outrigger distance to the ground on passenger's side – rear trailer
15	Accelerometer	PCB 3713E1150G	0 – 50G	6 – 30 VDC	Analog	A3-50-1	Longitudinal, lateral, and vertical acceleration – tractor cab
16	Accelerometer	PCB 3713D1FD3G	0 – 3G	6 – 30 VDC	Analog	A3-3-1	Longitudinal, lateral, and vertical acceleration – tractor frame
17	Accelerometer	PCB 3713E1150G	0 – 50G	6 – 30 VDC	Analog	A3-50-2	Longitudinal, lateral, and vertical acceleration – front trailer
18	Accelerometer	PCB 3713D1FD3G	0 – 3G	6 – 30 VDC	Analog	A3-3-2	Longitudinal, lateral, and vertical acceleration – rear trailer
19	LiDAR sensor	LeddarTech M16	0 – 25 m (0 – 85 ft)	12 – 24 VDC	Digital	LD-1	Articulation angle between the tractor and the front trailer
20	LiDAR sensor	LeddarTech M16	0 – 25 m (0 – 85 ft)	12 – 24 VDC	Digital	LD-2	Articulation angle between the front trailer and the rear trailer
21	GPS	Garmin GPS 18x-5Hz	N/A	5 VDC	Digital	N/A	Tractor travelling speed and path
22	GPS	Chang Hong Information GPS Magnetic Antenna	N/A	2.3 – 5.5 VDC	Digital	N/A	Tractor traveling speed and path
23	IMU	SparkFun Electronics LSM9DS1	0 – 8G	1.9 – 3.6 VDC	Digital	IMU-T	Accelerations and angular rates in 3D – tractor cab

24	IMU	SparkFun Electronics LSM9DS1	0 – 8G	1.9 – 3.6 VDC	Digital	IMU-A	Accelerations and angular rates in 3D – front trailer
25	IMU	SparkFun Electronics LSM9DS1	0 – 8G	1.9 – 3.6 VDC	Digital	IMU-B	Accelerations and angular rates in 3D – rear trailer
26	Time of Flight Sensor	ST Microelectronics VL53l0X	0 – 2 m	2.6 – 3.5 VDC	Digital	TF1	Outrigger distance to the ground on driver's side – front trailer
27	Time of Flight Sensor	ST Microelectronics VL53l0X	0 – 2 m	2.6 – 3.5 VDC	Digital	TF2	Outrigger distance to the ground on passenger's side – front trailer
28	Time of Flight Sensor	ST Microelectronics VL53l0X	0 – 2 m	2.6 – 3.5 VDC	Digital	TF3	Outrigger distance to the ground on driver's side – rear trailer
29	Time of Flight Sensor	ST Microelectronics VL53l0X	0 – 2 m	2.6 – 3.5 VDC	Digital	TF4	Outrigger distance to the ground on passenger's side – rear trailer

Appendix E

This section provides lateral acceleration data of selected stock tests as introduced in Chapter 8.

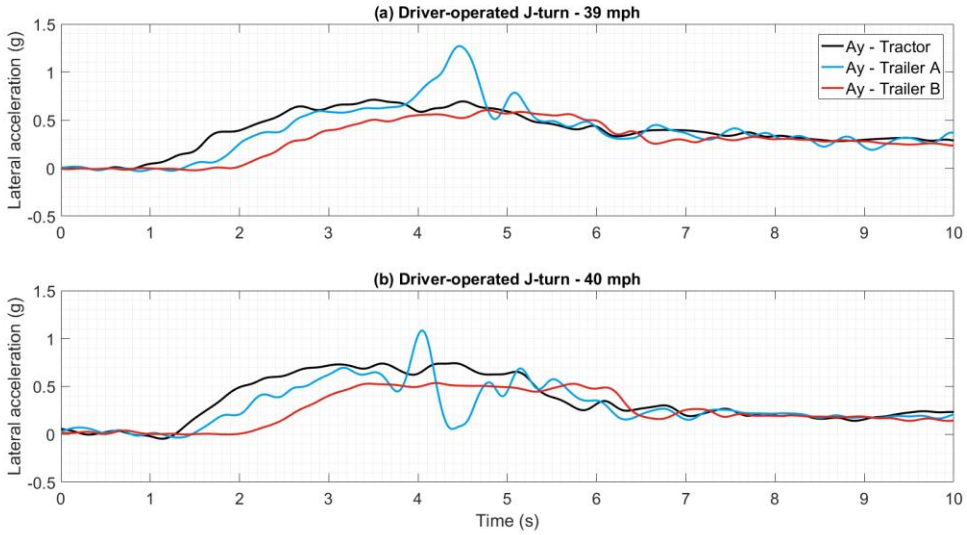

Figure E-1. Lateral acceleration data of stock driver-operated J-turn tests at (a) 39 mph and (b) 40 mph.

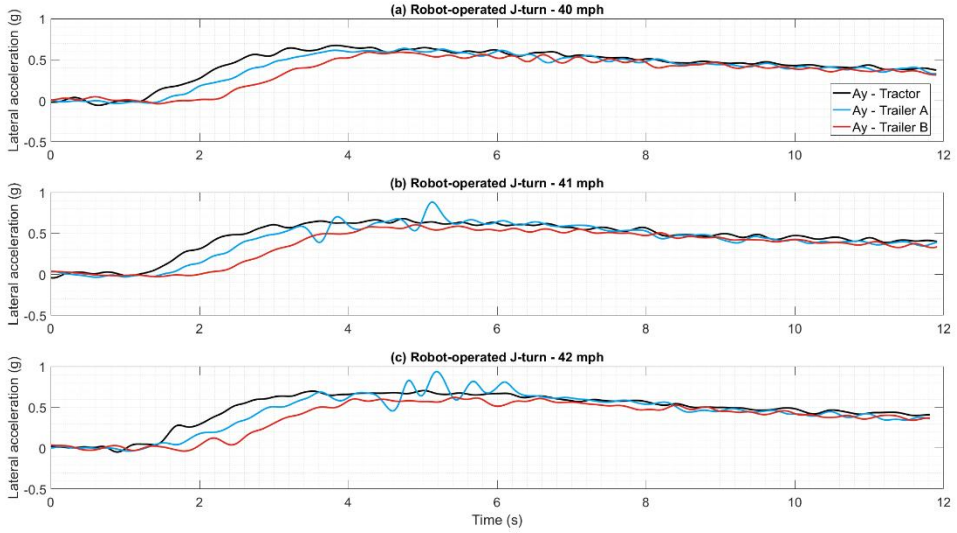

Figure E-2. Lateral acceleration data of stock robot-operated J-turn tests at (a) 40 mph, (b) 41 mph, and (c) 42 mph.

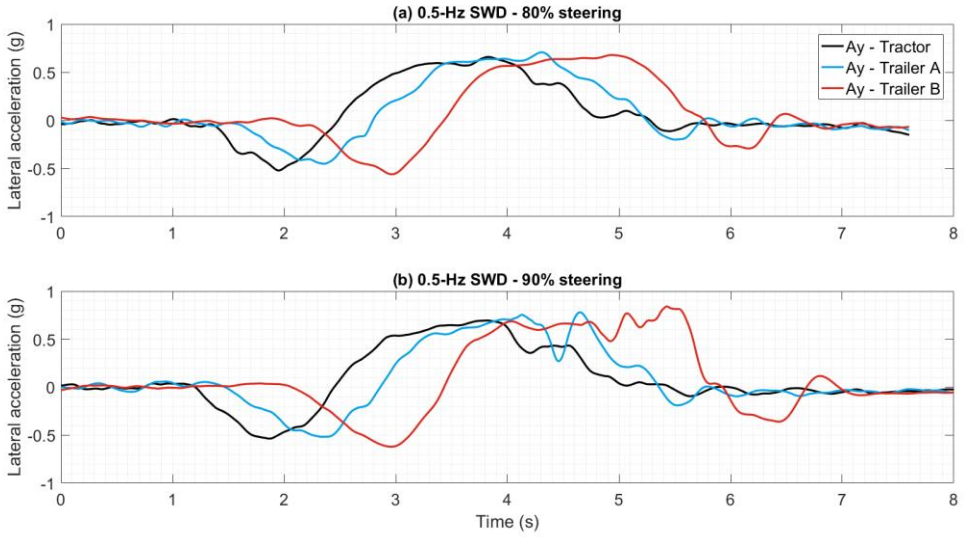

Figure E-3. Lateral acceleration data of stock 0.5-Hz SWD tests with steering at (a) 90% and (b) 100%.

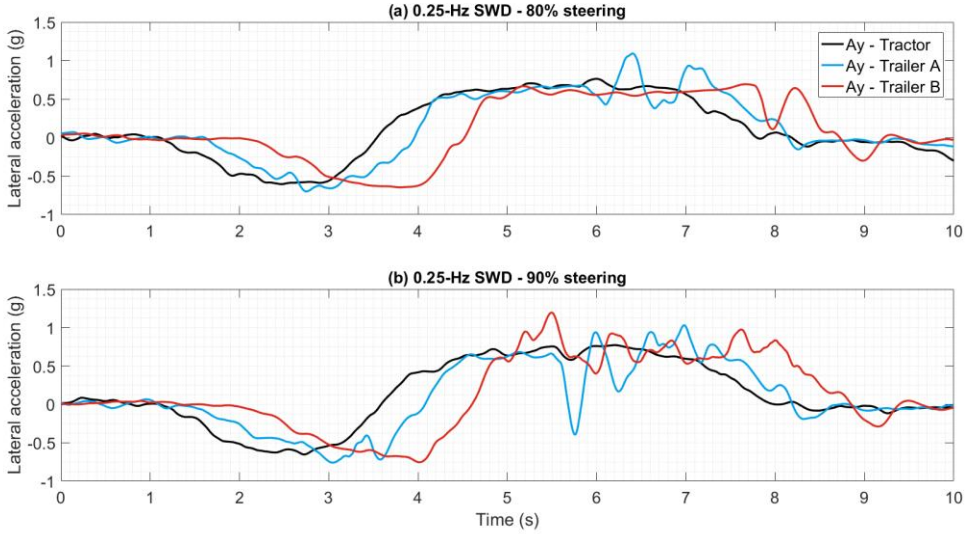

Figure E-4. Lateral acceleration data of stock 0.25-Hz SWD tests with steering at (a) 90% and (b) 100%.

Appendix F

This section provides lateral acceleration data of selected tests with an empty rear trailer or a tractor-based ESC system as introduced in Chapter 9.

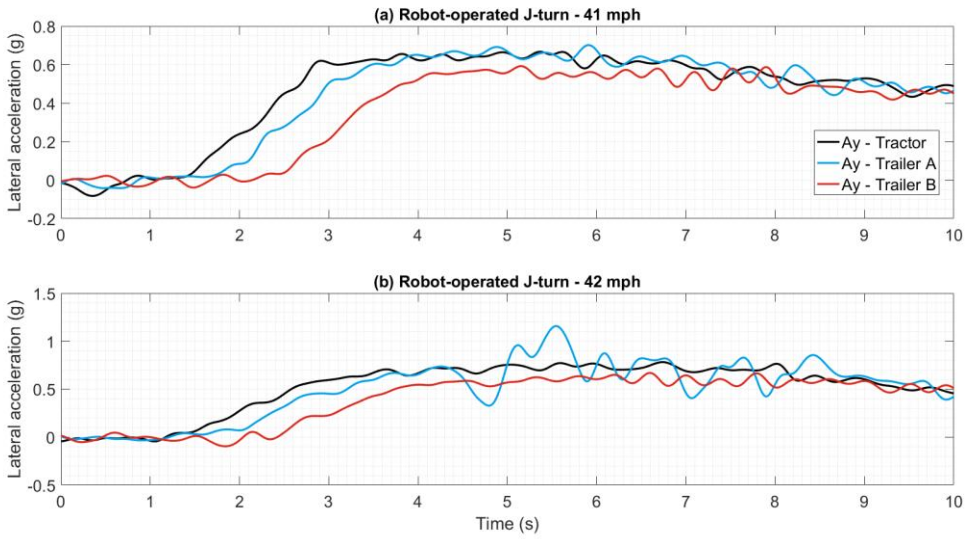

Figure F-1. Lateral acceleration data of robot-operated J-turn tests with an empty rear trailer at (a) 41 mph and (b) 42 mph.

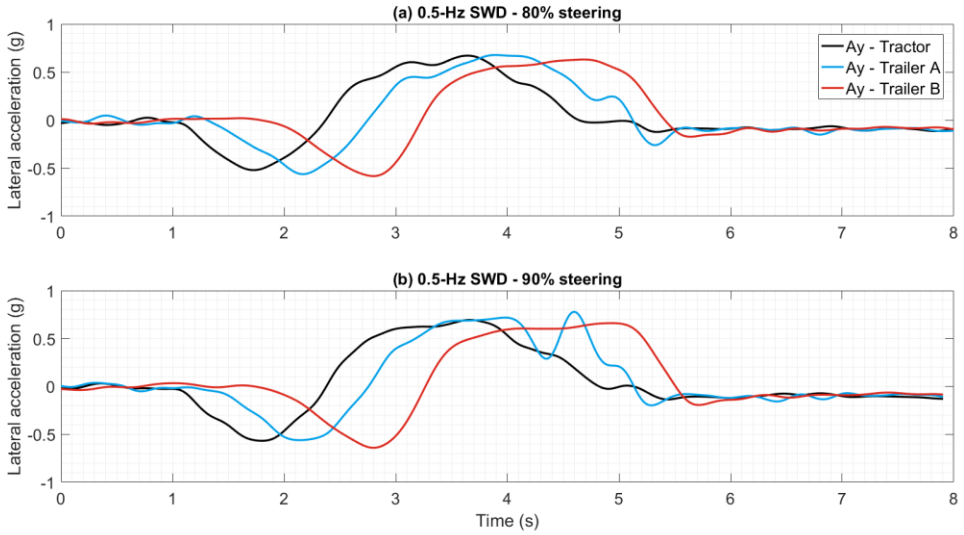

Figure F-2. Lateral acceleration data of 0.5-Hz SWD tests with an empty rear trailer at (a) 80% and (b) 90% steering.

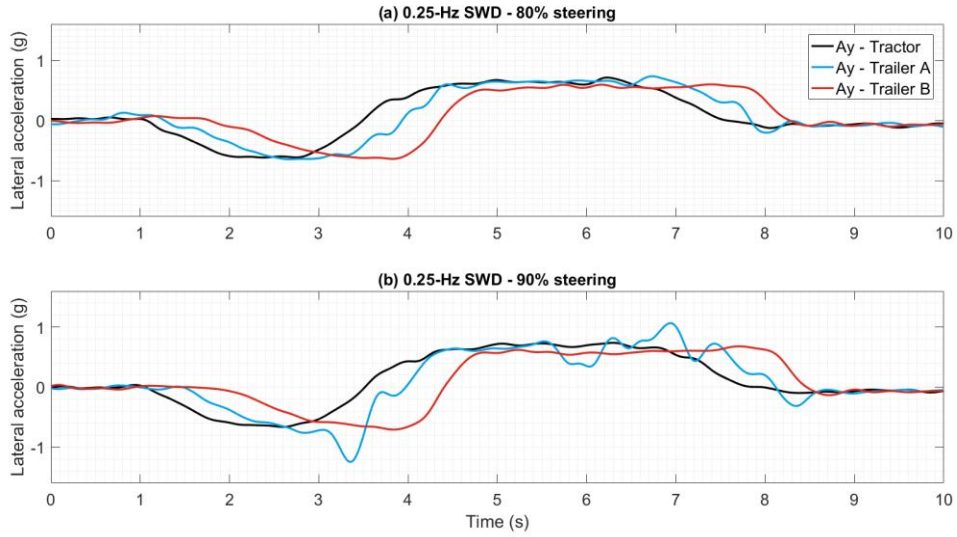

Figure F-3. Lateral acceleration data of 0.25-Hz SWD tests with an empty rear trailer at (a) 80% and (b) 90% steering.

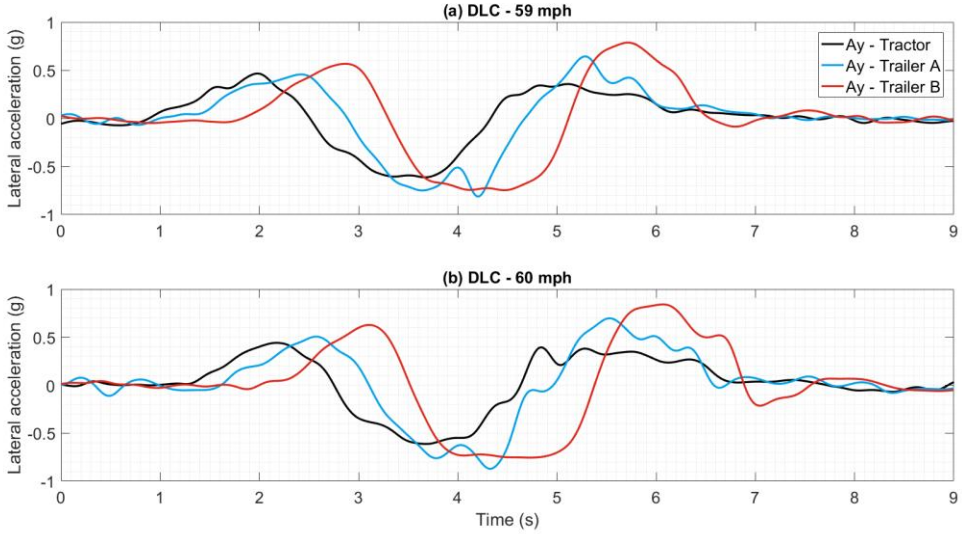

Figure F-4. Lateral acceleration data of DLC tests with an empty rear trailer at (a) 59 mph and (b) 60 mph.

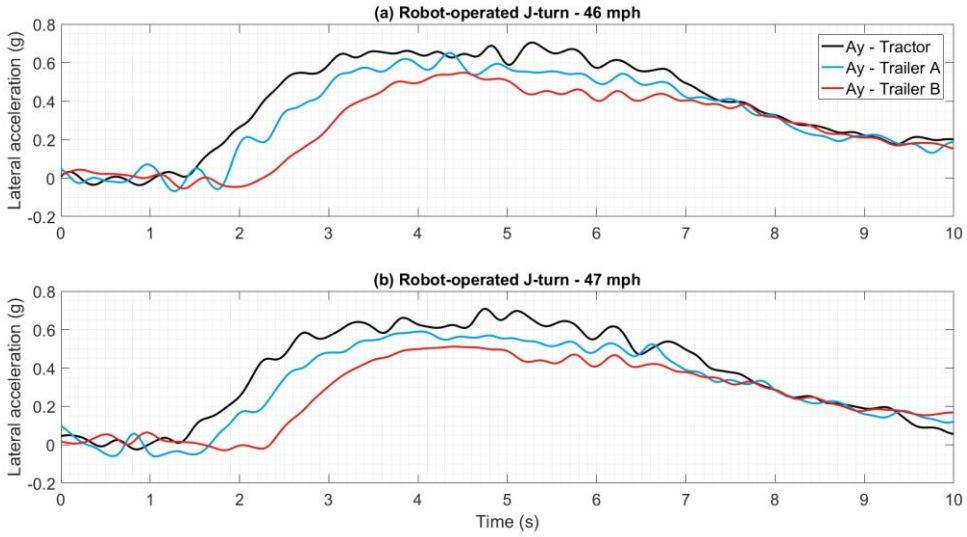

Figure F-5. Lateral acceleration data of robot-operated J-turn tests with a tractor-based ESC system at (a) 46 mph and (b) 47 mph

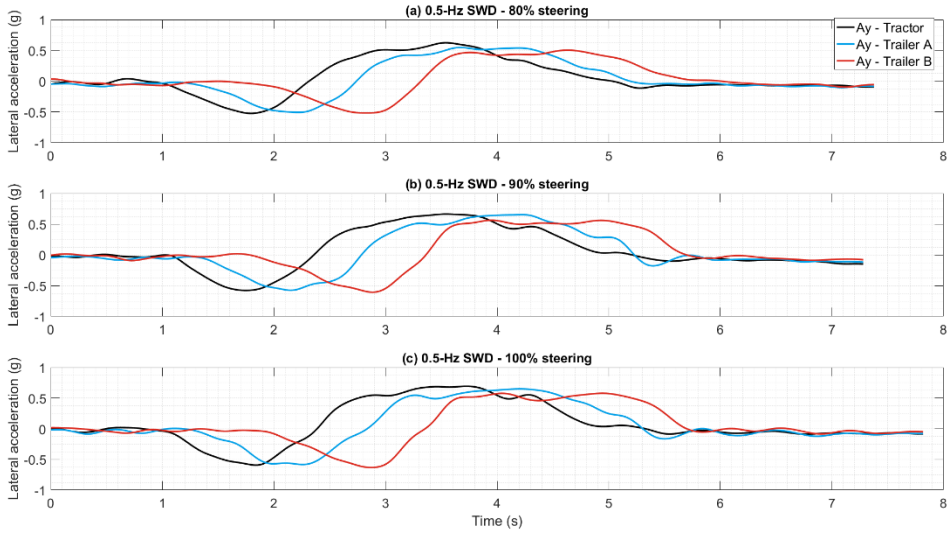

Figure F-6. Lateral acceleration data of 0.5-Hz SWD tests with a tractor-based ESC system at (a) 80%, (b) 90%, and (c) 100% steering.

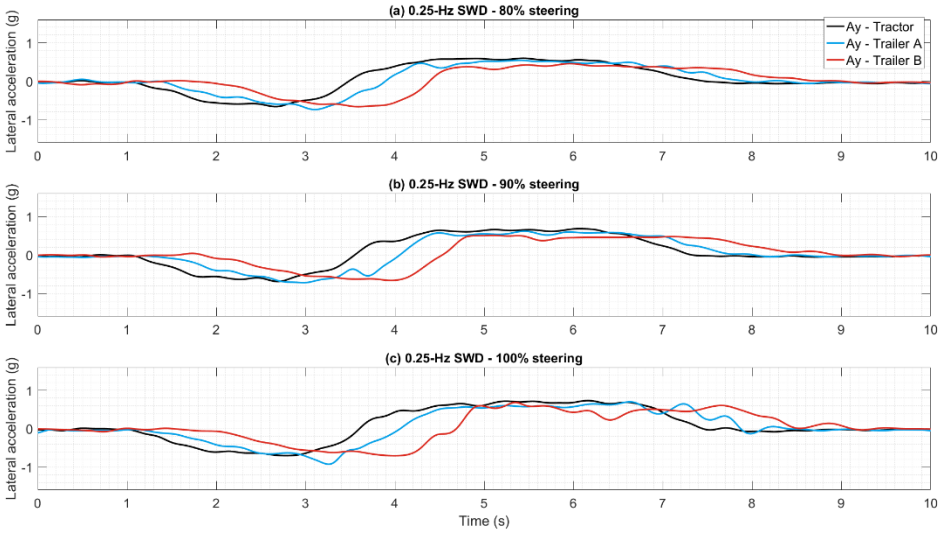

Figure F-7. Lateral acceleration data of 0.25-Hz SWD tests with a tractor-based ESC system at (a) 80%, (b) 90%, and (c) 100% steering.

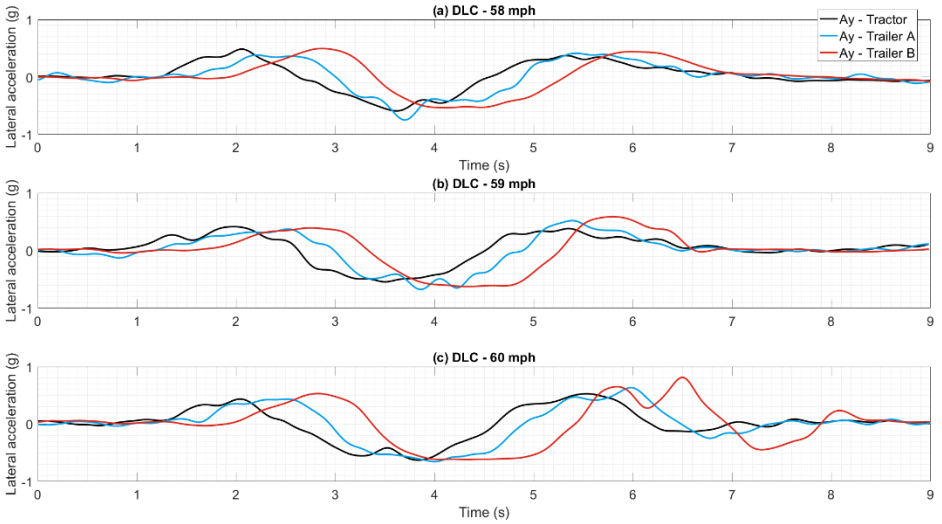

Figure F-8. Lateral acceleration data of DLC tests with a tractor-based ESC system at (a) 58 mph, (b) 59 mph, and (c) 60 mph.